

CONCEPTUAL AND STRUCTURAL DESIGN OF ADAPTIVE MEMBRANE STRUCTURES WITH SPOKED WHEEL PRINCIPLE – FOLDING TO THE PERIMETER

vorgelegt von
Master of Science – M.Sc.
Motoi MASUBUCHI
Japan

von der Fakultät VI – Planen Bauen Umwelt
der Technischen Universität Berlin
Institut für Bauingenieurwesen
zur Erlangung des akademischen Grades
Doktor der Ingenieurwissenschaften
Dr.-Ing.

genehmigte Dissertation

Promotionsausschuss:

Vorsitzender:	Prof. Dr.-Ing. Klaus Rückert
Gutachter:	Prof. Dr. sc. techn. Mike Schlaich
Gutachterin:	Prof. Dr.-Ing. Annette Bögle
Gutachter:	Prof. Dr.-Ing. Christoph Gengnagel

Tag der wissenschaftlichen Aussprache: 25.09.2012

Berlin 2013

D 83

ACKNOWLEDGMENTS

The research work was carried out at the Chair of Conceptual and Structural Design (Fachgebiet Entwerfen- und Konstruieren Massivbau) at TU Berlin.

I would like to express my sincere thanks to my supervisor Prof. Mike Schlaich for his scientific guidance, and for sharing his insights into the problem, and practical hints and tips necessary for me to carry out this work. I feel honored and fortunate to have completed my doctoral study under his supervision. I would like to extend my sincere application to Prof. Annette Bögle for her continuous support as well as for her personal and professional advice on various aspects of my work. She has always encouraged, inspired and motivated me throughout this research. My sincere thanks to Prof. Christoph Gengnagel for sharing his expertise and scientific advice on the topic. Special thanks are also due to Prof. Klaus Rückert for agreeing to be the Chair of my doctoral committee.

I thank all my colleagues at the Chair of Conceptual and Structural Design for their help, continuing friendship and warm atmosphere. I am especially grateful to Christian Hartz and Achim Bleicher for their continuous help and advice. The same goes to Gwénaél Derrien for his help and many interesting discussions during his Master thesis work under my supervision.

To strengthen the practical aspect of my research, I spent six months at the office, schlaich bergemann und partner in Stuttgart, Germany. I am grateful to my colleagues, Dipl.-Ing. Knut Göppert, Dipl.-Ing. Christoph Paech, Dipl.-Ing. Knut Stockhusen and Dr. Hiroki Tamai, for the guidance they provided me on practical design aspects, and for collaborating with me on this work subsequently.

For the study of historical development of retractable membrane roofs, special thanks to Prof. Jörg Schlaich and Dipl.-Ing. Rudolf Bergemann. I would like to thank Prof. Félix Escrig, Prof. Ken'ichi Kawaguchi, Dipl.-Ing. Alfred Rein, Dipl.-Ing. Christian Kühler and Dipl.-Bibl. Christian Assenbaum, for much valuable information for this research.

I am grateful to the Union Foundation in Japan for their financial support for a part of my research, and to Norgren GmbH who supplied the air cylinders for the study model.

I also would like to thank Dr. Sriram Narasimhan, Alissa Beck, P.E. and Dr.-Ing. Kerstin Puller for their help with the English language and also for their valuable scientific comments.

Last, but certainly not least, I want to thank my parents Fumio and Nanae, and my sister Kay for their unconditional support. There are no words to match my gratitude to my father who has not only been my father, but also my tutor. I am also grateful to Ikumi who patiently supported me during this arduous work. Without their understating and love, this dissertation would never have been completed.

ABSTRACT

Functionally-adaptive structures are increasingly being demanded by infrastructure owners, who need to utilize space for multiple purposes, optimally. Convertible roofs fall under this category, for example, an event space with a retractable roof could be used for sports games in an open condition and for music concerts in the closed condition.

To date, several membrane retractable roofs combined with a spoked-wheel structure have been designed and constructed. The advantage of this combination is that the light weight and flexibility of the membrane allows it to be moved and positioned easily, while the spoked wheel structure -similar in construction to a bicycle wheel- provides a lightweight support system for the membrane. Thus large areas can be covered with a relatively small amount of material. Furthermore, since their profiles are small, large transparency in the overall appearance can be obtained.

Most of the membrane retractable roofs with spoked-wheel structure store the folded membrane in the center, when the roof is open. A bundle of folded membrane remains in the center of the roof, which is not favorable, for instance, for broadcasting; the bundle casts a shadow in the playing field. There are also aesthetic considerations in leaving this membrane at the centre. However, if the textile membrane can be folded to the perimeter of the roof, these problems would be solved. There will be no shadows on the field and moreover this creates a free opening. This is the basic motivation of the current research.

Any proposed solution has to deal with two aspects: first, there is a geometrical issue, and second, a structural question concerning the prestressing of the membrane. The geometrical issue presents an inconsistency between the required shape of the membrane and the radial cable. Amongst several approaches to overcome these problems, two practical geometrical solutions have been developed.

In the first approach, the membrane strips are shaped so that the radial cables are aligned straight in space. Generally, the structural behavior of the membrane is related to its geometry. Therefore, the main challenge in this approach is how to obtain the doubly curved structural form of the membrane that can also satisfy the condition of the foldability. The proposed solution here is to change the boundary condition of the membrane to an intermediate state between prestressed and non-prestressed. This geometrical alternation could be achieved by the vertical movement of the entire compression ring. This 'raised compression ring' method is developed and discussed as the 'case study A'. In addition to the structural analysis, the feasibility of this method was checked through the physical model that the author built in the laboratory of TU-Berlin in Germany.

For the second approach, the radial cables are curved, thus rectangular membrane strips can be used. The main challenge of this approach is how to introduce the prestressing force uniformly in the textile membrane. The solution is to lift the cable girders along with the textile membrane. One advantage of this mechanism is that a minor shift of the anchor point of the upper cable efficiently causes a major lift of the whole structure. The kinematic behavior of the cable girders was revealed through an exhaustive parameter study. Then, these analytical results were transferred to the prestressing system of a retractable membrane roof.

KURZFASSUNG

Räume, die sich an die jeweiligen Bedürfnisse anpassen können, (Mehrzweck- bzw. funktional adaptive Konstruktionen) werden von Bauherren immer mehr gefordert, da sie eine optimale Nutzung unter veränderlichen Randbedingungen ermöglichen. Eine Antwort darauf sind wandelbare Strukturen, so wie ein wandelbares Dach, das eine Nutzungsvielfalt von z.B. großen Hallen zulässt: je nach den Anforderungen können Sportveranstaltungen oder Konzerte stattfinden, es sind Openair- bzw. Inhouseveranstaltung möglich.

Bisher wurden mehrere wandelbare Membrandächer kombiniert mit einer Speichenrad-Konstruktion entworfen und gebaut. Der Vorteil dieser Kombination ist klar: zum einen hat eine Membran ein geringes Gewicht und ist daher leicht zu bewegen. Zum anderen ist die Membran sehr flexibel und kann gefaltet werden. Das Prinzip eines Speichenrads, wie es beispielsweise für Fahrräder verwendet wird, ist zugleich ein sehr effizientes Konstruktionssystem, da es hauptsächlich aus Zugelementen besteht und ebenfalls ein geringes Gewicht aufweist. So können große Spannweiten mit einer geringen Menge an Material erreicht und aufgrund der geringen Abmessungen der Tragprofile kann zugleich eine große Transparenz erzielt werden.

Die meisten beweglichen Membrandächer mit einer Speichenrad-Konstruktion falten sich bei der Öffnung des Dachs zur Mitte hin auf. Folglich hängt dann die zusammengefaltete Membran in der Dachmitte und wirft einen Schatten auf das Spielfeld. Dieses ist für Fernsehübertragungen sehr nachteilig. Außerdem beeinträchtigt das über dem Spielfeld hängende Membranbündel den freien Blick in den Himmel und somit das ästhetische Erscheinungsbild. Eine Faltung der Membran in die entgegengesetzte Richtung, also zum Dachrand hin, würde diese Probleme lösen: es käme zu keinem Schattenwurf der Membran auf das Spielfeld und eine freie Öffnung über dem Spielfeld wäre erreicht! Dies ist die grundlegende Motivation dieser Arbeit.

Eine mögliche Lösung für ein wandelbares Membrandach mit Faltung zum Dachrand muss sich mit zwei Aspekten befassen: zum einen mit der geometrischen Umsetzung, zum anderen mit der Aufbringung der Vorspannung der Membran. Die geometrische Problemstellung beruht auf der Inkonsistenz zwischen der erforderlichen Form der Membran und den gerade verlaufenden radialen Seilen des Speichenrades. Unter den verschiedenen Ansätzen, die zur Lösung aufgezeigt wurden, sind zwei praktische und mögliche Lösungen weiter entwickelt worden.

Für den ersten Ansatz werden die Membranstreifen so geformt, dass die radialen Seile gerade verlaufen können. Im Allgemeinen ist das Tragverhalten einer Membran durch ihre Geometrie bedingt. Daher ist bei diesem Ansatz die größte Herausforderung, die Membran in eine doppelt-gekrümmte Form zu überführen und gleichzeitig die Faltbarkeit zu gewährleisten. Die vorgeschlagene Lösung verändert die Randbedingung der Membran im nicht vorgespannten und im vorgespannten Zustand. Die geometrische Veränderung kann durch die vertikale Bewegung des gesamten Druckrings durchgeführt werden. Diese Methode wird 'bewegliche Druckring-Methode' genannt und in 'Fallstudie A' eingehend analysiert und diskutiert. Dabei wurde neben der strukturellen Analyse auch die Umsetzung dieser Methode anhand eines physikalischen Modells überprüft, das der Autor im Labor der TU-Berlin in Deutschland gebaut hat.

Beim zweiten Lösungsansatz dienen Seilbinder dazu, die radialen Seile zu krümmen, so dass zwischen den Radialseilen rechteckige Membranstreifen verwendet werden können. Bei diesem Ansatz stellt die gleichmäßige Aufbringung der Membranvorspannung die größte Herausforderung dar. Durch das Anheben der Seilbinder, die die textile Membran 'mitziehen', kann die Vorspannung erzielt werden. Dieser Mechanismus nutzt den Vorteil, dass eine kleine, nach außen gerichtete, Verschiebung der Ankerpunkte der oberen Seile des Seilbinders eine große Verformung der gesamten Struktur nach oben verursacht. Das kinematische Verhalten der Seilbinder wurde in einer umfassenden Parameterstudie untersucht, die analytischen Ergebnisse auf das bewegliche Membrandach übertragen und so ein neuartiges Prinzip zur Vorspannung umgesetzt.

TABLE OF CONTENTS

ACKNOWLEDGMENTS	iii
ABSTRACT	v
KURZFASSUNG	vii
TABLE OF CONTENTS	ix
LIST OF SYMBOLS.....	xiii
1. Introduction	1
1.1. Background, aims and scope of research.....	1
1.2. Outline of thesis.....	3
2. Review of State of the Art	7
2.1. Introduction	7
2.2. Bull-fight Ring in Jaén, Spain	7
2.3. Retractable roof system with twisted membrane.....	9
2.4. Retractable membrane roof system folding to the perimeter	10
2.5. Rigid movable structure which opens to the perimeter	11
Part 1 A Comprehensive Study of Foldable Membrane Roofs with Primary Cable Structures.....	13
3. Characteristics of a Retractable Roof.....	15
3.1. Introduction	15
3.2. Typology of motion.....	15
3.3. Required energy for motion.....	18
3.4. Driving mechanism	19
4. Textile Membrane and its Foldability	21
4.1. General description.....	21
4.2. Material.....	21
4.2.1. Polymer.....	21
4.2.2. Fibers and Fabrics.....	22
4.2.3. Coating	23

4.2.4.	Combination of fabrics and coatings	24
4.2.5.	Membrane for folding structures.....	25
4.3.	Mechanical properties of membrane.....	26
4.3.1.	Non-linearity	26
4.3.2.	Geometrical form	27
4.4.	Numerical calculation	28
4.4.1.	Calculation methods for static membrane structures	28
4.4.2.	Calculation method for folding membrane structure	29
5.	Historical Development of a Retractable Membrane Roof Bunching in a Single Point..	33
5.1.	Introduction.....	33
5.1.1.	Brief history of retractable roofs	33
5.1.2.	Development of the retractable membrane roof bunching in a single point.....	34
5.2.	Development of single mast system.....	36
5.2.1.	Roger Taillibert.....	36
5.2.2.	Frei Otto	38
5.2.3.	End of the single mast system.....	39
5.3.	Vision for a large scale roof.....	40
5.3.1.	Multimedia Stadium.....	40
5.3.2.	Montréal Stadium.....	41
5.4.	Development of spoked wheel system.....	43
5.4.1.	Transfer from a mast to a spoked wheel	43
5.4.2.	Bull-fight Ring in Zaragoza	43
5.4.3.	Rothenbaum Stadium.....	46
5.4.4.	Frankfurt Stadium	47
5.4.5.	Kufstein Fortress	47
5.4.6.	Warsaw Stadium	48
5.4.7.	BC Place Stadium	49
5.5.	Development of the dimension of roofs.....	50
5.6.	Load bearing behavior of a membrane surface	51
5.7.	Summary of the history	52
6.	Spoked Wheel Structural System.....	53
6.1.	Principle of a spoked wheel structure	53
6.1.1.	Brief history of the development of a spoked wheel	53

6.1.2.	Definition of a spoked wheel structure.....	54
6.1.3.	Advantage of its lightness	55
6.2.	Historical development of a spoked wheel roof.....	56
6.3.	Morphology	58
6.4.	Structural principle	59
Part 2	Development of Foldable Membrane Roofs Opening towards the Perimeter	63
7.	Foldable Membrane Roof with Spoked Wheel Structure Folding from Inside to Outside 65	
7.1.	Introduction	65
7.2.	Geometrical challenges.....	67
7.2.1.	Geometrical boundary conditions.....	67
7.2.2.	Geometrical boundary conditions in tensioned status	86
7.2.3.	Summary of geometrical challenges.....	94
7.3.	Method for the introduction of prestressing force into membrane.....	96
7.3.1.	Mechanism for the introduction of prestressing force.....	96
7.3.2.	Summary of method of introducing prestress force	99
7.4.	Overview of the case studies	101
7.4.1.	Structural Analysis	101
7.4.2.	Dimensions and Materials for case studies	101
7.4.3.	Load Case for case studies	102
8.	Case Study A – Raised Compression Ring Mechanism.....	111
8.1.	Introduction	111
8.2.	Morphology	111
8.3.	Detail considerations	112
8.3.1.	Extension cable.....	113
8.3.2.	Water tightness	114
8.3.3.	Minimizing the size of the central hub	115
8.4.	Structural Analysis	116
8.4.1.	Calculation model.....	116
8.4.2.	Results of static analysis.....	117
8.4.3.	Results of transition analysis	119
8.4.4.	Actuator Design.....	122

8.5.	Model construction	124
8.5.1.	Details consideration.....	124
8.5.2.	Material and Dimension.....	125
8.5.3.	Actuator design	127
8.5.4.	Construction process	127
8.5.5.	Result	128
8.6.	Discussion	130
9.	Case Study B – ‘Minor Shift - Major Lift’ Mechanism.....	131
9.1.	Introduction.....	131
9.2.	Parameter study of static- and kinematic cable girder	131
9.2.1.	Advantage of kinematic cable girders.....	131
9.2.2.	Calculation model and parameters.....	132
9.2.3.	Summary of the results of the parameter study.....	134
9.3.	Principle model	137
9.4.	Analysis and design of a retractable roof structure.....	139
9.4.1.	Geometrical consideration	139
9.4.2.	Analysis of kinematic cable girder.....	141
9.4.3.	Global model analysis.....	141
9.4.4.	Results of static analysis	142
9.4.5.	Results of transition analysis.....	144
9.5.	Discussion	145
10.	Conclusion and Discussion	147
	LIST OF TABLES	151
	LIST OF FIGURES	153
	Reference	163
	Appendix A – Required Energy for Motion - Reference data for the diagram in Fig. 3.3	169
	Appendix B – An Alternative Solution (Pneumatic system)	171
	Appendix C –Parameter Study of Kinematic Cable Girders	175
	Appendix D – List of Retractable Roofs.....	183

LIST OF SYMBOLS

a	Width of a membrane strip
a_m	Width of a membrane strip with the position m
A	Name of a point / Area
A_i	Combination of reduction factors
A_{res}	Safety factor
c	Circumference / Compression ring
C	Compression Force
C_e	Exposure coefficient
C_t	Thermal coefficient
C_{pe}	External pressure coefficient for wind pressure acting on the external surfaces
C_{pi}	External pressure coefficient for wind pressure acting on the internal surfaces
C_{ALT}	Altitude factor
C_{DIR}	Direction factor
C_{TEM}	Reduction factor for temporary or provisional structures
D	Compression force
E_i	Cable girder's elevation
EA	Cables stiffness
f	Function
f_d	Allowable stress
f_{tk}	Tensile strength
f_u	Sag of the upper cable
h	Height
i	Iteration number
K	Stiffness matrix
K_M	Material stiffness matrix
K_G	Geometric stiffness matrix
L	Name of edge line / Length / Electrical power to move a roof [kW]
m	Position at a membrane strip
n	Number of radial cables / Raising-factor
p	Force
PX	Reaction force in x-direction [kN]
PY	Reaction force in y-direction [kN]
Q	Weight [t]
q_{ref}	Reference wind pressure
r	Radius
R_d	Design resistance
s	Snow Load
S	Tension force
s_k	Characteristic snow load on the ground
S_k	Characteristic load effects
T	Tension ring / Tension Force
U	Deformation

v	Vertical force
V	Running velocity [m/min] / Prestressing force
V_u	Prestressing force in a upper cable
W	Travel resistance [kgf/t]
w_e	Wind pressure acting on the external surfaces
w_i	Wind pressure acting on the internal surfaces
xx	Warp direction of a membrane
yy	Weft direction of a membrane

Greek Letters

α	Inclination angle of a membrane strip
Γ	Safety factor
Δ	Input parameter
η	Mechanical efficiency
θ	Twisted angle of a membrane strip
μ_i	Snow load shape coefficient
v_{ref}	Reference wind velocity [m/s]
$v_{ref,0}$	Basic value of reference wind velocity [m/s]
ρ	Air density [kg / m^3]
γ_f	Load-factor
γ_M	Material safety coefficient

Others

ASCE	American Society of Civil Engineers
ASD	Allowable (permissible) stress design
BC	Before Christ
B.C.	Boundary Condition
ETFE	Ethylene Tetrafluoroethylene
FE	Finite Element
GFRP	Glass fiber-reinforced polymer
IASS	International Association for Shell and Spatial Structures
LC	Load case
PC	Polycarbonate
PES	Polyester
PET	Polyethylene Terephthalate
PTFE	Polytetrafluoroethylene
PVC	Polyvinyl chloride
SLS	Serviceability limit State
THV	Tetrahydrocannabivarin
ULS	Ultimate limit State
UV	Ultraviolet
WCSE	World Congress on Space Enclosure

1. Introduction

1.1. Background, aims and scope of research

No more bundles up in the air, instead a clear view of the sky when the movable membrane roof is open; this is the research vision. This dissertation aims to develop new folding methods for a movable textile membrane roof, which is folded to the perimeter of the roof, and to study the feasibility for large span structures such like stadium roofs.

Usually our buildings and structures are passive. They are built to satisfy more or less only one function. Currently multi-purpose space is being demanded more often for optimal use, and retractable, i.e., functional-adaptive roofs, are perhaps an answer to this requirement [Schl 04]. Using functional-adaptive roofs, a single space can be used for different purposes, for example an open stadium roof allows open-air sport events, while closed it can be used in inclement weather and/or for cultural events like concerts. So far quite a large number of retractable roofs have been built and they show a wide variety of form and motion.

However, since heavy structures are more difficult to be moved and since they consume more energy for movement, light weight structures and materials are more suitable for retractable roofs; they can move faster and more easily. Due to their flexibility they can be folded, which allows for compact storage of the structural materials in open condition. Moreover, they are aesthetically pleasing.

Foldable textile membrane roofs combined with a primary spoked-wheel structure are amongst the most advanced light-weight retractable roofs. A spoked wheel structure is a well-known light weight structure: it consists of radial spokes and a compression ring. As all members experience only axial forces under dead load, large areas can be covered with a relatively small amount of material.

Thus, large movable roofs can be built and operated in a sustainable way, i.e., with minimum use of building material and minimum use of energy for moving the roof; not to mention the overall good appearance.

Up to now this combination has been applied to only a few practical examples: the bullfight-ring in Zaragoza, the football stadium in Frankfurt, the tennis-ground in Rothenbaum, the open air event place in Kufstein and the stadiums in Warsaw, Bucharest and Vancouver – all of them successfully working. The roof in Warsaw is regarded as one of the largest movable roofs of its kind in the world – it is called the world's largest convertible cabriolet.

All such roofs open towards their center where the folded membrane is stored.

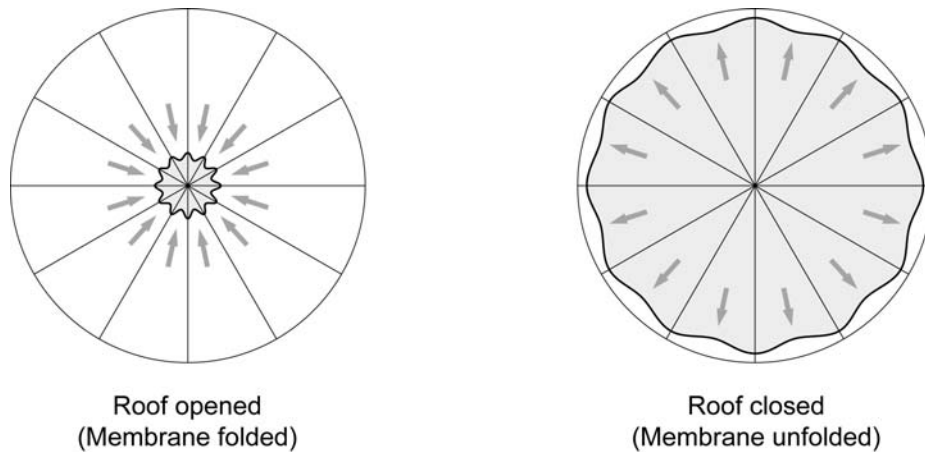


Figure 1.1 *Folding in the center (left: open configuration, right: closed configuration)*

But there is one critical issue with this system. All roofs described above open towards the centre of the roof, that is to say, the textile membrane is folded and stored in the centre when the roof is open. This means even in the open situation there is no unobstructed view into the sky possible: a bundle of folded membrane remains at the centre as a floating block. Furthermore, the bundle is difficult to maintain at the centre and can easily be damaged in windy conditions. Also, this is unfavorable for broadcasting; the bundle creates a shadow on the playing field and interferes with an ideal appearance.



Figure 1.2 *Movable roof with the membrane moving along a spoked wheel structure, Frankfurt, Germany [Göp 07a]*

However, if we can fold the textile membrane away from the centre, i.e., to the perimeter of the roof, these problems could be solved. Since the membrane is stocked along the edge, it is easy to protect and to maintain the material. There will be no shadow on the field and moreover this will result in an unobstructed view. Thus, a movable membrane cover that opens towards the perimeter of the roof is a sufficient solution to avoid these problems. This is the basic motivation of this research.

However, this design approach is not a novel one: Felix Escrig and Jose Sanchez designed a similar retractable roof for the bullfight-ring in Jaén, Spain in 1998. They employed a spoked wheel structure as a primary one and the inner textile membrane could be folded from the inside to the outside. Still, the roof in Jaén was a simple prototype and could stand just one year till it was damaged in strong winds. The complex geometrical issues, which arise in this type of the roof, have still not been resolved completely. Therefore, the aim of this dissertation is to reveal all the geometrical challenges and to develop prototypes which could satisfactorily perform in all these conditions. The results indicated two solutions and their feasibility for large scale structures, and were confirmed statically (dimensions, stress,...), kinematically (driving system, electrical supply,...), and physically (drain path, water tightness in the centre of the roof,...).

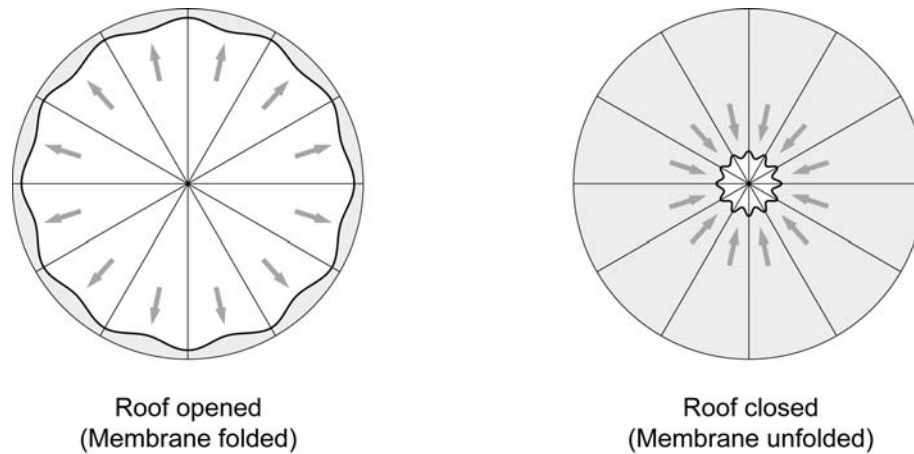


Figure 1.3 *Folding on the perimeter (left: open configuration, right: closed configuration)*

1.2. Outline of thesis

This dissertation mainly consists of two parts. The first part is a comprehensive study of foldable membrane roofs with primary cable structures that consists of a study of its character, material, history and primary structure. The second part is the development of foldable membrane roofs opening towards the perimeter on the basis of the knowledge obtained in the first part.

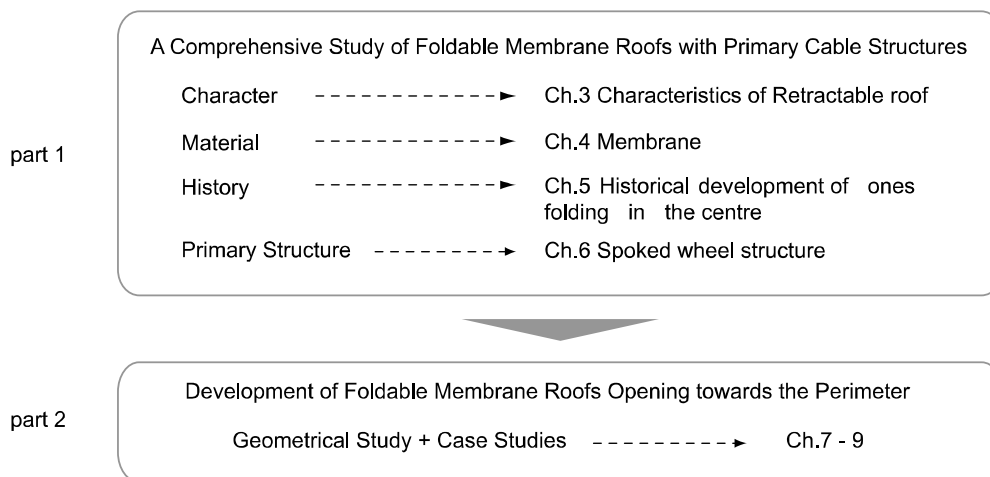


Figure 1.4 *Structure of this dissertation*

In Chapter 2 the relevant literature will be reviewed and the only realized prototype by Felix Escrig and Jose Sanchez will be described: the bullfight-ring in Jaén, Spain constructed in 1998 and demolished in 1999.

In Chapter 3 the characteristics of retractable roofs are presented. A special focus will be placed on three important aspects of designing a retractable roof: the general topology of retractable roofs, the required energy for the movement and the driving mechanisms.

Chapter 4 serves to study the characteristics of textile membrane as a structural material. Textile membranes are very light and flexible materials, and they can only be used as a building material through tensioning them. Therefore, their foldability and the methods of

introducing prestress are key aspects to be addressed and special attention will be paid to them in this study.

Chapter 5 shows realized examples of foldable roof structures with the membrane bunched in one single point in an open condition, and their historical development. Since the 1950s, Frei Otto and Roger Taillibert have designed foldable membrane roofs with masts and the textile membrane folded and hoisted at the top. This retractable roof system has been upgraded by Jörg Schlaich and his team with the bull-fight ring in Zaragoza in 1989. They employed a spoked wheel structure instead of a mast, because the spoked wheel structures are more reliable as a primary structure, without losing the efficiency and the transparency of the former system. Up to now this has been applied to comparatively few practical examples as mentioned above. The major projects will be described in detail.

Chapter 6 serves to present the characteristic of a spoked wheel structure. Its brief history, morphology, and structural principles will be described.

Based on the knowledge obtained from Chapter 2 to 6, possible folding methods towards the perimeter of the roof will be developed and described in the second part of the dissertation.

Chapter 7 describes the principal problems which arise when a continuous circular membrane cover opens towards its perimeter and the possible solutions will be developed and described.

First the geometrical problem will be addressed. However, in this phase, the configuration of the textile membrane will be defined just geometrically, namely the pre-tensioning force in the membrane will not be considered, in order to keep this complex geometrical issue as simple as possible. In the closed situation, the whole area should be covered with one continuous membrane, because joints in the surfaces of textile membrane are a weak point from a maintenance stand-point, as well as from water and wind penetration resistance. However, a flat continuous membrane is clearly cannot be folded towards the outer edge of the roof, because the length of the membrane in the direction of circumference changes along the radius. The possible folding methods will be developed by studying a radial membrane strip as a part of the continuous membrane between each radial cable. To be folded to the perimeter, this membrane strip must have a constant width along the radius. In other words, the membrane strip must have a rectangular shape, even though the required shape of the membrane and the primary form of a spoked wheel are not consistent. This geometrical inconsistency can be solved by twisting the membrane strips perpendicular against the horizontal edge of the outer ring in order to fit them to the form of a spoked wheel; however the minimum distance between two adjacent straight radial cables is not constant along the radial direction. It becomes smaller at the centre of the cables, and this causes problems for the mobility of the membrane strip. Above all, there is interdependence between the shape of the membrane strip and the one of the radial cable, and its inconsistency is the main question.

Among several approaches to overcome these geometrical questions, two geometrical solutions will be developed, at first without and then with the consideration of the corresponding form of the textile membrane in tensioned status. For the first solution, the membrane strips are shaped so that the radial cables can be straight in space. For the second solution, the radial cables are curved, thus rectangular membrane strips can be used. To develop these solutions further, the basis for structural analysis is discussed and the load cases are determined in accordance with practical design codes.

Then, two suggested solutions will be developed in chapters 8 and 9 as case studies. In the first approach, the radial cables remain straight in space, whereas the outer edge of the membrane strip is inclined, and therefore the line of the outer edge of the roof is not smooth. In order to fold this membrane toward the perimeter, the fixed support points of the outer edge

of the membrane strip must be moved vertically toward the level of the roof's surface. This geometrical alternation of the boundary condition could be conducted by the vertical movement of the entire compression ring. In Chapter 8, this 'raised compression ring' method will be developed as 'case study A'. The whole geometry of the roof as well as some details such as the extension cable, water tightness, and minimizing the size of the central hub will be considered at first. Then, structural analysis will be conducted with an integrated model in unfolded configuration. The transition process of introducing a prestressing force into the membrane will be also analyzed by using an iterative method. Furthermore the feasibility of this method and the details will be checked through a physical model that author built at TU-Berlin.

In the second approach, the radial cables are curved by adding the hanger cables that serves cable girders. To introduce the prestress force uniformly in textile membrane, these cable girders are lifted up together with the textile membrane, which is similar to one of the convertible bridges over the Duisburg Inner Harbor in Germany. One advantage of this mechanism is that a minor shift of the anchor point of the upper cable causes a major lift of the whole structure. The study of this 'minor-shift and major-lifting' approach will be presented in Chapter 9 as 'case study B'. The kinematic behavior of the cable girders will be revealed at first through an exhaustive parameter study. Then, these analytical results will be transferred to the intended notable prestressing system of a retractable membrane roof. The principle of the movable mechanism will be demonstrated by the physical study model. Finally, structural analysis of the textile membrane and the radial cables will be carried out using geometrical non-linear finite element method.

In Chapter 10 conclusions and recommendations for further study will be presented.

Finally, another possible solution using a pneumatic system will be presented, and all the results of parametric studies of the kinematic cable girder and a list of existing retractable roofs all over the world will be shown as appendices.

2. Review of State of the Art

2.1. Introduction

In this chapter the literature and projects related to the thesis will be reviewed and discussed. Already in 1972 Frei Otto conceptualized a foldable membrane roof opening to its perimeter as shown in the figure below. However, this idea was not explored further. And only one project has been realized: Felix Escrig and Jose Sanchez designed a foldable membrane roof that opens from inside to outside for the bull ring in Jaen, Spain in 1998 (see section 2.2). A unique principle by twisting the membrane was developed by Ozawa and Kawaguchi, but this idea has not been realized as a practical structure yet (see section 2.3). And in 2001 Kühner developed the principles in his diploma thesis (see section 2.4)

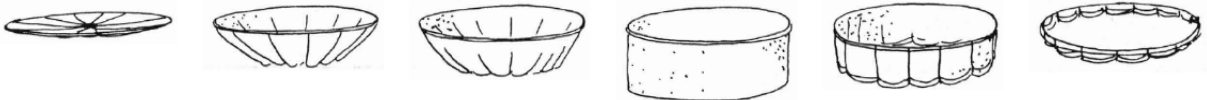


Figure 2.1 Sketch, membrane roof opening toward the perimeter [Ott 72]

Finally, some examples of rigid movable structures that open to the perimeter will be reviewed briefly (see section 2.5).

2.2. Bull-fight Ring in Jaén, Spain

The bull-fight ring in Jaén for 11000 spectators was inaugurated in 1960. In 1998 this became the first roof-covered ring in Andalusia with a textile membrane, which was designed by Felix Escrig and Jose Sanchez. But the roof structure did not last long; one year later it was damaged in strong winds.



Figure 2.2 Exterior and interior of the bullring in Jaén, Spain (courtesy of Felix Escrig)

The membrane roof of the bull-fight ring consists of two parts: one outer fixed membrane roof and an inner retractable one, which opens toward the outer edge. These components exploit the principle of the spoked-wheel: one concrete compression ring located at the outer edge,

one tension ring in the perimeter and one central flying mast are united though prestressed radial cables. The roof skin of the outer stationary roof is a high point membrane structure supported by 8 masts. The upper radial cables of the inner roof serve track lines of foldable textile membrane. The roof area was 5000m² including 3000m² for the inner retractable roof.

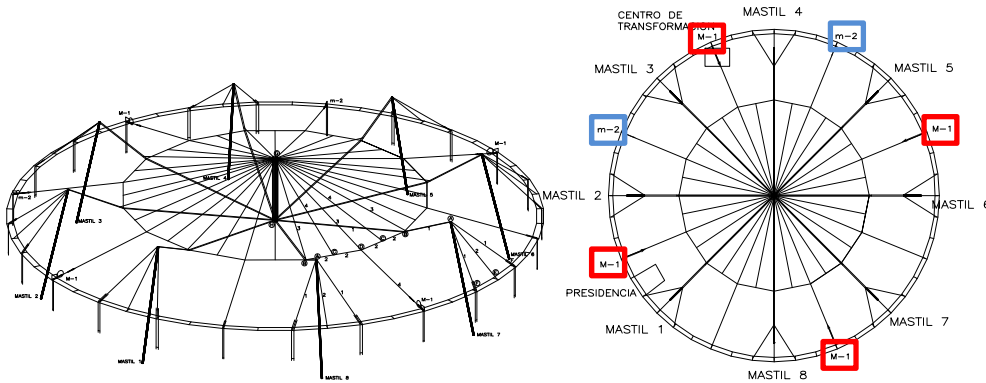


Figure 2.3 Radial cable structural system of the bullring in Jaen (left), Plan of bullring in Jaen with the information of the place of the motors (M-1(red): driving motor, m-2(blue): auxiliary motors) (right) (courtesy of Felix Escrig)

Four main motors moved 16 points through 32 pulleys using a continuous cable. The duration time to open and to close was less than 20 minutes.



Figure 2.4 Sequential view of retractable membrane roof from closed state to opened state (courtesy of Felix Escrig)

The pulleys are located radially at the top of the centre flying mast in horizontal configuration as shown two left figures below. The right figure shows pulleys which stand vertically on the

outer edge of the roof. Endless driving wires between them, therefore, are twisted in 90 degrees.

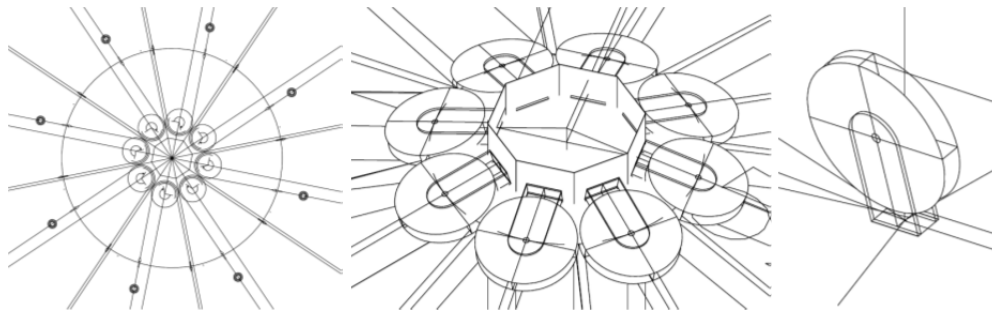


Figure 2.5 Pulleys on the top of the centre flying mast in plan (left) and in 3D (middle) and pulley in vertical on the outer edge of the roof (right) (courtesy of Felix Escrig)

Four driving motors and two auxiliary motors were installed alternately along the outer edge of the roof. In order to close the roof, the membrane is deployed first by the driving motors and then in the last phase the auxiliary motors help to close the roof tightly. “M-1” indicates driving motor and “m-2” the auxiliary motors in Figure 2.3 right. However, by such simple prestressing mechanism the membrane roof assumingly could not be closed perfectly. It allowed rain intrusion through the gap between membrane textile and the central flying mast.

2.3. Retractable roof system with twisted membrane

Ozawa and Kawaguchi developed a unique mechanism for a membrane roof [2000]. A membrane which is cylindrical in an unfolded configuration is folded by twisting to cover the area below. The major advantage is the simplicity of the required driving system: two compression rings in the top and bottom of the cylinder are rotated against each other, in different directions.

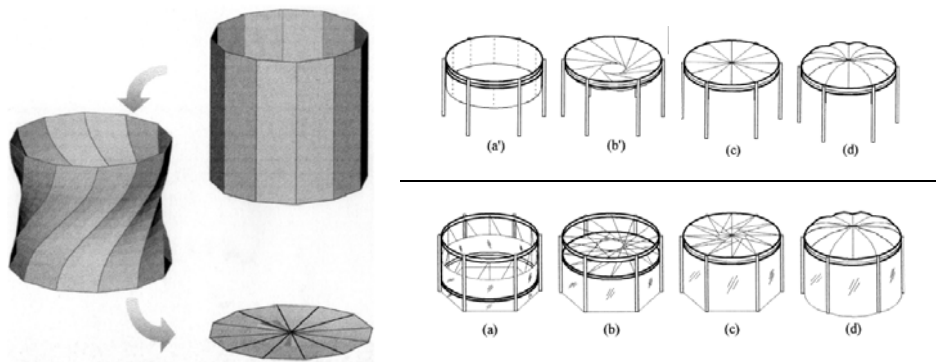


Figure 2.6 Folding pattern of cylinder membrane (left), Air-inflated type (upper right) and air-supported type (lower right) [Oza 00]

For applying this mechanism to a roof structure, the height of the cylinder in unfolded state becomes an essential issue. However by folding a cylinder membrane along the middle line of its height it could be reduced by 50%. Through this folding, the overlapped membranes generate a semi-closed space inside. The membrane can be tensioned by applying inner air pressure in this space (see Figure 2.6 upper right). Another option for prestressing the membrane is also called air-supported system: the upper or lower half of the cylinder membrane is replaced by cables so that roof's surface becomes a single layer. Then the inner

air pressure of the space enclosed will be increased, but then the entire space becomes necessary (see Figure 2.6 lower right).

The mechanism of this system is very simple and therefore has a lot of potential to be applied in a real structure. However the compatibility of the geometry is problematic. The form of the roof in folded- and unfolded states is satisfactory, but in the transition state between folded and unfolded there is incompatibility of the geometry. The textile membrane is forced to undergo large deformations. Also, since sharp folding lines occur when the membrane is folded, the membrane material is burdened under cyclic bending stress. The height of the cylindrical membrane in the unfolded configuration is also another problem, even though it can be reduced by half, as mentioned above.

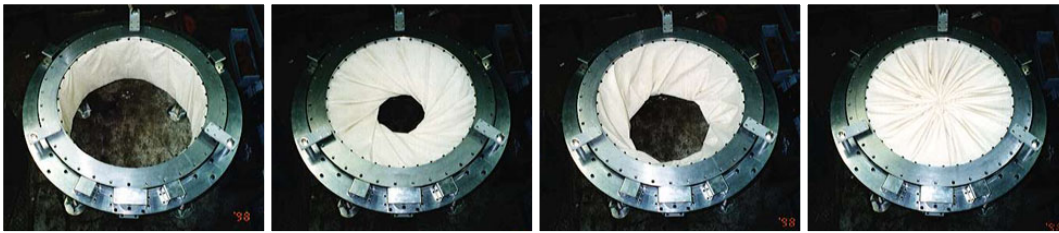


Figure 2.7 Physical test model (courtesy of K. Kawaguchi)

2.4. Retractable membrane roof system folding to the perimeter

Kühner had developed a retractable membrane roof system folding to the perimeter in his diploma thesis at Stuttgart University [2001]. A circular flat continuous membrane could not be folded towards the outer edge of the roof, because the length of the membrane in the direction of circumference changes along the radius. When the circular shape in plan is changed to the n-square form as shown in Figure 2.8 left, it becomes clear that a part of a continuous membrane defined in a triangular area of this n-square form must have a constant width H along the radial direction. This is possible if the tendons of the outer edge of the n-square stood in a vertical position at the center as shown in Figure 2.8 right. In this way, the horizontal outside edge length corresponds to the vertical center length.

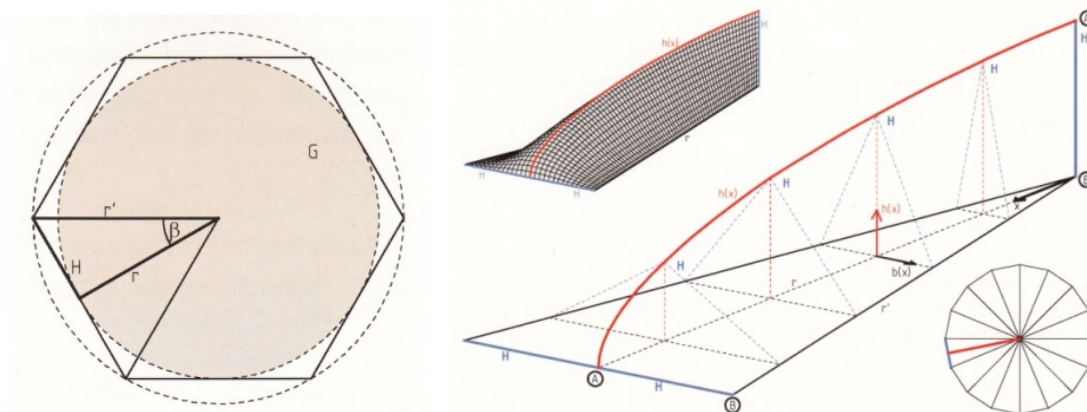


Figure 2.8 n-square form in plan (left) and the geometrical lines of the part of the membrane roof (right) [Küh 01]

In order to satisfy this ideal geometrical condition, two different main structural systems, a spatial steel truss and a cable girder, were considered and the former was adapted for further

study. As a case study, the retractable roof with its diameter ca. 75m was designed as shown in figure 2.9. After closing the roof, the textile membrane would be prestressed by pulling down the outer edges of the membrane carried out by the actuators.



Figure 2.9 A case study model of which membrane roof is folded to the perimeter [Küh 01]

2.5. Rigid movable structure which opens to the perimeter

Scissor structures have been developed by many inventors, designers and engineers since 1960s, and expanding them in radial directions is one of the main challenges. The most well-known recently developed mechanism is one by Chuck Hoberman. One of the architectural applications of his mechanism is Iris Dome constructed for Expo Hannover in 2000. This scissor dome opens from the centre to the perimeter.

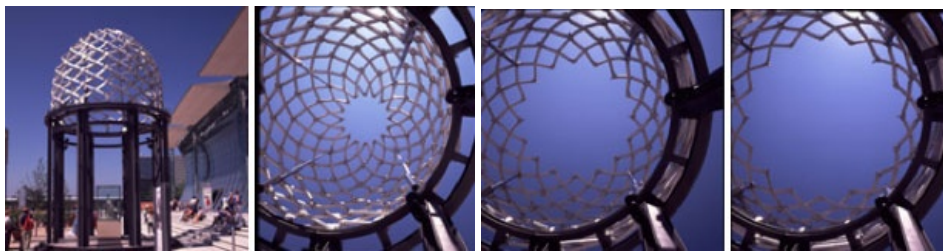


Figure 2.10 Iris dome on Expo Hannover, Germany [Hob 12]

Although a lot of studies have been conducted all over the world, still very few roofs are realized which open to the perimeter. One exception is Qi Zhong Centre Court Stadium constructed in Shanghai, China in 2005 which is a tennis hall with a capacity of 15,000. The roof is divided into eight parts, and all of them rotate horizontally. It takes 8 minutes for the roof to open.



Figure 2.11 Qi Zhong Centre Court Stadium designed by Environmental Design Institute + Naomi Sato (Architect) and SDG (Engineer) [Bau 12]

**Part 1 A Comprehensive Study of Foldable
Membrane Roofs with Primary Cable
Structures**

3. Characteristics of a Retractable Roof

3.1. Introduction

This chapter presents the characteristics of retractable roofs: their typology, the effort necessary for motion; in particular, the required electrical power and the driving mechanism. The typology expresses the diversity of retractable roofs and the study of required electrical power demonstrates the advantage of applying lightweight materials to retractable roofs.

3.2. Typology of motion

Frei Otto developed a table in his book [Ott 72], which is often referred to as the classification of the retractable roofs.






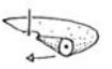


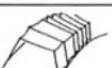







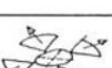





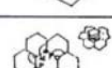

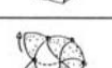
BAUART/ CONSTRUCTION SYSTEM	ART DER BEWEGUNG/ TYPE OF MOVEMENT	BEWEGUNGSRICHTUNG/DIRECTION OF MOVEMENT			
		PARALLEL/PARALLEL	ZENTRAL/CENTRAL	ZIRKULÄR/CIRCULAR	PERIPHER/PERIPHERAL
MEMBRANEN, TRAGKONSTRUKTION FESTSTEHEND/ MEMBRANES, SUPPORTING STRUCTURE STATIONARY	RAFFEN/ BUNCHING				
	ROLLEN/ ROLLING				
MEMBRANEN, TRAGKONSTRUKTION BEWEGLICH/ MEMBRANES, SUPPORTING STRUCTURE MOVABLE	SCHIEBEN/ SLIDING				
	KLAPPEN/ FOLDING				
	DREHEN/ ROTATING				
STEIFE KONSTRUKTIONEN/ RIGID CONSTRUCTIONS	SCHIEBEN/ SLIDING				
	KLAPPEN/ FOLDING				
	DREHEN/ ROTATING				

Figure 3.1 Classification of the retractable roofs [Ott 72]

Based on this, a matrix is developed which expresses the variety of retractable roofs according to simple physical and mathematical laws (Table 3.1). Rigid body dynamics is a study of motion of rigid bodies in physics. One rigid three-dimensional body with no-deformable volumes is supposed, and its motion is characterized by its six degrees of freedom (translation and rotation in three directions). A rigid body is replaced with a two-dimensional rigid plate (in four degrees of freedom) as a plane roof.

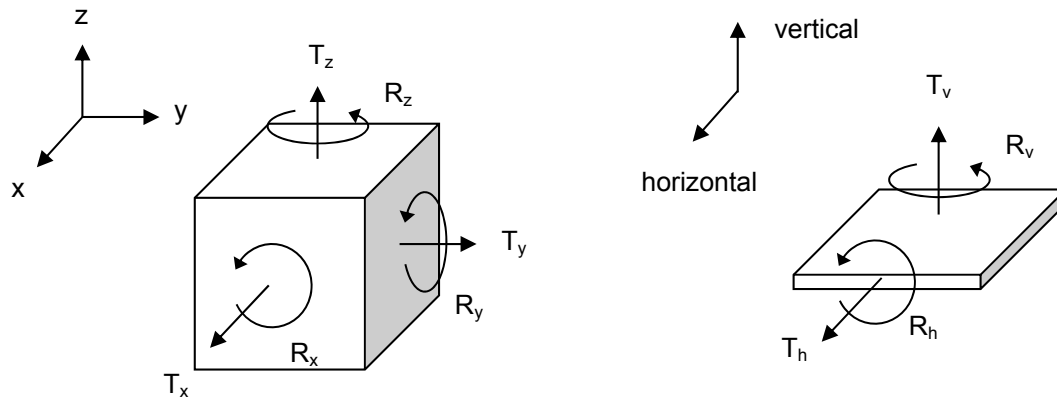


Figure 3.2 6 degree of freedom of a rigid body (left) and 4 degree of freedom of a rigid plate (right)

The movement of this rigid plate can be described by the type of motion and by the axis of motion. The types of motion are either translation or rotation. Translation means moving the plate in space while its orientation remains the same. Accordingly, rotation means changing its direction in space while its position remains the same. The axis of motion can be defined by two directions, horizontal and vertical.

Adding to these four types of motion, a retractable roof has one unique motion type: changing its dimension. When a retractable roof is opened, it must be stored near the opening. But the storage space is limited in most cases. Therefore, for the storage a size reduction or a change of the form of the opening part of a roof is important. This changing of dimension can be explained in Euclidean space such as: the path of moving a “one-dimensional” line becomes a “two-dimensional” plane. As a physical behavior, there are four fundamental types of changing the form of a roof’s surface: overlapping, folding/bunching, rolling and deforming by air.

Now, the different directions and the different possibilities of size reduction are combined, and the resulting motion matrix shows the typology of retractable roofs. Motion of one rigid cover can be defined by one axis, whereas motions of a roof consisting of several independent movable parts or a continuous membrane can be expressed using multiple axes. When the axes of motion are multiple, each axis can freely be orientated, but in most cases they are controlled with the aim of opening the space. The movement directions are mostly oriented to the stored place: peripheral and central.

The cases of multiple axes motion are described according to the storage space in lower half of Table 3.1.

Table 3.1 Typology of retractable roofs

Coordinate System		Size reduction for storage				
		none	overlap	fold / bunch	role	deform by air
Single - axis motion						
Translation	Horizontal					
	Vertical					
Rotation	Horizontal					
	Vertical					
Multiple - axis motion						
Translation	Horizontal	peripheral				
	Central					
Rotation	Horizontal	peripheral				
		Central				
	Vertical	peripheral				
		Central				

3.3. Required energy for motion

The required energy to move retractable roofs is determined by an equation based on the running velocity, loads and mechanical efficiency. The equation is expressed as [AIJ 93]:

$$L = \frac{V \cdot W \cdot Q}{6120 \cdot \eta} [kW] \quad \text{with} \quad \begin{array}{l} L : \text{Electrical power to move a roof [kW]} \\ V : \text{Running velocity of a roof [m/min]} \\ W : \text{Travel resistance [kgf/t]} \\ Q : \text{Weight of a roof [t]} \\ \eta : \text{Mechanical efficiency} \end{array} \quad (3.1)$$

Consequently, the weight of the retractable roof has a large influence on the required energy for motion. Accordingly, the diagram (Fig. 3.3) was drawn based on the data of the weight and the area of few existing retractable roofs. The reference data is included in the Appendix A. It shows the relationship between the required energy for different types of existing retractable roofs as a function of their size. Compared to retractable roofs of rigid structures, membrane retractable roofs tend to be less influenced by the scale factor. The amount of required energy for membrane retractable roofs is smaller than the ones of rigid structures. However, most of the membrane roofs require additional energy to introduce prestressing force into the textile membrane.

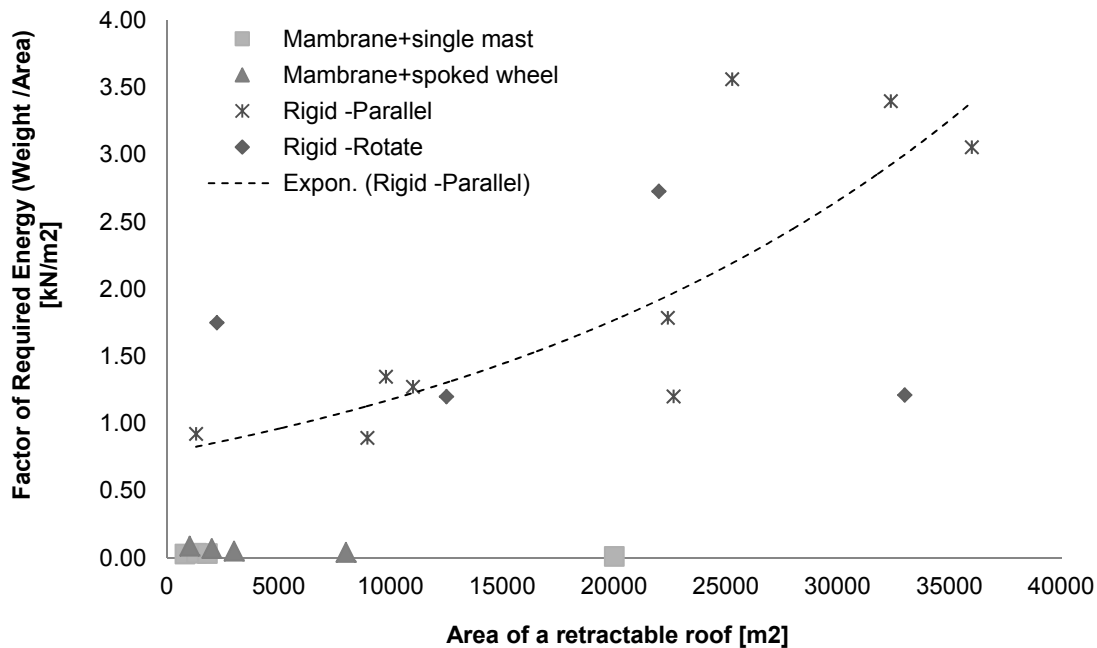


Figure 3.3 Energy required for moving of different types of retractable roofs

3.4. Driving mechanism

Three different devices are required for the point supporting foldable membrane roof structure. A folded membrane fabric is unfolded by a driving device such as a winch system, and then the edge points are locked by a fixing device, for instance a lock-pin system. Finally, the membrane fabric is stressed in tension with the aid of actuators.

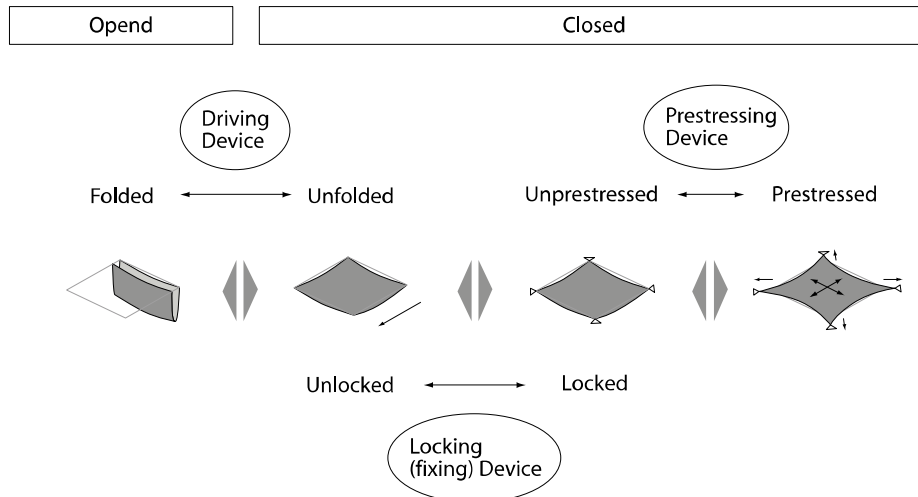


Figure 3.4 Required devices for the point supporting foldable membrane roof

Driving system which has been adopted for the point supporting foldable membrane roofs is a pulley system, in which a pulley runs on a cable during folding/unfolding the membrane. According to Otto [1972], a powered pulley is called a tractor, and its driving force for making it travel along the cable is provided by a built-in motor. Large contact pressure is required for introducing an appropriate level of friction between the tractor and cable, since the tractor moves by means of frictional force. An additional problem arises due to the supply of electrical power and the weight of tractors and motors. A non-powered pulley, called trolley (or also carriage), moves along the cable while folding/unfolding the membrane. Trolley is a passive unit, therefore it must be either pulled by the cable, or pushed by a tractor.

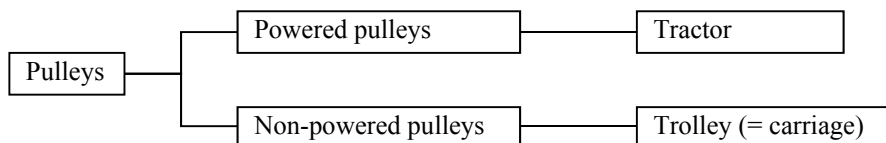


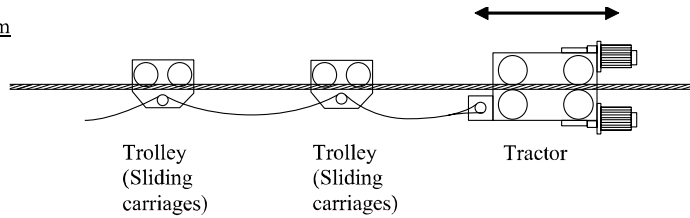
Figure 3.5 Unit of pulleys for the point supporting foldable membrane roof

Driving system of the point supporting foldable membrane roof consists of a combination of these two units. Two kinds of driving systems have mainly been adopted in the realized projects.

In a tractor system, a tractor is moved by a built-in motor. The other trolleys (sliding carriages) that run along the same cable are pushed and pulled by the tractor. As, in general, each tractor has its own power line, the method of power supply to the tractor must be always considered. In a stationary drive system, the required driving force is supplied through winches installed at the fixed part of the roof. The system is required to appropriately and

mechanically adapt to the change in driving direction between extension and retraction. [Ish 00] In a “closed” system, the driving carriage is moved by an endless cable for which only one motor is necessary. However the endless cable must always be in tension to transfer the forces from the motor. In an “open” system, two winches are used for each direction of the movement of the driving carriage. Tension force in a driving cable is not necessary in this system.

Tractor system



Stationary driving system

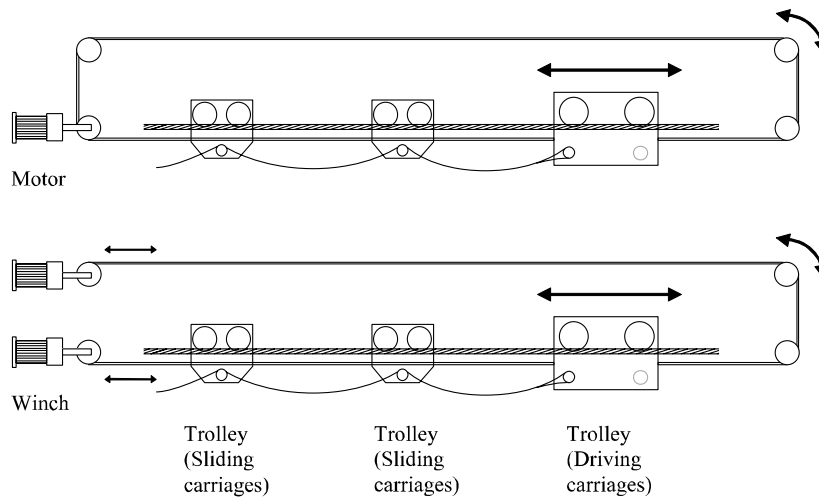


Figure 3.6 Two driving systems for the point supporting foldable membrane roof

For a retractable membrane roof with single mast system that had been often constructed in 1960s and 70s, the tractor system had often been applied, whereas for ones with spoked wheel structure that have started to be constructed in 1990s, the stationary driving system has been used. This history will be described in detail in Chapter 5.



Figure 3.7 A tractor of the Allwetterbad in Düsseldorf constructed in 1977 (left) (photo taken by author in 06/2012) and sliding carriages of the Frankfurt Stadium constructed in 2005 (right) (courtesy of schlaich bergmann und partner)

4. Textile Membrane and its Foldability

4.1. General description

Fabrics in architectural use have long been in use, since ancient times, but they were mostly only for temporary use. From the 1950s, pioneers such as Frei Otto started to develop the structural principles of fabric for permanent use as a building material. Membrane uses tension as the primary method of transferring loads in a structure. Energy and material conservation can be achieved due to its light-weight, translucent and reflective properties. The unique physical properties of fabric are its flexibility and foldability, which has been efficiently exploited to some membrane retractable roofs. This chapter deals with this characteristic aside from the general description about textile membranes.

4.2. Material

Modern textile membranes used in architecture are woven and coated fabrics, or mono-plastic films, and most of their components (fiber, coating and foil) are made from synthetic polymers. In this section the polymers often adopted for coating and fiber of the textile membrane will be explained, and their combinations for the product will be shown using a matrix.

4.2.1. Polymer

‘Poly-’ is a prefix meaning ‘many’, and a polymer is a synthetic material, which is a large molecule composed of repeated small units (monomers). Polymer is often used as a synonym for plastic and has become an indispensable material in modern life. Polymers are mainly classified into three kinds according to the way the organic molecules are bonded together.

The first one is thermoplastic, which is also known as a thermo-softening plastic. Since their molecules are not cross linked, they have relatively low strength and a low heat resistance. Thermoplastic turns to a liquid when heated, and freezes in cold temperatures. Most of the plastics that we use in our daily lives are thermoplastic.

PVC (**poly**vinyl chloride) is the most commonly used synthetic material in the building industry. It has good ageing resistance, excellent resistance to chemical attack and, comparing to other thermoplastics, good fire protection. However PVC is brittle and therefore needs plasticizers to be added (softeners).

Polyester (sometimes shortened to PES or PEs Polyester) is a general term for a group of polymers having high tensile strength and high elastic modulus. PC (Polycarbonate) and PET (polyethylene terephthalate) belong to this category. PET fibers are important for membranes and often simply called polyester by manufactures [Kni 11].

A fluoropolymer is a fluorocarbon based polymer, and the most well-known polymer of this group is Teflon®, a brand name of PTFE (**Poly**tetrafluoroethylene) developed by DuPont Co.

A fluoropolymer is characterized by high resistance to heat and low friction. It has very low mechanical strength and therefore is not generally suitable as a construction material except in PTFE fabrics and pneumatically prestressed foils (ETFE (Ethylenetetrafluoroethylene) and THV). PTFE is also often used as a membrane coating, and it provides the fabrics with strain resistance on its surface.

Next, there are elastomers. As their molecules are cross-linked, they cannot be melted once they have been produced. An elastomer is viscoelastic (colloquially referred to as “rubber” or “elastic”) and has low Young's modulus and high yield strain (very high extensibility). Elastomers are not used for membrane construction, with the exception of silicon rubber which has very high heat resistance.

Finally, there are thermosets, also known as thermo-setting plastics. Thermoset materials are usually liquid (reactive resin) and cured through heating generally above 200 °C. Once hardened a thermoset resin cannot be melted down again to a liquid. The molecules are strongly cross-linked and therefore thermosets have higher strength and better durability than the others. Epoxy resin or GFRP (glass fiber-reinforced polymer) are categorized here*.

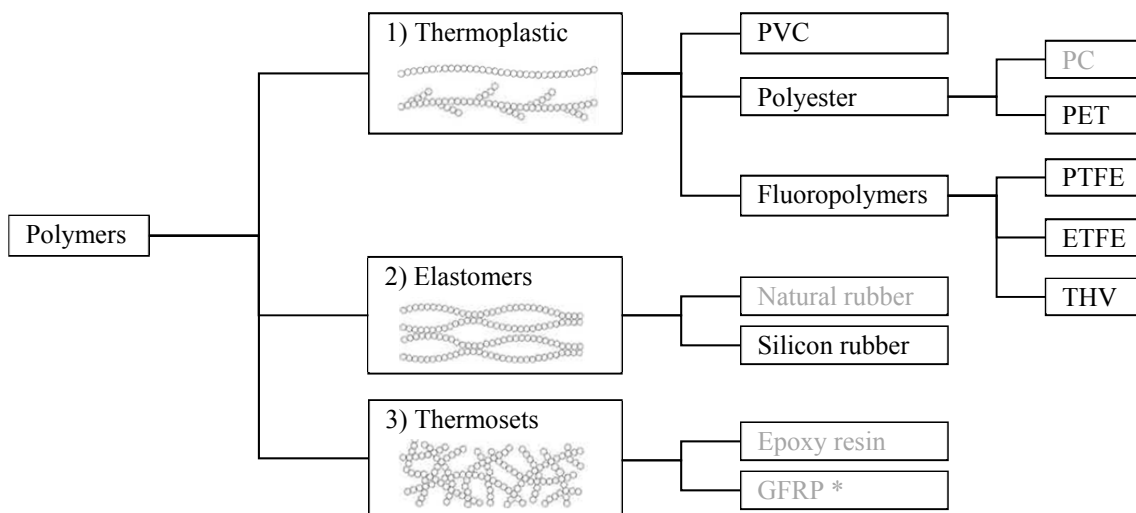


Figure 4.1 Classification of polymers according to the chemical structures (image figures of the molecules from [Kni 11]) (*A glass fiber is not polymer, but GFRP is a resin which is reinforced by glass fiber.)

4.2.2. Fibers and Fabrics

Membrane products can be divided into two groups based on their load bearing properties: isotropic and anisotropic. With the exception of plastic sheeting such as ETFE film, most products used for buildings are anisotropic and are divided into three types according to the mature of their manufacture [Kal 04]:

- Mesh fabric (knitted)
- Woven fabric
- Non-woven fabrics (fleece, felt,..)

Among those, woven fabric is a suitable material for architectural use, due to its load-dispersing capabilities. Orthogonal threads of woven fabric consist of several hundred fibers.

Until 1950s, textile membranes used for temporary tents or sun shades are made from natural fiber. But most of the modern textile membranes for architectural use are made from polymer fiber. Glass fiber is an exception and categorized as inorganic fiber as shown in diagram below. “Organic” is defined with reference ones that contain carbon bonds, and “inorganic” is when they are not organic compounds.

Fiber is a production form of the raw materials and has higher strength than their raw form. The strength of the material is improved through the production phase of melting and stretching. Although carbon fibers have a much higher elastic modulus than other fibers, the cost is still a large issue. Since glass fiber has high strength and does not burn, they are one of the most frequently used textile membranes and permanent building materials. However compared to others, glass fiber is very sensitive to folding. That is the reason why glass fiber’s fabric is generally not suitable for using as a folding membrane.

Polyester (PET fiber) is also a very important raw material for textile membrane. PET fiber is very flexible and therefore has a very good folding resistance. Therefore polyester fabric is suitable and often used for folding membrane structures. However since their stability against UV radiation is very low, they must be coated.

Aramid fiber is very light and has high strength in tension but less suitable for applications that occur in bending or compression. Its low resistance to heat and UV light are big disadvantages. The foldable membrane roof of the Olympic stadium in Montreal might have been the only case of a membrane made of aramid fiber. Its fabric ‘Kevlar’ is the registered trademark for an aramid synthetic fiber, developed by DuPont.

The strength of PTFE fiber is lower than others; however, it has high flexibility and good resistance to folding. Therefore PTFE is very suitable for folding membrane materials.

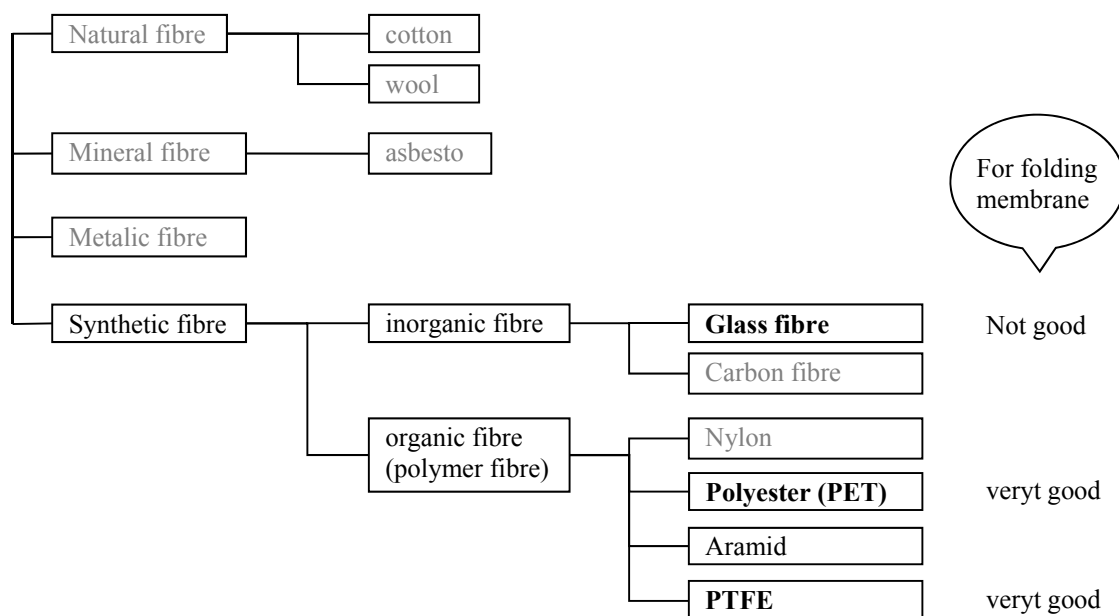


Figure 4.2 Classification of fibers showing typical ones

4.2.3. Coating

When fabric is uncoated, its service life period is extremely short, in general. Following benefits are achieved by coating both faces of a fabric [For 04][Kal 04]:

- a) Protecting the yarns against damage caused by UV, abrasion, atmosphere
- b) Rain and moisture proofing
- c) Stabilizing unstable fabric geometry
- d) Providing material to permit heat-sealed seams
- e) Influencing the resistance to soiling and the life of a fabric

PVC, PTFE and silicone are common materials for membrane coating. PVC coating is susceptible to UV radiation and therefore has a short life span. PTFE has better self-cleaning property than silicone, but more expensive. Silicon rubber has higher flexibility than PTFE.

Acrylics and PVDF (Polyvinylidene fluoride) and their mixtures are often used for coating. For the foldable membrane in the Frankfurt stadium, PVDF is coated on the upper surface of the membrane PVC coated polyester.

4.2.4. Combination of fabrics and coatings

PVC-coated polyester fabric and PTFE-coated glass fibre are often used for membrane projects nowadays. The common combination of coating and the fabric of the membrane are shown along with their brief historical transition in Figure 4.3.

Since 1960s air domes have been developed in USA, and PVC-Nylon has been used often for this purpose. Polyester as fabric material has been researched since early 1960s; however they could only be made practical since the 1970s. Since then polyester has been used more often than nylon, primarily due to its better weather-ability.

At the same time, PVC coated glass fiber fabric has been continuously used, even though its number of the applications are few. One example is the US Pavilion for EXPO 70 in Osaka. Since 1970s PTFE coated glass fabric has proved its high quality in an increasing number of permanent membrane structures. PTFE, however, can only be coated on fabrics with high melting point. Therefore polyester fabric coated with PTFE is not possible.

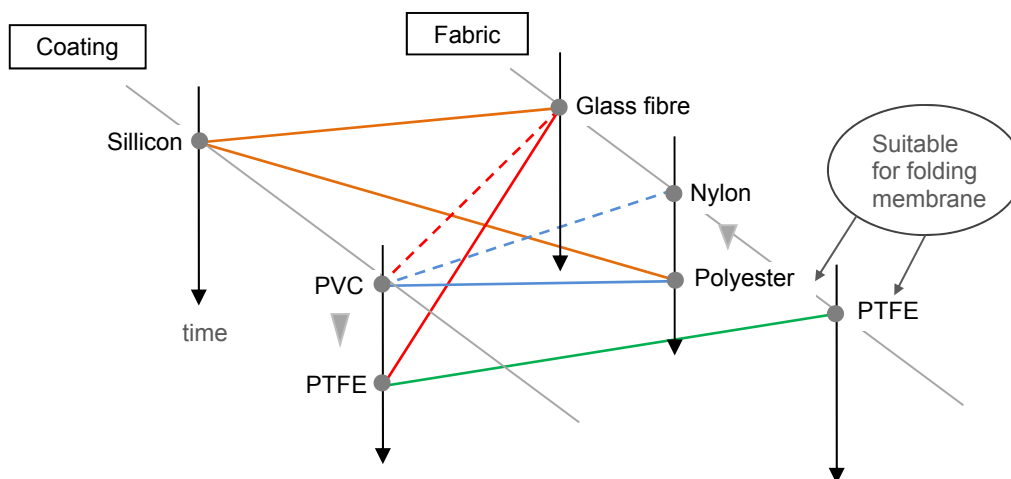


Figure 4.3 Common combinations of the coating and fabric of membrane with historical transition

4.2.5. Membrane for folding structures

Among the three typical membrane materials (PVC-coated polyester, PTFE-coated glass fibre and PTFE fabric coated with fluoropolymer), PTFE fabric is the most flexible material as shown in Figure 4.4 left. Lightness, foldability and flex cracking resistance are the deciding factors for convertible membrane design [Kni 11]. Figure 4.4 right demonstrates that uncoated PTFE fabric is more flexible than the coated one.

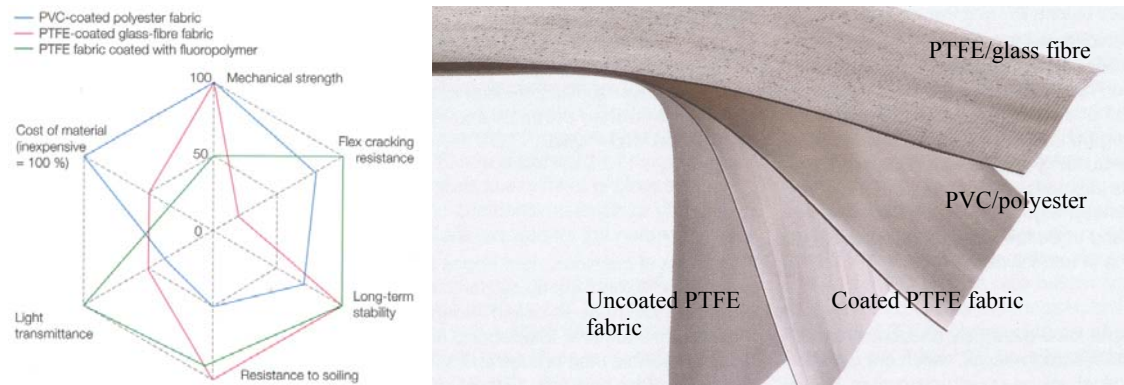


Figure 4.4 Comparison of three typical membrane materials (best value in each case taken as 100%) (left), Four different membranes with similar strength (right) [Kni 11]

Göppert et al. describe the selection of suitable material for an application where the material is subjected to folding cycles. The selection depends on the following main aspects [2011]:

- *environmental conditions (indoor / outdoor / climate)*
- *loading conditions (wind / snow / rain / hail / temperature)*
- *number of envisaged cycles within the lifespan of the material*
- *required protection level (water, wind, sun, temperature)*

In the same reference paper, they mention that materials made from Polyester (PES) or PTFE fibres are the most suitable fabrics for membranes:

PES fibres need to be protected from UV light, for which the state of the art would be either PVC or Silicone. It is important to mention that if PVC is used, it must be ensured that softeners are kept in the PVC to avoid embrittlement of the coating over time.

Fluoropolymer coated woven PTFE can be used with and without PTFE coating. The latter is the water tight version of a highly translucent membrane with excellent self-cleaning properties and good folding behaviour.

PTFE fabric has higher flex cracking resistance than PVC-coated polyester fabric. Even after 10,000 folding cycles, it displays almost no signs of wear [Koc 04]. However, it is expensive and has only half of the strength of PVC-coated polyester. PTFE fabric tends to creep significantly due to permanent loading. Therefore prestressing force and span length should be kept small.

Recently, TENARA® Fabric, trademark for a PTFE fabric developed by Sefar has been applied to foldable roofs in Fortress in Kufstein (Austria), the Wimbledon centre court, and BC Place in Vancouver.

Mechanical properties of common fabrics which are available for folding membrane roofs are displayed in Table 4.1.

Table 4.1 Mechanical properties of common “foldable” fabrics [Kni 11]

Fabric /Coating		Weight [g/m ²]	Reaction to fire *	Tensile strength (warp/weft) [N/50mm]	Tear propagation resistance(warp/weft) [N]	Service life	Cost of raw materials **
Polyester /PVC	Type I	750	B1	3000/3000	300/300	15-20 years	15-45%
	Type II	900		4200/4000	500/500		
	Type III	1100		5800/5400	850/800		
	Type IV	1300		7500/6500	1200/1200		
	Type V	1450		10000/9000	1800/1800		
Polyester /THV	Type I	1150	B1	3500/3000	700/700	No data available	60-140%
	Type II	1200		5000/4500	600/600		
Coated PTFE fabric		1080	B1	4000/4000	798/752	>25 years	100-140%
Uncoated PTFE fabric		320	B1	2000/2050	365/330	>30 years	120-170%
		530	S1-d0 (EN 13501)	4000/3700	669/550		

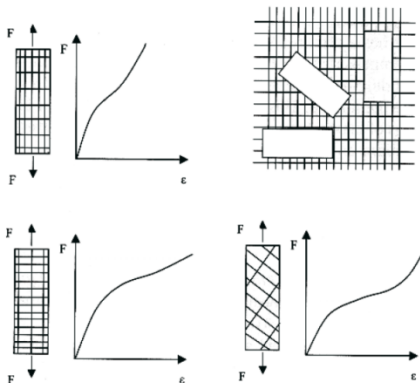
* Building materials class to DIN 4102

** Compared with the average price for PTFE/glass (100%)

4.3. Mechanical properties of membrane

4.3.1. Non-linearity

From the material tests it is clear that membrane fabric is anisotropic, and the relation between the stress and strain is non-linear. Anisotropic property arises from the weaving process. Normally, the warp threads have larger stiffness and a smaller breaking elongation than the weft threads, because they are prestressed during the manufacturing process, and therefore have less wavy form. Surface coating and seals affect tearing strength.

**Figure 4.5 Anisotropy shown in different fibre orientations [Blu 90]**

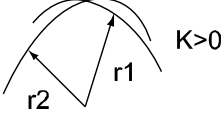
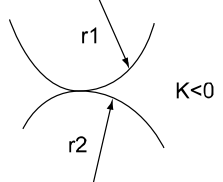
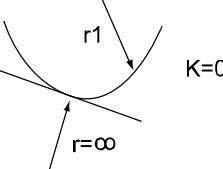

4.3.2. Geometrical form

The type of a surface is defined by the Gaussian curvature. When it is positive, the centers of radii of the two principle curvature are on the same side and its surface is called synclastic. Out of the family of membrane structures, the pneumatically prestressed forms belong to this. Whereas when it is negative, the centers of radii are located on different sides and its surface is called anticlastic. Mechanically prestressed membrane surfaces mostly form this shape. When it is zero the surface is defined by only a single curvature and the other one is defined infinity.

As discussed, textile membrane can be rolled and folded. One large advantage of deformable membrane structures is this efficient size reduction that can be achieved. Gaussian curvature however shows that a membrane surface can be rolled and unrolled only when their surfaces are defined by zero Gaussian curvature. When it is positive or negative, membrane surface is doubly curved and therefore cannot be easily rolled/unrolled.

The type of membrane structure with a Gaussian curvature of zero is therefore limited in its dimension, because the flat surface is easily ponded by rain- and snow water or flapped by wind. That is why only small dimensional rolling membrane construction, such as common sunshades, can be seen.

Table 4.2 Gaussian curvature ($K=k_1*k_2=1/r_1*1/r_2$) and the possibility of its surface deformation

			folding	Rolling
Double curvature	Synclastic	 $K > 0$	OK	not possible
	Anticlastic	 $K < 0$	OK	not possible
Single curvature		 $K = 0$	OK	 OK

Any prestressed membrane surface is characterized by the close interaction between form and structure. Sufficient stiffness could be achieved by increasing the curvature of the surface. Figure 4.6 right shows that increasing curvature of its surface leads to smaller support reactions, and the prestressing level has less influence.

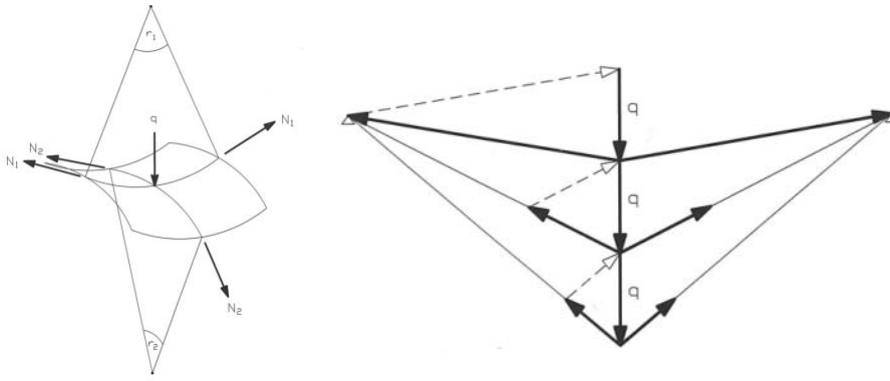


Figure 4.6 Equilibrium models: increasing resistance to loading through alternations of the angle of the system axes to each other [Sei 09]

4.4. Numerical calculation

4.4.1. Calculation methods for static membrane structures

The main structural character of a membrane is the load transfer with only normal forces, and there are no bending moments. The structural analysis for membrane structure is very different from standard analysis where the form is given and stays more or less the same even under deformations. Then the stresses are just the result of deformations under loads. In contrast, in the case of a textile membrane the stresses have to be prescribed to find the corresponding form. The final shape is unknown before this form-finding calculation.

The production plan of a membrane structure is called a cutting pattern. The membrane is disassembled into unstressed, plane pieces. For generating the cutting pattern, the size of the strip must be compensated not only for the gap between the stressed and unstressed status but also for creeping of the material [Top 07]. Consequently, the process of the planning (structural design) of membrane structure is an inversed of its construction process as shown in Figure 4.7.

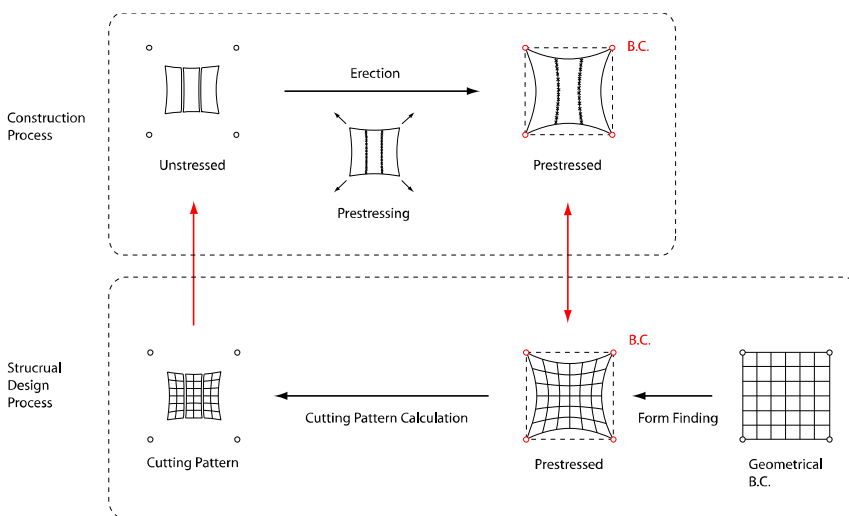


Figure 4.7 Brief difference between the construction process and the designing (numerical simulation) process

Different numerical methods are available for form finding and for non-linear analysis of membrane structures. The well referred methods are:

- Non-linear Finite Element Methods
- The Force-Density method
- Dynamic Relaxation

For the case studies in this dissertation, the finite element methods will be applied. In the case of the finite element method, structures have to be analyzed with non-linear theory because cable and membrane are geometrically non-linear structures. The stiffness matrix is expressed as:

$$K = K_M + K_G \quad (4.1)$$

Where K_M is the material stiffness matrix and K_G is the geometric stiffness matrix. For form-finding the Young's modulus is set to almost 0, because the strains should not cause stress modifications. The equilibrium is ensured only by the prestressing force. However the Young's modulus of zero is not possible, because in the case of flat membrane the in-plane stiffness cannot be achieved.

4.4.2. Calculation method for folding membrane structure

Simulation of introducing prestressing force into the textile membrane

Special attention must be paid for the numerical analysis of the foldable membrane structure. Adding to common static analysis, the process of introducing prestressing force into textile membrane should be analyzed to assess the relation between the reaction force and the positions of edge nodes of the membrane. The author will use "inverse" calculation for the case studies of this dissertation.

The process of introducing the prestressing force is similar to the construction phase of any cable structures, and an inverse calculation is often conducted for its analysis. Erection studies are undertaken in the reverse sequence of the intended process on site. Starting from the final stressed state, the tension in the stressed elements can be gradually reduced using tension control or element length adjustment in successive analysis [Koc 04]. One actual example of this kind of analysis is shown in Figure 4.8 that is the cable roof of the stadium in Stuttgart (shown also in Fig. 6.6 in Chapter 6). Actual construction scheme was followed to the results of numerical analysis. 40 cable trusses laid out on the stand were lifted up together with the inner tension ring. The graph shows the cable was tensioned with a travel of 1.4m and the prestressing force meanwhile increased from 450kN to 2300kN. It reveals that in such tensioned structures, prestressing force is dramatically increased by the final, albeit small displacement.

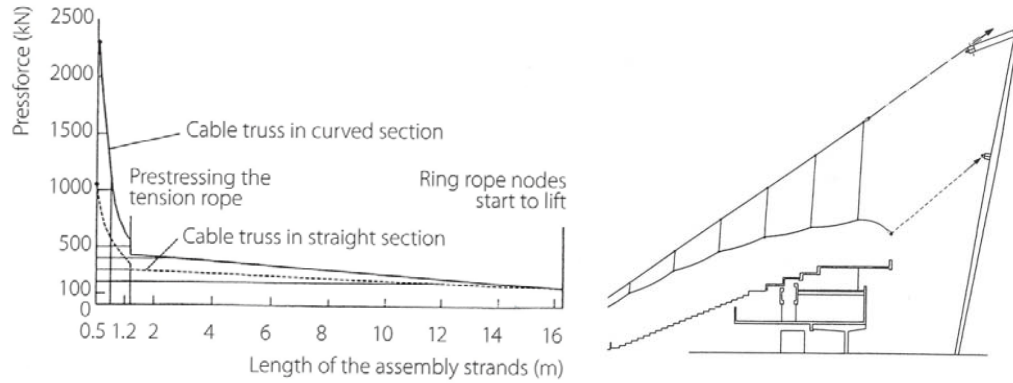
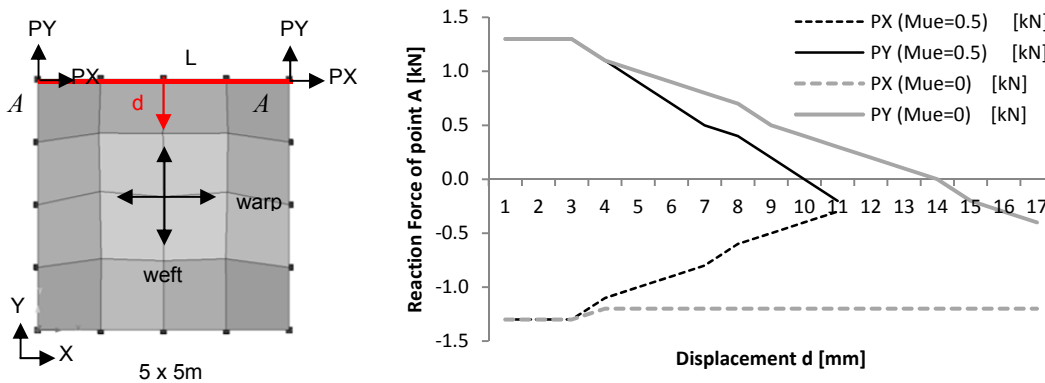


Figure 4.8 Cable force during the lifting procedure (left) and its schematic illustration (right) [Ber 00]

Using a simple model it was checked whether such an inverse calculation is valid also for a thin element under biaxial in-plane stresses. Figure 4.9 shows the test of a square planar membrane (5x5m), of which all four end nodes are fixed, and the other edge nodes are fixed but free in the y direction. In a form finding process it is prestressed 2.0kN/m for both warp and weft direction that corresponds to x- and y directions, respectively. In one calculation, the upper side L is moved 1mm in the negative y direction to release the prestressing force, and the calculation is iterated until it stops. The reaction force of x- and y direction of the moving point A is observed and plotted. Two different membranes with its Poisson's ratio 0.5 and 0 are tested to check whether proper behavior of the reaction force could be observed or not. When the Poisson's ratio is 0.5, the numbers of PX and PY decrease at the almost same rate, and when 0, number of PX remains almost constant. From this result, it would be proven that the reversed calculation might be valid also for a thin element under biaxial in-plane stresses, that is to say, membrane structure that has an orthotropic material property.



- Performed using the Finite element program SOFiSTiK
- Geometrical nonlinear effects are taken into account
- Same material property of membrane as one shown in Section 7.4 was applied

Figure 4.9 Simple model of tension releasing calculation

Figure 4.7 is modified for the folding membrane structure. Instead of the construction process, the folding/unfolding process is shown in Figure 4.10. Reversed calculation for tension releasing is conducted to assess the reaction forces of the membrane edge points. It should be noted that this reversed calculation and the cutting pattern calculation are different and do not relate with each other. The author will use the cutting pattern to check the movability of the membrane.

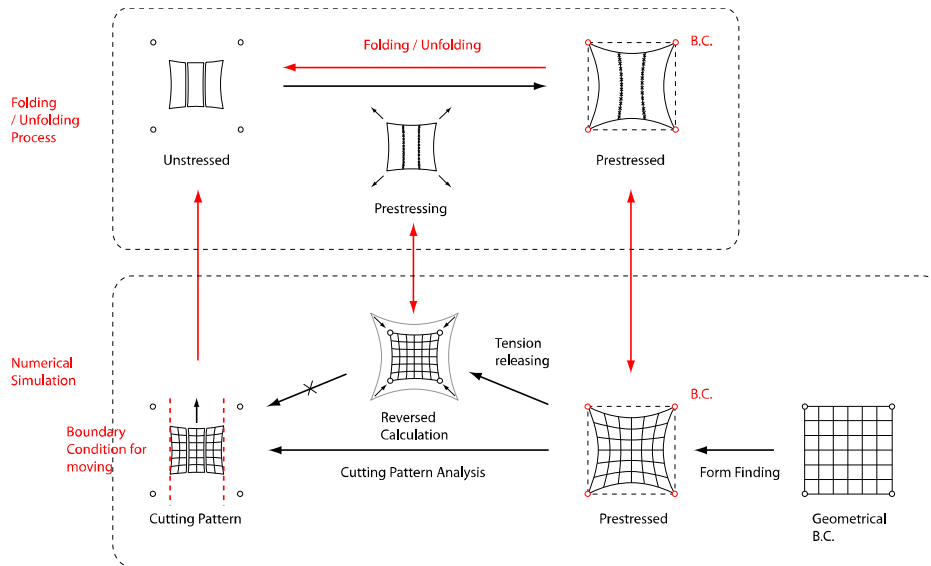


Figure 4.10 The process of the construction and the planning of folding membrane structure

Simulation of folded and intermediate folding states

The folded and intermediate folding states of a retractable membrane have traditionally been studied by physical models, although it can be difficult to recreate the scaling of both membrane self-weight and stiffness. Numerical modeling of the folding process has its origin in the simulation of clothing (both static and dynamic) developed by the computer graphic based animation industry [Koc 04].

In the design of inner retractable roof of the Commerzbank-Arena in Frankfurt, the physical model was built to obtain a deeper understating of the complex geometrical processes during folding of the membrane. Special fabrics from the apparel industry were used for the model because, as for most scaled models, the correct weight and the correct bending stiffness are necessary to obtain useful results. The folding is strongly dependent on both parameters.

Furthermore, the size of the folded package of the textile membrane had to be investigated in order to design the storage place. First, it was simulated by the software of the automobile industry (air bag folding) that was not a standard one in the construction industry. To simulate the folding process, the finite element must be defined as a contact element. But the solution was not good enough to obtain useful results. One of the reasons might be that the parameters ranged quite widely. However, it proved the result of the scaled models. Finally it was tested by a mock-up of one eighth of the roof. This final check has proved that the chosen volume of the video cube could be sufficient [Göp 07a+b].

LS-DYNA user input
Time = 10.836



Figure 4.11 The investigation of the inner retractable roof of Commerzbank-Arena Frankfurt, computing simulation (left) [Göp 07b] and mock up model (right) [Göp 07a]

5. Historical Development of a Retractable Membrane Roof Bunching in a Single Point

5.1. Introduction

The historical development of a retractable membrane roof bunching in a single point will be described in this chapter. The study will be focused on the persons who have contributed to this development.

5.1.1. Brief history of retractable roofs

The first well known large-scale movable roof in history is the Coliseum in the Ancient Roman era. The roof for the protection from sunlight could be moved manually. The detailed roof system is unknown, but their existence has been confirmed by documents from that period or remains of their columns in the ruins, and so on. Its dimension is assumed to be between 5700 and 23000 m² [Ott 72]; anyway this is quite large and such enormous retractable roofs have not been constructed again until the modern times.

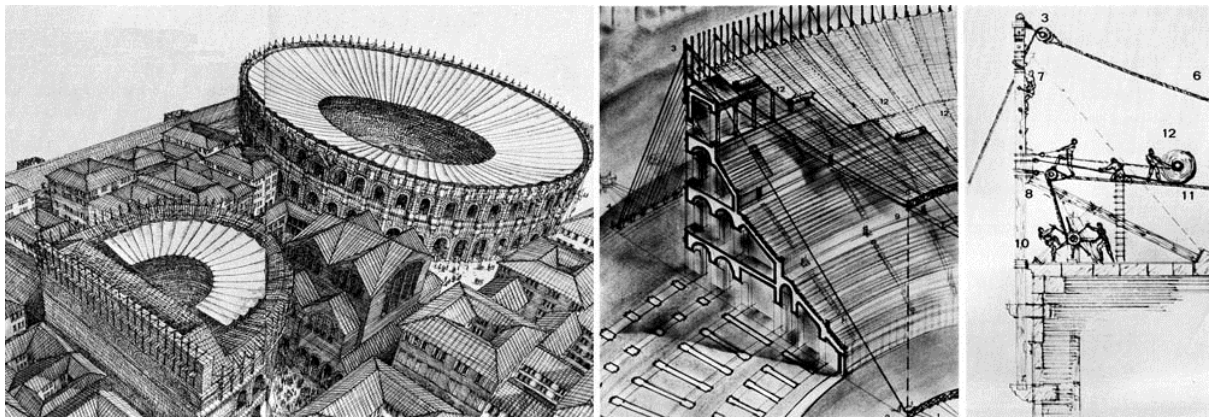


Figure 5.1 The appearance of the convertible roof of the Colosseum [Gra 79]

Since 1930s small movable roofs have been constructed. According to the study by Otto and his team, the roof for a swimming pool in Rotterdam, Netherlands, constructed in 1935, is probably the first modern convertible roof [1972]. In the early times, the designer used crane technology, because cranes have been used long in history and their standards and specifications were well established. The crane technology opened the possibility for large scale retractable roofs. Pittsburgh Civic Arena in the United States in 1961 is considered as the first large scale movable roof (127m span length) that could be operated for opening and closing based on modern technology. Since then a lot of big stadiums have started to be covered with movable roofs. The main reason is an economical one; there is significant financial risk, if a scheduled event in a stadium was cancelled due to unfavorable weather. Covering by a stationary roof can be a solution. However the audience prefer open-air due to the exposure to natural sky, light, and air flow. Thus movable roofs are the preferred solution.

Except for the swimming hall, each country has different use and hence, a different demands for their sports facilities. For instance, in Japan, large retractable roofs have been often been used for baseball stadiums. In USA, retractable roofs are chosen for American Football stadiums. In Spain, a large number of retractable roofs have been constructed for bullfight rings. In many countries, retractable roofs would eventually find their use in football stadiums. Football is nowadays one of the most popular sports internationally, and hence, several football stadiums with retractable roofs have been constructed in many countries.

5.1.2. Development of the retractable membrane roof bunching in a single point

Retractable roofs can be divided into two basic types: soft and flexible roofs, for which geometry can be changed by folding, bunching or rolling up, and rigid roofs that consist of several movable segments of fixed shapes. In modern times, advances in engineering and the development of high-strength fabrics have opened up new dimensions for movable roofs [Gen 01]. The retractable roof described in this chapter is the one with the membrane folded and gathered in one localized area (loosely, phrased as a point). In this type of folding, the membrane is suspended point-wise from the supporting structure.

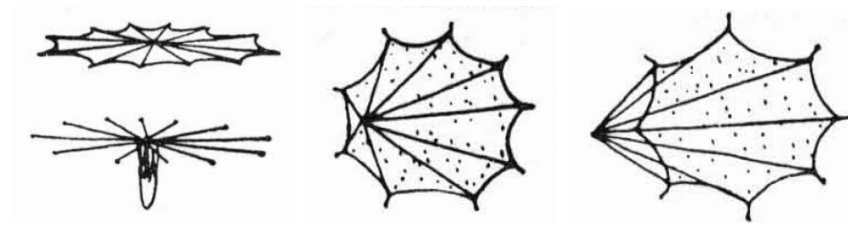


Figure 5.2 Three types of centrally folding system [Ott 72]

In 1950s Frei Otto and his team in Germany, who are often regarded as pioneers of modern architectural membrane structures, started studying retractable membrane roofs. One of their achievements is the development of the principle of bunching membrane covers. With French architect Roger Taillibert, they designed and constructed several membrane roofs with single masts in Germany and France. The retractable roof for the Olympic Stadium in Montreal in 1988 marked a turning point of this system due to all the problems related to its specific design and size.

Here, German engineer Jörg Schlaich and his team were involved in the realization. For them this experience was the beginning of further development in retractable roofs using the principle of bunching in a single point. They combined this principle with the spoked wheel structure instead of a single mast, and thus a very efficient large scaled roof was realized. Their retractable roof for a Bull-fight ring in Zaragoza, Spain, constructed in 1990, became a prototype for this type of structure. Its development is still ongoing mainly by the team of Schlaich and one of their partners, Knut Göppert, who designed and constructed numerous light-weight stadium roofs throughout the world. The history is summarized in the Figure below.

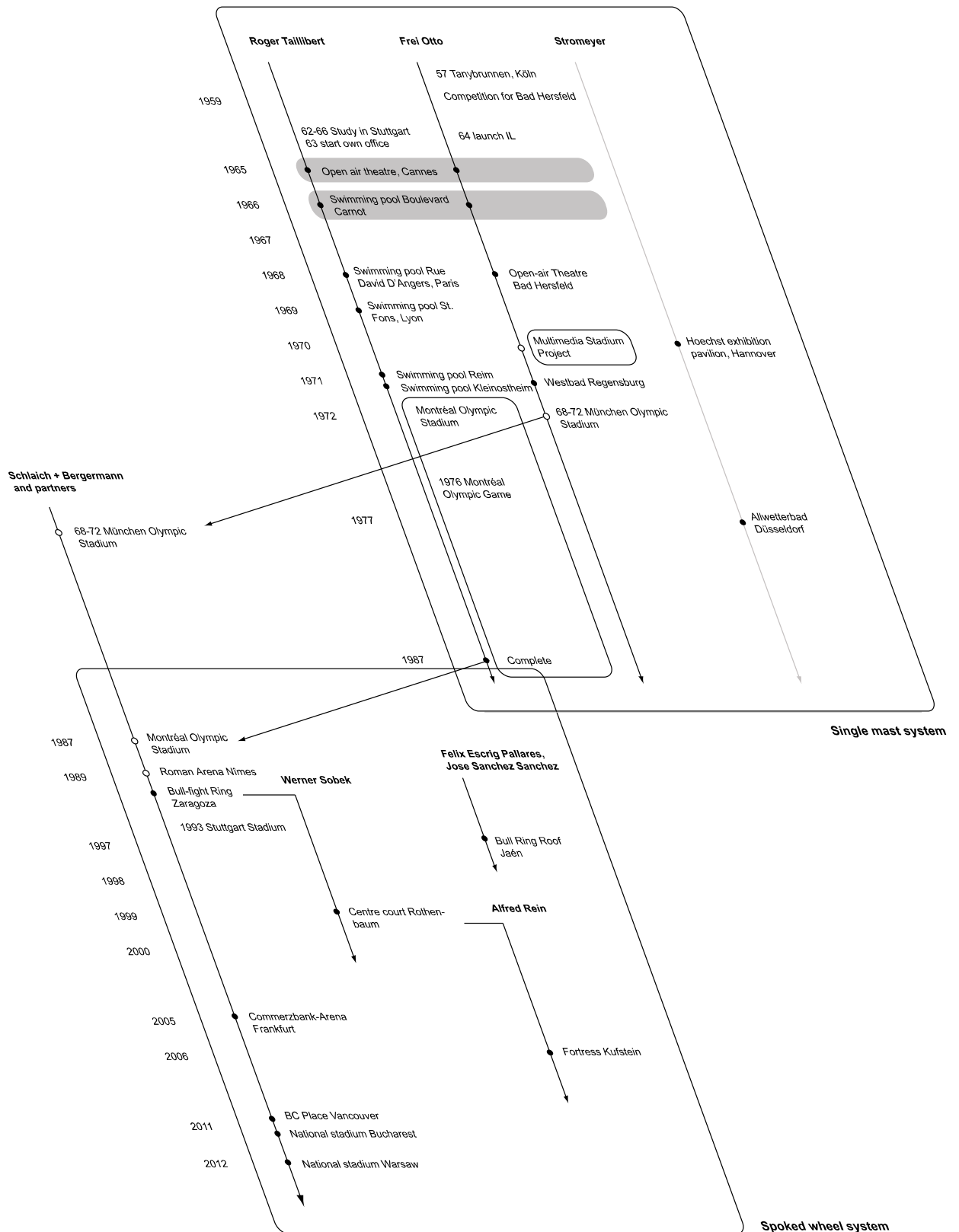


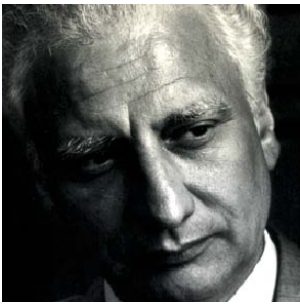
Figure 5.3 History of retractable roofs bunching in a single point single mast system

5.2. Development of single mast system

There are two key persons for the birth of the folding membrane roofing system. One is French architect, Roger Taillibert (1926-) and the other is German architect/researcher Frei Otto (1925-), who worked together at the beginning, but separated later. They left a large footprint for the development of this type of the retractable roof.

5.2.1. Roger Taillibert

Taillibert is an architect who was born in Châtres-sur-Cher and studied architecture at the Ecole des Beaux Arts in France and also in KTH in Stockholm, where he became aware of “another vision of the architecture, more constructivist” [Tai 12]. He explored concrete due to its wide and varied potential. In 1970s he worked with Heinz Isler (1926-2009, Switzerland), well known shell builder, on the design of several concrete thin shell structures. His unique architectural line could be realized by the technological development of prestressed concrete and prefabrication. His strongest invention, however, would not be for engineering efficiency but rather for architectural curved lines. Taillibert would like to move away from the cubic motif that is fundamental to Functionalist Architecture. He follows a main stream of architectural design in the second half of the 20th century, in which several architects looked for new organic style architecture.



“I am essentially working with curves because I do not believe in the straight line that I consider to be meant for the storage. The curve is the dynamism. It also looks a little like a sculpture, as energy is going through it.....”

Figure 5.4 Portrait of Taillibert and his own description about the design attitude for the curves (Both from [Tai 12])

The contact between Taillibert and Otto started in the early 1960s. After receiving his degree, Taillibert visited Stuttgart and stayed four years (1962-1966) in the Institute for Lightweight Structures (IL) which was chaired by Otto, in order to study textile membranes for practical use in architecture.

In 1963, he founded his own office. After the success of the design of his first swimming pool in Deauville (1966), which is covered by thin concrete shell vaults, he obtained an opportunity to design sports facilities in France by the French National Department of Sports. At the beginning of 1960's, the French government encouraged research for designing buildings for swimming pools with shorter construction periods as well as less expensive solutions than those used at that time. Thus Taillibert proposed an experimental and challenging solution; the roof structure consists of cables and membrane which are supported by one high mast. With the use of extremely light weight materials they could cover large spans very efficiently. Furthermore the roof could be opened and closed in a few minutes with very low energy.

The first realized retractable roof was for the Open Air Theatre in Cannes, France (1965). Taillibert asked Otto to support the design process as the planning and construction time was limited to two months and Otto had already developed the concept of this new type of the roof

in his head and was more or less just waiting for its realization. The 25.5m high slender mast was guyed by several cables and it supported 8 stay-cables connected to one continuous membrane with an area of approximate 1000m^2 . When it is retracted, the membrane roof hanged compactly at the top of the mast. 16 small trolleys (8 end trolleys, the rest is middle trolleys) suspend the membrane and they are moved by winches. Three independent winches were installed for the end trolleys and the middle trolleys, and the last one was directly connected to the tow cable (Figure 5.5 right). In this early phase, the membrane is not prestressed, therefore it can easily be flapped by the wind. Thus, the roof has to be retracted when the wind velocity is larger than 10 m/sec.

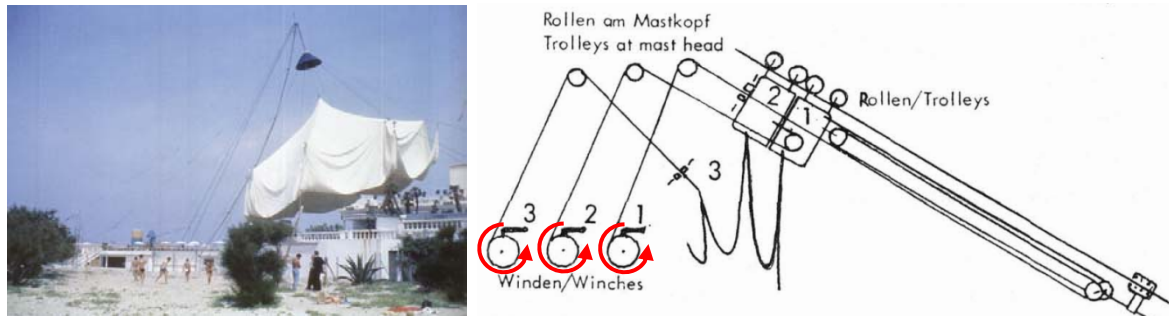


Figure 5.5 Appearance of the retractable roof in Cannes, France (left) [Ner 05] and its driving system (right) [Ott 72]

The first retractable roof for a swimming-pool was constructed in Boulevard Carnot in Paris in 1967, with the aid of Otto and his team. They designed and constructed the retractable roof, which is able to adapt the swimming baths to all weathers and seasons. A total area of 1800m^2 was covered by a single textile membrane that is suspended from the 16m high mast.

The large development in technology from both the Canne project and the Carnot project led to the development of the driving system for the membrane roof. The mechanical system is a combination of a stationary winch and cable tractor system. To deploy the roof, 14 cable tractors pull the edge points of the roof to the edge anchor points. The tractor has three wheels, and only one wheel is driven. The friction between the wheels and membrane is enough for hanging the membrane but not for introducing the prestressing force. Pretensioning of the textile membrane is accomplished by slowly tightening the two winches installed in the mast foot (Figure 5.6 right). The process of extension and retraction process is automatic; the motors for the cable tractors and the winches are controlled by computer controllers.

In winter, condensation on the roof skin is prevented by two warm air curtains and the temperature in the interior space is kept at 25 degrees. This warm temperature could help prevent the accumulation of snow on the roof skin.

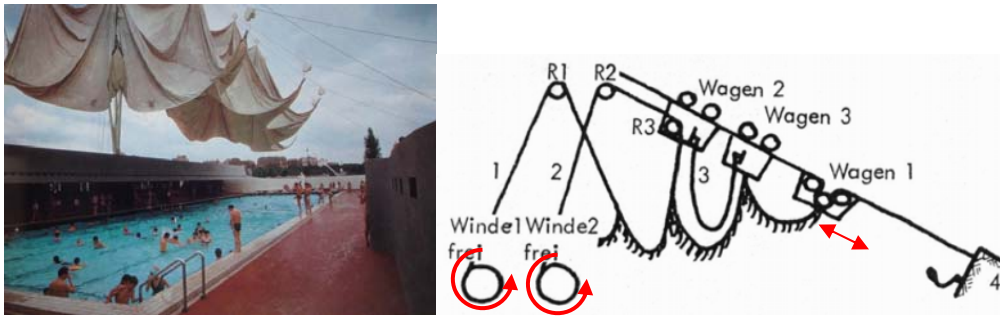


Figure 5.6 *Appearance of the retractable roof in Boulevard Carnot in Paris, France (left) [Fab 70] and its driving system (right) [Ott 72]*

Taillibert registered a patent for this experimental roof system in 1967. The success of the roof in Boulevard Carnot gave him another opportunity to design and construct successful projects in David D'Angers (Paris, 1969), Saint-Fons (Lyon, 1970) and Reims (1971). But their construction principles were mostly same, and no significant development could be found.

5.2.2. Frei Otto

Frei Otto was born in Siegmars, a suburb of Chemnitz in Germany and studied architecture in Berlin. Participating in the World War II as a fighter pilot triggered him to pursue the subject of light weight structures, which require minimizing use of energy and material. Following the call of Fritz Leonhardt, Otto founded the institute of Lightweight Structures (Institute für leichte Flächentragwerk) at the University of Stuttgart in 1964. His systemic research accelerated the development of textile membrane structures and their practical use for architecture and engineering.



- 1957 - Dance Pavilion at the Federal Garden Exhibition, Cologne
- 1967 - West Germany Pavilion at Expo 67 Montreal
- 1970 - Tuwaiq Palace, Saudi Arabia
- 1972 - Roof for Olympic Stadium, Munich
- 1975 - Multipurpose Hall of the Federal Garden Exhibition, Mannheim
- 2000 - Japanese Pavilion at Expo, Hanover

Figure 5.7 *Portrait of Frei Otto [Ott 96] and his major works*

Also in the field of retractable roofs, the achievement of Frei Otto and his colleagues has been highly acclaimed as pioneering work and has contributed greatly to its development [Ish 00]. Otto designed his first large span convertible roof for the open-air theatre in Killesberg, Stuttgart, however it was not executed. The next chance was the idea competition in Bad Hersfeld, Germany that was performed in 1959. The new roof was desired in order to undertake open-air performances at the summer festival in any weather condition. The following three conditions were required for the roof construction: no alternation of the surrounding historical buildings, no detraction of the spatial impression of the Roman stage scene, and availability of the roof only in the case of necessity.

The proposed idea by Otto and his team was a retractable membrane roof with a single mast system, which became prototypes of the roof later in Cannes and Boulevard Carnot described

above. Even though there was a competition held and a winner chosen, this did not lead to the actual construction. After eight years, Otto finally received an offer from the city administration of Bad Hersfeld, and the construction was executed in 1968.

Whereas Taillibert applied the same structural principle repeatedly to a series of swimming facilities in France, Otto tried to develop the system incrementally. The significant development can be featured in its driving system.

A drive mechanism of stationary winches that were applied in Cannes and Boulevard Carnot were not used for this project, because the numerous trolley cables demanded a great amount of cable materials. In this project, specially developed cable tractors were used, and thereby the cost could be considerably reduced. The cable tractor built by the local company Haushahn in Stuttgart consists of two caterpillar undercarriages. It is held with each other and to press against the trolley cable by a pretensioning force, which offers a minimum of cable strains. The motor (380V) is attached to the side of the tractor. All motions of the cable tractors are programmed so that all tractors reach at the pre-set position simultaneously during the extension or retraction. The roof skin whose area is 1315m^2 is prestressed by these edge tractors. Pretensioning on the edge of the roof skin is 100kp/m^2 (ca. 1.0 kN/m^2), and the driving strength of the edge tractor is 1300kp (ca. 13kN).

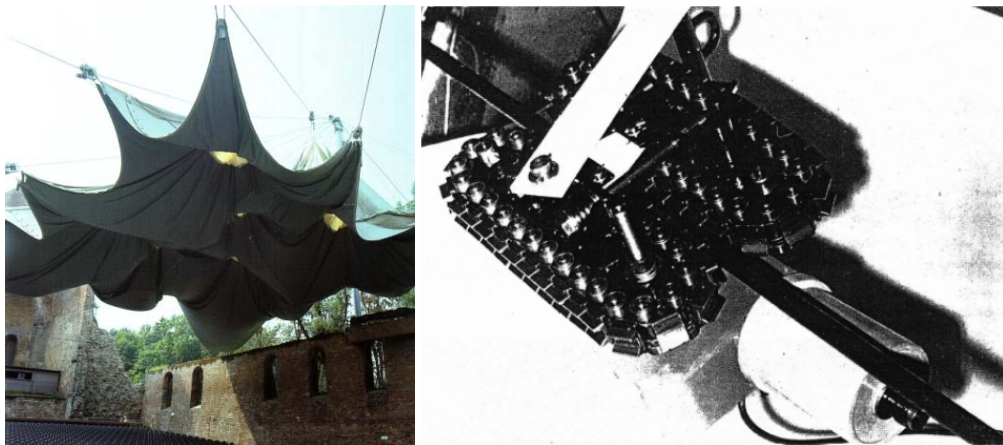


Figure 5.8 Appearance of the retractable roof in Bad Hersfeld, Germany (left) [Ner 05] and its driving system (right) [Ott 72]

5.2.3. End of the single mast system

Otto and his team had designed and constructed a similar type of the roof for the swimming pool in Regensburg, Germany in 1972. The cable tractor would be more simplified and refined than the one in Bad Hersfeld. However, since the completion of the roof in Regensburg, neither Taillibert nor Otto designed this type of retractable roof subsequently. Probably there is only one similar type of the retractable roof for a swimming pool constructed afterwards in Düsseldorf designed by German tentmakers Stromeier with IPL Ingenieurplanung Leichtbau in 1977. Stromeier had pioneered exciting innovations in the history of tensile structures in a long-term partnership with Frei Otto. The roof still exists, but has not been retracted for several decades. It is likely to be replaced sooner or later.



Figure 5.9 Allwetterbad Düsseldorf, photos taken by author in 06/2012

In the Book of complete works of Otto [Ner 05], Möller wrote in the description about the retractable roof in Regensburg:

The great enthusiasm with which this innovative technology was initially welcomed did not last very long. The trolley mechanism was prone to malfunctioning, and the low insulating effect of the membrane caused high heating costs. During renovations and alterations in the mid-1980s, the roof was replaced with a conventional structure.

Also in another literature [Koc 04], Habermann wrote the following in the chapter of the history of membrane buildings:

The gap between the ambitions and the technology available was still too great. Practical solutions were achieved only in those cases where a retractable roof was required without the necessity of sealing off the covered space climatically.

It is not unreasonable to assume that the retractable membrane roof with a single mast has not solicited the interests of clients any more after the 1970s. In the case of swimming hall, one of the greatest issues would be in terms of energy consumption. On a visit to the Allwetterbad in Düsseldorf in June 2012, it was observed that there was inadequate tension in the membrane between the retractable roof and surrounding edge walls, which allowed wind flow to and from the gap. In the case of Regensburg, the pneumatic cushion was installed there to fill this gap after several years since the construction. The insulation problem might have been very critical for this type of retractable roof.

5.3. Vision for a large scale roof

5.3.1. Multimedia Stadium

One of the major works of Frei Otto is the roof of the main stadium for the München Olympics in 1972, for which he joined as a consultant. However, Otto actually did not even enter the competition for this project held in 1967. Instead, Otto drew some sketches for a convertible roof structure for large areas and published them in the same year.

In 1970, the feasibility study based on that sketch and named ‘Multimedia Stadium’ project was carried out with financing from Hoechst AG. The height of the main mast was 180m and the diameter was 5-6m, which was supposed to allow visitors access its interiors. A retractable large membrane hung from the mast, covering an area 60,000m², which was not only the playing field but also the surrounding grandstands, including restaurants, cafes,

exhibition area and shopping centre, and so on. This unique project was suspended due to the oil shock in the early 1970s.

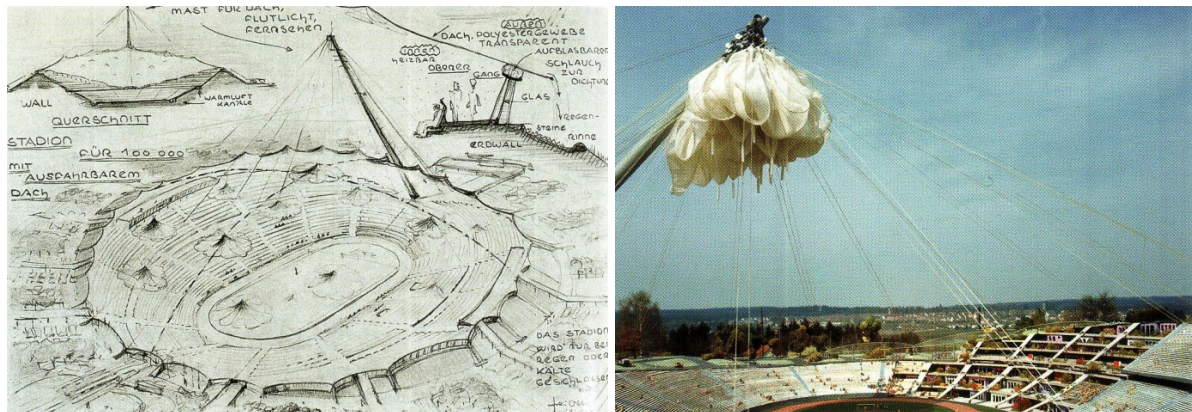


Figure 5.10 Multimedia stadium the sketch and the physical model [Ner 05]

5.3.2. Montréal Stadium

Even though it is not clear whether the ‘Multimedia Stadium’ project influenced or not, Taillibert realized a large scale roof of this construction principle as a main stadium in Montréal, Canada for the Olympic Games held in 1976. The scale of the building is much larger than his series of swimming pools constructed in France and Germany. The capacity of the stadium was 65,000, and the area of the elliptical inner retractable roof covering the tracking field is 20,000m². The inclined tower that suspended the roof was 168m height, and an observation deck is located on its top. The outer stationary part of the roof is prestressed concrete which cantilevers 60 to 80m over the stand.



Figure 5.11 Retractable Roof of the Olympic Stadium in Montréal [Hol 97]

This Olympic stadium invoked great controversy among engineers, for instance, in the panel discussion organized by WCSE (World Congress on Space Enclosure) and IASS (International Association for Shell and Spatial Structures conference) held right before the opening of the Olympic Games, and in the magazine of the ASCE (American Society of Civil Engineers). Mamoru Kawaguchi, who was in attendance in the panel discussion, wrote:

..in the case of Montreal, it is undeniable fact that there was an important error on the selection of the structural system due to no appropriate proposals from the engineers,

and this led the construction of such wasteful Olympic building, which has forced the local residents to bear the burden for decades. [Tsu 12 (Author translated)]

Ignoring the scale factor and an absence of structural efficiency would lead to critical issues for such large scale structures. In combination with other factors such as demonstration of the constructor on site, only one third of the tower was completed on time.

The remaining part of the structure was finalized in 1987, 11 years after the Olympic Games. Local engineering firm Lavalin was appointed to complete the construction, and they asked German engineer, Jörg Schlaich, for consulting on the project. The team followed the original design of Taillibert but worked thorough redesigning for the snow load and all the lifting mechanisms. The feasibility and reliability of the snow melting system was of great concern.

The fabric roof was suspended from 26 points, and 17 edge cables are anchored with the same number of points. Special fabric, PVC coated Kevlar-membrane, was used which has a relatively high strength (ca. 600 kN/m). Schlaich and his team were not satisfied with the choice of the material, because it was found to be rigid and brittle and sensitive to ultra-violet radiation. But changing the material was not acceptable due to cost and strength issues [Hol 97].

A very unique operating system and a prestressing mechanism had been developed. Three different kinds of winches were set for hoisting, retaining and storing the membrane, respectively. For opening and closing the roof, movement of the membrane is operated by the hoist winch located at the base of the tower. The motion was stabilized by a retaining winch at the 17 anchor points on the stationary roof. 26 suspension points of the membrane were connected to the hoist winch by the suspension cables that were connected in series with the hoisting cables. These ‘suspension + hoisting’ cable turned the direction in the saddle rollers at the top of the tower. The third winches are installed at the bottom of the niche, a specially designed space for storing folded membrane at the top of the tower. The movement of the membrane is controlled with a ‘lasso’ cable roped around the lower perimeter.

Pre-tensioning of the membrane was done by using hydraulic jacks at the anchorage of the suspension cables. These center-hole jacks, in which the suspension cable ran through, were located at the tower and shifted the socket of the suspension cables. Extension of the piston by 0.7 to 1.0m introduced a uniform biaxial stress in the roof skin, from about 3 to 10 kN/m.

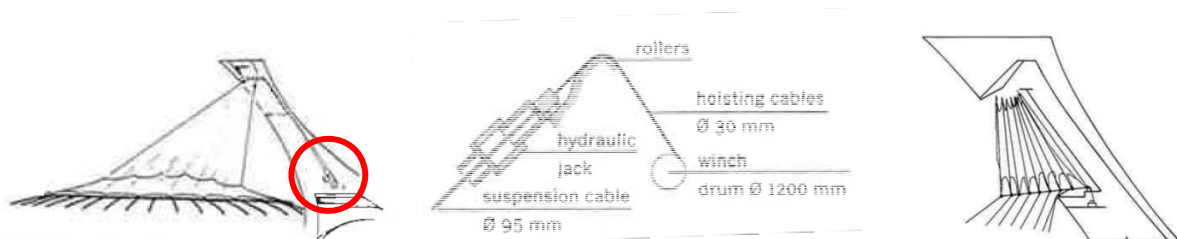


Figure 5.12 Retractable Roof of the Olympic Stadium in Montréal [Hol 97][Ish 99]

Such a complicated system for both hoisting and prestressing the membrane resulted from the geometrical issue of initial conceptual design. In order to withstand heavy snow loads, the diameter of the suspension cable had to be quite large (95mm in initial design). This would be problematic to reel the cables with winch drums for retracting the roof. In that case, 6 meters' drum would be necessary, which was impossible to install in the limited space at the top of the tower. A breakthrough was achieved by dividing the suspension cable into two cables and connecting them serially: a larger diameters suspension cable with a smaller diameter hoisting

cable. This made the diameter of the drum much smaller, and then other minor problems were automatically solved.

5.4. Development of spoked wheel system

5.4.1. Transfer from a mast to a spoked wheel

Even though the roof of Montréal could survive severe snowing suitably, the major damage of membrane in 1993 triggered its replacement by a rigid stationary one. Schlaich described this as follows.



Though the result (of Montreal Stadium roof)(..) was not satisfactory but probably could not better without accepting major changes of the original design of the architect Roger Taillibert, we learned a lot, so that we considered it as pleasure to apply this experience when designing the Roof for the bull-fight arena in Zaragoza, Spain. [Ish 93]

Figure 5.13 Portraits of Jörg Schlaich [Bög 03]

But according to an interview by the author in 2012, he also mentioned that these two projects are very different from an engineering point of view. The geometrical configuration of Montreal was eccentric, whereas one of Zaragoza is symmetric that could make the system much simpler.

From the unusual but challenging Montreal project, Jörg Schlaich and Rudolf Bergermann, based in Stuttgart and working with Otto for the Olympic stadium roof in München, gained fruitful experience and have led great technical innovations in retractable roofs with the principle of bunching at a single point. Since then, their office schlaich bergermann und partner has played a central role in that development as shown by the diagram in Figure 5.3.

5.4.2. Bull-fight Ring in Zaragoza

The existing old bull-fight arena had been constructed at the end of the 18th Century, and a roof was erected for the extension of its architectural function. Until the construction of the roof, the arena had been unused 350 days in a year. The required conditions for a new roof were difficult: to guarantee the performance of a concert or musical event, a roof must cover and protect the whole arena. However, the roof must be opened for the bull-fight-events. Furthermore, since a new roof is laid on an existing old building, the weight of the roof should be small as possible and should not interfere with the picturesque view of the old arena. Preferably invisibility from the outside was required [Ber 00]. Thus a self-contained cable-supported membrane roof with a retractable inner roof was chosen to satisfy such difficult questions.

In an interview conducted in 2012 by the author, Rudolf Bergermann who was charged with this project noted that their other project of Roman Arena Nîmes in France in 1988 would

influence to the conception of Zaragoza. The roof in Nîmes was not a retractable one, but a removable roof that was used only in winter. The two layers of foldable PVC-coated polyester membranes consisted of an air cushion and stabilized by an outer compression ring. Both roofs are self-contained tensioned structures that were installed for the historical buildings, and the foldability of a membrane fabric was suitably exploited. Very limited time scheduling from conceiving to the construction was also a common characteristic of both projects.



Figure 5.14 Retractable Roof of Bull-fight ring in Zaragoza (left) and Roof of Roman Arena Nîmes (right) [Bög 03]

A spoked wheel consists of three main elements radial spokes, an outer compression ring and an inner hub. Since all members are exposed only to axial forces under dead load, large areas can be covered with small amounts of material. Furthermore in contrast to the mast system, a large foundation is not necessary, because its structural system is closed: Tension forces in the radial spokes are perfectly balanced to the compression force in an outer ring under dead load.

Thus, construction of a large scale movable roof becomes possible. Furthermore, a spoked wheel structure can have a central opening, and the retractable roof can be installed there according to functional requirements. The primary structure of the inner roof can follow the same principle as the outer roof. The geometrical and structural simplicity for this combination of outer fixed and inner retractable roofs are the great advantages of this system.

Comparing to a mast system, the disadvantage might be only the storage place. In a mast system folded membrane is stored at the high point and a clear sky is possible when the roof is opened. However in the spoked wheel structure a membrane bundle must stay in the centre of the roof, when the roof opens.

Since Zaragoza, the retractable membrane roof combined with a spoked wheel structure has been developed little by little, mostly for large scale roofs. From a historical point of view, it could be said that the roof in Zaragoza has made a turning point in the development of

membrane retractable roofs. Schlaich could be regarded as a mediator who transferred from a mast to a spoked wheel as a primary structure for a folding membrane roof.

The roof is circular in plan and consists of one compression ring at the outer edge, two tension rings and a central hub. The primary structure of the outer stationary roof is as follows: The outer steel compression ring is a box section 800x500mm filled with concrete to provide a sufficient counterweight. 64 lower and 32 upper radial cables are attached to the compression ring and to 16 tubular steel columns at the outer end. The 6m height columns secure the distance between the upper and lower tension rings to ensure the adequate out-of-plane stability. The primary structure for the inner roof is a 'second' spoked wheel that is integrated with the 'first' one of the outer stationary roof: 16 upper and 16 lower radial cables attached to the steel columns are gathered to one central common node. The retractable membrane is suspended from the lower radial cables by a sliding carriage.

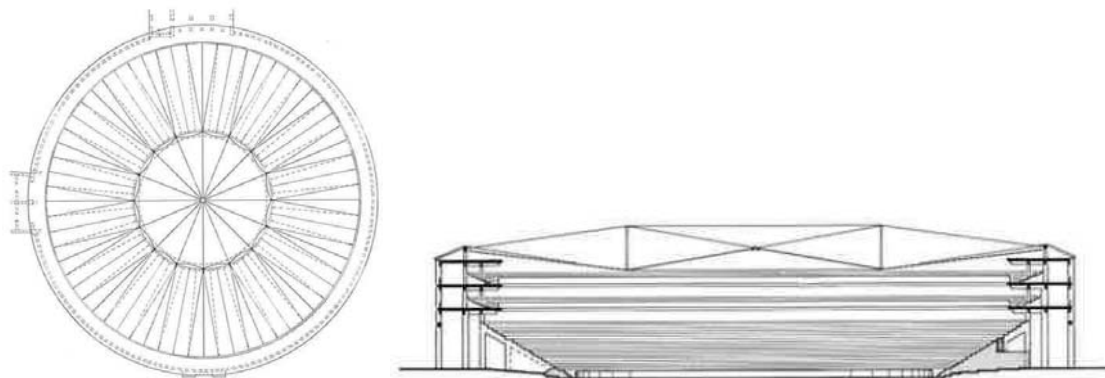


Figure 5.15 Retractable Roof of Bull-fight ring in Zaragoza [Hol 97]

In Zaragoza, not only the structural system but also the driving and prestressing system has been developed further. Until then high cost and slow-moving tractor units were exploited. But the driving system and the pretensioning system in Zaragoza were clearly separated, because their required functions were completely different. The radial movement of the fabric over a long distance (ca. 17m) could be operated very quickly, and very small force is required, because the textile membrane is extremely light and minimum friction force is expected for sliding of the carriages. Since movement direction is mostly horizontal, effect of gravity has not to be considered. On the other hand, pre-tensioning membrane requires only few centimeters' movement, but by high forces. The speed of movement is not important.

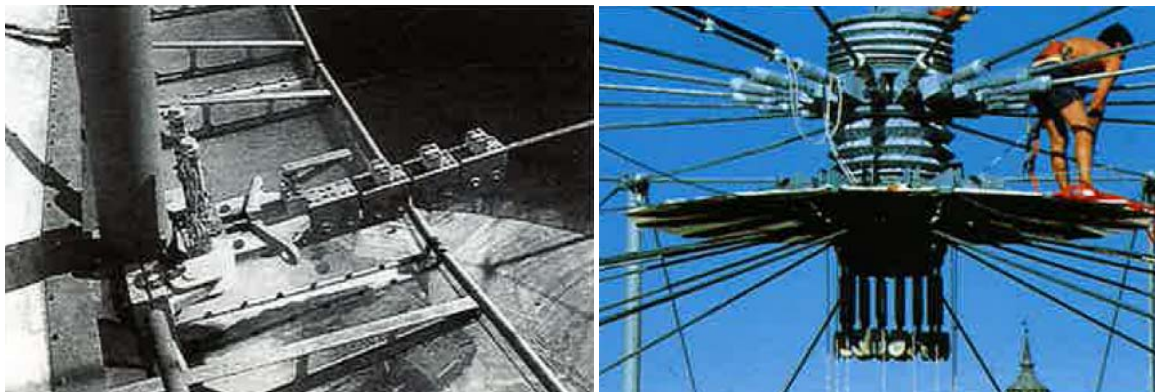


Figure 5.16 Retractable Roof of Bull-fight ring in Zaragoza [Ish 99]

16 motors located at the bottom of each steel column draw the outer edge of the membrane out to the lower rim through the endless cable loops. The membrane forms a Chinese hat, when the front ‘driving’ carriages arrive at the final outer position. Then two pins are inserted into the driving carriage by a pneumatic system for locking. Finally, the central movable node is lifted by the screw jack by ca. 70cm to introduce sufficient prestressing force into the membrane. The entire process is monitored by sensors and controlled by a computer.

Since the membrane could easily be broken by movement errors of the driving carriages, the reliability of the operating system was very important. In the design phase, non-contact optical sensors used for adventure rides were investigated, because they have extreme accurate control system to accelerate, brake and stop their heavily loaded cars [Mor 04]. The development resulted in not only the optimum design in terms of drive and control technology but also a considerable cost savings and an important increase in the robustness and reliability of the design. Since its start of operation in 1990, the roof has been operated several hundred times without any trouble. [Bla 99]

5.4.3. Rothenbaum Stadium

Werner Sobek who worked in the office of schlaich bergemann und partner, and found his own company, designed the Tennis court in Hamburg, Germany in 1999. The major difference here compared to Zaragoza is its asymmetric positioning of the inner roof, which is intended to prevent shadows casting on the centre court and to shield the player on the court from a shadow.

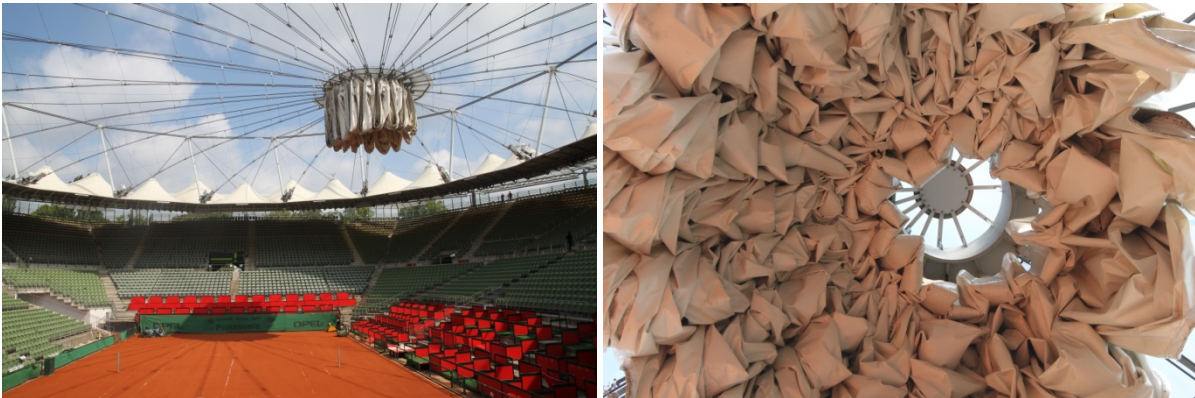


Figure 5.17 *The Rothenbaum Center Court in Hamburg (photos taken by author in 06/2011)*

In this condition every sliding carriage must be moved at a different speed, because all the radial cables have different lengths. The movement of the inner roof is completely automatic and carefully controlled by contactless sensors. The prestressing of membrane textile is done by 18 hydraulic jacks located at the outer edge of the inner roof. High accuracy is required for their operations, because membrane is easily damaged or collapsed by the force of hydraulic jacks.

The primary structure has been stiffened by connecting the upper and lower radial cables of both the inner and outer roofs, using hanger cables, so that they work together as a load bearing structure. This mechanism has made the large scale of the retractable membrane roof possible. At 3000m², this was the largest convertible textile roof at that time.

By adopting this change, the form of the sliding carriage had to be changed. In Zaragoza, the sliding carriage has a hole in the middle, and the radial cable runs through it. However, in

Rothenbaum, this is difficult due to the presence of hanger cables. Therefore, the sliding carriage is hooked to two cables arranged in parallel to provide stable gliding conditions.

5.4.4. Frankfurt Stadium

The construction form using spoked wheel principle proved to be extremely efficient and became the prototype for numerous stadium roofs throughout the world designed by schlaich bergemann and partner [Kni 11]. Knut Göppert is one of their directors (Partner since 1998) and has served as a key person for the design and construction and its development. The roof of the football stadium in Frankfurt, Germany constructed in 2005 is an archetype for their successive stadium projects which have an inner retractable membrane roof. The construction principle of Frankfurt is almost the same as the former ones in Zaragoza or Rothenbaum. However, the scale of the retractable roof is much larger (8000 m²), and its rectangular shape is different. The roof is designed only for summer, but for extreme summer conditions like hail storms, 65% of reduced snow load is applied for design. The membrane roof is folded up into the central video cube and protected against severe environmental conditions through the year. For driving the membrane, a motor-operated winch is used.

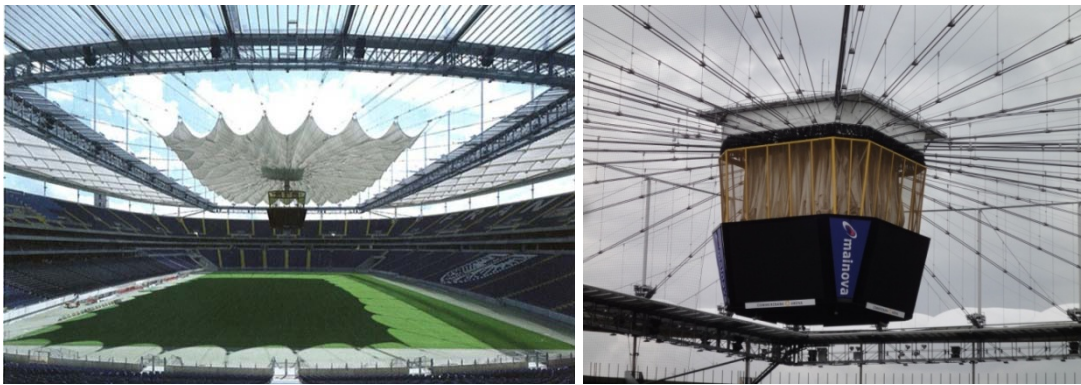


Figure 5.18 The Commerzbank-Arena Frankfurt, unfolding of the retractable roof (left) [Göp 07a] and the central video cube protecting the folded membrane (right) (taken by author in 06/2012)

5.4.5. Kufstein Fortress

Engineer Alfred Rein who studied by Frei Otto and worked in the office Werner Sobek Ingenieure designed a similar type of retractable roof for an area ca. 2000m² at the historical fortress in Kufstein, Austria, which is today a major tourist attraction. The membrane is made from PTFE coated fabric, which has good flexibility, flex cracking resistance, and durability.



Figure 5.19 The retractable roof at Kufstein, Austria (left) [Rei 12], a part of the webbing belt of the retractable roof (PES 50x3mm ultimate strength 80kN) (centre and right, photos taken by author at the office Kugel+Rein in 01/2009)

5.4.6. Warsaw Stadium

National stadium in Warsaw, Poland was constructed for hosting the European Soccer Championship in 2012. The required conditions for the retractable roof were stringent: a large scale (maximum ca. 70m spanning) structure also intended for winter use. The engineer schlaich bergemann and partner realized it as single layer membrane (no air cushion system) with single layer cables (without stabilization by hanger cables). This primary structural system is the same as the one for Zaragoza; however, the required size for the roof for Warsaw (11,000m²) is 11 times larger than Zaragoza, and instead of a circular shape, the shape approaches a square. Even with 60 upper radial cables for the primary structure of the inner roof, a relatively organized bottom view is provided because of relatively few structural elements between the central hub and the upper tension ring. In light of this, the retractable roof for Warsaw can be considered a milestone for single layer roofs [Göp 11].

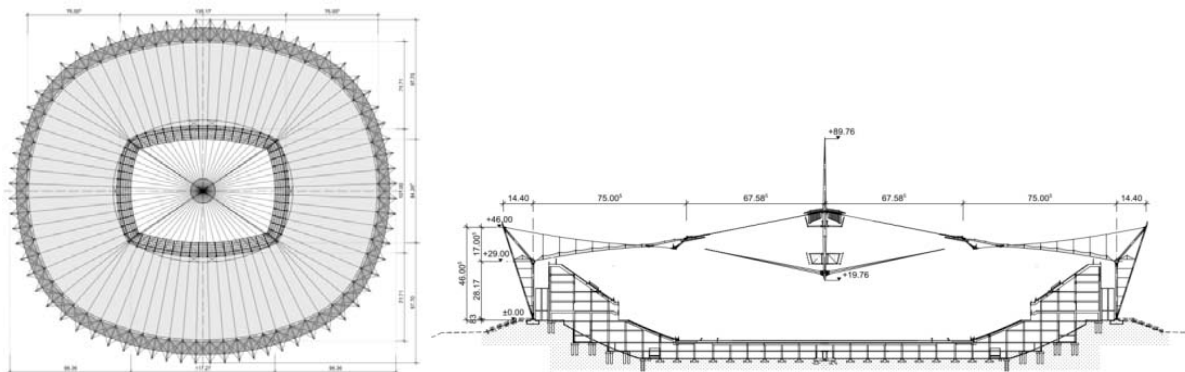


Figure 5.20 National Stadium Warsaw [Göp11]

For each radial cable, one driving carriage and eleven sliding carriages are installed. To reduce the weight of the components, sliding carriage made of Polyamide is applied instead of one of steel with sliding pads.

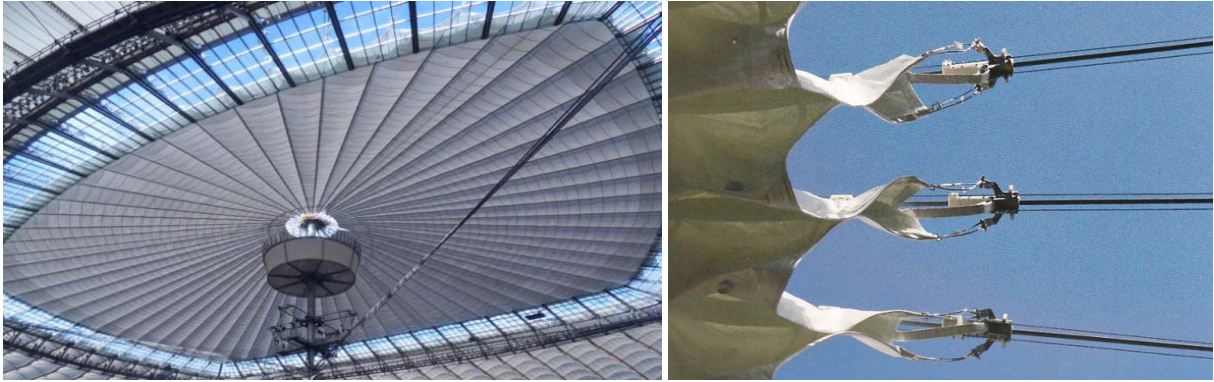


Figure 5.21 National Stadium Warsaw, retractable roof (left) [sbp 12] the driving carriage of the retractable membrane roof in Warsaw [Jae 12]

5.4.7. BC Place Stadium

The multi-sports facility BC Place in Vancouver, Canada was the largest air-supported stadium in the world when it was first built in 1982. However, in 2007 a tear occurred in the roof skin, and the whole roof quickly deflated. After repairs, it was decided that whole roof needs to be replaced. Schlaich bergemann und partner and Geiger Engineers constituted the design team.

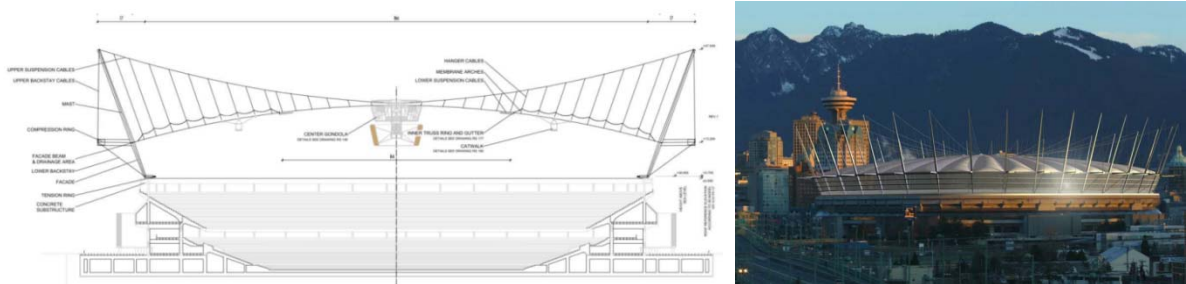


Figure 5.22 BC Place in Vancouver, section and appearance [Göp 11]

There is a novel structural principle using a pneumatic system used in BC place to additionally stabilize the membrane. By this the inner retractable roof, open in summer and closed in winter or for special events, provides sufficient inclination and stiffness to prevent ponding and to limit the stress of membrane under severe snow load (1.75kN/m^2 according to local code). When the roof is unfolding, first the radial Polyester belts between the adjacent cushions are mechanically prestressed using the hydraulic cylinder located at the perimeter of the inner roof such as the other retractable roofs described above. Then, the cushions are inflated to a pressure of 500 Pa to 2000 Pa according to the environmental condition. The required load is decided by the information from the magnetic sensor attached to the hanger cables. For retraction of the roof, the inner air is removed by an exhaust system through a perforated tube located inside of the cushions. The performance checks for all these phases were checked in full scale mock-up of two cushions. The transformation of the roof takes 20 minutes.

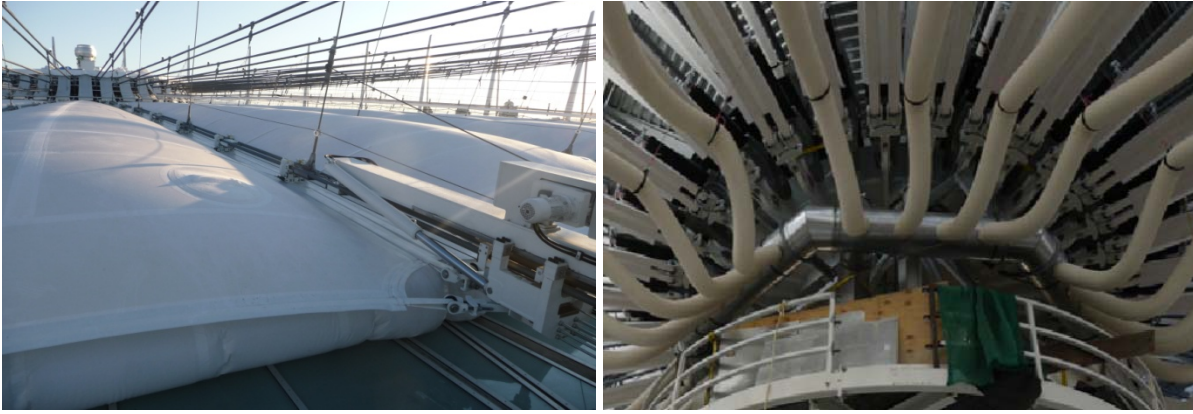


Figure 5.23 Inflated retractable roof in BC Place (left) (courtesy of schlaich bergemann und partner/C. Paech), Air ducts in the central Hub (right) [Ten 12]

Furthermore the same type of stadium roof is constructed in Bucharest and has been on design in Brazil, both designed by schlaich bergemann und partner.

5.5. Development of the dimension of roofs

Figure 5.6 shows the historical transition of the size of the retractable roof bunching in a single point. Every architectural building is built for different purpose; therefore the dimension cannot be regarded simply as a factor for the development. However it is in some cases possible to show some relationships. Membrane retractable roofs with a single mast from middle 60s to 70s are almost the same size. One reason for that is that most of them are for covering swimming pools, therefore it is not necessary to cover an area larger than 2000m^2 .

Apparently the $20,000\text{ m}^2$ for Montreal Stadium was different from the other ones of the same system. Even from this curve, the reason is clear why the Montreal roof has resulted in controversy.

In contrast to the single mast, the development of ones with spoked wheel principle is steadier. Starting from 1000m^2 in Zaragoza, it has now reached to $11,000\text{m}^2$ in Warsaw.

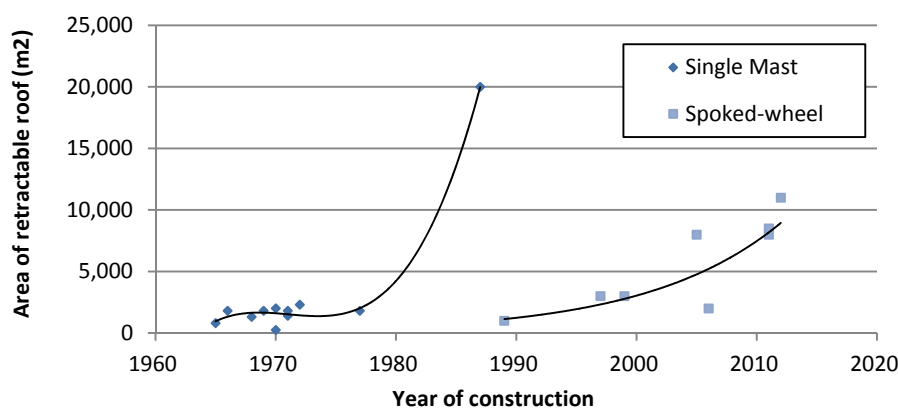


Figure 5.24 Historical transition of the size of the retractable roof bunching in a single point

5.6. Load bearing behavior of a membrane surface

As discussed in Section 4.3.2, any prestressed membrane surface is characterized by the close interaction between form and structure. Sufficient stiffness could be achieved by the double curvature of the surface.

In most cases of a foldable membrane roof with a spoked wheel structure, the prestressing force is introduced by actuators located at the outer edge of the roof. They pull the edge nodes of the membrane outward in radial direction to ensure that sufficient prestressing force can be introduced in the radial direction. However the question is how to tension the membrane skin also in the circumference direction.

In Zaragoza, the membrane surface is relatively flat, because there is no curvature of the radial cables. Therefore the roof is more sensitive to fluttering, and careful operation is required. The roof in Warsaw is similar, but the inclination of the roof is much larger. Hence, there is little threat against snow ponding.

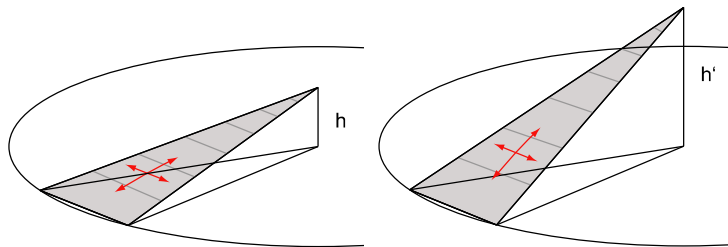


Figure 5.25 Uniaxial forces of foldable membrane with spoked wheel primary structure (Left: type of Zaragoza roof, Right: type of Warsaw roof)

In Rothenbaum, Frankfurt, Kufstein and Bucharest, the prestressing force in the circumference direction is mainly achieved by the form of cable girder. When the cable girder is curved in radial direction in a positive curvature, the prestressed membrane surface should have a negative curvature in the circumference direction, even though it is only a slight curvature.

In Vancouver, the double layered membrane is inflated to resist severe snow loading. Therefore the membrane has a synclastic surface.

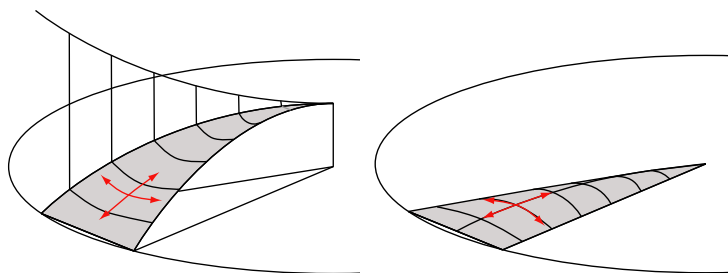


Figure 5.26 Uniaxial forces of foldable membrane with spoked wheel primary structure (Left: type of cable girder such as Frankfurt Stadium, Right: type of pneumatic system such as BC-Place, Vancouver)

Furthermore, since most of these roofs are not circular but oval or close to rectangular shape in plan, the lengths of the adjacent radial cables are not always constant. Therefore the membrane between the two adjacent radial cables has different vertical coordinates in circumferential direction as shown in Figure 5.27. This height difference creates a curvature of the membrane skin. In Warsaw, the adjacent radial cables are anchored at the different

heights in the central hub. Hence this height difference is even larger. (see Figure 8.6 in Chapter 8)

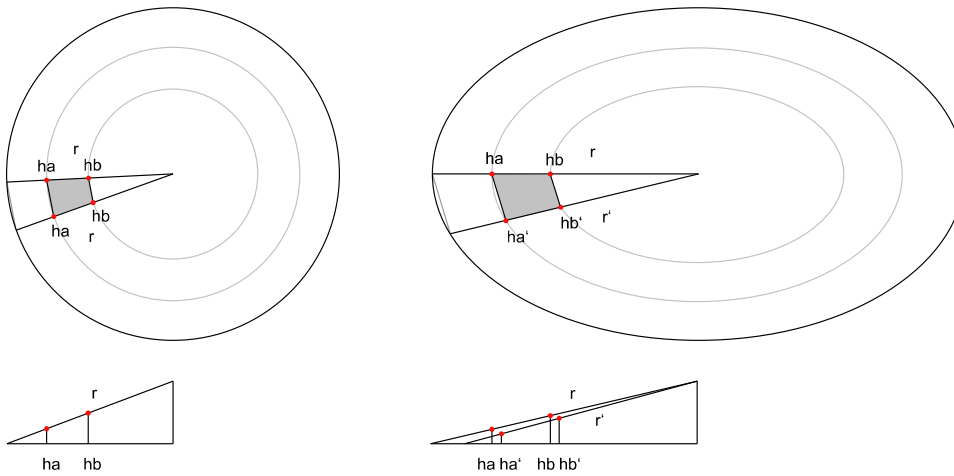


Figure 5.27 Different vertical coordinates in circumference direction (left: circle, right: Oval in plan)

5.7. Summary of the history

The entire history of the development of a retractable membrane roof bunching in a single point has been studied and described in this chapter. The author emphasized on people who were engaged in each project, because technology is often developed through people. The study revealed that the development of this retractable roof structure has been made possible by people from Stuttgart, Germany, or at least related to this place.

Frei Otto is the most important person with regards to the invention and a comprehensive development of membrane structures. Taillibert who studied and was inspired by Otto had many opportunities to realize the projects. Both pioneers had a strong ambition for the realization of large scale retractable roofs, however the project of Otto was suspended and Taillibert's Montreal Stadium can be regarded as a failure.

Jörg Schlaich, an engineer based in Stuttgart who worked together with Otto for München Olympic Stadium, is well known for his innovation in a wide variety of light weight structures. He was responsible for combining retractable membrane with a spoked wheel. Engineers who followed Schlaich contribute to the development and maturing of this technology. The largest retractable roof is the one in Warsaw, where the size reached nearly 11000m².

6. Spoked Wheel Structural System

6.1. Principle of a spoked wheel structure

6.1.1. Brief history of the development of a spoked wheel

The wheel is one of the greatest inventions in human history. By using wheels even a heavy load can be transported with a minimum of energy. A wheel can dramatically decrease the friction force between the load and the ground surface. However, wheels of an early date (around 3000 BC) consisted of planks, which were extremely heavy. Therefore, the wheel with planks could be used only for short distances. Earlier than 2000 BC, the great innovation was achieved by connecting the central hub to the outer rim with spokes. This ‘spoked’ wheel spread out fast all over the world, from Mesopotamia to China. But these spokes were still compression elements. No further innovations were made until the beginning of the 1800s. Sir George Cayley, an English engineer and one of the most important persons in the history of aeronautics, had designed the first ‘tensioned’ spoked wheel that was more efficient and lighter than the conventional compression spokes [Beu 05].

The American inventor, Buckminster Fuller noted this evolution as a starting point of the reversion of structural strategy of human being [Kra 99]. The load transfer system of the tension spoked wheel is unique: when a load is applied on the centre hub of a bicycle wheel, the load does not only go down to the ground through the spokes as a compression force (decreasing the pre-tensioning force) but also goes up as a tension force (increasing of the pre-tension force). From the spokes the load is transmitted into the ground through the rim, which is stabilized by the tension forces of the radial spokes. Modern spoked wheels are extremely light in comparison to the load they can carry: their weight is only around 1.5kg without tire, but they can carry up to 7,000N (ca. 700kg) [Ino 02].

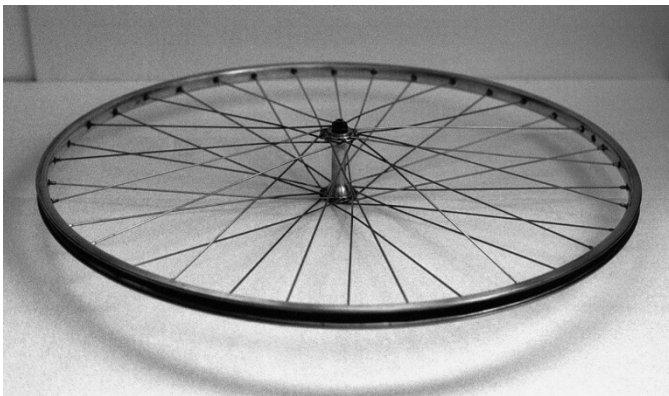


Figure 6.1 A typical spoked wheel

6.1.2. Definition of a spoked wheel structure

A spoked wheel could be defined as a self-contained structure which consists of a compression ring, a central compression hub and radial tension spokes. Schlaich categorizes it as a tension structure as shown in Figure 6.2. According to the mirror axis of compression and tension, it is located at the opposite position of the shell structure that is subjected to pure compression forces under self-weight.

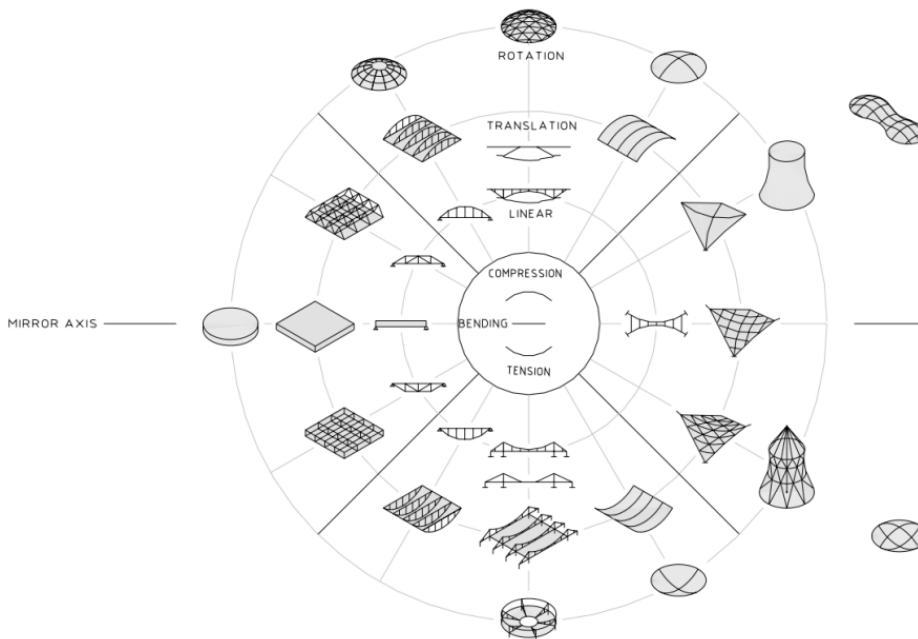


Figure 6.2 The order of structures [Schl 06]

One frequently asked question is whether the spoked wheel could be defined as a kind of tensegrity structure. Tensegrity is a structural principle based on the use of discontinuous components in compression and continuous tension members. Buckminster Fuller, who introduced the term tensegrity as a contraction of tensional integrity, noted a spoked wheel as a kind of primitive tensegrity structure.



As I wondered whether it was now possible for man to inaugurate an era of thinking and conscious designing in the terms of comprehensive tensions and discontinuous compressions, I saw that his structural conception of the wire wheel documented his intellectual-designing break-through into such thinking and structuring. That is, the compressional hub of the wire wheel was clearly islanded or isolated, from the compressional "atoll" comprising the rim of the wheel. As these compressional islands were only interpositioned in structural stability by the tensional spokes, I said that this was dearly a tensional integrity, where tension was primary and comprehensive and compression secondary and local. This reversed the historical structural strategy of man [Kra 99].

Figure 6.3 R. Buckminster Fuller and the model of tensegrity structures [Ful 61]

The definition of tensegrity has been discussed over the last several decades, but René Motro described that nowadays a consensus has been reached classifying tensegrity structures in several classes: for class I the compressed components are single struts, while in class II several struts are contiguous [Mun 11]. In accordance with that definition, a spoked wheel structure can be defined as a tensegrity structure of class II.

Another controversial theme regarding the definition is the difference between spoked wheel roofs and “cable domes”. Cable domes have often been constructed in the USA for large scale roofs such as of sport event halls. The tension ring of a spoked wheel could be exchanged by several numbers of rings arranged in the radial direction. Each ring would be connected by diagonal cables. Geiger dome (Figure 6.4 left) is a well-known structural system that was developed by the American engineer David Geiger. The first realized Geiger domes are the Seoul Olympic Gymnastic Hall and Fencing Hall constructed in 1986. In Geiger domes, the membrane cladding between four support points is shaped like a saddle to achieve sufficient stiffness against vertical loads. Another structural system of the cable domes is the Aspension dome (Figure 6.4 right), whose connection cables are arranged in zigzag form. In Aspension domes, a triangle meshing form provides the stiffness of the cladding. The stability of the Aspension dome against geometrically-not-affine loads would be higher than the one of the Geiger dome (smaller deformation occurs), however more complicating joint details would be necessary. The cable domes could also be defined as a tensegrity structure in class II, however the difference between spoked wheel roofs and cable domes would not be clear.

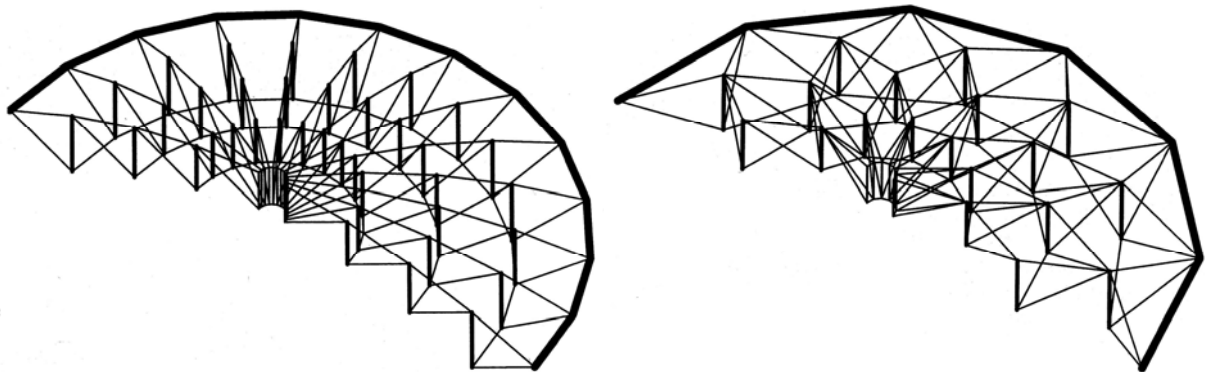


Figure 6.4 Variation of the Cable dome: Geiger Dome (left) and Aspension Dome (right) [Schl 97]

6.1.3. Advantage of its lightness

The advantage of using the spoked wheel principle for large scale roof structures is clearly shown in the graph in Figure 6.5, in which conventional cantilever roofs (continuous line) are compared to the spoked wheel roof (dotted line) in regards to their weight. The vertical axis indicates the amount of required construction materials (only self-weight). The weight of a cantilevering roof with a span of 35m is defined as 100%. Compared to the cantilever roofs, spoked wheel structures tend to be less influenced by the scale factor. The larger the roof length is, the larger the difference of the weight between the cantilever and the spoked wheel becomes. The weight for cantilever roofs dramatically increases when the roof length becomes large. The required amount of steel reached 400%, when the cantilever length is 60m. One typical example, Beijing National Stadium, often called Bird's Nest, is categorized in this cantilever type. The Gottlieb-Daimler-Stadium in Stuttgart is an example of the spoked wheel

roof, and its mean weight is about 13 kg/m^2 [Ber 00]. Whereas, the mean weight of the Beijing National Stadium is about 700 kg/m^2 , and the used amount of the steel reached 42,000t. [Tsu 12]

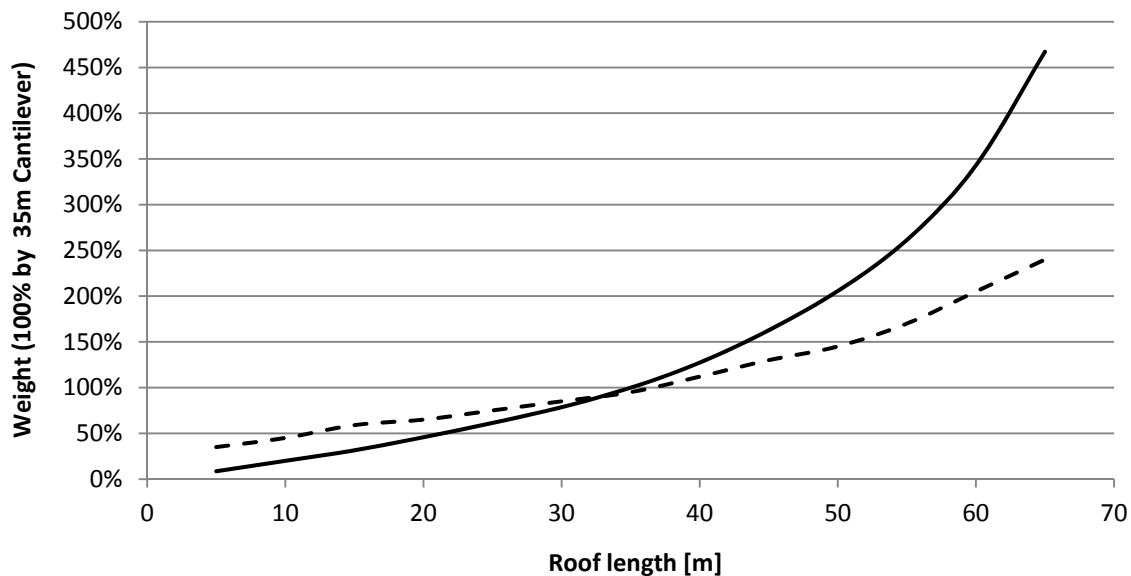


Figure 6.5 Weight comparison: Cantilever (dot line)– Spoked wheel Structure (line) (Internal study, Courtesy of schlaich bergemann und partner)

6.2. Historical development of a spoked wheel roof

The spoked wheel principle was first applied for large scale roofs in 1960s. The American Pavilion designed by Edward Durell Stone at the Brussels Universal and International Exposition in 1958, the New York State Pavilion designed by Philip Johnson in 1964 and the roof of the Oracle Arena in Oakland designed by Skidmore, Owings and Merrill in 1966 were the well-known examples of this early stage. In the roof of the Oracle Arena, single layer cables were configured in radial direction, and its global stability against vertical load is ensured by the weight of reinforced concrete beams placed on each cable.

Since the late 1980s, the spoked wheel principle has been applied for stadium roofs with a central opening. One of the most well-known examples at this early date is the roof of Gottlieb-Daimler-Stadium (named Mercedes-Benz Arena since 2008) in Stuttgart designed by schlaich bergemann und partner. Only small foundations were allowed due to the existence of mineral water close to the ground surface. The self-equilibrating effect and the lightness of the spoked wheel structural principle were efficiently utilized to realize it.

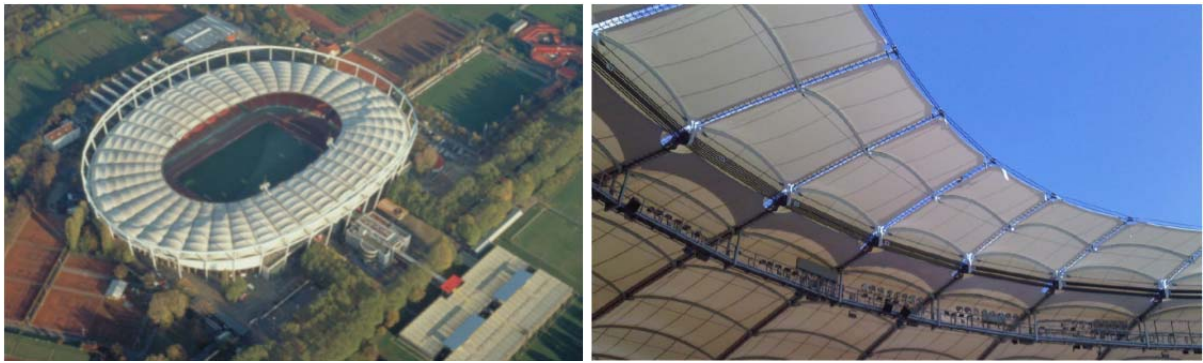


Figure 6.6 An aerial view of Gottlieb-Daimler-Stadium in 1993 (Left) and the roof from the lower angle with extended part constructed in 2011 (Right) [sbp 12]

Like many structural engineers, Schlaich recognized the bicycle wheel structures as one of the most beautifully optimized tensile hybrid structural system [Mun 11]. The Gottlieb-Daimler-Stadium became a prototype of a large number of the stadium roofs all over the world (as shown in Table 6.1) designed and developed by schlaich bergemann und partner since then.

Table 6.1 Stadium roofs using spoked wheel principle (Courtesy of schlaich bergemann und partner)

Stadium	Country	Seats	Roof area [m ²]	Cladding material	Completed year
Mercedes-Benz Arena, Stuttgart	Germany	55000	34000	PVC-Membrane	1993
Bukit Jalil National Stadium, Kuala Lumpur	Malaysia	100000	38500	PVC-Membrane	1997
Estadio Olímpico, Sevilla	Spain	57000	25000	PVC-Membrane	1999
HSH Nordbank Arena, Hamburg	Germany	55000	35000	PVC-Membrane	2000
Sports Dome, Pusan	South Korea	56000	34000	PTFE-Membrane	2001
National Stadium Abuja	Nigeria	60000	33000	PTFE-Membrane	2002
Inchon Munhak Stadium, Incheon	South Korea	52000	32000	PTFE-Membrane	2002
Stadium im Allerpark, Wolfsburg	Germany	35000	15.000 + 8.000	fixed: PVC Membrane + retractable: Membrane (Pneumatic)	2002
Commerzbank Arena, Frankfurt	Germany	52000	29.000 + 8.000	fixed: PVC Membrane + retractable: PVC Membrane	2005
Jaber Al-Ahmad Stadium	Kuwait	65000	44500	PTFE-Membrane	2007
World Cup 2010 Stadium, Durban	South Africa	75000	46000	Membrane	2008
Jawaharlal Nehru Stadium, Delhi	India	75000	45000	Membrane	2009
World Cup 2010 Stadium, Green Town, Cape Town	South Africa	68000	45000	Glass	2009
Nelson Mandela Bay Arena, Port Elizabeth	South Africa	42000	34000	Membrane/Aluminum	2009
FNB Stadium, Johannesburg	South Africa	95000	27000	Membrane	2009
National Stadium, Warsaw	Poland	55000	50000	Membrane	2011

6.3. Morphology

A hanging roof with one outer compression ring and one inner tension ring is too flexible against vertical loads. There are two possible fundamental forms: one consists of one compression ring and two tension rings, the other has two compression rings and one tension ring. The Bukit Jalil National Stadium, Kuala Lumpur in Malaysia is an example for the former and the Gottlieb-Daimler-Stadium is one for the later as shown in Figure 6.7 below. In the Bukit Jalil National Stadium the membrane roof is located on the upper spoked cable, whereas in the Gottlieb-Daimler-Stadium on the lower cable. The drain path follows the inclination of the roof.

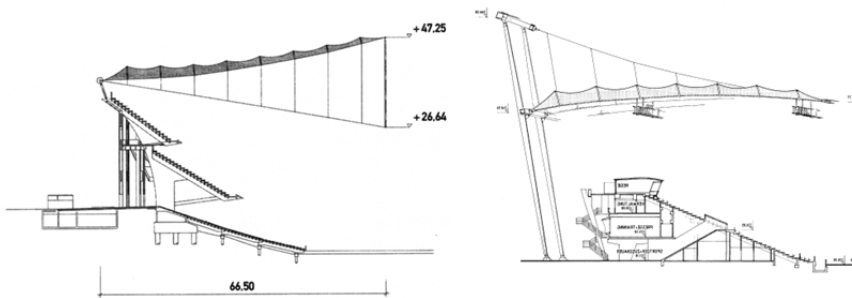


Figure 6.7 Sections of Bukit Jalil Stadium (Left) and Gottlieb-Daimler-Stadium (Right) [Ber 00]

In both cases a central hub of a spoked wheel could be replaced by a tension ring, which is required for stadium roofs that demand a central opening. For sports stadiums such as football, tennis or athletics stadiums, oval forms in plan are demanded more often than circular ones. This distortion is possible by varying the spacing of the compression rings.

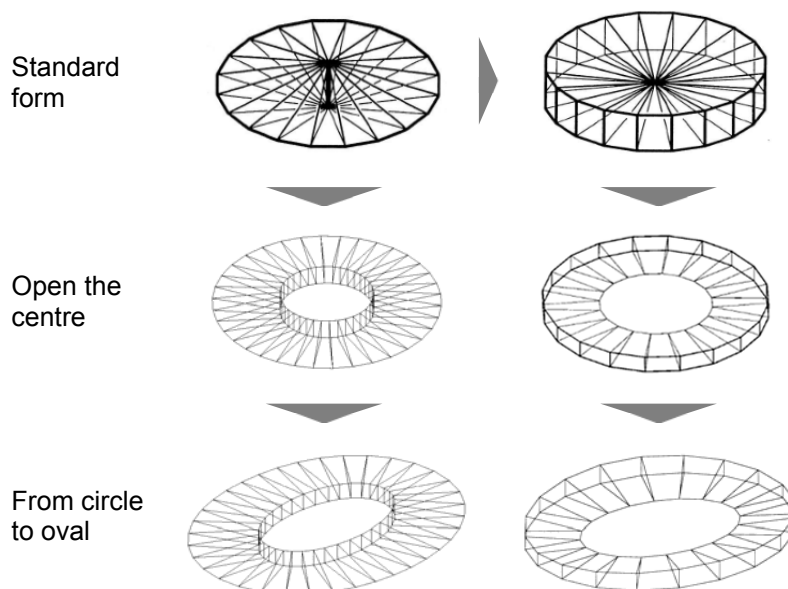


Figure 6.8 Variation of the forms of the spoked wheel roofs (the figures from [Ber 00])

In most realized membrane retractable roofs with spoked wheel structures, these two fundamental forms are interlocked; one for the outer stationary roof and the other for the inner retractable roof. The variations of the combination are shown in Table 6.2. Against the

distributed load the spoked wheel roof can resist by geometric affine transformation, however against the point load it would be very flexible and the resulting deformations would be large. Thus, most spoked wheel roofs are stabilized by connecting the upper and lower cable by hangar cables.

Table 6.2 Variations of the combination of the two spoked wheels

Outer stationary roof		Inner retractable roof		Combination	Examples
	+		=		Zaragoza
	+		=		Frankfurt Rothenbaum
	+		=		Bucharest
	+		=		Warsaw

6.4. Structural principle

The spatial structural system of the spoked wheel roof can briefly be explained as follows: The spoked wheel roof is fixed at the outer ring and strongly prestressed inward. This prestressing force (indicated as V in the figure below) is the sum of the tension force in a ring cable (S) that is balanced by the compression forces in the outer rings. When a downward load, for instance snow load (P), is applied on the spoked wheel structure, it is mainly carried by a compression force in the lower cable (D). This compression force should always be smaller than the prestressing force in the upper cable (V_u).

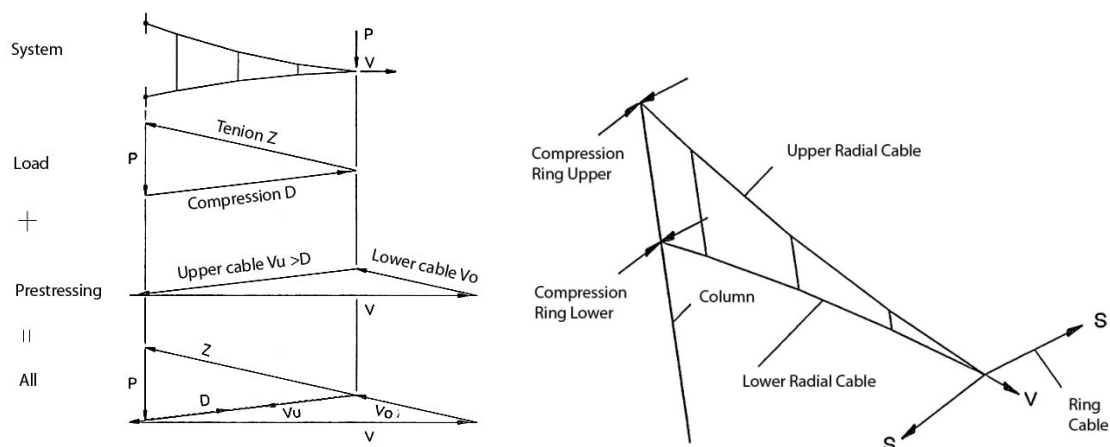


Figure 6.9 Cable truss – Normal forces (left), Development of radial prestress [Ber 00]

The force of the compression rings must be constant and equal to one of the tension rings. Therefore, if the roof form is oval in plan such as at the Stuttgart stadium, the prestressing

forces of the radial cables are not constant due to the variation of the radii of the compression ring. The tension forces in the curved sections are greater than in the straight sections.

These geometric-affine structural behaviors are demonstrated using a simple FE model. (Figure 6.10) The study model is oval in plan with almost the same geometrical configuration as the one of Gottlieb-Daimler-Stadium but only a one layer spoked wheel (one compression and one tension ring). A prestressing force 10,000 kN is applied in the tension ring, and the axial forces of each member are estimated by a non-linear calculation. The right figure shows the axial force of the tension ring and the radial cables. The values of the radial cables vary according to the position. Larger tension forces occur at the positions of the ring where the bending angle is larger.

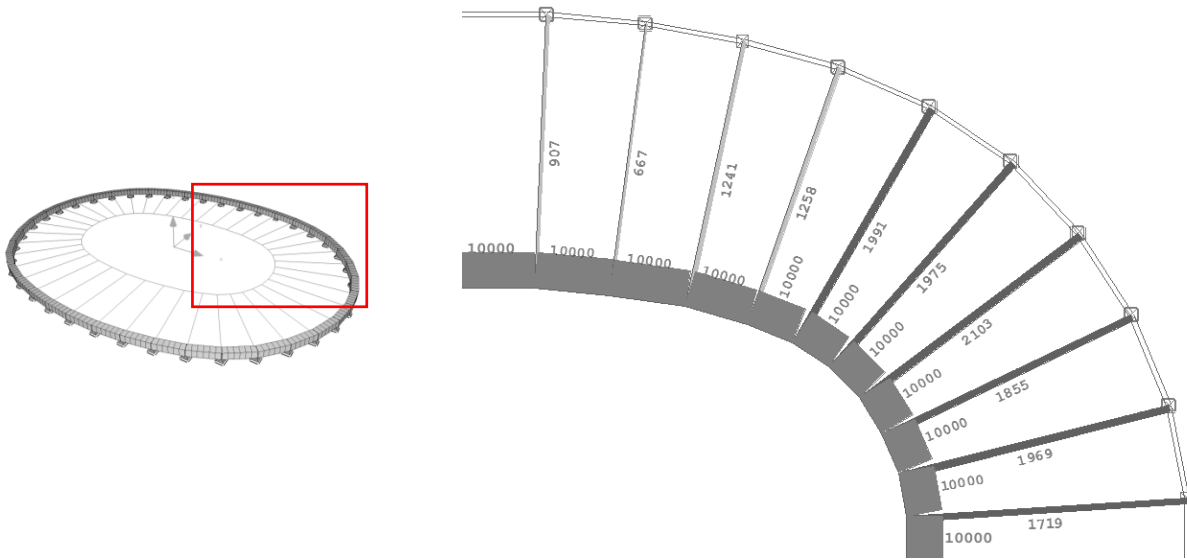


Figure 6.10 A simple study model; one fourth of an oval-form spoked wheel, axial force (kN) in the tension rings and in radial cables

The geometrical limitation of the spoked wheel structure is that the angle of the bend in the compression ring must be equivalent to the bend of the tension ring. The parameter study of the roof of Pusan Dome in South Korea indicates how much it adds to the costs, if the shapes of the compression and tension ring differ. (Figure 6.11) Here a roof that has oval opening had to be fitted to the already constructed outside concrete structure whose configuration is circular in plan. The graph clearly shows that the more the opening shape deviates from the circle, the more material, here steel, is required: 600% more steel would be necessary for an oval opening 200/140 in contrast to the perfect circular-circular solution.

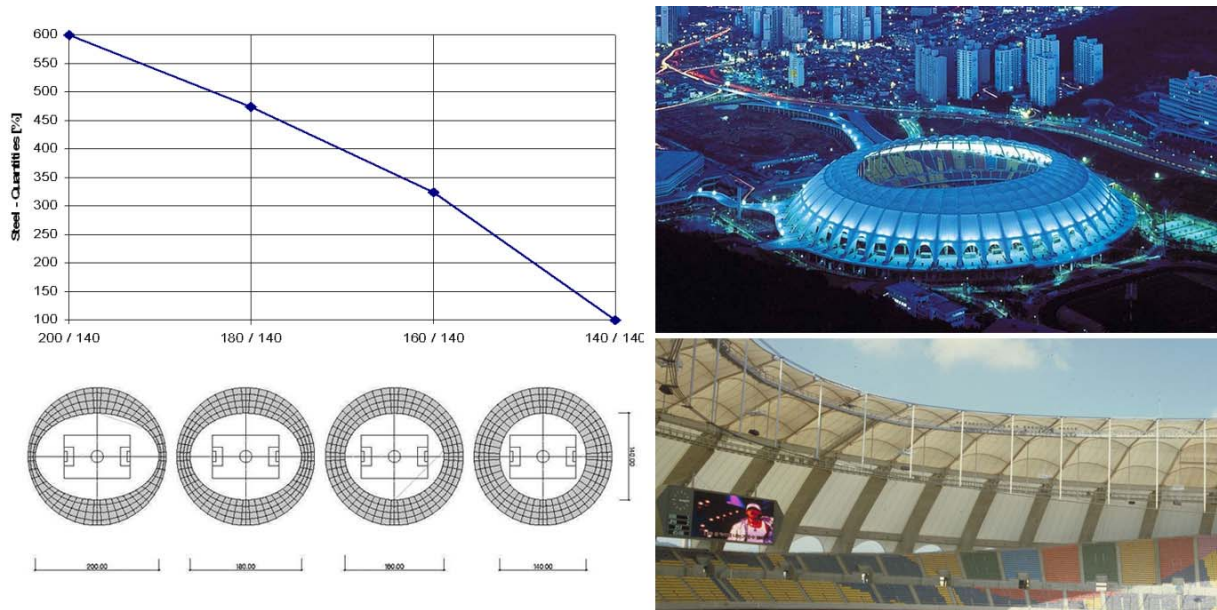


Figure 6.11 Variation of inner roof opening of Pusan Dome, South Korea (The figures from [Ber 00], the pictures from [sbp 12])

In reality, the shape of a football court is not even oval but rectangular; therefore the rectangular opening roof would be the best for the football stadium roof. The difference between an oval and a rectangular layout are the corners that attract much more tension forces in the radial cables due to the larger angle of the kink. In the roof of the AOL Arena in Hamburg, in order to adapt the inner opening as far as possible to the rectangular football court, three cables each were concentrated on the four corners of the tension rings.

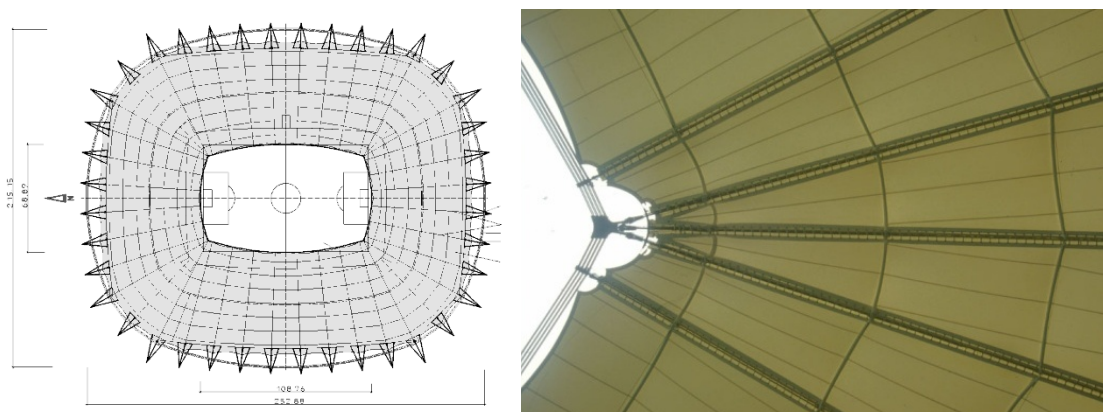


Figure 6.12 AOL Arena in Hamburg: plan view (left) and the corner as built from the lower angle (right) (The figure from [Ber 00], the picture from [sbp 12])

Wider varieties of the structural form are possible for the spoked wheel roof. The one compression – one tension ring system is also possible and has been realized for example by combining it with a cable girder system (AOL-Arena, Hamburg), by making the global roof shape being a saddle form (Jaber Al Ahmad Stadium, Kuwait) or by weighting the roof with steel trusses and glass cladding (Greenpoint Stadium, Cape Town). Instead of a cable girder, a prestressed membrane can be utilized for the direct inter connection of the upper and lower cables, as it was done at the Olympic stadium in Sevilla.



Figure 6.13 AOL-Arena, Hamburg / Jaber Al Ahmad Stadium, Kuwait / Olympic stadium in Sevilla / Greenpoint Stadium, Cape Town (in clockwise direction from upper left hand) [sbp 12]

Part 2 Development of Foldable Membrane Roofs Opening towards the Perimeter

7. Foldable Membrane Roof with Spoked Wheel Structure Folding from Inside to Outside

7.1. Introduction

The study of the required energy for the movement in Chapter 3 makes it obvious that a textile membrane roof with a spoked wheel structure is one of the most economical solutions for retractable roofs. Light-weight materials like textile membranes are most effective for retractable roof structures. Due to their light weight, they can be moved fast, easily and precisely. Due to their flexibility they can be folded, which allows for the compact storage of the structural material in open conditions as shown in Chapter 4. A spoked wheel structure, as described in Chapter 6, is a well-known light-weight structure and large areas can be covered with relatively small amounts of material. In combination, the spoked wheel structure is the fixed primary structure and the folding membrane is the secondary structure.

But there is, among others, one critical issue to this system which will be discussed here. All existing roofs with this structural system open toward the centre of the roof. Therefore, even in the open situation there is no unobstructed view of the sky; a bundle of folded membrane remains in the centre as a floating block. There the bundle is difficult to maintain and can be more easily damaged in windy weather conditions. Also this is unfavorable for broadcasting. The bundle creates shadows on the playing field. Furthermore, it interferes with an ideal appearance.

All these problems could be solved, if the textile membrane can be folded into the opposite direction i.e. to the perimeter of the roof. A membrane stocked along the edge would be easy to protect and to maintain. It would make no shadows on the field, and moreover a free opening would be created.

The geometrical complexity is the main obstacle for this system. Therefore, this chapter serves to clear the geometrical problems and to show their possible solutions.

Unique characteristics of a foldable membrane roof are its foldability and necessity of prestressing force. During the procedure of opening and closing, a rigid movable roof has only two configurations: open and closed. In contrast, a foldable membrane roof has three configurations: folded, unfolded and prestressed as shown in Figure 7.1. In the unfolded status the textile membrane is under no significant tension, whereas in the prestressing status the stiff double curved surface is created. This alteration of the configuration of the textile membrane is one of the keys to designing this kind of structure.

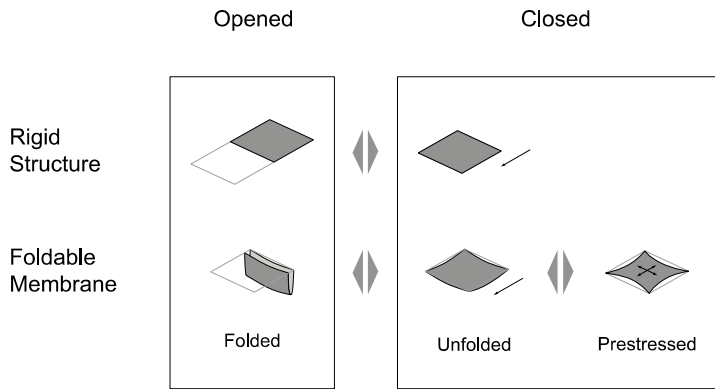


Figure 7.1 The differences in the number of configurations between rigid movable roof and foldable membrane roof

The diagram shown in Figure 7.2 is the design flow that the author follows to develop the foldable membrane roof opening to the perimeter. First, the geometrical problems will be described in section 7.2. To solve them, the boundary conditions of the roof need to be clarified. However, in this stage, the configuration of the textile membrane was defined just geometrically, that is to say, no prestressing force was considered. For instance, the flexible edge of a tensioned textile membrane becomes a curve under prestress, but for the study of the geometrical boundary conditions in 7.2.1, all edge lines are simply linear.

In the next step, both the boundary conditions and the corresponding form of the textile membrane under prestress will be considered. The double curved surface or the curved edge lines of the textile membrane will be checked mainly for the foldability of the textile membrane. This study will be shown in 7.2.2 as a geometrical condition in tensioned status.

As discussed in the previous chapter 4, it is also essential to evaluate how the prestressing force will be introduced into the membrane. This will be discussed in section 7.3. Here, kinematic methods for the introduction of the prestressing force into the membrane, which have structural and economical considerations, will be developed by the author. An overview of case studies will be described in the last section of this chapter, section 7.4.

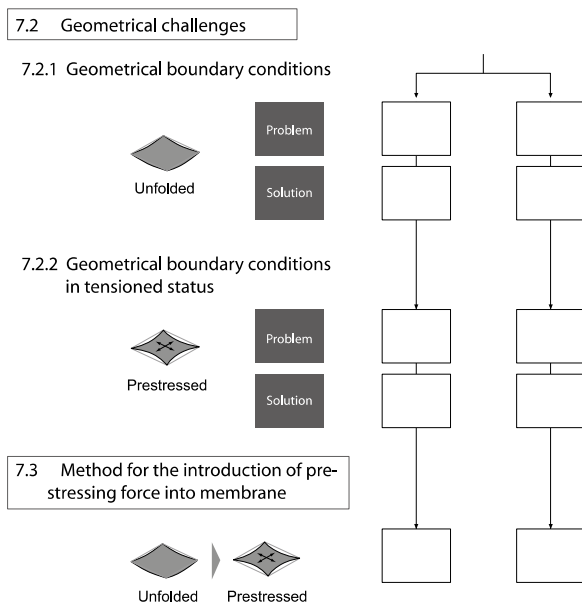


Figure 7.2 Diagram of design flow and the corresponding number of the section

7.2. Geometrical challenges

7.2.1. Geometrical boundary conditions

The main issue for the foldable membrane roof with spoked wheel structure folding from inside to outside lies in the geometrical boundary conditions of the textile membrane against the radial arrangement of a primary structure. First the geometrical compatibility of a whole continuous membrane and spoked wheel structure will be discussed. Then one membrane strip will be focused on, and its compatibility will be cleared.

The geometrical compatibility of a whole continuous membrane and spoked wheel structure

The essential question for opening the membrane roof from the inside to the outside is a geometrical one. In the closed situation the whole area should be covered with one continuous membrane, because joints in the surfaces of textile membrane are a weak point regarding maintenance as well as water and wind tightness. However, already simple geometry shows that a flat continuous membrane is not able to move towards the outer edge of the roof, because the length of the membrane in the direction of circumference changes along the radius.

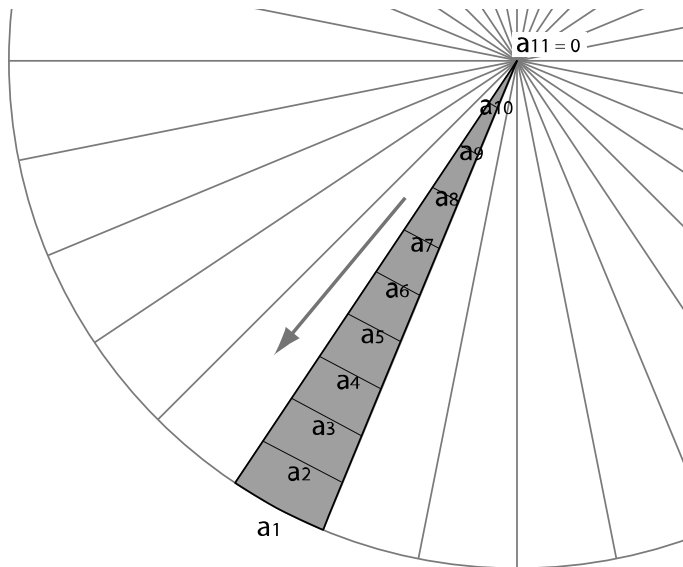


Figure 7.3 A strip, a part of continuous membrane roof and the width a

The gray area in Figure 7.3 presents a part of the continuous membrane and a_m indicates the width of a membrane strip, starting with $m=1$ on the outside. To open the roof to the perimeter, the width a_{m+1} must be always greater than or equal to the width a_m . Therefore, two variations of the shape of membrane strip can be conceived: one is the case of $a_m = a_{m+1}$, in which the form becomes rectangular. The other case is $a_m < a_{m+1}$, in which the form is trapezoidal. For further development the rectangular membrane strip is chosen here because it is the most economical shape.

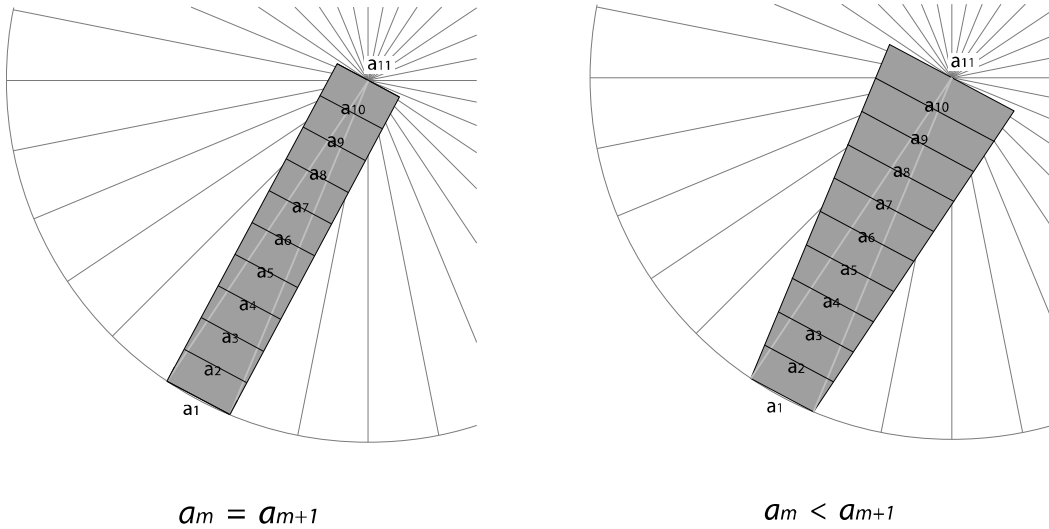


Figure 7.4 Possible membrane strips with the width a

Here a width of a rectangular membrane strip a is calculated as:

$$a = \frac{c}{n} = \frac{2\pi \cdot r}{n} \quad (7.1)$$

where c : Circumference of the roof
 n : Number of radial cables

When membrane strips are rectangular, a continuous membrane covering the whole roof's area has the form of a cylinder. It stands on the circumference of the roof and is folded down towards the centre of the roof. Then the height h of the cylinder will be nearly equal to the radius r .

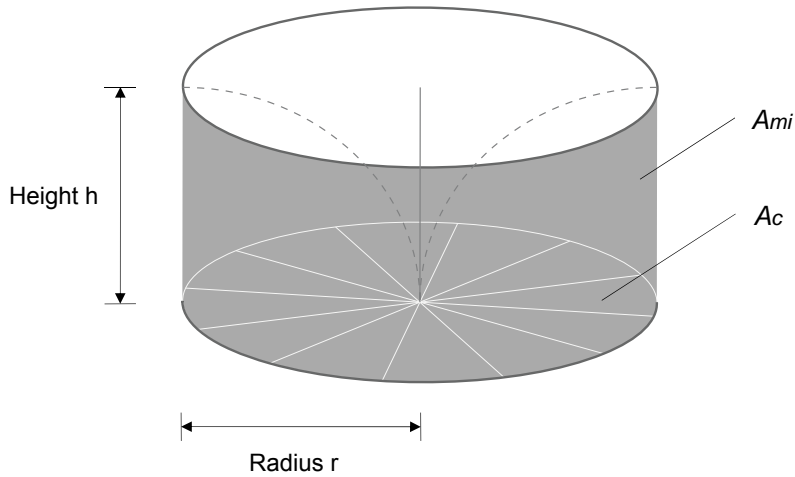


Figure 7.5 A minimal required membrane cylinder composed of rectangular strips

The minimum amount of membrane that requires covering a whole area of the roof by this means is approximately calculated as:

$$A_{\min} = \text{Circumference} \times \text{Height} = 2 \cdot \pi \cdot r \times h = 2 \cdot \pi \cdot r \times r = 2 \cdot \pi \cdot r^2 \quad (7.2)$$

The required area to be covered by textile membrane corresponds to the bottom face of the cylinder:

$$A_c = \pi \cdot r^2 \quad (7.3)$$

Therefore,

$$A_{\min} = 2 \cdot A_c \quad (7.4)$$

From this simple calculation we can recognize that at least double the amount of material is required to cover the surface area by this means.

The next question is how this rectangular strip can be converted to the triangle shape needed to cover the spoked wheel structure. One of the simplest ideas is that the membrane strip is folded to fit to the form of the radial spokes. If one rectangular membrane strip is folded along the two adjacent radial lines as shown in Figure 7.6, the height of the roof in the centre is half of the width of membrane strip, because the edge in a_{11} is folded in the middle and overlapped.

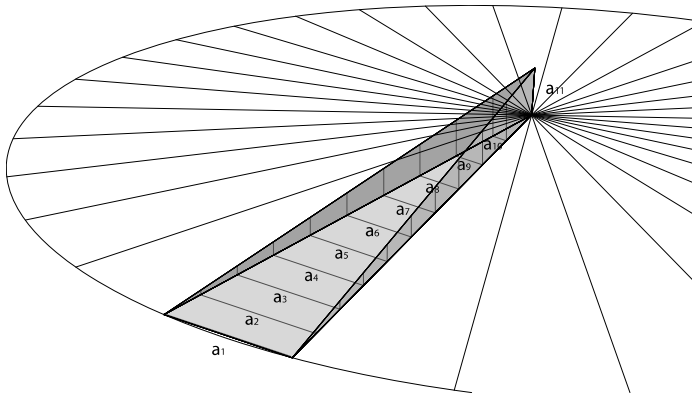


Figure 7.6 A membrane strip folded to fit to a radial form

The cylindrical membrane is divided into rectangular strips. To allow the membrane to fold, not only should the long sides be straight, but also the outer edge. But then the actual form is not a circular cylinder, instead it is a polygonal cylinder, as seen from the top. As shown in Figure 7.7, the straight line of the outer edge of the membrane strip works as an axis of rotation..

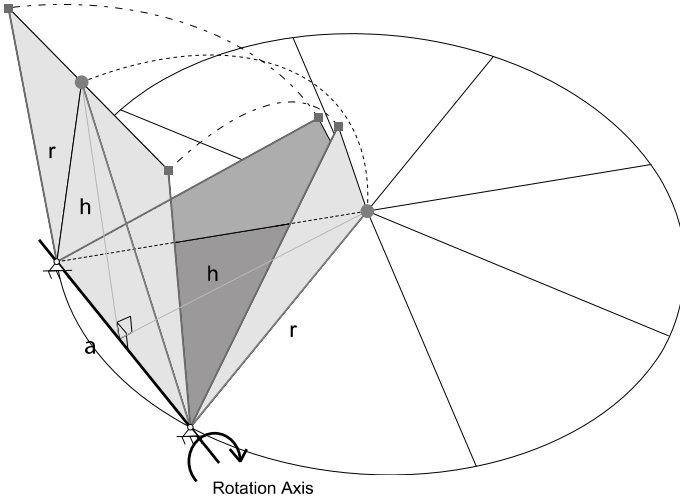


Figure 7.7 The rotation of one strip of a continuous membrane

Accordingly the height of the continuous membrane h cannot be equal to the radius of the roof r , because the height h must be perpendicular to the rotation axis. They are expressed from Pythagorean Theorem:

$$r^2 = \left(\frac{a}{2}\right)^2 + h^2 \quad (7.5)$$

With substitution of (7.1) h becomes:

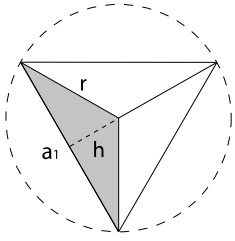
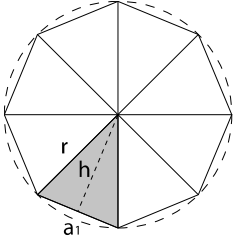
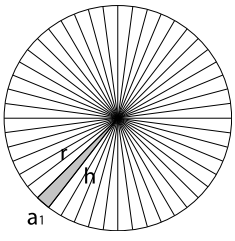
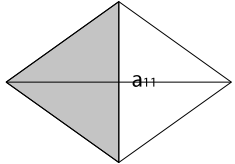
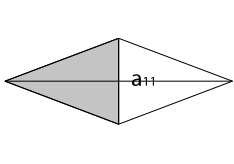
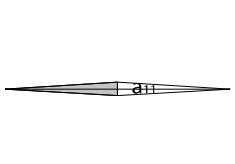
$$h = \sqrt{1 - \frac{\pi^2}{n^2}} \cdot r \quad (7.6)$$

When n is very large, the height of the cylinder h is nearly equal to the radius r , therefore the roof shape becomes circular. On the other hand when n is very small, the difference between h and r is large then the shape of the roof becomes polygonal that is far from desired circular shape.

Also, the width of a membrane strip a , which is determined by the number of radial cables n with equation (7.1), determines the height of the roof in a closed configuration. A small number of n leads to a large value for a_1 . Since the membrane strip is a rectangular form, a large value for a_1 means a large value for a_{11} , which leads to a large height of the roof. A small value for a_1 leads to a small value for a_{11} , and then the height of the roof becomes also small.

Thus the number of radial cables n directly determines the geometry of a roof and should be decided based on structural- and esthetical considerations as described in Table 7.1.

Table 7.1 Geometrical change according to the number of radial cables

Number of radial cables n	Minimum ($n=3$)	(Polygonal form)	Maximum ($n = \text{infinite}$)
Top view	 $h \neq r$		 $h \cong r$
Side view			
Structural point	<ul style="list-style-type: none"> - larger dimension of radial cable (large load is transmitted) - significant higher membrane stress and higher possibility of ponding due to the large span 		<ul style="list-style-type: none"> - smaller dimension of radial cable - less membrane stress and less ponding threat
Esthetical point	<ul style="list-style-type: none"> - polygonal form - more transparent (less number of cables) - large height of a spoked wheel 		<ul style="list-style-type: none"> - circular form - cables becomes obstacle from the ideal view - small height

Also the geometrical compatibility of the continuous membrane and the spoked wheel structure must be considered. There are two types of spoked-wheel structures as described in Chapter 6: one has one compression ring on the outer edge and two tension rings in the centre, the other has one tension ring in the centre and two compression rings in the outer edge. As shown before, the height of the closed roof seen in the cross section needs to increase toward the center of the roof due to the described geometrical folding conditions. Therefore, a cylindrical continuous membrane can be effectively combined with the first type of spoked wheel structure: one outer compression ring and two inner tension rings. Here the textile membrane can be guided by both upper and lower radial cables. It is safer against the uplifting wind in the transition state of the textile membrane. If a cylindrical continuous membrane is combined with the second type of spoked wheel structures - two outer compression rings and one inner tension ring - the membrane is guided only by the lower radial cables of the spoked wheel structure and is relatively free against wind load not only in deployed state but also in transition state, which demands more careful operations for opening and closing the roof.

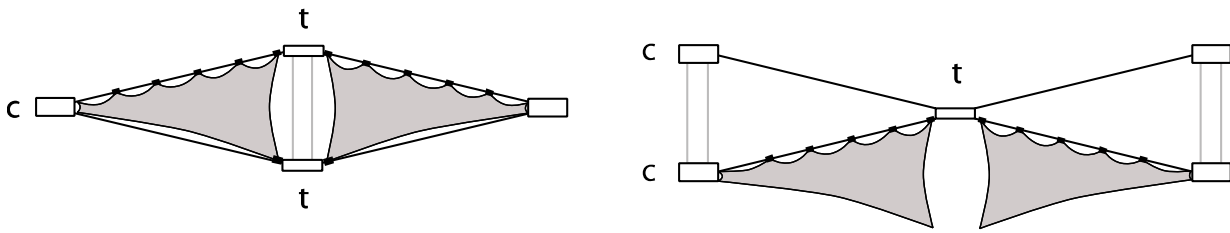


Figure 7.8 Possibilities of the combination of spoked wheel structure and membrane and the drain lines (c: compression ring, t: tension ring)

The drain path is also essential for the determination of the geometry. The folded membrane has ridge and valley lines, and rain water always runs along the valley lines. Therefore, if the valley line is sloping down toward the centre of the roof, special attention must be paid. There are simply two possibilities: one is adding pipes sloping down to the outer edge of the roof for draining off rainwater. The other is changing the geometry of the roof. The centre of the roof is hoisted up until the valley lines of the surface becomes horizontal or leaned down toward the outer edge of the roof. This may require additional radial cables. The compatibility of membrane and spoked wheel structures and drain system must be always taken into account.

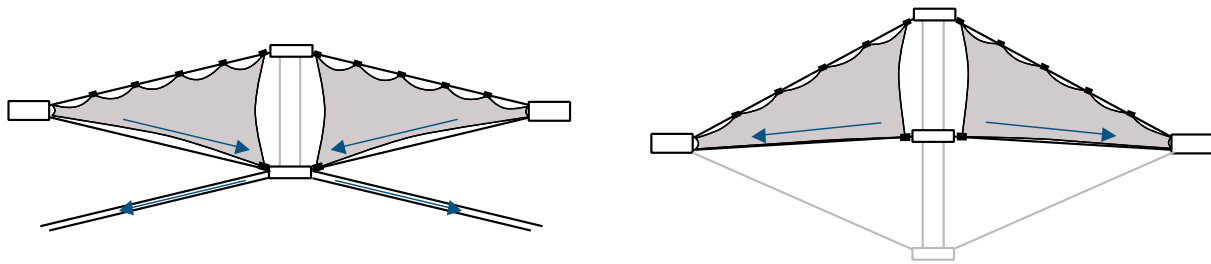


Figure 7.9 Two possibilities for a drain path, if valley line of the roof surface is sloping down toward the centre of the roof (Left: adding pipes for draining off rainwater, Right: changing the geometry with additional radial cables)

The cylindrical continuous membrane roof can be unfolded in both upward and downward directions. But it is obvious that if the membrane roof is opened in an upward direction, it is exposed high wind pressure in the horizontal direction, and if opened in a downward direction, it remains inside the building and will become an obstacle. Thus it is clear that this cylindrical textile membrane must be folded in the vertical direction as well.

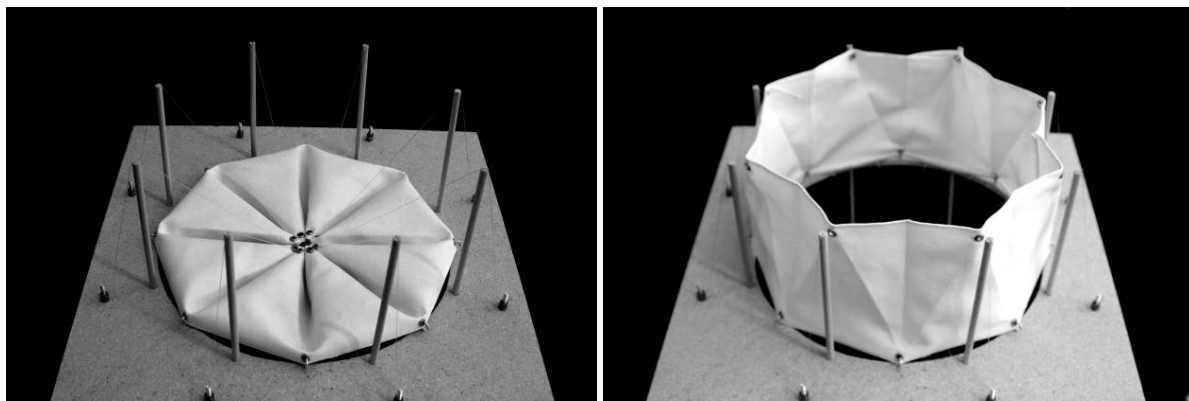


Figure 7.10 Physical model: opened in the upward direction

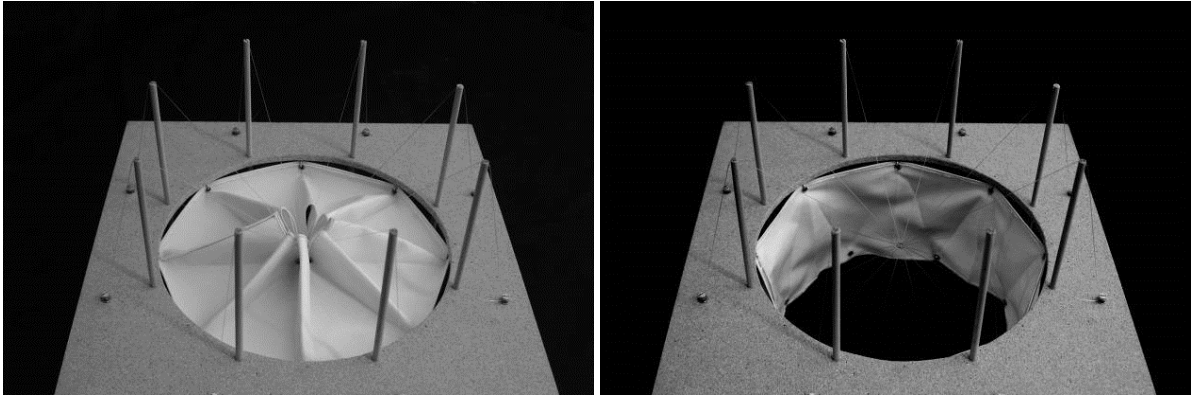


Figure 7.11 Physical model: opened in the downward direction

This can be easily solved if the rectangular membrane strip is twisted by 90 degrees instead of folding. A membrane strip will be gradually inclined from the edge of the roof toward the centre, and at the centre it stands perpendicular to the plane of the roof. The result of this twisting method is the same as the folding method as shown above. The difference is only whether the lower long edge of membrane strip is constrained by the radial cable or not.

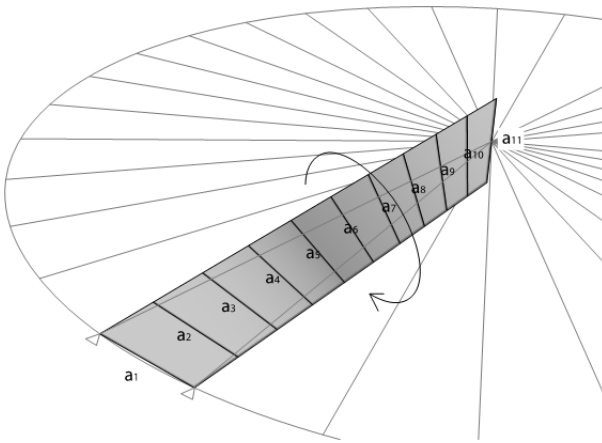


Figure 7.12 A rectangular strip with the width a twisted in clockwise direction

When one strip is twisted in a clockwise direction, the adjacent strips must be twisted in a counter-clockwise direction so that the textile membrane can be continuous. Therefore, radial cables need to be arranged up and down and the continuous membrane has ridge and valley lines forming a wave like shape.

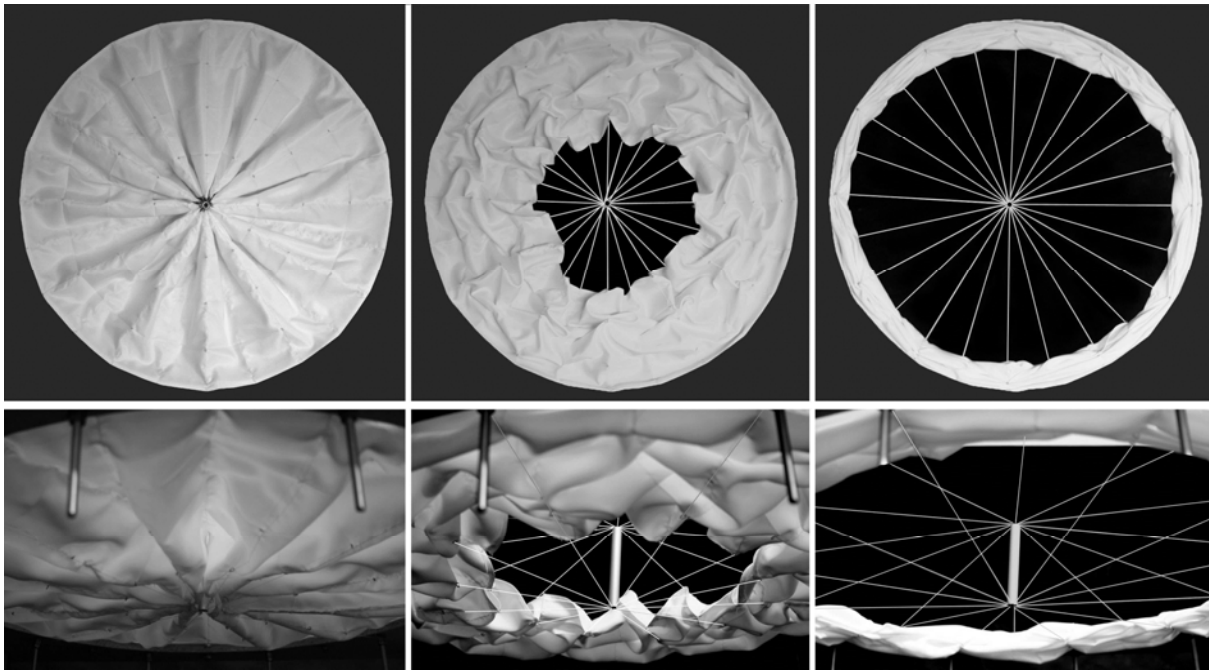


Figure 7.13 A physical model of a membrane retractable roof using the ‘twisting’ method (left: closed configuration, right: open configuration)

Felix Escrig and Jose Sanchez constructed a retractable roof of the bullfight-ring in Jaén, Spain in 1998 by the means described in Chapter 2. The height of the central flying mast was longer than the minimum requirement of the membrane in its unfolded state, in order to permit the membrane to fold between the upper and lower radial cables at the perimeter. A shorter flying mast would mean that the membrane bundle would touch the lower radial cable and could be damaged easily when it was folded. But anyway the textile membrane was not folded completely at the outer edge of the inner roof but was instead slightly inside, as shown in Figure 7.14 left. The gap between inner retractable roof and stationary outer roof was covered by additional fabrics, as shown in Figure 7.14 right.

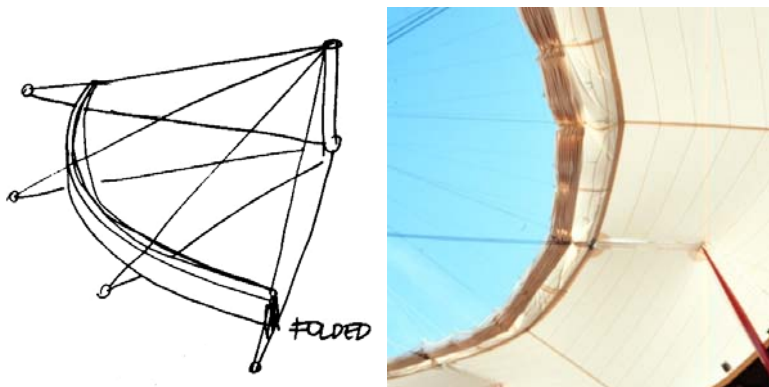


Figure 7.14 The position of the bundle of textile membrane (Left), Membrane textile covered the gap between inner and outer roof (Right) (courtesy of Felix Escrig)

The geometrical compatibility of a membrane strip and spoked wheel structure

Challenge

Another geometrical challenge is that the minimum distance between two adjacent straight radial cables is not constant along the cables. The figure projected to the perimeter of the roof (left in Figure 7.15) makes it clear: whereas the width a_1 and a_{11} are a , the widths from a_2 to a_{10} are smaller than a .

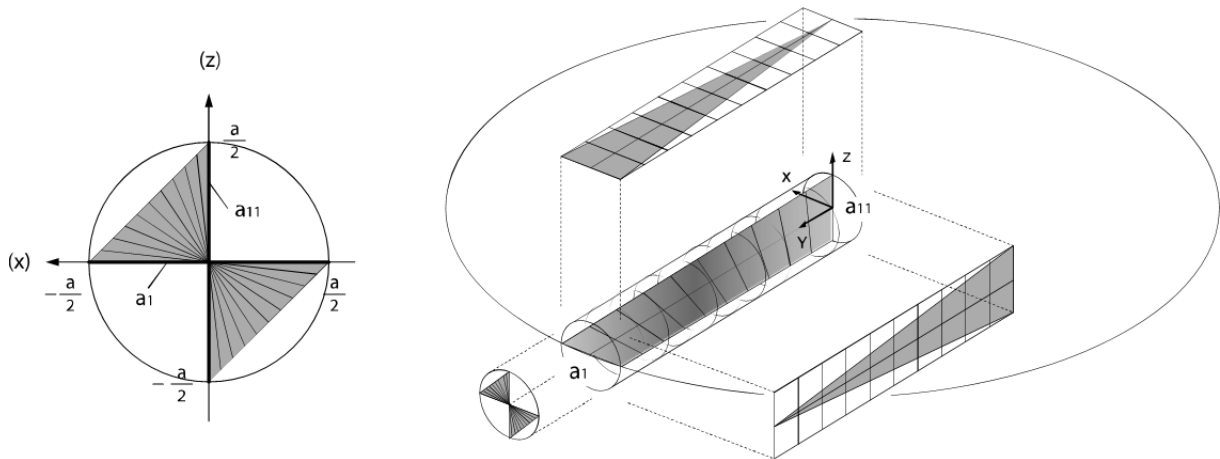


Figure 7.15 Figure projected to the perimeter of the roof (Left). Three-dimensional figure of a twisted membrane strip (top view, side view and view from the perimeter) (Right)

Accordingly, the distance between two radial cables becomes smaller in middle of the cables. Therefore, the form of the membrane strip becomes a ‘waisted’ shape.

This curve can be seen using a physical model. All elastic strings of the physical model in Figure 7.16 are straight in space, even after the two circular discs are rotated against each another around the central bar. It is clear that the distances of any two strings are smaller in the middle of the central bar. The same applies to the roof, in which the distance between two adjacent straight radial cables are closer in the middle and, therefore, the shape of membrane strip between the cables has to be waisted.

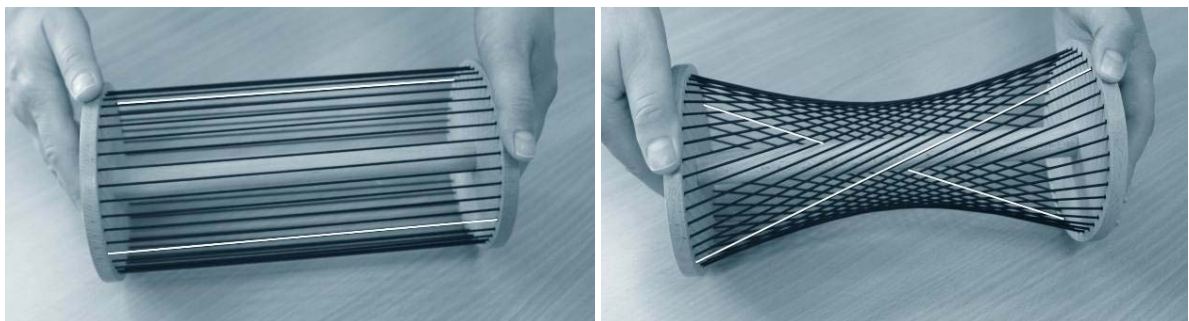


Figure 7.16 A mathematical model called a hyperboloid

Accordingly, the waisted curve can be expressed using the formula of a hyperboloid of one sheet as follows. In mathematics, a hyperboloid is a surface in three dimensions that can be

described by the equation with the twisted angle θ , the width of the membrane strip a , and the radius of the roof r :

$$\frac{x^2 + z^2}{\left(\frac{a}{2}\right)^2 \cdot \cos^2\left(\frac{\theta}{2}\right)} - \frac{\left(y - \frac{r}{2}\right)^2}{\left(\frac{r}{2}\right)^2 \cdot \cot^2\left(\frac{\theta}{2}\right)} = 1 \quad (7.7)$$

The original point of the coordinate above is set in the center of the roof. The value of y is the distance from the center of the roof to the outer edge as shown in Figure 7.17.

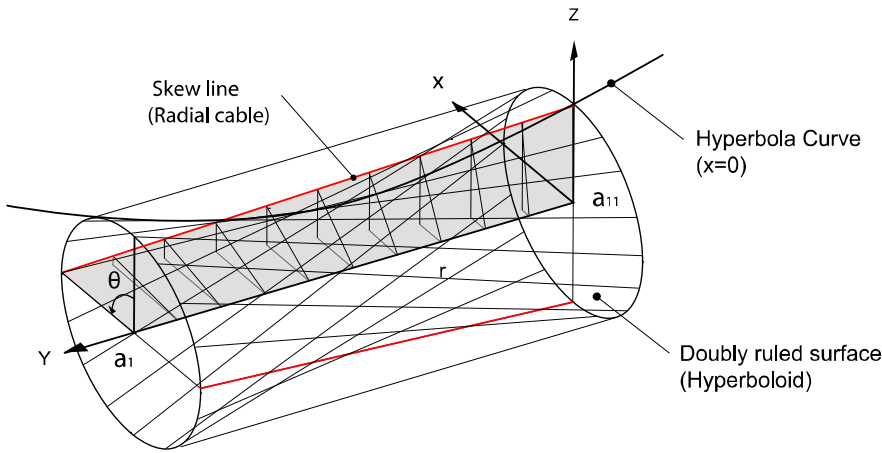


Figure 7.17 3-D Diagram of hyperboloid with the twisted angle θ

Since a hyperboloid of one sheet is a doubly ruled surface, it can be defined by the revolution of not only a skew line but also a curve (hyperbola), around its one central axis. When a constant value for x or z is taken in equation (7.7), then an equation of a hyperbola can be obtained to express the waisted curve of the membrane strip. With $x=0$ in (7.7), for instance:

$$\frac{z^2}{\left(\frac{a}{2}\right)^2 \cdot \cos^2\left(\frac{\theta}{2}\right)} - \frac{\left(y - \frac{r}{2}\right)^2}{\left(\frac{r}{2}\right)^2 \cdot \cot^2\left(\frac{\theta}{2}\right)} = 1 \quad (7.8)$$

With $\theta = 90^\circ$, radial cables can be drawn as in Figure 7.18. However this figure does not show the cutting pattern of a membrane strip but the group of the lines of distance between two adjacent straight radial cables.

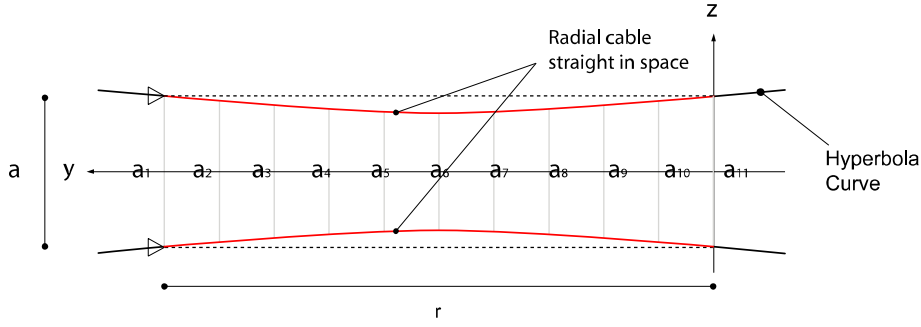


Figure 7.18 Distance between two straight radial cables

The critical problem of this “waisted” form is the movability of the membrane strip. Figure 7.18 shows that the width a_6 is smaller than a_5 , therefore, it cannot be fully moved to the perimeter.

If the membrane strip stays rectangular, we need to achieve the geometrical compatibility between the radial cables and rectangular membrane strip.

The edge lines of the long sides of the rectangular membrane strip can be expressed as follows. The curve is expressed by $f(y)$, corresponds to $[x]$ on a projected plane of top view and $[z]$ of side view, when the coordinate system is set the same as in Figure 7.15.

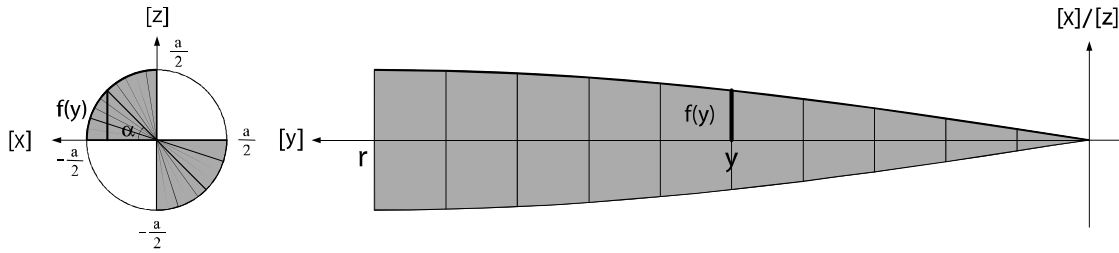


Figure 7.19 Figure projected to the perimeter of the roof (left). One projected to the top and side (right)

The function $f(y)$ is expressed also in the view from the perimeter of the roof as shown in left diagram in Figure 7.19. When the inclination of the narrow side of a membrane strip from the level of the roof's surface is expressed as a degree of angle α , $f(y)$ is as follows:

$$f(y) = \frac{a}{2} \cdot \sin \alpha \quad (7.9)$$

The inclination angle α is in proportion to y and when $\alpha = 0^\circ$, $y=0$ and when $\alpha = 90^\circ$, $y=r$. Therefore α can be expressed with y :

$$\alpha = \frac{90}{r} \cdot y \quad (7.10)$$

(7.9) becomes with substitute of (7.10):

$$f(y) = \frac{a}{2} \cdot \sin\left(\frac{\pi}{2r} \cdot y\right) \quad (7.11)$$

Thus the edge lines of the long side of a membrane strip are spatial curves and can be expressed as a sine curve in projection as shown Figure 7.20 below. Certainly some smooth

stretching of both long sides of the strip must be considered. To be precise, this twisted membrane strip is not any more rectangular. The sum of inner angles of area bounded by two adjacent width of membrane strip and two radial lines is not 360 degrees.

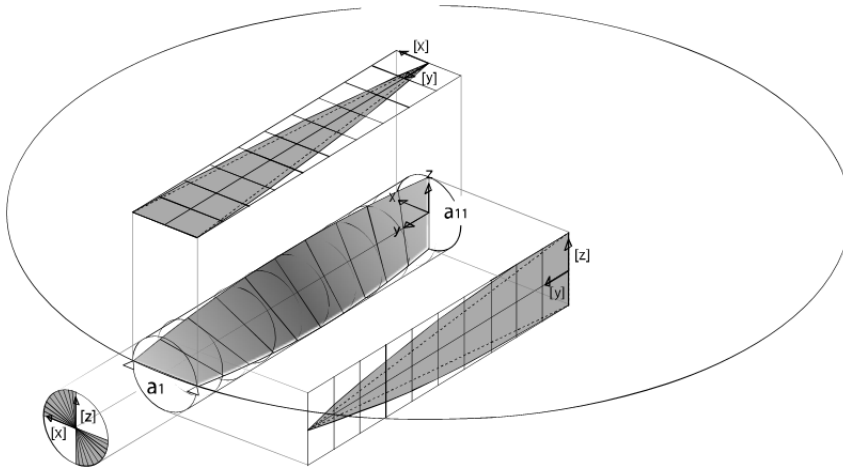


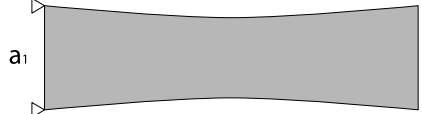

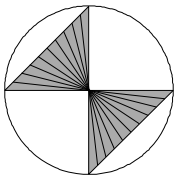
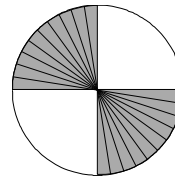
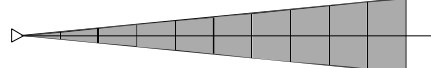
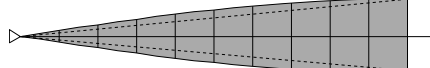
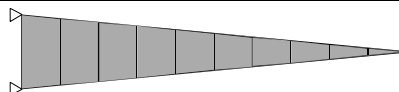
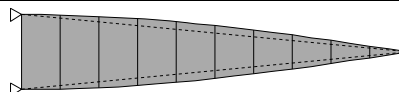
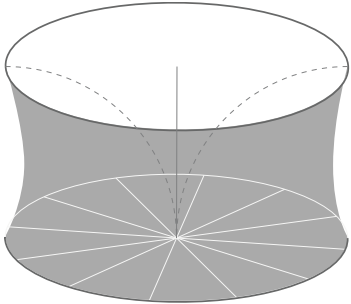
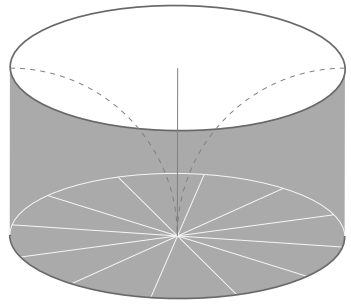
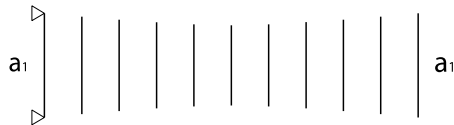
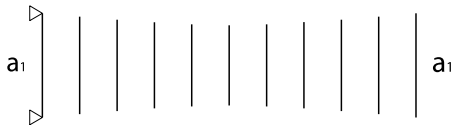
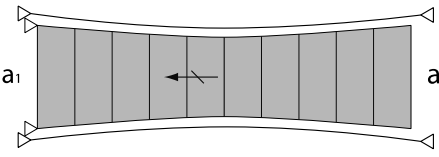
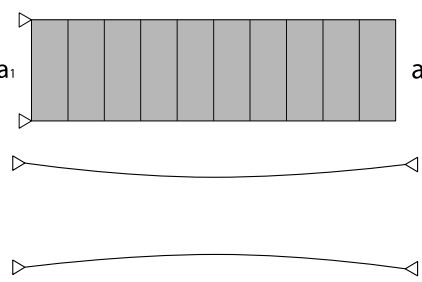
Figure 7.20 Three-dimensional figure (top view, side view and view from the perimeter)

A geometrical issue of this curve is that it is not compatible with the straight lines of radial cables. Also one membrane strip cannot be connected to the adjacent strip to make a continuous membrane roof.

Consequently, it becomes clear that there is an interdependency between the shape of the membrane strip and the shape of the boundary cable. These interdependencies are summarized in Table 7.2. If the membrane strip has a “waisted” shape, it can be fitted to the boundary cables. But a movement outwards is not possible, because it has the shortest width in the middle of the strip. This case of the waisted strip is shown in the left column in the table.

Vice versa, a membrane strip with rectangular shape may be moved but it cannot be fitted to the boundary cables arranged in space as radial cables of spoked wheel structure. They are straight in space, but the distance between two adjacent boundary cables is not constant. The case of the rectangular membrane strip is shown in the right column in the table.

Table 7.2 Two types (waisted and rectangular) of membrane strips and respective geometric problems

	Waisted membrane strip	Rectangular membrane strip
Form of the membrane strip		
view from the perimeter		
side view		
top view		
Appearance of the whole continuous textile membrane		
Distance between adjacent radial cables		
A membrane strip and the boundary cables		
Form compatibility	OK	Not good
Membrane movable	Not good	OK
Problem	Cannot move outwards	Curved lines of long side of a membrane strip are not compatible with the straight lines of radial cables

Solutions

There are several approaches to overcome these geometrical challenges. One approach for the waisted membrane strip is to take only half of the membrane strip since the problem is that the shortest width occurs in the middle. If only the half of membrane strip is used, then the membrane strip has the shortest width on the edge of the roof and movement becomes possible. A possible approach for the rectangular strip is to change the form of radial cable by adding other structural elements. The form of the cable girder fit to the rectangular shape of membrane strip was investigated. These two approaches will be described in the following pages.

The geometrical solution for the waisted membrane strip (Half membrane strip)

The problem of the waisted membrane strip is that the shortest width is in the middle of the membrane strip. Therefore, one of the simplest ideas is to set the outer edge of the roof in the middle of the membrane strip. This is the same as taking half of the waisted membrane strip. Thus the membrane strip has the shortest width on the edge of the roof and consequently the problem of the movability would be eliminated.

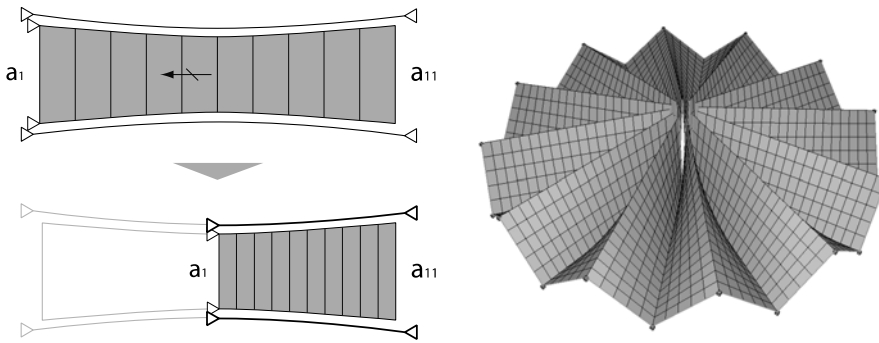


Figure 7.21 An idea to use half of a membrane strip (left) and an appearance of the whole roof (right)

This is geometrically synonymous with another approach: a membrane strip is twisted 45 degrees and the length of the width a_{11} is decided to satisfy the required geometrical condition $a_m \leq a_{m+1}$. From this it becomes clear that the different twisting angle θ gives the different required width a_{11} . Of course, if the membrane strip is twisted less than 90 degrees, the edge of the membrane strip at the outer edge of the roof a_1 must be inclined against the roof's surface. The line of the outer edge of the roof becomes zigzag as shown in Figure 7.21. This zigzag form requires additional considerations for the compression ring.

When the value of θ ranges 0 from 90 degrees, each minimum required width a_{11} will be calculated as follows. The left diagram in Figure 7.22 shows the view from the perimeter. The radius of the inner small circle is set to a_1 and the one of the outer large circle is a_{11} . To satisfy the required condition $a_m < a_{m+1}$, the point on the z-axis of the large circle is connected tangentially to the point A of the small circle. This connecting line becomes the edge line of the membrane strip of the long side. α is the inclined angle against the roof's surface at the outer edge of the roof, and in this approach the following must be always satisfied: $\alpha + \theta = 90$.

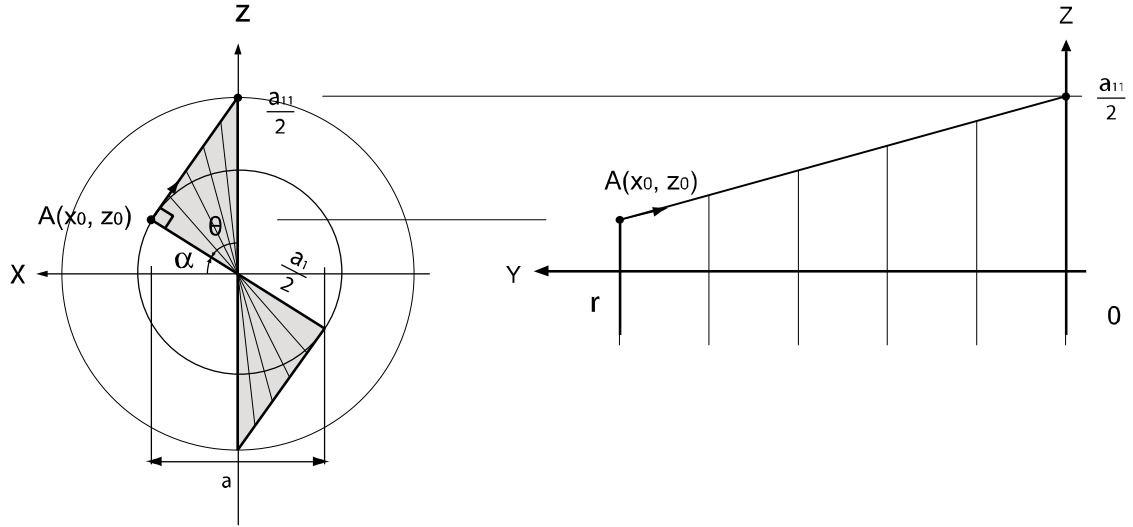


Figure 7.22 Diagram showing view from the perimeter (left). The edge line of the long side of the membrane strip on the vertical plane (V) extruded from a straight line of the radial cables (right).

The equation of the line on the tangential point $A(x_0, z_0)$ can be calculated using the equation of a circle:

$$x_0 \cdot x + z_0 \cdot z = \left(\frac{a_1}{2}\right)^2 \quad (7.12)$$

Then it becomes:

$$z = -\frac{x_0}{z_0} \cdot x + \frac{\left(\frac{a_1}{2}\right)^2}{z_0} \quad (7.13)$$

Since the point A lies on the circle, it can be also expressed as:

$$\begin{cases} x_0 = \frac{a_1}{2} \cdot \cos \alpha \\ z_0 = \frac{a_1}{2} \cdot \sin \alpha \end{cases} \quad (7.14)$$

The intersection point of the tangent line and the z-axis becomes the half of the width of the membrane strip at the center of the roof a_{11} . With the substitution of (7.14), the equation (7.13) becomes:

$$\frac{a_{11}}{2} = z(x=0) = \frac{\left(\frac{a_1}{2}\right)^2}{\frac{a_1}{2} \cdot \sin \alpha} = \frac{\frac{a_1}{2}}{\sin \alpha} \quad (7.15)$$

And then,

$$a_{11} = \frac{a_1}{\sin \alpha} \quad (7.16)$$

At the same time, the width of one membrane strip must be a on roof's surface, therefore:

$$a_1 = \frac{a}{\cos \alpha} \quad (7.17)$$

With the substitution of (7.17), equation (7.16) becomes:

$$a_{11} = \frac{a}{\sin \alpha \cdot \cos \alpha} = \frac{2a}{\sin 2\alpha} \quad (7.18)$$

The diagram of the equation (7.17) for a_1 and (7.18) for a_{11} is drawn in Figure below.

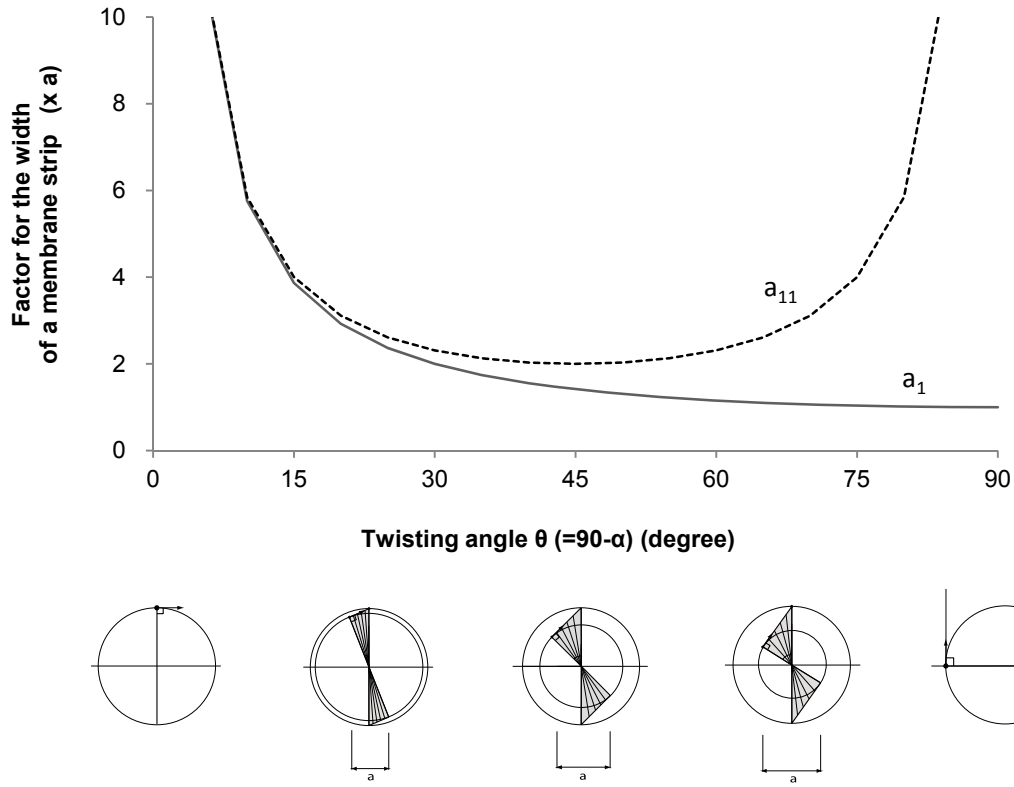


Figure 7.23 Required width of the membrane strip against the different twisting angle of the membrane strip

The curve of a_1 is 1.0 when $\theta = 90^\circ$, but it goes to infinity when $\theta = 0^\circ$. The curve of a_{11} goes to infinity when $\theta = 0^\circ$ and when $\theta = 90^\circ$. The curve of a_{11} gets the minimum value of 2.0 when $\theta = 45^\circ$. This corresponds to the one of the half strip approach. Consequently it can be said that the half strip approach is most economical for the width a_{11} .

This diagram also provides an answer for the frequently asked question: when the membrane strip is twisted 90 degrees and its width at the centre of the roof becomes much larger than the one at the outer edge, is it possible that two required conditions (a membrane strip forms 'waisted' by the straight edge line and its width is $a_m < a_{m+1}$) can be simultaneously satisfied

as shown in Figure 7.24? From the fact that a_{11} becomes infinite for $\theta = 90$ in the diagram in Figure 7.23, it becomes clear that this cannot occur.

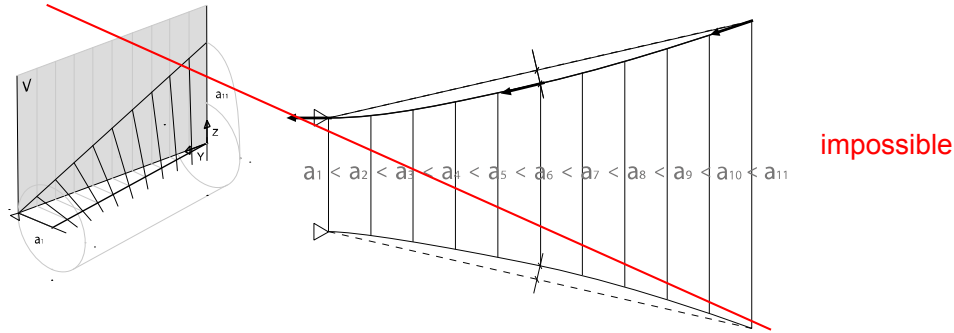


Figure 7.24 The 3-D diagram and the imaginary plane between two adjacent radial cables

By twisting 45 degrees, the length a_1 must be $\sqrt{2}a$. Consequently the length a_{11} in the center becomes $2a$.

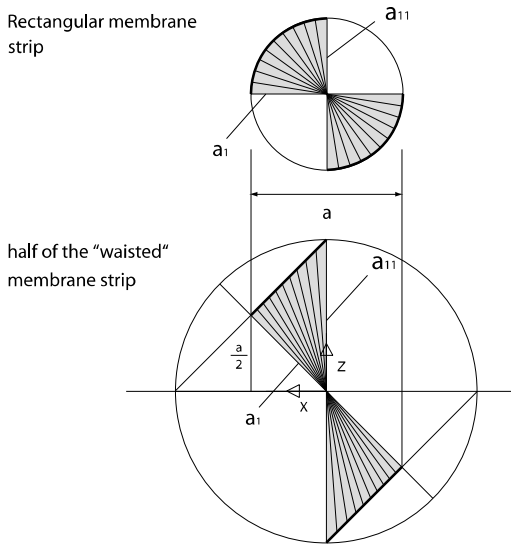


Figure 7.25 Diagrams in view from the perimeter

Thus it becomes clear that a bigger amount of textile membrane is required. The amount of the area of the half strip can be approximately calculated with the integration of the equation (7.8) with $\theta=45$.

$$A_{\text{halfstrip}} = 2 \times \int_r z \cdot dy = 2 \cdot \left(\frac{a}{2}\right)^2 \cdot \cos^2\left(\frac{\theta}{2}\right) \times \int_r \sqrt{1 + \frac{\left(y - \frac{r}{2}\right)^2}{\left(\frac{r}{2}\right)^2 \cdot \cot^2\left(\frac{\theta}{2}\right)}} \cdot dy \quad (7.19)$$

When the amount of the triangle area between the two radial cables (equal to the gray are in Figure 7.3) is quantified as 1.0, the required area for the rectangular membrane strip is 2.0 as discussed with the equation (7.4). The amount of the area for the half strip is 3.2.

The geometrical solution for the rectangular membrane strip (Cable girder)

Using a rectangular membrane strip and changing the form of the cables is a simple and feasible geometrical solution. Similar basic studies were also done by Kühner in [2001] and schlaich bergemann und partner in 2008 [Pae]. In this thesis this principle is analyzed in depth and its compatibility is checked through a physical model.

When using a rectangular membrane strip the essential question will be the description of the spatial curved form of the long side edge as described above. Therefore, if their projected lines can be straight in top view, a rectangular strip can be employed. The following will explain how to reach this. Due to the twisting of the membrane strip, an exact rectangular membrane strip cannot be used and a modification of this shape is needed. Therefore, the rectangular membrane strip will be approximated as the group of lines shown in Figure 7.26 with gray lines. They have all the same length in correspondence to the width of the membrane strip. When these lines are twisted around a central radial line, it is obvious that the movement of the lines follows the surface of a cylinder. Thus the boundary line we are searching for lies on the surface of the cylinder. Certainly, the shape of this membrane strip is not rectangular any more. But it allows the movability.

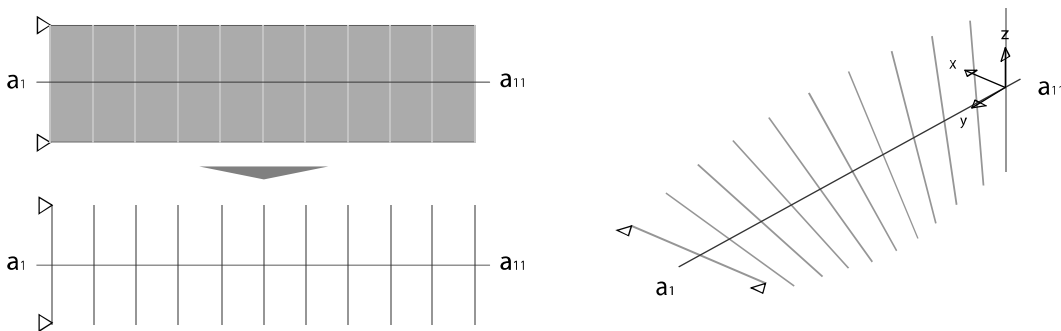


Figure 7.26 Changing a rectangular membrane strip

The next issue is the shape the curve of the boundary edge. If the cylinder is cut by a vertical plane raised up from the desired ideal straight line of the radial cables, one curve appears on the cut surface (Figure 7.27).

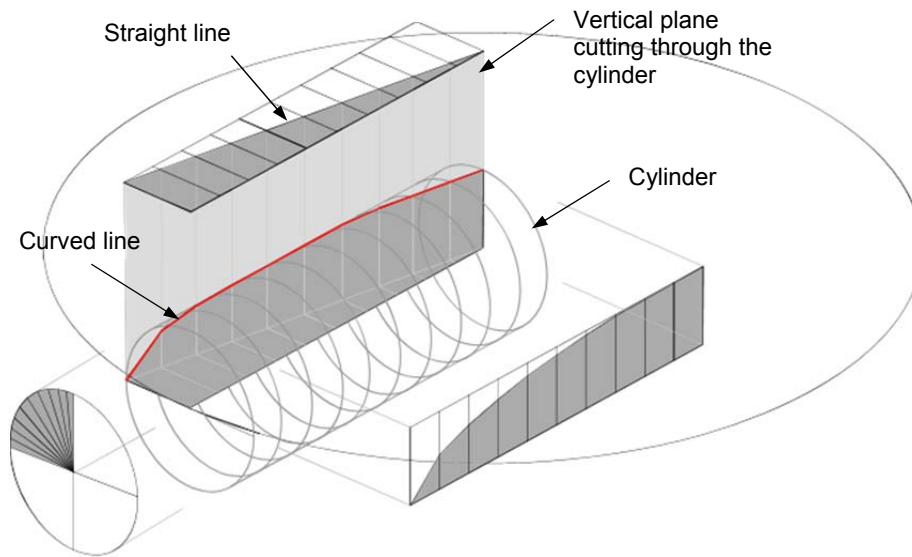


Figure 7.27 A rectangular membrane strip with ellipse curve

This curved line on vertical plane (V) can be expressed by the Cartesian geometry as follows.

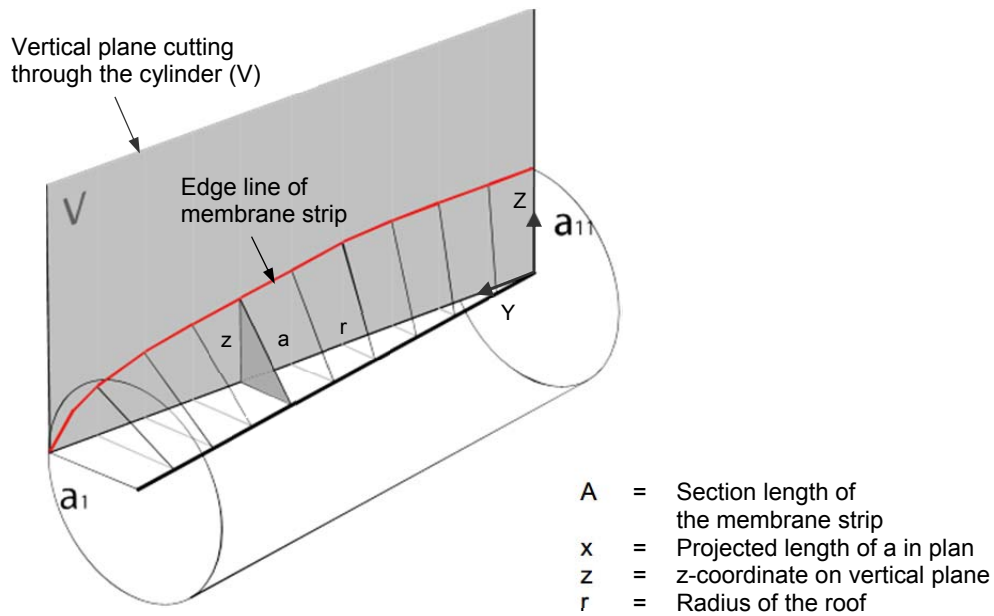


Figure 7.28 Mathematical ellipse form

The projected length x can be calculated as homologous deformation:

$$x = \frac{y \cdot a}{r} \quad (7.20)$$

From Pythagorean Theorem:

$$z^2 = a^2 - x^2 = a^2 - \frac{y^2 \cdot a^2}{r^2} \quad (7.21)$$

Therefore:

$$\frac{y^2}{r^2} + \frac{z^2}{a^2} = 1 \quad (7.22)$$

This corresponds to the equation of the ellipse. In mathematics, the types of curves obtained by intersecting a cylinder are a pair of parallel lines or an ellipse, in which the circle is a special case of the ellipse. Using this elliptical curve for the edge line of a membrane strip, both the movability of textile membrane and the geometrical compatibility between membrane and radial cables can be achieved.

The required area for this membrane strip is approximately 2.0 against 1.0 of the triangle area in Figure 7.4. The form of the membrane strip is not any more rectangular but the dimensions remain almost the same. The membrane strip can be twisted around the axial line in the center as well as around the edge as shown Figure 7.29.

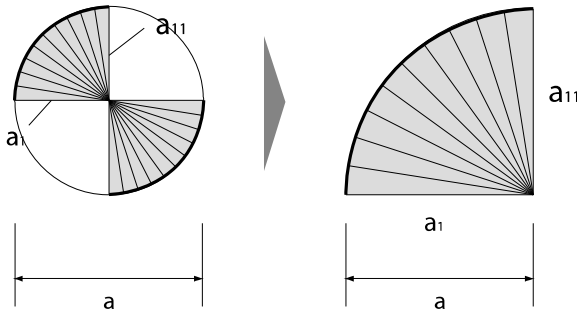


Figure 7.29 Changing axis of twisting from the center to the edge in a two dimensional diagram from the perimeter

7.2.2. Geometrical boundary conditions in tensioned status

In the last section, two approaches to deal with the geometrical challenges were described. One approach is for the waisted membrane strip, and the solution is to take half of the membrane strip. The second approach is for the rectangular strip, and the solution is to change the form of radial cable by adding other structural elements.

As the next step, these geometrical boundary condition need to be discussed under the consideration of the unique characteristic of tensioned fabric. Any textile membrane must be tensioned to work as a structure having sufficient stiffness. Form and stress distribution is indivisible for membrane structures.

7.2 Geometrical challenges

7.2.1 Geometrical boundary conditions



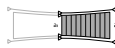
Unfolded

Problem

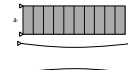
Solution



„Waisted“ form
Unable to move
outwards



Half strip



„Rectangular“ form
Incompatible with
radial cables



Cable girder

7.2.2 Geometrical boundary conditions in tensioned status



Prestressed

Problem

Solution



Figure 7.30 Design flow up to the geometrical boundary conditions

The major geometrical problem of folding of tensioned fabric is described by Frei Otto and his team: *If one does not wish to hang the membranes loosely between the cables but rather wisher to pretension them, geometric problems become a major factor. A membrane attached at the edges and hung between two parallel cables slackens more and more as it is slid toward the middle. A membrane which is folded together in the middle can be evenly extended toward both sides and accordingly stretched. In this form, it cannot be moved to the side without becoming overextended.* [Ott 72]

Figure below shows that the pretensioned fabric between two parallel cables is folded in the middle. Clearly the problem is again the waisted form of a membrane strip. But here “waisted” arises not from the geometry but from the condition of prestressing force. Thus the challenges and solution for the half strip- and for the cable girder approach need to be discussed.

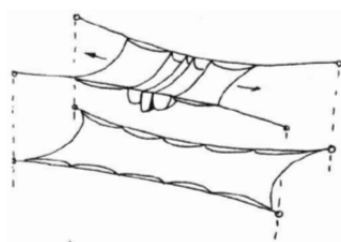


Figure 7.31 pretensioned fabric between two parallel cables cannot folded to the side but only folded in the middle [Ott 72]

Challenge of the half strip approach and its solution

A critical issue of the half strip approach is the pretensioning of the textile membrane. When pretensioning all boundary edge lines of a membrane strip are not straight but need to be curved: the upper edge line of the long side forms a concave curve and the lower edge line is convex curve. But such a shape of the membrane strip does not fulfill the required condition $a_m < a_{m+1}$, because it has the shortest width in the middle. Also all edge lines in the long side of the membrane strip were assumed as straight lines, but due to their self-weight the boundary cables are physically not possible to be straight.

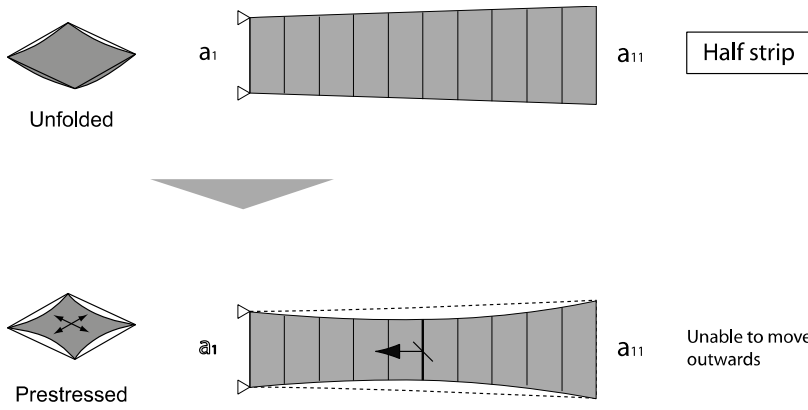


Figure 7.32 Problem of the half strip approach

Therefore, it is clear that if using the half strip, some special ways of introducing prestressing force must be considered. Physical approaches can be considered as following: One is adding ballast on the lower cables. This is like a stressed ribbon bridge which is stiffened by a comparable heavy concrete deck. Form stability is achieved by pretensioning through loading. Another idea is adding a cable into the membrane strips that forms a curve with negative curvature as shown right figure below. However, this would impart prestress into only the upper part of the membrane, and it would leave the portion below the cable without prestress. Therefore, this physical approach is possible but not rational.

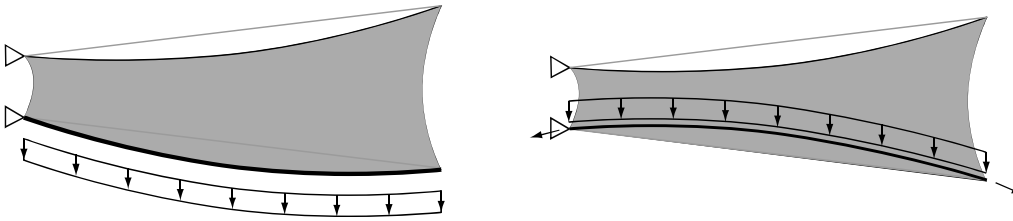


Figure 7.33 Some ideas for prestressing membrane strip

Thus it is obvious that an alternative approach has to be developed. The issue is how the two opposed conditions can be fulfilled simultaneously: the first required condition is the prestressed membrane. Then the shortest width has to be in the middle ($a_1 > a_2 > \dots > a_6 < a_7 < \dots < a_{11}$). The second condition is the movement. Then the width of the membrane strip must be $a_m < a_{m+1}$.

The author developed one solution to satisfy these two conditions. The key is to change the boundary conditions when the membrane strip is under tension and when there is no tension. In order to transition from the tensioned to the no-tensioned status, the outer edge of the membrane strip must be brought back in parallel with the global horizontal (Figure 7.34). This releases the prestressing force in the membrane strip. Obviously the widths of the membrane strips remain same ($a_1 > a_2 > \dots > a_6 < a_7 < \dots < a_{11}$), however the pretensioning status and the geometry of the boundary cables are changed. In this new geometry the required condition $a_m < a_{m+1}$ can be fulfilled. The key of this solution is that the inclined outer edge of the membrane strip a_1 is larger than the required width of membrane strip in the level of the roof's surface a : $a_1 = \sqrt{2}a$. Now an alternative condition $a_6 > a$ must be checked to guarantee the movability of the membrane strip to the outer edge of the roof.

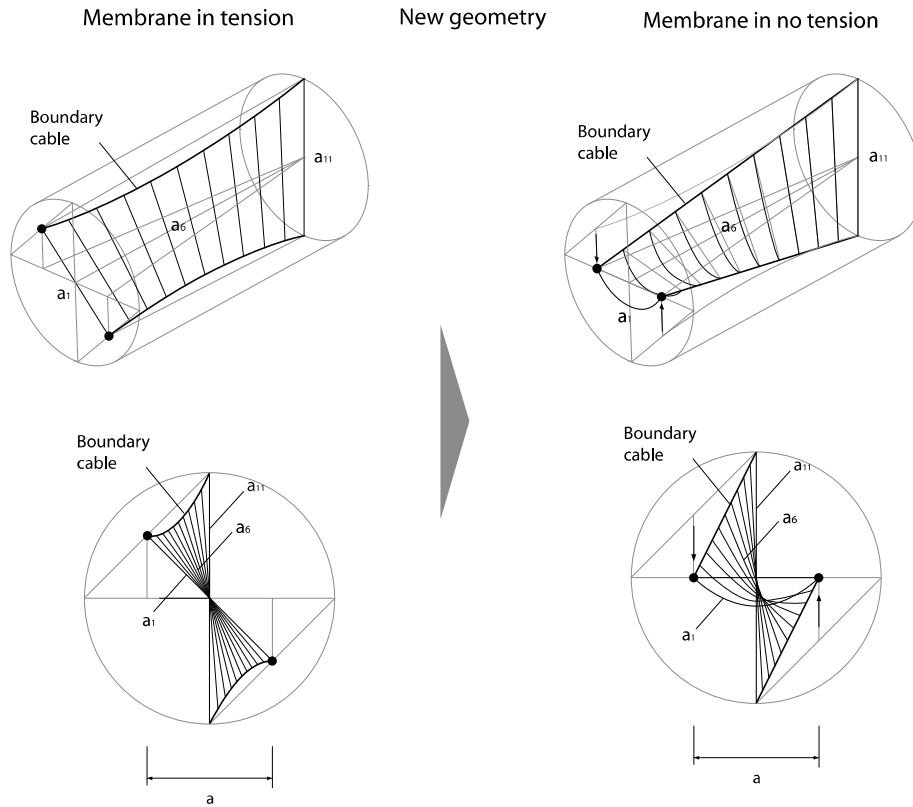


Figure 7.34 Two geometrical configuration of a membrane strip

The curvature of the edge curve of the membrane strip is determined physically: by the level of prestressing force and material property (stiffness of membranes and cables). Strong prestressing force causes large curvature of the edge curve of membranes. (Figure 7.35)

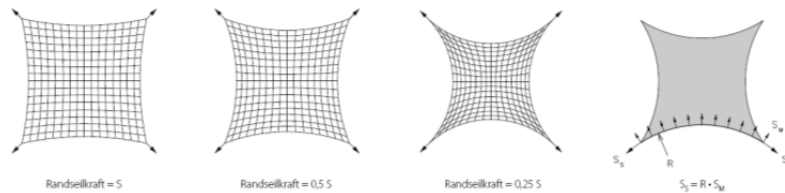


Figure 7.35 Variation of the edge rope radius and edge rope force [Sei 09]

Therefore the consistency of this approach was not analytically but numerically verified by the cutting shape of the membrane strip. The figure below shows one membrane strip, a part of the whole roof shown in Figure 7.36, with the radius $r=18.0m$ and prestressing force in membrane 2.0 kN/m . If the lower cable is constrained by trolleys, the curvature of the lower cable becomes smaller, but here no trolleys are attached.

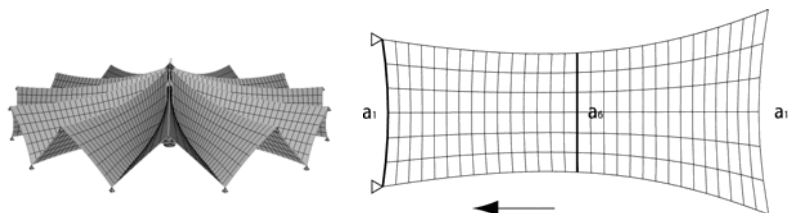


Figure 7.36 FEM model of the whole roof after the form finding process (left) and the cutting shape of a membrane strip (The compensation value is zero) (right)

We obtained the values of width $a_6 = 5.3[m]$. Since $a_1 = \sqrt{2}a$, an inequality expression is achieved as: $a\left(\frac{a_1}{\sqrt{2}}\right) = 4.7[m] < a_{\min} = a_6$

Thus the condition $a_6 > a$ is fulfilled and the validity of this approach is verified. But the length of radial cable also changes by this means. This must be considered and will be discussed in next section.

The consistency was also tested through the physical model. Two pictures in Figure 7.37 show that when the outer edge of the membrane roof forms zigzag line, the textile membrane cannot be folded completely. The radial cable is kinked in the picture right. On the other hand if the outer edge line of the membrane roof becomes flat, the textile membrane can be folded completely.

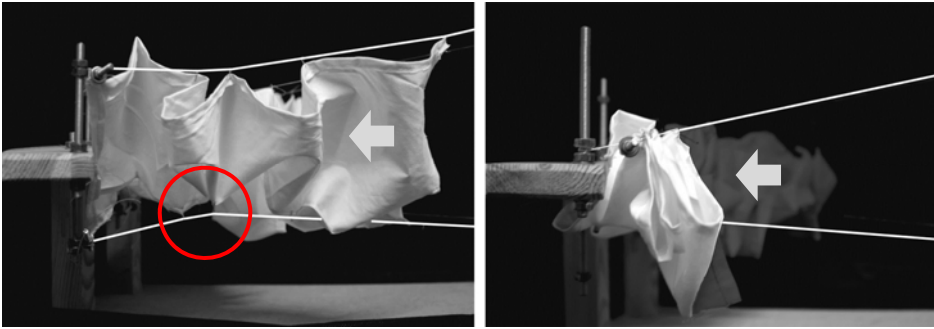


Figure 7.37 A physical model of the one eighth of the roof in two different configurations

The process of unfolding the textile membrane was observed using the physical model of one eighth of the roof. In the last (fourth line of the pictures), the geometrical configuration was changed and the textile membrane was in tensioned.

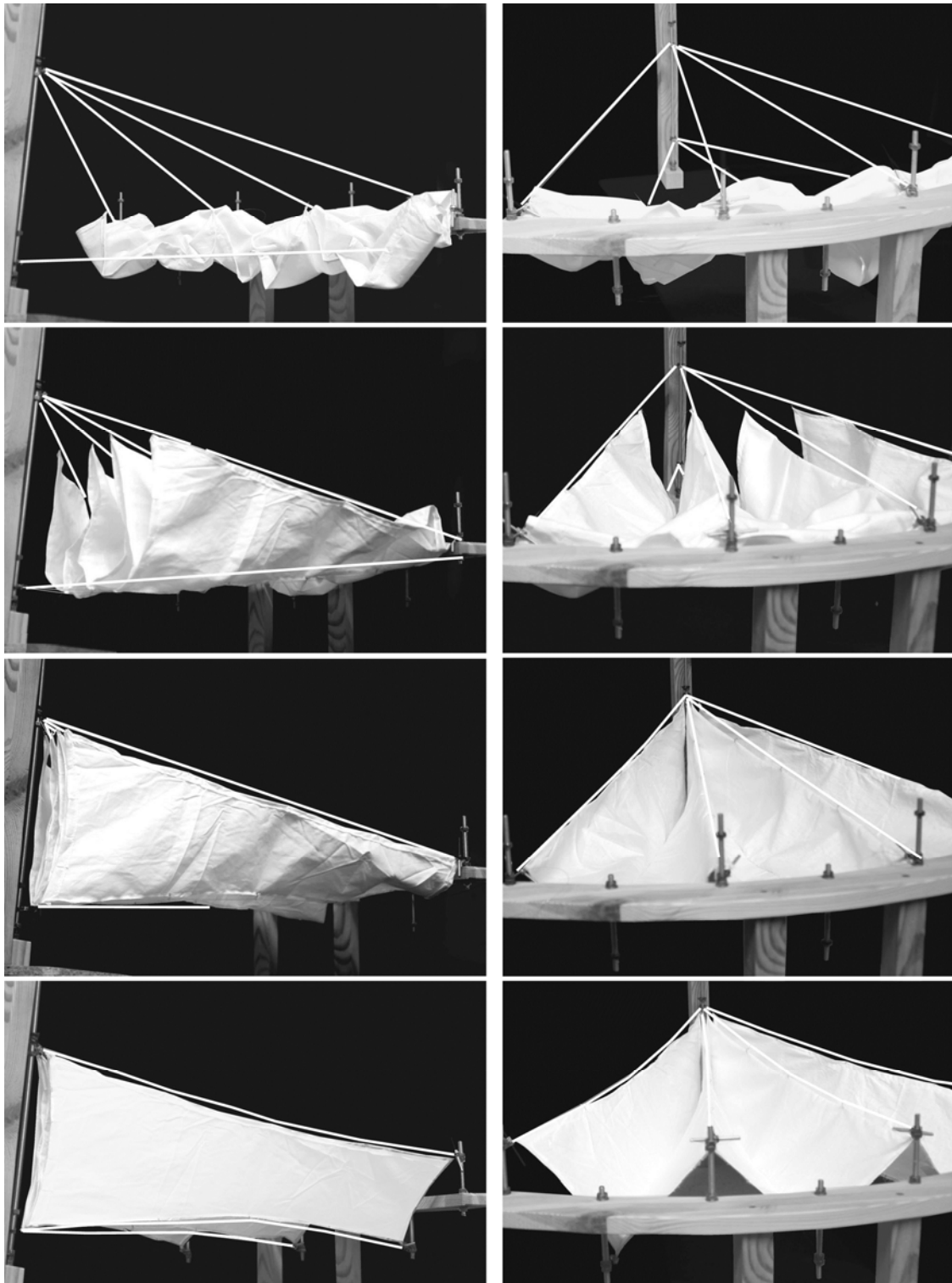


Figure 7.38 A physical model of the one eighth of the roof in an unfolding procedure

Challenge of the cable girder approach and its solution

Also for the cable girder approach the question is: how to achieve pre-tensioning in the entire membrane? To keep the width constant there is no curvature in the membrane strip in the circumference direction, therefore apparently some curvature in the radial direction is necessary. One simple idea is to hang up the lower long side edge of the membrane strip to reach a convex curved line. By then the upper edge line must be also hung up as much as the lower edge to keep the constant width of membrane strip.

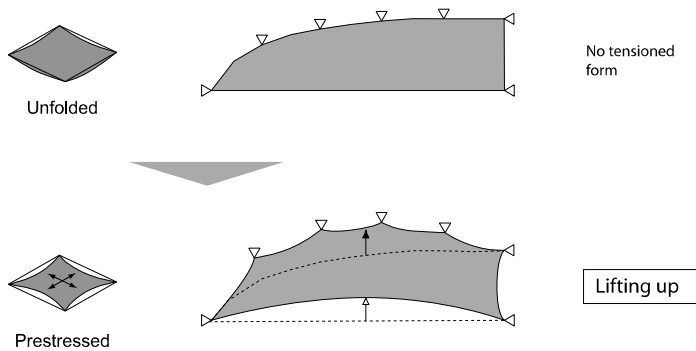


Figure 7.39 Problem of the cable girder approach and its solution (side view of a membrane strip)

A physical model of one eighth of the roof was built to confirm the analytical thoughts and to get a deeper understanding of the processes of unfolding the textile membrane. The upper guide lines (ridge lines) were constructed as arch structures and the lower lines (valley lines) were constructed using cables.

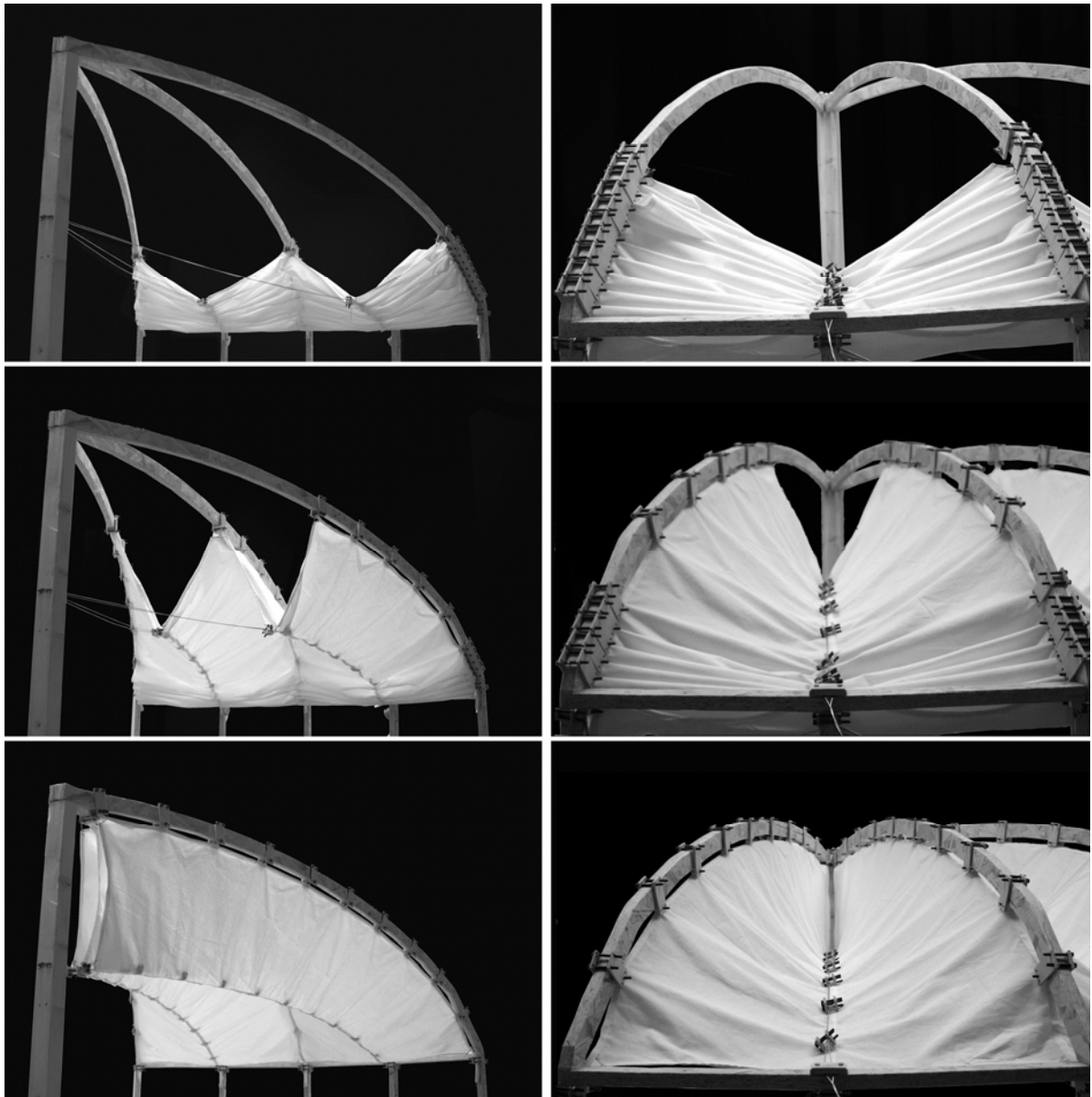


Figure 7.40 The physical model of one eighth of the roof using an arch as upper guide line

The shape of one membrane strip is shown from different views. The view from the top shows that this membrane strip is fit to the shape of radial spoked wheel structure and the view from the perimeter shows the width of the membrane strip is constant. The cutting pattern of this membrane strip can be gained by commercial computing software. It is clear that the membrane strip is not any more rectangular shape, but the widths of membrane strip are kept constant along the radial direction of the roof.

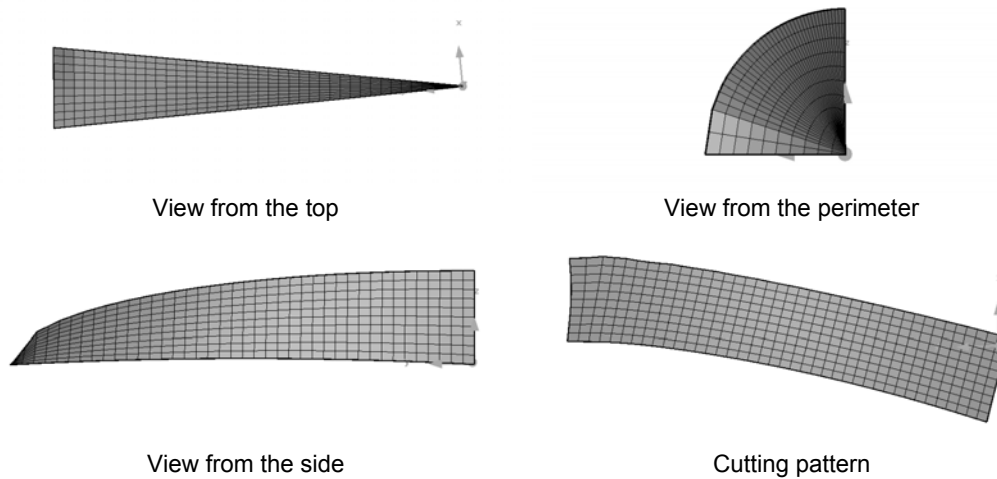


Figure 7.41 One membrane strip. View from the top, perimeter and the side and the cutting pattern

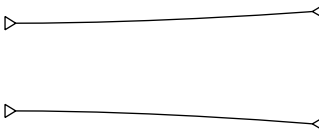
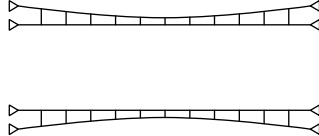

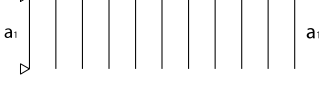
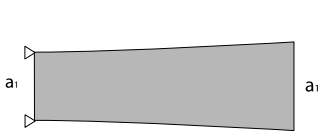
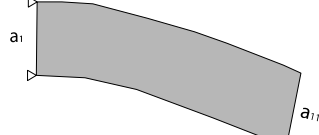
7.2.3. Summary of geometrical challenges

From the geometrical study in this section it becomes obvious that two approaches (1. half strip and 2. cable girder) are reasonable and feasible. These two are summarized in one Table below.

The ‘half strip’ approach is a simple geometrical solution. This simplicity leads to high transparency of the structure. Since all outer edges of the membrane strips are inclined forming zigzag line, two compression rings are necessary at the outer edge of the roof. However, when the roof opens, only radial cables will remain in space. This is the great advantage of this approach. But the large issue is the way of introducing of the prestressing force into the textile membrane. Changing the boundary condition is the solution to overcome the conflicted geometrical conditions. The required amount of textile membrane is relatively large: in comparison with the area to be covered A_c (in Equation 7.3) here $3.2 \cdot A_c$ becomes necessary.

The ‘cable girder’ approach is a kind of mathematical solution. It was solved by analytic geometry. The cable girder becomes necessary to form the ellipse curve for the upper edge line of a membrane strip. Here more structural elements remain when the roof opens, thus the ideal transparent view will be achieved to a lesser extent. Since the width of membrane strip can remain constant, the required amount of material stays at $2.0 \cdot A_c$.

Table 7.3 Two approaches for geometrical solutions

	Half strip approach	Cable girder approach
Radial cable		
Distance between adjacent radial cables		
Shape of a membrane strip		
Required Amount of membrane	$3.2 \cdot A_c$	$2.0 \cdot A_c$
Possible way for introduction of prestressing force	kinematic	kinematic

7.3. Method for the introduction of prestressing force into membrane

As a next step mechanisms for introducing the prestressing force into the textile membrane will be discussed. At first general things about the introducing of prestressing force into the textile membrane will be described. Then the mechanisms for both approaches (half strip and cable girder) will be explained respectively. Although pneumatic mechanism is also possible to give the pretensioning force into the textile membrane, the author will focus only on the kinematic mechanism in this paper.

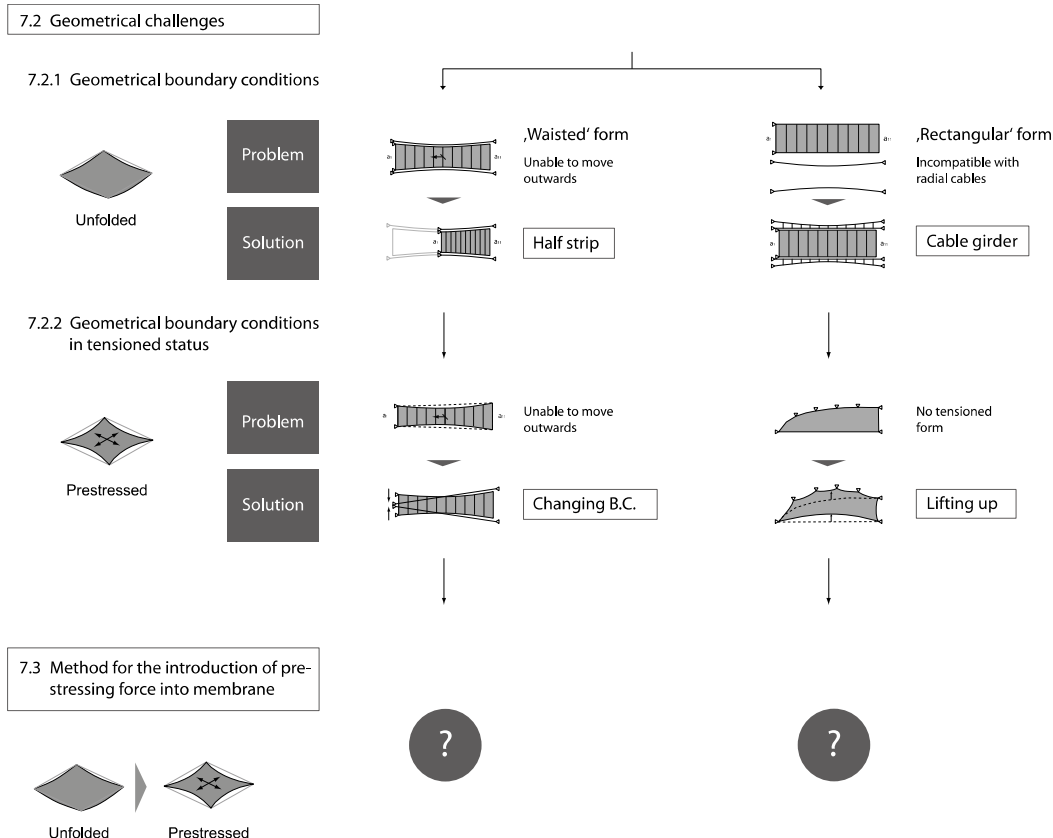


Figure 7.42 Development of the foldable membrane roof opening center to the outside: geometrical study to the method for pretensioning

7.3.1. Mechanism for the introduction of prestressing force

Biaxial pretensioning forces are necessary for membrane in architectural use. The membrane strip is spatially twisted but its surface can be defined by radial- and circumference direction. Here warp direction is set in radial direction and weft in circumference. The warp direction is named as ‘Nxx’ and the weft direction is as ‘Nyy’ as shown in Figure 7.43.

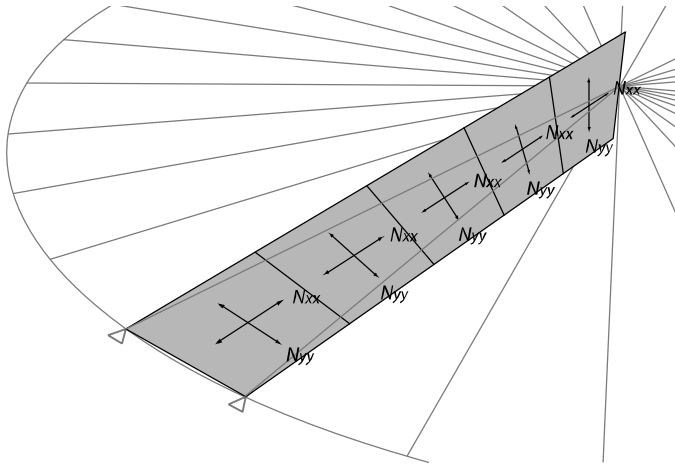


Figure 7.43 One membrane twisted strip and its warp (N_{xx}) and weft (N_{yy}) directions

Prestressing force in a textile membrane is introduced through the boundary edge cables which are extended by the movement of the end nodes. In addition to the direction of prestressing, the level of tension force, its balance in warp and weft directions, and the travel length for prestressing are important to consider pretensioning procedure.

The mechanism for the introduction of prestressing force in the half membrane strip (for Case Study A)

The method for the introduction of prestressing force for the ‘half strip’ approach was already discussed in the last section. To put the membrane strips in tension, the centre and the outer edge points of the upper radial cable are moved vertically upward, and ones of the lower cable downward. Thus all four end nodes of the membrane strip are moved, which require very careful operation for both introducing and releasing prestressing force. Membrane can easily tear or be damaged by irregularly movement of end nodes due to high force of the operation. With this method, the weft direction of the membrane strip (N_{yy}) could be mainly stressed. The warp direction (N_{xx}) would be prestressed by an orthotropic material behavior of membrane fabric.

Changing the boundary condition requires a special attention for the outer compression ring. For the vertical movement of the fixed support point of the membrane strip at the outer edge of the roof, the whole compression ring could be raised up or lowered down. In doing so, horizontal force from the prestressed membrane strip is always transferred to the outer ring as compression force, and no bending moment would be occurred. However, to raise the compression ring, its weight must be taken into account.

This method is named as “raised compression ring method”, and the mechanism will be studied further with structural analysis and a physical model, as the case study “A” in next Chapter.

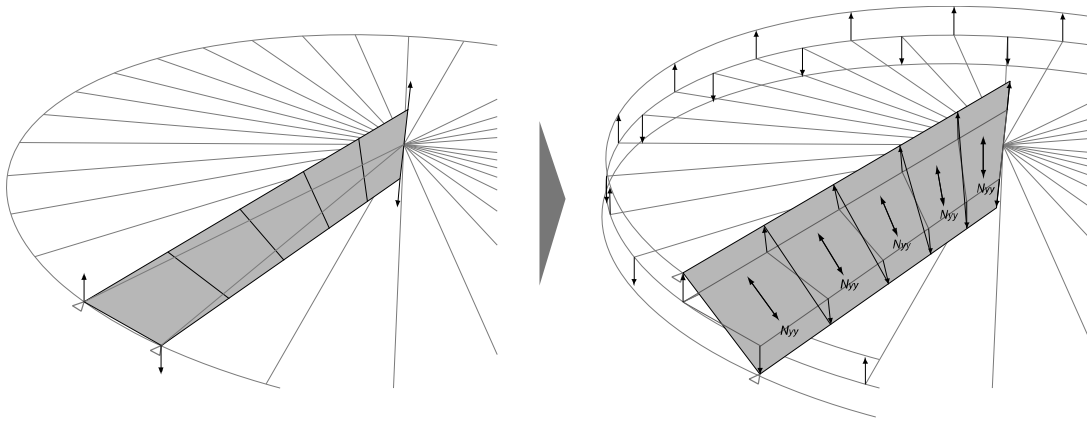


Figure 7.44 Introduction of prestressing force into membrane in both surface directions

The mechanism for the introduction of prestressing force in the rectangular membrane strip (for Case Study B)

The arches shown in the physical model in Figure 7.40 are compression elements, thus generally their dimensions are quite thick. Since tension elements can be much slimmer and more efficient, the next step is to transfer the arches into a cable girder. Here, both the upper guide lines (ridge lines) and the lower lines (valley lines) were modeled with cable elements. Especially the ellipse curves for the upper guide lines were formed by cable girder structures.

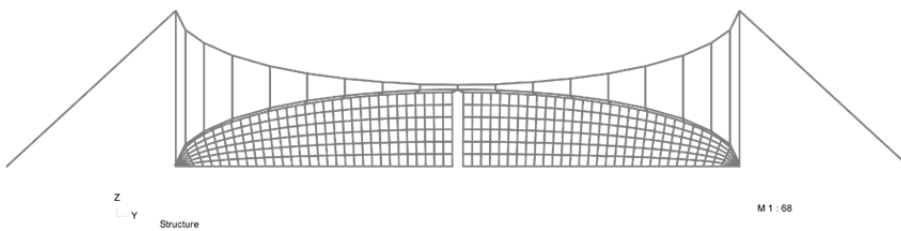


Figure 7.45 Model of the whole roof (sectional view)

A possible idea for the introduction of prestressing force in the membrane was drawn from the kinematic mechanisms of the Inner Harbor Bridge in Duisburg, Germany. The span of this back-anchored suspension bridge is 73 meters and the four slender masts are 20 meters with the diameter 42 centimeters. The deck can be raised up in about 5 minutes. Three positions of the arch height are pre-set to allow different size of ships to pass and the maximum arch height is 9.2 meters.



Figure 7.46 Movable bridge in Duisburg (eng.: schlaich bergemann und partner) [sbp 12]

The great advantage of this mechanism is the achievement of large deformation with minimal input. Hydraulic cylinders attached at the ends of each four stay cables can be extended or

retracted in 3 meters maximum. When it is retracted, the stay cables shorten and the masts pivot outwards. This causes the position of the main cables and hangers to change and the deck consisting of precast concrete elements automatically lifted upwards into an arched shape. Usually large deformation in the sag caused by small horizontal shift of the anchorage is regarded as unfavorable effect in this kind of structures. But this effect is efficiently used here: 1.7 meters horizontal move of the mastheads caused by 3 meters shorting of the stay cables leads 8.1 meters humping of the arch deck. [Bög 03]

This mechanism can be exploited for the introduction of prestressing force in the membrane strip. Through lifting up the cable girders by hydraulic cylinders attached to the back stay cables, the membrane fabric suspended from the lower radial cable is also lifted up then could be prestressed. With this method, the membrane strip would be mainly pulled in the radial direction. Hence, the warp direction (N_{xx}) would be mainly prestressed, which make the weft direction (N_{yy}) also in tension by an orthotropic material behavior of membrane fabric.

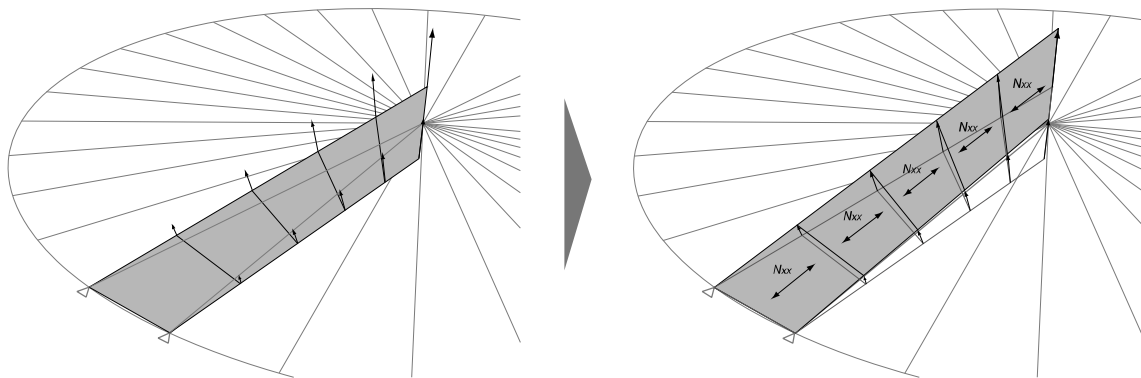


Figure 7.47 Introduction for prestressing force into membrane in both directions

The large advantage of applying this mechanism is that ‘Minor shift’ causes ‘Major lift’. Also, in contrast to the raised compression ring method, an actuator to introduce prestressing force is not necessary in the centre of the roof. This can make the structure of the central hub simpler and more transparent visually. This mechanism will be studied further in structural analysis and a physical model as the case study “B” and described in Chapter 9.

7.3.2. Summary of method of introducing prestress force

The two mechanisms for the introduction of the prestressing force into the textile membrane were introduced in this section.

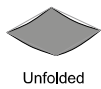
One mechanism is for the half membrane strip and is named raised compression ring method: the outer compression ring is raised and lowered to change the boundary condition for the membrane strips.

The other mechanism is for the rectangular membrane strip and is named minor shift - major lift mechanism. The fundamental idea came from the movable bridge in Duisburg, Germany; the deck is lifted up by hydraulic cylinders attached on the back stay cables. Here in the project, the cable girder and textile membrane are lifted up together, which introduces prestressing force into the membrane. Large deformations caused by a small shift is the key for this mechanism.

These two kinematic approaches will be developed further as case studies in following sections.

7.2 Geometrical challenges

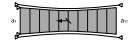
7.2.1 Geometrical boundary conditions



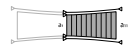
Unfolded

Problem

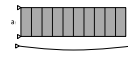
Solution



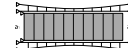
„Waisted“ form
Unable to move outwards



Half strip



„Rectangular“ form
Incompatible with radial cables



Cable girder

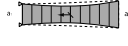
7.2.2 Geometrical boundary conditions in tensioned status



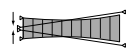
Prestressed

Problem

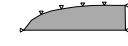
Solution



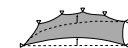
Unable to move outwards



Changing B.C.



No tensioned form



Lifting up

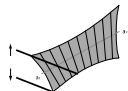
7.3 Method for the introduction of pre-stressing force into membrane



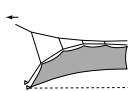
Unfolded



Prestressed



„Raised compression ring“ Method



„Minor shift - Major lift“ Method

Case Study A

Case Study B

Figure 7.48 Development of the foldable membrane roof opening center to the outside

7.4. Overview of the case studies

7.4.1. Structural Analysis

Two approaches will be developed as case studies in following chapters. In case study A, a roof using half of waisted membrane strip will be analyzed, and in case study B, the kinematic system consisting of rectangular membrane strips and cable girders will be studied. The kinematic cable girder will be analyzed through parameter studies.

A structure must resist even the most unfavorable applied load in its life span. As a feasible study, the structural analysis will be done by using Eurocode, and dimensions and load cases will be described here.

7.4.2. Dimensions and Materials for case studies

Geometry and Dimension

The geometry and the dimension are set as follows. Circular shape in plan is selected due to its simplicity. The graph in Figure 6.5 in Chapter 6 indicated that light weight structure becomes efficient from an economical point of view when its span is larger than approximately 35 m. Therefore, 36m is given for the value of the diameter of the roof. This is same as an existing roof in Zaragoza.

Diameter of the roof	d	: 36.0 m
Radius of the roof	r	: 18.0 m
Number of trolley in a radial cable	t	: 5
Circumference	$c = \pi \cdot d$: 113.1m

Material properties

Applied material properties are as follows. Typical values of the material property are chosen from the commercial product catalog. However, some values which required calculation such as E-modulus of a membrane are mostly not included here, because these values relate to the material non linearity. The values shown with an asterisk are values only for use in the numerical analysis.

Membrane (Polyester / PVC. Typ III):	Thickness	1 [mm]
	Weight	1 [kg/m ²] (= 10.5 [kN/m ³])
	Ultimate tensile strength (warp/weft)	115/100 [kN/m] (= 5750/5000 [N/50mm])
	Tensile strain (warp/weft)	15/25 [%]
	Translucency	4-9 [%]
	E-module (warp/weft)*	1.30 / 0.94 [GPa]
	Poisson's ratio*	0.49
	Shear modulus*	55900 [kN/m ²]
Strap and Belt for Trolleys (Polyester):	Thickness	1 [mm]
	Weight	2 [kg/m ²]
	Ultimate tensile strength	490 [kN/m]
	Elongation	7 [%]
	E-module*	4.2 [GPa]
Edge Cable (Spiral Strand – Stainless Steel):	Diameter	14.1 [mm]
	Characteristic breaking load	141 [kN]
	Limit tension	86 [kN]
	Weight	78.5 [kN/m ³]
	E-module	160 [GPa]
	Metallic cross section	117 [mm ²]

7.4.3. Load Case for case studies

Allowable Stress Design

Currently the limit state approach is employed as the design concept for most national codes including Eurocode. A limit state indicates the required performance criteria when the structure is subject to loads. The design criteria correspond to safety and functionality of the structure, of which the building and its part must be secured against applied design load. In many cases two principal criteria are applied: the ultimate limit state (ULS) and the serviceability limit state (SLS).

An allowable (or permissible) stress design (ASD), in which the stresses in the structure at the largest applied loads should not be exceed the yield stress of the construction material, seems already old concept for structural design. However European Design Guide for Tensile Surface Structures [For 04] suggests that a limit state approach (with partial safety factors applied to the loads and also the material properties) may not be appropriate for the assessment of the strength of the stressed fabric. The main reason of that is because the geometry of the tensile surface structure is dependent on both the magnitude and distribution of loading. Geometry change particularly affects non-uniform loading distributions. Also there is small impact to use factored loading to the prestressed fabric structure, because the variation in material characteristics and the factors for the rupture strength of the unused new fabric are large.

Thus, the analysis of textile membrane is normally done using the calculation method based on an allowable stress design. However, the supporting structures such like steel frames should be assessed using the concept of limit state. Unfactored design loads were applied to a full non-linear analysis method and resulting stresses was factored according to Eurocode 3.

Normally the textile membrane and the supporting structure are calculated by the same numerical model but assessed separately by each approach.

Most of the values for membrane material referred to in this section are derived from European Design Guide for Tensile Surface Structures.

Safety Factor of textile membrane

Design practice in Germany typically adopts a stress factor approach applying the unfactored design loads. A factor depending on loading type is incorporated to a reduction factor of materials.

Based on the PhD thesis of Minte [1981], the following summarized safety factors are derived from various tests by material experts for stadia projects. By European Design Guide for Tensile Surface Structures, the allowable stresses are defined as follows:

$$f_d = \frac{f_{tk}}{\gamma_f \cdot \gamma_M \cdot \gamma_{A_i}} = \frac{f_{tk}}{A_{res}} \quad (7.23)$$

where:

- f_d = allowable stress
- f_{tk} = tensile strength defined as 5%-fractile of at least 5 strips 10cm wide, tested at 23 °C
- γ_f = load-factor
- γ_M = material safety coefficient for all approved materials: 1.4 within the fabric surface, or = 1.5 for connections
- A_i = combination of reduction factors depending on load case.

The value of the global safety factor for the material are provided in ranges, but the maximum value that the Design Guide suggests was taken for the structural analysis.

Table 7.4 Global safety factor for the material

type of load case	description of load case P: Prestress G: Self-weight S: Snow W: Wind	duration of loading	load safety factor	material safety factor	reduction factor for biaxial stresses	reduction factor for long term loading	reduction factor for local environmental effect	reduction factor for high temperatures		total safety factor for membrane material
			γ_f	γ_M	A_0	A_1	A_2	A_3	γ_{calc}	$\gamma_{total, mem}$
1)	(P+G)	long	1.5	1.4	1.2	1.7	1.2	1.0	5.1	6.4
2)	(P+G)+S	long	1.5	1.4	1.2	1.7	1.2	1.0	5.1	5.1
3)	(P+G)+W	short	1.6	1.4	1.2	-	1.2	1.0	3.2	3.2

Strength of welded seams depends on the adhesion of coating onto the weave, the welding parameters and the seam width [For 04]. The following numbers are proposed for welded widths that are a simple overlap weld for the standard range of PVC coated polyester membrane. Typ III is chosen for this project.

Proposed seam width:	Type I	40 mm
	Type II	60 mm
	Type III	80 mm
	Type IV	80 mm
	Type V	100 mm

Global safety factor for welded seams with appropriate width for fabric types are calculated as follows, but the maximum number that the Design Guide suggests was taken for the structural analysis.

Table 7.5 Global safety factor for welded seams

type of load case	description of load case P: Prestress G: Self-weight S: Snow W: Wind	duration of loading	load safety factor	material safety factor	reduction factor for biaxial stresses	reduction factor for long term loading	reduction factor for local environmental effect	reduction factor for high temperatures		total safety factor for membrane material
			γ_f	γ_M	A0	A1	A2	A3	γ_{calc}	$\gamma_{total, mem}$
1)	(P+G)	long	1.5	1.5	1.2	2.5	1.2	1.0	8.1	9.5
2)	(P+G)+S	long	1.5	1.5	1.2	1.5	1.2	1.0	4.9	4.9
3)	(P+G)+W	short	1.6	1.5	1.2	-	1.2	1.0	3.5	3.5

For other materials following numbers were chosen as typical composite factors: 2.5 for cables and 3.0 for webbing belt.

Limit state assessment

A stress check of the textile membrane is done assuming a 30% increase in stiffness. In addition to that, the deformation of the textile membrane (Ponding) must be carefully examined.

Avoidance of ponding is important for finding the initial prestress shape of tensile structures. All area of the surface of the tensile structure must be positive for drainage. Also this positive inclination must be maintained under load-induced deformations. An accumulation of snow or ice may cause deformation of the surface, in which melting water and rain can collect. This may increase the depth of the depression, allowing more water to accumulate. This cycle could lead to structural collapse. Thus a surface of tensile structure must maintain a positive gradient even under the worst possible snow load conditions. The stiffness of the textile membrane is reduced 20% in a ponding analysis.

Design loads

After obtaining the equilibrium state by the form finding process, snow and wind loads are applied. Compared to the conventional building structures, light weight structures are affected more by wind and snow load, because the ratio of applied loading to the self-weight is large. The regular wind loads are defined by EC 1 [DIN 96].

Prestress Force in membrane

An appropriate prestressed force introduced in the textile membrane may be 1-5 kN/m in warp and weft direction. The minimum required prestress of membrane surface is given in the 'European Design Guide for Tensile Surface Structures'. It is suggested that lower prestress leads to an uneven or wrinkles on the membrane surface. For PVC coated Polyester membrane structure the prestress should not be less than 1.3 % of the average tensile strip capacity of the material in both the warp and weft directions. The minimum prestress levels for PVC coated Polyester membrane structure are given as follows [For 04]:

Minimum prestress level for PVC/Polyester membrane:	Type I	0.70 [kN/m]
	Type II	0.90 [kN/m]
	Type III	1.30 [kN/m]
	Type IV	1.60 [kN/m]
	Type V	2.00 [kN/m]

For foldable membrane structure minimum prestress force both in warp and weft direction seems reasonable to apply, because it brings a balance between the resistances of the textile membrane by the tension force and the resulting forces transferred to the stationary structure. The need for highly sophisticated device and material for introducing the pre-stressed force can be also avoided. The prestress force in the membrane was set to 1.3 kN/m but increased when more prestress force is necessary.

Long term effects such as creep causes change of prestress level and distribution, but these effects are not considered for this project because prestress force is re-introduced every time the roof is closed.

Snow Loads

Snow load is determined by the formula [DIN 96a] as follows:

$$s = \mu_i \cdot C_e \cdot C_t \cdot s_k \quad (7.24)$$

Where s_k : Characteristic snow load on the ground
 C_e : Exposure coefficient (generally taken equal to 1)
 C_t : Thermal coefficient (for normal standards of thermal insulation. taken equal to 1)
 μ_i : Snow load shape coefficient. being a function of the type of roof

All factors C_e , C_t and μ_i are given the value 1 and for the characteristic snow load a value of $1.13 \text{ kN} / \text{m}^2$ is taken (Zone III in Germany where altitude is less than 200m), which leads to the value of snow load $1.13 \text{ kN} / \text{m}^2$.

The retractable roof is designed to be deployed only in summer (between May and October). However, even in summer the roof must be capable of withstanding extreme conditions like storm, and this is taken into account as a reduced snow load. The full snow load is reduced to 65%. This concept is based on the design of the retractable roof of football stadium in Frankfurt. [Göp 07a] Thus Snow load is given here as: $0.65 \cdot s = 0.73 \text{ kN} / \text{m}^2$.

An asymmetrical load case is important for a light weight structure. The shape coefficient is given as shown in Table 7.6 below.

Table 7.6 Snow loads

Type	μ	Ce	Ct	sk [kN / m ²]	s [kN / m ²]
Symmetrical	1.0	1	1	0.73	0.73
Asymmetrical	2.0	1	1	0.73	1.46
	1.0	1	1	0.73	0.73

During the moving operation of the roof wind and snow load is eliminated in calculation. This leads the careful operation of moving the roof in the reality.

Wind loads

The reference wind pressure q_{ref} is expressed as:

$$q_{ref} = \frac{\rho}{2} v_{ref}^2 \quad (7.25)$$

Where v_{ref} : Reference wind velocity [m/s]
 ρ : Air density [kg / m³]

Air density is affected by altitude and depends on the temperature and pressure to be expected in the region during wind storms. Normally 1.25 was taken for the value. [DIN 96b]

Reference wind velocity is determined as:

$$v_{ref} = C_{DIR} \cdot C_{TEM} \cdot C_{ALT} \cdot v_{ref,0} \quad (7.26)$$

Where $v_{ref,0}$: Basic value of reference wind velocity [m/s]
 C_{DIR} : Direction factor
 C_{TEM} : Reduction factor for temporary or provisional structures
 C_{ALT} : Altitude factor

Germany is divided in 4 zones in which the basic reference wind velocity varies between 24.3 and 31.5 m/s. Direction factor C_{DIR} takes into account wind direction. A reduction factor for temporary or provisional structures C_{TEM} takes 1, unless otherwise specified in annex A of Eurocode 1 part 2-4 [DIN 96b]. Altitude factor C_{ALT} takes into account the altitude of building location and in the wind zones 1 and 2, for which the average wind velocity is relatively low. The coefficient is to be used for all constructions at an altitude above 800 meter. The following specific locations are applied.

Location : Berlin, Germany
Wind zone : 2 (inland. flat area with few buildings)
Altitude : 45 m above mean sea level

For this location $v_{ref,0} = 25.0$ m/s, $C_{DIR} = 1$, $C_{TEM} = 1$ and $C_{ALT} = 1$ are chosen and this gives:

$$q_{ref} = 0.39 [kN / m^2]$$

The total wind pressure acting on the surfaces is calculated by the subtracting the wind pressure on the external surfaces from the wind pressure on the internal surfaces. The wind pressure acting on the external surfaces of a structure is expressed as:

$$w_e = q_{ref} \cdot C_e(Z_e) \cdot C_{pe} \quad (7.27)$$

In which $C_e(Z_e)$: Exposure coefficient
 C_{pe} : External pressure coefficient

Also the wind pressure acting on the interior surfaces of a structure is expressed as:

$$w_i = q_{ref} \cdot C_e(Z_i) \cdot C_{pi} \quad (7.28)$$

In which $C_e(Z_i)$: Exposure coefficient
 C_{pi} : Internal pressure coefficient

The total wind pressure acting on the surfaces is given by:

$$w = w_e - w_i \quad (7.29)$$

The exposure coefficient considers the impact of several parameters on average wind velocity, such as terrain characteristics, presence or absence of obstacles, topography and height with respect to ground level. The most severe terrain (category 1. smooth flat country without obstacles) is chosen and the value sets 2.2.

The external pressure coefficient is determined by the geometry of the surface of the structure. Similar geometry is chosen from the literature [For 04] and the given values are exploited.

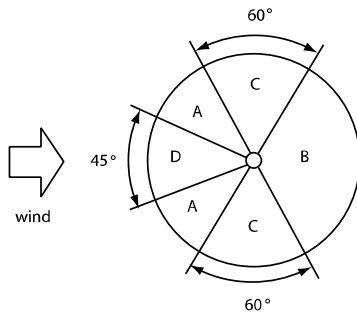


Figure 7.49 Zone Definition for the exposure coefficient (conical shape with open side) [For 04]

The internal pressure coefficient is distinguished by the opening ratio of side wall and takes a value between 0.8 (closed) and -0.5 (opened). A negative value indicates the suction force. The opened side wall is here considered and then -0.5 is taken for the value. The values of external and internal pressure coefficient and wind pressures are listed below.

Table 7.7 Wind pressure on the roof per load zone (+: pressure. -: suction)

q_{ref} [kN/m ²]	Zone	C _{pe}	w _e [kN/m ²]	C _{pi}	w _i [kN/m ²]	w [kN/m ²]
0.39	A	-0.15	-0.13	-0.50	-0.43	0.30
0.39	B	-0.60	-0.51	-0.50	-0.43	-0.09
0.39	C	-1.00	-0.86	-0.50	-0.43	-0.43
0.39	D1	0.40	0.34	-0.50	-0.43	0.77
0.39	D2	-0.20	-0.17	-0.50	-0.43	0.26

Load Cases

The analyses are done using unfactored loading in order to take into account the large deformation of membrane structures. Applied load combinations are listed as follows. The prestress and self-weight are taken in all load cases. The self-weight of the membrane is not reduced even for the case of uplift wind load, because it is very small. Since the snow load here is considered as a storm condition, wind and snow loads are not considered to act simultaneously.

Table 7.8 Load combinations with load factors

	Load case	membrane prestress	Self-weight	Snow Load 1 (Symmetrical)	Snow Load 2 (Unsymmetrical)	Wind Load 1	Wind Load 2
	LC	P	G	S1	S2	W1	W2
(P+G)	1	1.0	1.0				
(P+G)+S	2	1.0	1.0	1.0			
	3	1.0	1.0		1.0		
(P+G)+W	4	1.0	1.0			1.0	
	5	1.0	1.0				1.0

For stress analysis (membrane stiffness *1.3)

For ponding analysis (membrane stiffness *0.8)

Maximum allowable forces

Material strength with corresponding safety factors in each load case are as follows. All primary structural members were simulated in a computer model using geometrically non-linear analysis.

Table 7.9 Design resistance R_d divided by safety factor

for membrane material

type of load case	Load case combination	Duration of load-action	Total safety factor	Tensile strength in warp-direction	Allowable membrane-force in warp-direction	Tensile strength in fill-direction	Allowable membrane-force in fill-direction
			$\gamma_{\text{total, mem}}$	$f_{t,k,\text{mem,warp}}$	$f_{t,d,\text{mem,warp}}$	$f_{t,k,\text{mem,fill}}$	$f_{t,d,\text{mem,fill}}$
				[kN/m]	[kN/m]	[kN/m]	[kN/m]
1)	(P+G)	long	6.4	115	18.0	110	17.2
2)	(P+G)+S	long	5.1	115	22.5	110	21.6
3)	(P+G)+W	short	3.2	115	35.9	110	34.4

for membrane seam

1)	(P+G)	long	9.5	115	12.1	110	11.6
2)	(P+G)+S	long	4.9	115	23.5	110	22.4
3)	(P+G)+W	short	3.5	115	32.9	110	31.4

For strap and belt, $490/3.0 = \mathbf{163 \text{ [kN/m]}}$ will be used as a maximum allowable force.

8. Case Study A – Raised Compression Ring Mechanism

8.1. Introduction

In this chapter the raised compression ring method which was proposed in the last chapter will be developed further. The whole geometry of the roof will be considered at first as well as some details studies such as the extensional cable system, water tightness and minimizing the size of the central hub. The structural analysis will be done with an integrated model in the unfolded configuration. The process of transition will be also analyzed by using iteration calculation method. Furthermore the feasibility of this method will be checked through the physical model that author built at the TU-Berlin, Germany.

8.2. Morphology

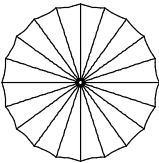
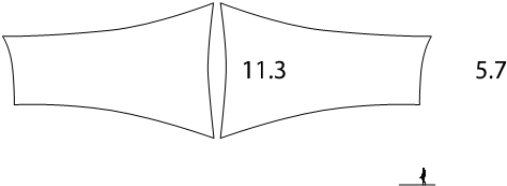
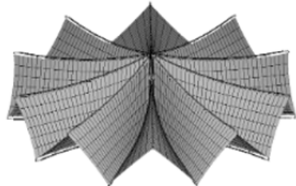
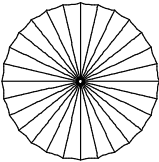
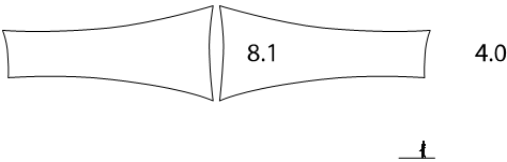
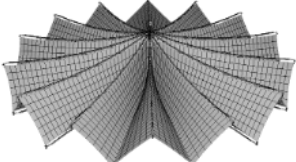
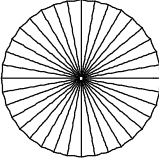
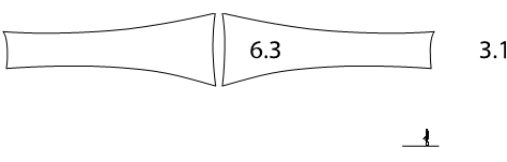
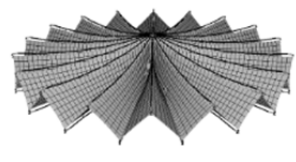
At first the factors related to the morphology of the whole roof will be considered. As discussed in Table 7.1 in the last chapter, the number of radial cables determines the geometry of a roof.

From a structural point of view the amount of required cross-sectional area of the radial cable is important. A large number of radial cables reduces the amount of stress on one section. The great advantage of this raised compression ring method is that no hanger cables are required. However a simple hanging radial cable is very flexible against loading. Therefore, a large number of radial cables is favorable.

As shown in Table 8.1, the required width of one strip at the outer ring in the roof surface's level a and at the center of the roof a_{II} , and thereby the proportions of the membrane strip, change largely according to the different number of the radial cables n . When n is small, for instance $n=20$, the required height of the spoked wheel becomes 11.3m, which is enormous against the roofs diameter 36m.

Considering the above mentioned two points, the number of radial cable $n=36$ is chosen.

Table 8.1 Geometrical change according to the number of radial cables by the half strip method

Number of radial cables n	Top view	Sectional view with $a_{11}(m)$ and $a(m)$ (bottom right: human scale 1.6m)	3-D Figure after form finding calculation
20			
28			
36			

The drainage system also must be considered. There are two possibilities for drain paths as shown in Figure 7.9 in the last chapter. In the fundamental shape of the half strip method, the valley line along the radial cable slopes down toward the centre of the roof. Hence additional pipes that slope down to the outer edge of the roof must be installed in order to drain off rainwater. Otherwise, the shape of the half strip can be changed: the centre of the roof is hoisted up until the valley lines of the surface becomes horizontal or leaned down toward the outer edge of the roof, which requires additional radial cables at the bottom of the flying mast. In this case study, the former is chosen to keep the geometrical challenges simple and clear.

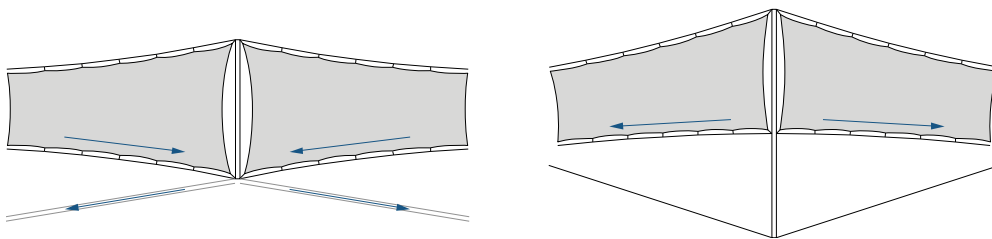


Figure 8.1 Two possibilities for drain path by the half strip method (Left: adding pipes for draining off rainwater. Right: changing the geometry with additional radial cables)

8.3. Detail considerations

Next the required details for the raised compression ring method will be considered.

8.3.1. Extension cable

Special attention must be paid to the alternation of the required length of the radial boundary cables during raising and lowering of the compression rings. A small physical model was constructed to study the movement mechanism and force flow of this system. A cable is fixed at the point on the top of the mast on the left-hand side of the model in Figure 8.2, and it spans across to the connection point on the right-hand side. The mast on the left side has to be imagined as the flying mast at the centre of the roof, and the one on the right-hand side as the outer edge of the roof. The direction of the cable is deflected by the saddle that can be moved vertically along the masts and joined to the elastic spring in outside of the masts. An elastic spring is used here just as a device to compensate the alternation of the cable length. According to the vertical position of the saddle, the lengths of the cable and the elastic spring are altered.

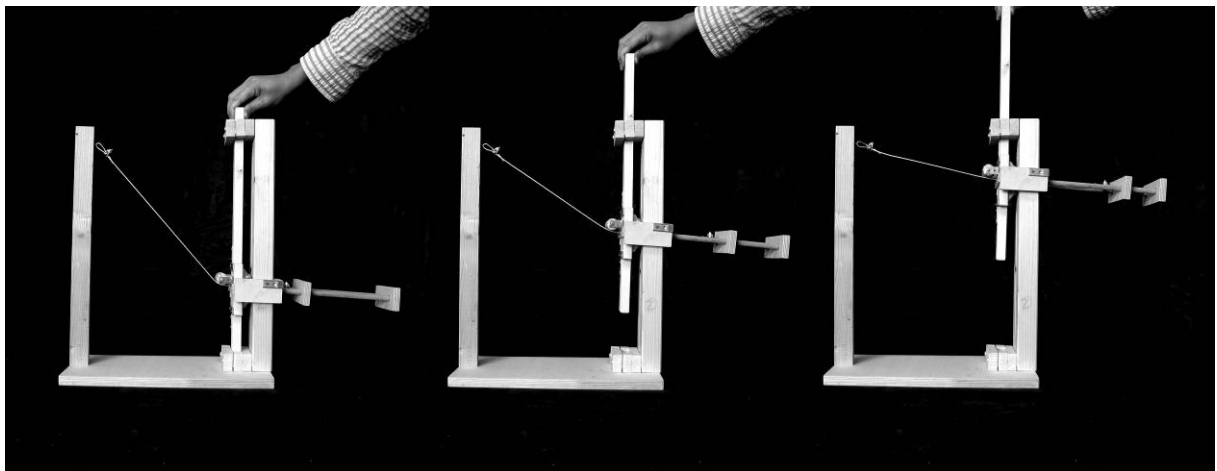


Figure 8.2 A physical study model for the extension cable

The force from the tensioned spring is transmitted to the mast through the struts tied with the saddle. The red arrow in Figure 8.3 below shows the internal force in this system. Since the saddle, the elastic spring and the struts move together, no extra stress appears in the structure except the vertical force (v) applied on the saddle by changing the direction of the cable. This one unit system can be included to the compression rings.

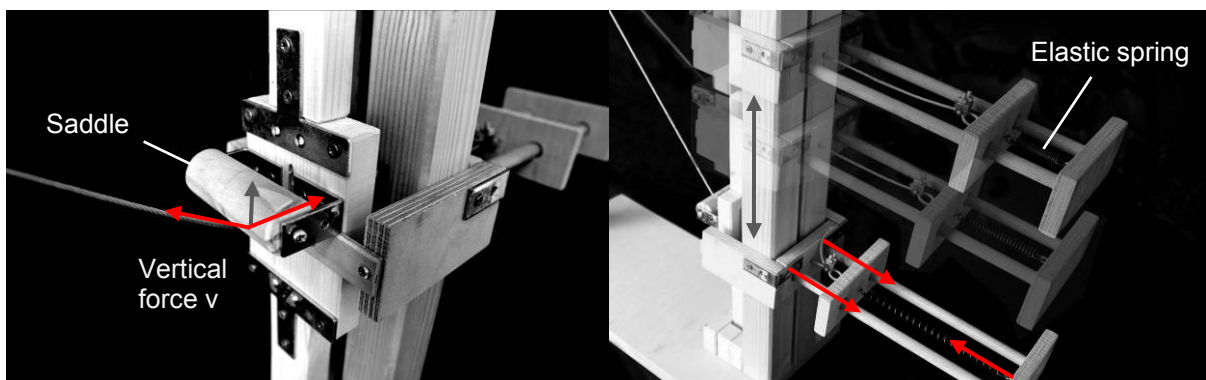


Figure 8.3 Details of a physical study model for the extension cable and internal force flow

It must be also cared how to compensate the alternation of the required length of the radial boundary cables. One simple solution is using elastic spring as an extensionable cable. The advantage will be that no extra device to control the extension part becomes necessary. An

elastic spring is automatically elongated according to the required length of the cable. However, change of the length of an elastic spring causes large variation in the tension force in the cable. Also the required size for elastic spring is problematic. Examples of elastic springs stabilizing a glass façade with tensioned cables are shown in Figure 8.4. These elastic springs work for small variation in cable length due to external factors such as temperature or wind loading on the facade. Even for such small variation, the cross section of the elastic spring must be much larger than one of the cables. For a large scale roof, the required diameter of the radial cables is normally much larger than one for the glass façade. Hence using the elastic spring for a large scale roof is not feasible.



Figure 8.4 Examples of spring bearings for a glass façade (Sony Center in Berlin (left)(photo taken by author) and the entrance area of the University of Bremen (ZBUB) (right) [Sob 04]

Another possibility is to attach an additional element which automatically slides out from the side of the primary structure according to the changing length of the radial cable. The principle of the Katzbuckel bridge in Duisburg, Germany shown in Figure 7.46 illustrates this idea. However, the extension part for the roof structure would not be rigid elements, as they are in the bridge. Therefore some additional devices such as hydraulic jacks become necessary to control the length and the prestressing force of the cables.

8.3.2. Water tightness

Water tightness is very important for retractable roofs. By the raised compression ring method, driving carriages first move along the radial cables from the outer edge to the center of the roof, when the roof closes. Then they move vertically when the textile membrane is prestressed. One idea for water tightness is, therefore, attaching the vertical walls on the central hub of the roof. The picture in Figure 8.5 demonstrates this idea. In this case, the upper cable trolleys are fixed when the textile membrane is prestressed. The plates are arranged in a zigzag form around the central hub and each plate is slightly curved to make the convex curve so that membrane can be fit to the plates tightly.

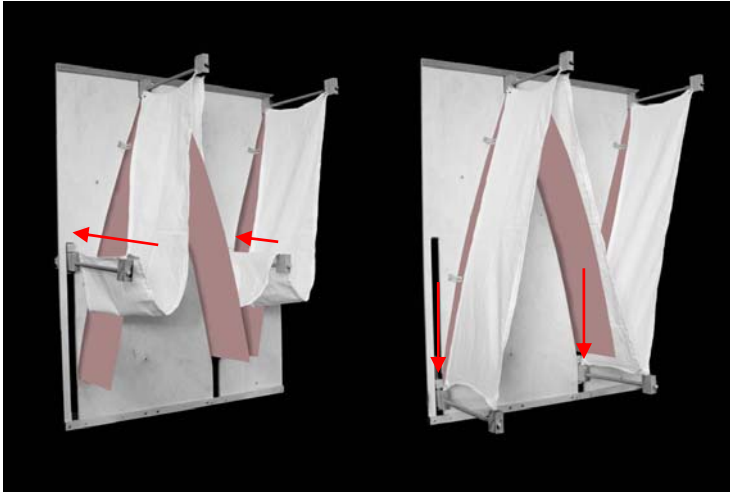


Figure 8.5 A physical study model for water tightness of the raised compression ring method. a part of the central hub (left and centre), a simple image of the appearance (right)

8.3.3. Minimizing the size of the central hub

Minimizing the size of the central hub of the roof is also important. By the raised compression ring method, the following items must be gathered at or built into the central hub:

- driving carriages.
- a prestressing device for the membrane.
- locking devices for the driving carriages.
- radial cables and their anchors
- wire ropes for the driving system and their anchors.

In most cases the number and the size of the radial cables anchors would be decisive for the dimension of the central hub. Figure 8.6 shows it: the central hub of the Commerz Bank Arena in Frankfurt, Germany demonstrates that there is almost no space between two adjacent cable anchors. In case of Warsaw, the positions of the adjacent cable anchor are changed up and down to minimize the size of the central hub. The roof in Zaragoza demonstrates that the dimension of the central hub is decided from the same factors, even if a screw jack is installed inside the hub. (Figure 5.16 in Chapter 5)

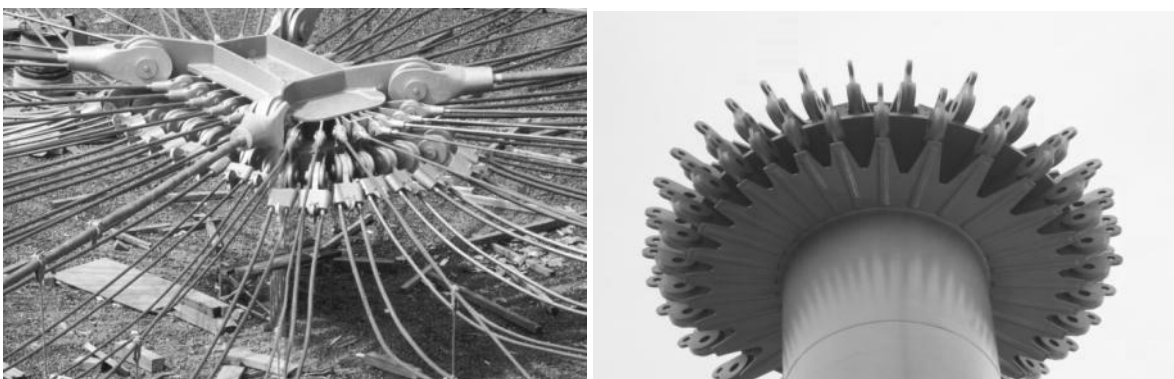


Figure 8.6 Central hub of the Commerz Bank Arena in Frankfurt (left) [Ale 05] and of the National Stadium in Warsaw (right) (Courtesy of schlaich bergemann und partner)

However, the conditions for the minimum required dimension of the central hub change when the textile membrane is folded to the perimeter. The locking device must be built into the central hub, because the driving carriages must be locked there. Therefore the size of the whole central hub must be normally larger than the one of the roof folding to the center.

8.4. Structural Analysis

The structural analysis of textile membrane and radial cables are carried out using finite element method. Geometrical nonlinearity effects are taken into account. The analysis is performed using the Finite element program SOFiSTiK that is one with particular emphasis on civil- and structural engineering.

8.4.1. Calculation model

36 radial cables are chosen for modeling in the structural analysis. The width of a single membrane strip and the height of the flying mast are automatically decided from this number of radial cables. As described in the last chapter, the required height of the flying mast becomes two times of the width of the membrane strip.

Number of radial cable	n	: 36
Width of a single membrane strip	$a = \pi \cdot d / n$: 3.14 m
Height of flying mast in the centre	$h = 2a$: 6.28 m

The equations of upper and lower edge lines of a membrane strip in y-z plane are:

$$z(y) = -\frac{h}{2}y + h \quad (\text{for upper radial cable}) \quad (8.1)$$

$$z(y) = \frac{h}{2}y - h \quad (\text{for lower radial cable}) \quad (8.2)$$

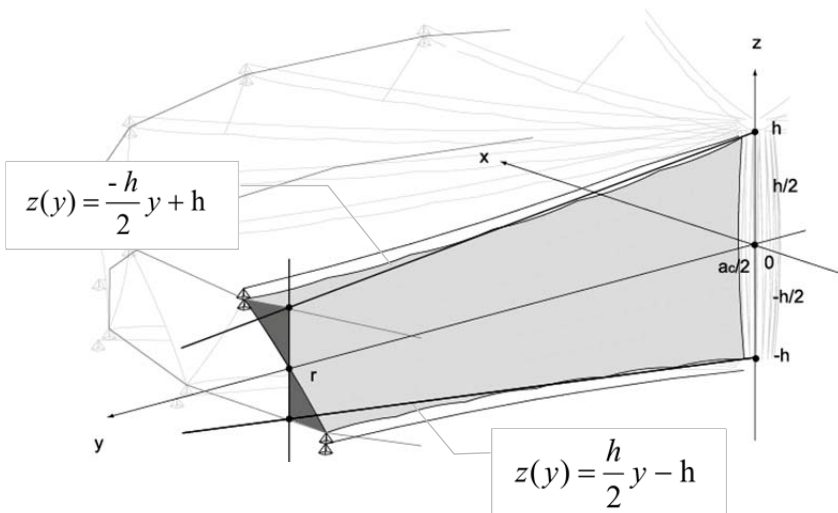


Figure 8.7 Equations of the upper and lower radial edge of one membrane strip

The weight of the flying mast including actuators installed in the centre of the roof is ignored in this numerical model. In reality, extra fixed radial cables must be applied to allow movement of all edge nodes in the center of the roof. All of the weight of the flying mast and

the actuator and the reaction force against the actuator force is transferred through these fixed radial cables to the outer edge.

Also temperature loading is not considered for this structural analysis. Although textile membrane is sensitive material for temperature loading, it is supposed that a retractable roof is used only in summer as described in the previous chapter.

Assumption of the carriages

All bearing points and joint details are implemented as realistically as possible. Since observing the contact between the membrane and cable is important, the membrane and cable should be not analyzed separately. Thus the connection becomes essential. The carriage can be moved only in the cable direction and there are several approaches to simulate this condition.

One possibility is a coupling support. The support point of the membrane and the corresponding point of the radial cables are defined as a coupling point that can slide in one local direction. However this coupling method is very sensitive and careful operation is needed.

Therefore, a simple truss element is used to connect the two points. This is much simpler and less error occurs even in the transition analysis. In this case the support point of the membrane can move but the amount of allowable sliding is limited. The truss element moves like a pendulum, and its amplitude defines the amount of allowable sliding. To make the amount of allowable sliding larger, the length of truss is set as 300 mm. The edge point of both membrane and cable in the centre of the roof are connected to a flying mast as fixed points.

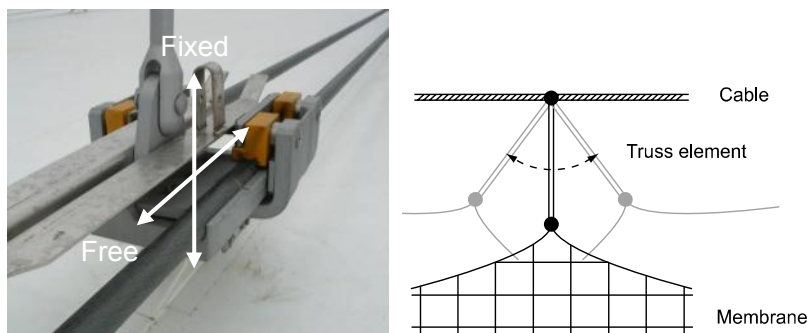


Figure 8.8 Carriage of retractable roof in Commerz Bank Arena (left) (Courtesy of schlaich bergemann und partner) and the simulated model in the analysis (right)

8.4.2. Results of static analysis

The stress- and ponding analysis are performed as static analyses. Firstly in the form finding process, membrane stiffness is reduced with the factor $1e-4$ and the following prestressing forces are given simultaneously: 1.3kN/m in Nxx-direction and 1.8 kN/m in Nyy-direction.

Only the validation of stress analysis and the geodesic height of a load case in which the largest deformation in z-direction occurs will be shown here.

Stress analysis in membrane

Generally it should be verified that the summation of characteristic load effects S_k multiplied with a safety factor γ does not exceed the design resistance R_d :

$$S_d < R_d \quad (8.3)$$

The values of R_d for each material are described in the last chapter.

The normal roll widths of membrane fabrics are 2.05 and 2.50 m, however it is also possible to obtain woven in widths of up to approximately 5 m. [Sei 09] Since the required width of one membrane strip for this roof is 6.3 m in the center of the roof, the seams must be also considered in stress analysis.

The stress analysis of the roof membrane is performed using the corresponding load combinations together with a 30% increase in membrane stiffness, because textile membrane cannot be prestressed in reality like calculation result. Hence, increasing membrane stiffness ensures that the calculation produces conservative results.

Table 8.2 Validation of stress analysis

membrane material										
Type of load-case	load case	number of load-case-combination	warp				fill (weft)			
			Max. membrane force in warp-direction	Max. allowable membrane force in warp-direction	utilization	verification	Max. membrane force in fill-direction	Max. allowable membrane force in fill-direction	utilization	verification
			N_{xx} [kN/m]	$f_{t,d,mem,warp}$ [kN/m]	$N_{xx} / f_{t,d,mem,warp}$		N_{yy} [kN/m]	$f_{t,d,mem,fill}$ [kN/m]	$N_{yy} / f_{t,d,mem,fill}$	
1)	(P+G)	1	1.40	18.0	0.08	<1.0 ok	1.83	17.2	0.11	<1.0 ok
2)	(P+G)+S	2	3.57	22.5	0.16	<1.0 ok	5.61	21.6	0.26	<1.0 ok
		3	2.10		0.09	<1.0 ok	3.53		0.16	<1.0 ok
3)	(P+G)+W	4	4.27	35.9	0.12	<1.0 ok	5.59	34.4	0.16	<1.0 ok
		5	8.21		0.23	<1.0 ok	9.28		0.27	<1.0 ok

membrane seam										
Type of load-case	load case	number of load-case-combination	N_{xx}	$f_{t,d,seam,warp}$	$N_{xx} / f_{t,d,seam,warp}$		N_{yy}	$f_{t,d,seam,fill}$	$N_{yy} / f_{t,d,seam,fill}$	
			[kN/m]	[kN/m]			[kN/m]	[kN/m]		
1)	(P+G)	1	1.40	12.1	0.12	<1.0 ok	1.83	11.6	0.16	<1.0 ok
2)	(P+G)+S	2	3.57	23.5	0.15	<1.0 ok	5.61	22.4	0.25	<1.0 ok
		3	2.10		0.09	<1.0 ok	3.53		0.16	<1.0 ok
3)	(P+G)+W	4	4.27	32.9	0.13	<1.0 ok	5.59	31.4	0.18	<1.0 ok
		5	8.21		0.25	<1.0 ok	9.28		0.30	<1.0 ok

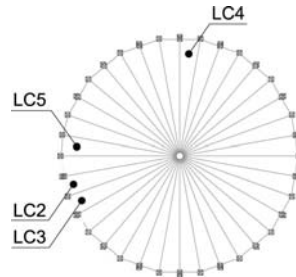
Others										
			Strap and Belt				Edge cables in membrane			
Type of load-case	load case	number of load-case-combination	N	$f_{t,d}$	N / $f_{t,d}$		N	$f_{t,d}$	N / $f_{t,d}$	
			[kN/m]	[kN/m]			[kN/m]	[kN/m]		
1)	(P+G)	1	53.2	163.3	0.33	<1.0 ok	37.1	86.0	0.43	<1.0 ok
2)	(P+G)+S	2	61.2		0.37	<1.0 ok	41.8		0.49	<1.0 ok
		3	61.1		0.37	<1.0 ok	37.8		0.44	<1.0 ok
3)	(P+G)+W	4	60.0		0.37	<1.0 ok	44.8		0.52	<1.0 ok
		5	74.3		0.45	<1.0 ok	57.0		0.66	<1.0 ok

Ponding analysis for the membrane surface

Even though this roof has no flat surface and furthermore a drain pipe is already considered to exist in the center of the roof, a ponding check was performed. The ponding analysis of the roof membrane is performed together with a 20% decrease in membrane stiffness, which is on the safe side. The minimum values of the deformation in the z-direction in each load case are described in Table 8.3.

Table 8.3 The minimum values of the deformation in z-direction in each load case with the corresponding node positions

LF	min Uz [mm]
LC 2	-161
LC 3	-70
LC 4	-198
LC 5	-329



The iso-area is checked to determine whether water will accumulate. The geodesic height that indicates the z-axis height of the membrane surface after deformations is displayed in Figure 8.9 below. Load case 5 has the largest deformation in z-direction. It becomes clear that water flows down to the center of the roof and no ponding occurs on the membrane surface.

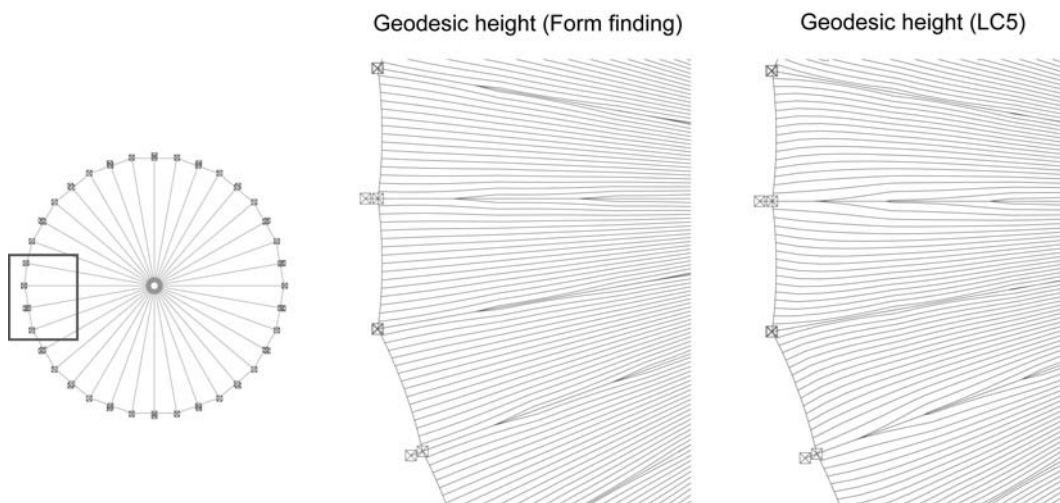


Figure 8.9 Geodesic height (Form finding and Load Case 5)

8.4.3. Results of transition analysis

As a next step, a transition analysis is performed. The aim is to observe and check the transition status of introducing prestressing force in the structural membrane. The transition analysis has been done by iteration of the non-linear static analysis performed in reverse order. It starts from the prestressed configuration and releases the initial prestressing force in the membrane by moving of the edge nodes step by step.

From a practical point of view, observation of the reaction force of the edge node of the membrane is enough. The structural behavior of textile membrane that occurs when prestress

is released is not significant. Therefore, the membrane, edge cable and radial cable are included in the model and only the self-weight of the structure is considered. The flying mast is not included in a numerical model. Instead, the edge points of the membrane and the cable are fixed as support points. Their support forces in z-direction are assumed as axial force transferred to the flying mast.

Since the load vector is not updated during the iteration process by SOFiSTiK, the loads have to be updated. Primary load cases are used in this analysis. Input values are shown in Figure 8.10. The edge nodes of both the membrane and the radial cable move simultaneously and in equal magnitude.

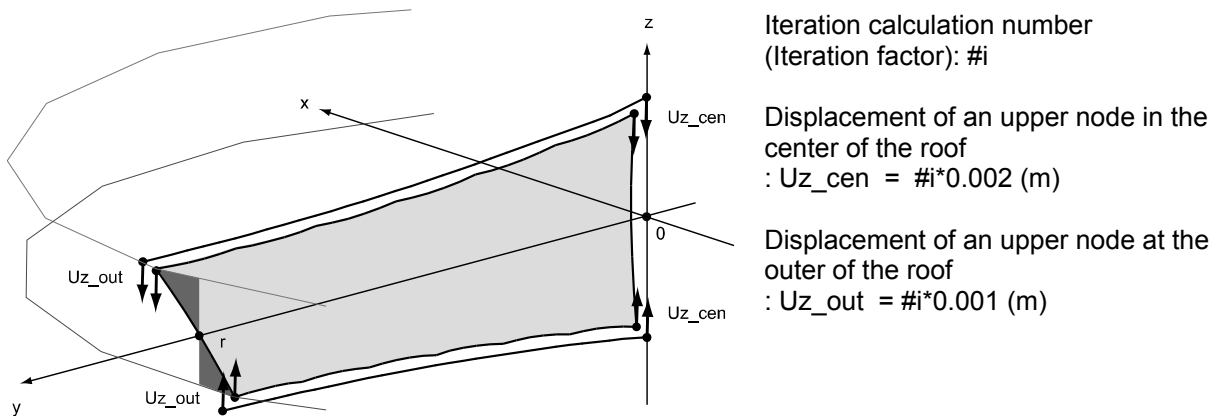


Figure 8.10 Input displacement of the edge node of membrane and radial cables

The introduction of prestressing force into the membrane is displayed in Figure 8.11: starting from the upper left and ending to the lower right (form finding). The magnitude of stress is shown with colors: compression stress is in red and tension stress is in blue. The figures in the left column show that the edge of the membrane is going slack and even begins to develop compression stress. However as described above, the behavior of slacking textile membrane cannot be simulated appropriately by this method. Note that all figures illustrate only the introduction of prestressing force into the textile membrane.

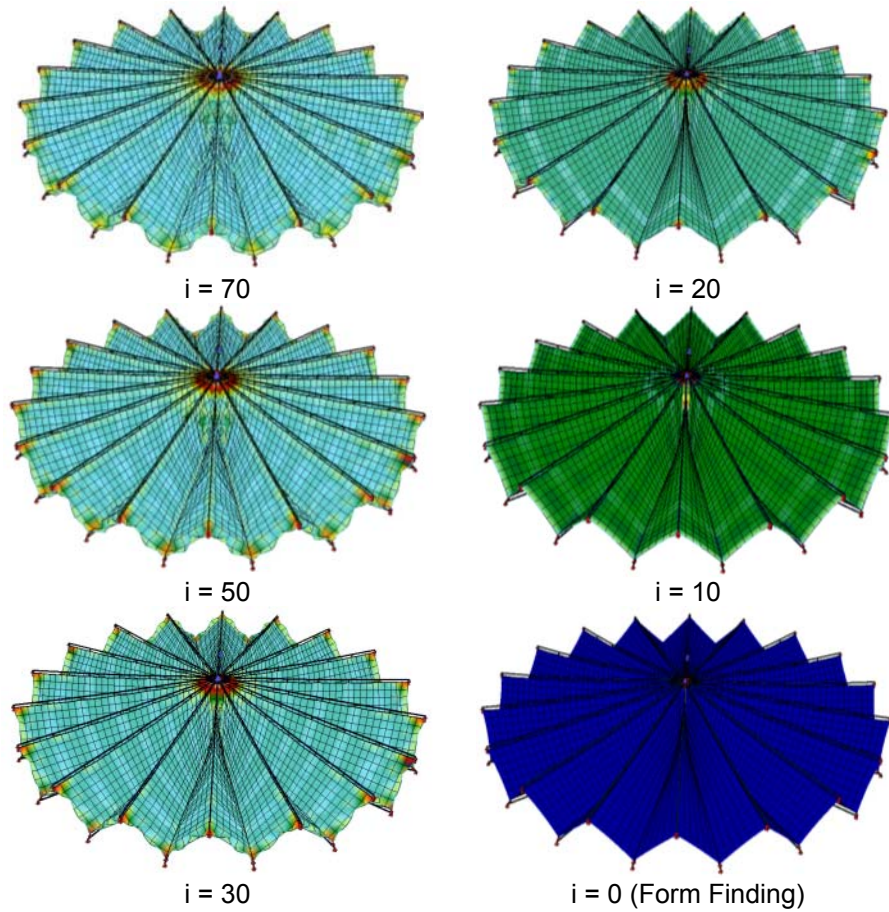


Figure 8.11 Transition of the Reaction force in Membrane

Reaction forces of textile membrane and radial cable are observed. Drastic reduction of the reaction forces are observed in all edge nodes from the $\Delta = 0$ to approximately $\Delta = 5$ to 7. The iteration stopped at a value of $\Delta = 77$.

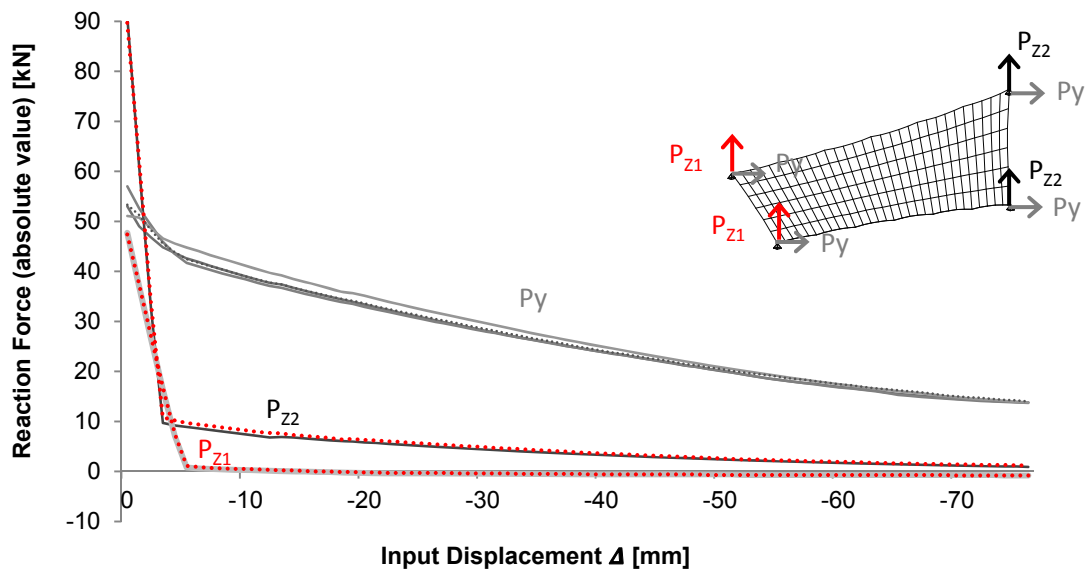


Figure 8.12 Reaction force in four edge node of the membrane strip in both y- and z-direction

Check of movability

The consistency of this method of introducing prestressing force is checked using a cutting pattern of the textile membrane. Figure 8.13 shows a cutting pattern of the membrane strip generated by SOFiSTiK. Shrinkage is apparent because the elongation is set to 3/3% in warp/weft direction in the material properties. The minimum width of this cutting pattern is measured from the figure.

$$a_{\min} = 4.03 \text{ m} < a = 3.14 \text{ m} \quad (8.4)$$

Since the value is smaller than the required width of a single membrane strip on the level of the roof surface, it can be verified that textile membrane can be folded to the outer edge of the roof.

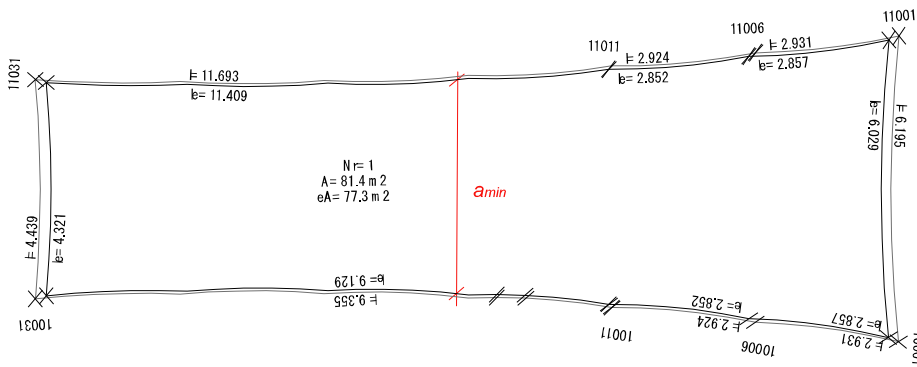


Figure 8.13 Cutting pattern of a membrane strip

8.4.4. Actuator Design

The required force for the actuators can be calculated from the reaction force of the textile membrane and the radial cables. Two edge nodes of a membrane strip at the centre of the roof are moved vertically by two actuators installed in upward and downward directions. The other two nodes at the outer edge of the roof are moved also vertically but together with the compression rings. Furthermore, two more actuators are necessary in the horizontal direction to provide sufficient tension force in the radial cables.

Here the required forces of actuators related to the two upper edge nodes are calculated. At the centre of the roof the force of the vertical actuator $P_{z_act_c}$ must be balanced the vertical reaction force of membrane P_{z_cen} , as shown in Figure 8.16.

$$P_{z_act_c} = P_{z_cen} \quad (8.5)$$

The point at the outer edge is not as simple as the one at the center of the roof, because the force of the radial cable and the weight of the compression ring must be considered. In the vertical direction, the vertical reaction force of the membrane P_{z_out} and of the radial cable P_{z_t} and the weight of the compression ring P_g must be balanced to the vertical actuator force $P_{z_act_o}$. In horizontal direction, the horizontal actuator force $P_{y_act_o}$ is balanced to the horizontal reaction force of the radial cable P_{y_t} .

$$P_{z_act_o} = P_{z_out} + P_g - P_{z_t} \quad (8.6)$$

$$P_{y_act_o} = P_{y_out} + P_{y_t} \quad (8.7)$$

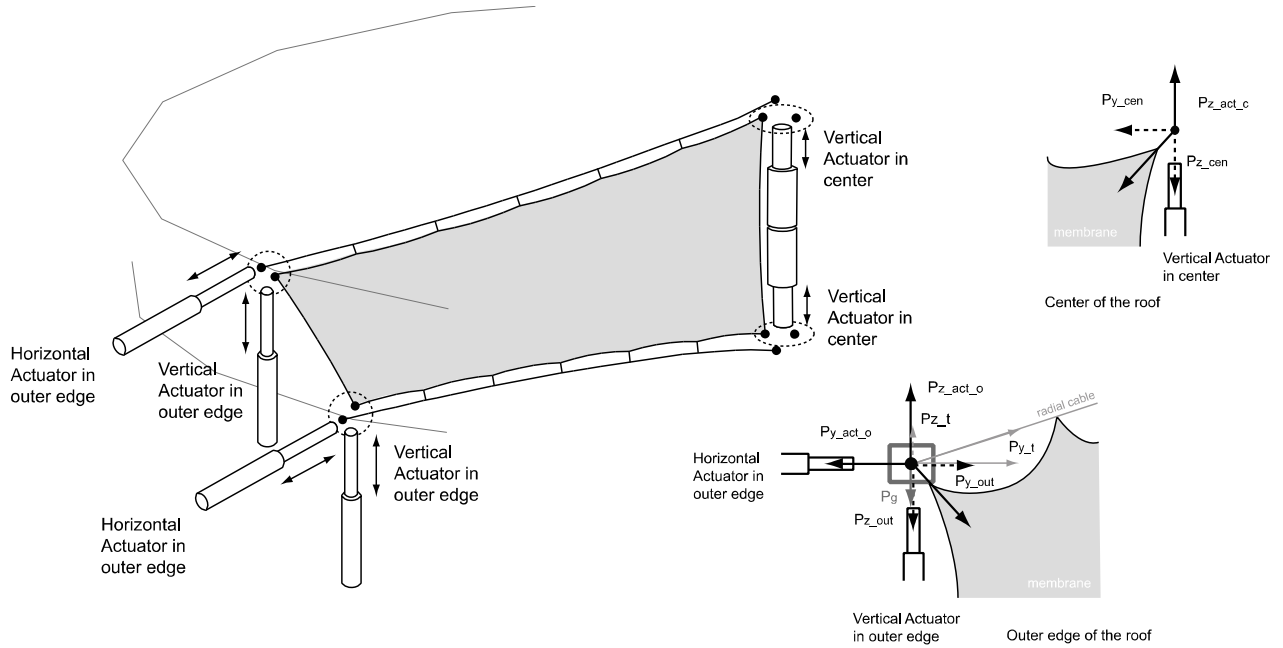


Figure 8.14 Position of actuators and force balance at the outer edge and the centre of the roof

Calculated maximum values of the reaction forces are as follows.

$$\begin{aligned} P_{z_cen} &= 90.7 \text{ kN} \\ P_{y_out} &= 57.0 \text{ kN} \\ P_{z_out} &= 47.7 \text{ kN} \\ P_{y_t} &= 478 \text{ kN} \\ P_{z_t} &= 17.5 \text{ kN} \end{aligned}$$

P_g is estimated as steel hollow section (400 x 400mm) including the weight of the horizontal actuator: $P_g = 13\text{kN}$

The values are substituted in the equation of (8.5), (8.6) and (8.7).

$$\begin{aligned} P_{z_act_c} &= P_{z_cen} &&= 90.7 \text{ kN} \\ P_{z_act_o} &= P_{z_out} + P_g - P_{z_t} &&= 47.7 + 13 - 17.5 = 43.2 \text{ kN} \\ P_{y_act_o} &= P_{y_out} + P_{y_t} &&= 57.0 + 478 = 535 \text{ kN} \end{aligned}$$

In the centre of the roof all edge nodes of the membrane can be moved together by one actuator. Therefore the required force of the actuator at the center is multiplied with half of the number of membrane strips. Thus the required force of the actuator becomes:

$$\begin{aligned} \text{Vertical actuator in the center of the roof:} & \quad \sim 1600 \text{ kN} \\ \text{Horizontal actuator at the outer edge of the roof:} & \quad \sim 550 \text{ kN} \\ \text{Vertical actuator at the outer edge of the roof:} & \quad \sim 45 \text{ kN} \end{aligned}$$

8.5. Model construction

Even though calculation results from the analysis seemed to be rational, the simulation of the exact interactional behavior of all movable components in the system has to be proven. The whole transition process cannot be analyzed easily even by modern computing technology. Therefore, the author designed and constructed a physical model of the whole roof. The main goals were to check the details and to validate the feasibility of the conceptual design of the raised compression ring method. Water tightness of the central hub was not considered in this model due to the size limitation.

8.5.1. Details consideration

Modifying the principle of the raised compression ring method

For the construction of the model, the principle of the raised compression ring method is modified in the following two points.

The structural analysis revealed that a large actuator force is necessary especially in the centre of the roof, because all of the cables and the membrane are gathered there in one point. To reduce the required loading, upper nodes of the membrane are fixed and only the lower nodes are moved by the actuator installed on the flying mast.

Moving both compression rings is difficult, because an immovable point is necessary to make the roof stand on the fixed ground. Therefore, in the model the lower compression ring is fixed and only the upper ring is raised up and down.

Consequently two edge points, out of the four edge points of the membrane strip are fixed.

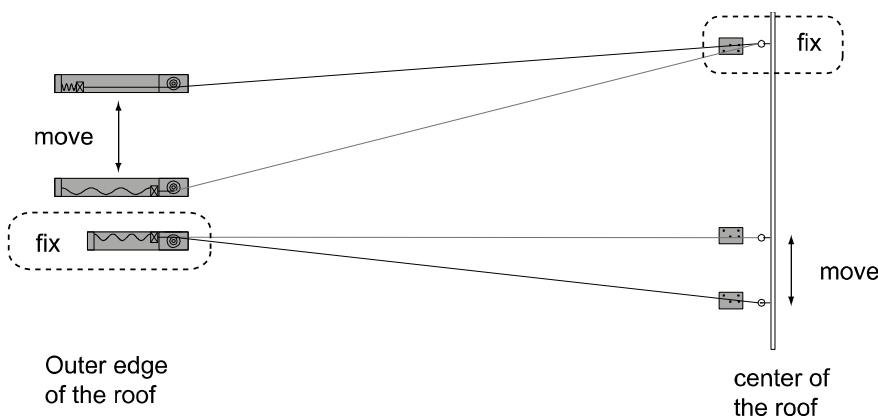


Figure 8.15 Sectional view of primary structure

The extensional cable system is built into the compression ring as one unit as shown in Figure 8.16 below. Elastic springs are used due to cost and simplicity. A small roller is installed for the functioning a saddle between the compression rings. The air cylinder to raise the whole upper compression ring is connected just below the saddle to make the force transfer through only one point. Tension force from the radial cable is transferred into the compression ring as displayed in the far right image in Figure 8.16.

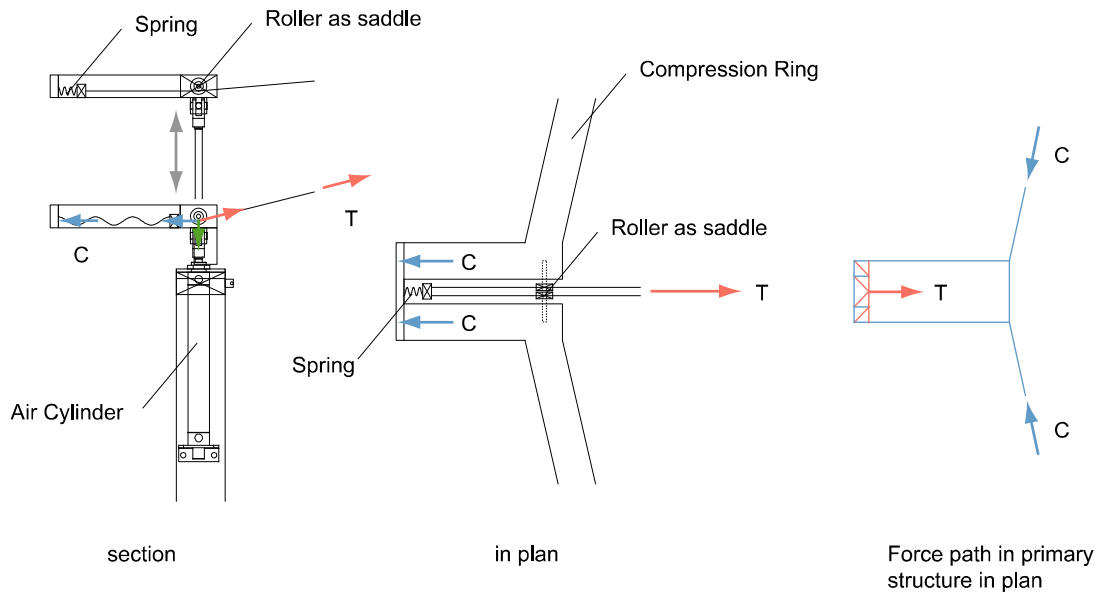


Figure 8.16 Extensional cable system at the outer compression ring

8.5.2. Material and Dimension

Wood is used for the main material of the primary structure because of its ease of handling. However most of the part of the central hub consists of steel and aluminum, because the dimensional accuracy is necessary for the mechanical part.

The diameter of the roof is chosen as 1.8m, which is 1:200 scale of a full size roof. The number of cables is 28. The upper and lower compression rings are constructed separately at first and then combined together with the actuator. Seven fixed cables are anchored in the lower compression ring.

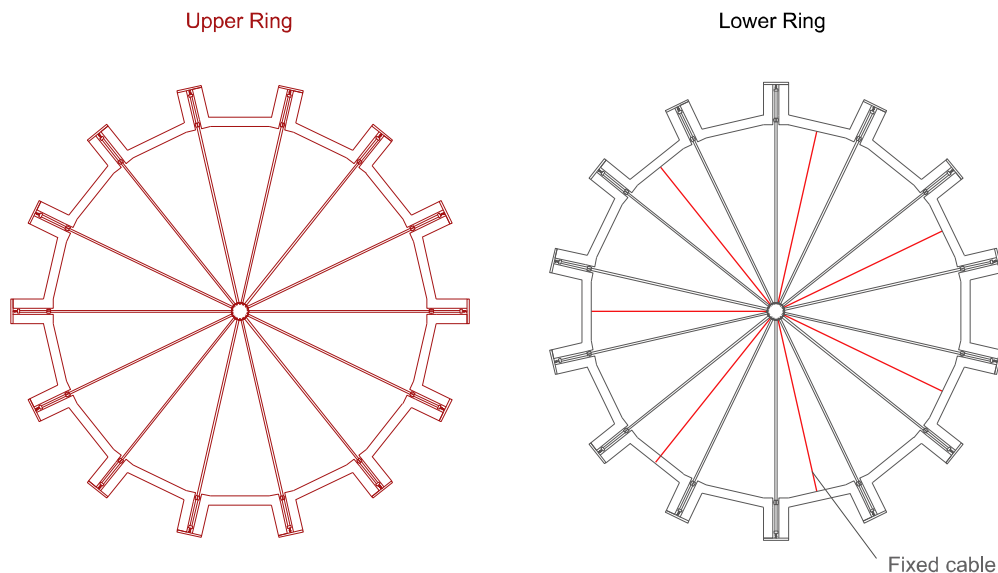


Figure 8.17 Two compression rings (red: upper ring and black: lower ring)

The upper compression ring is laid on the lower compression ring on site, with the positions of the radial cables staggered.

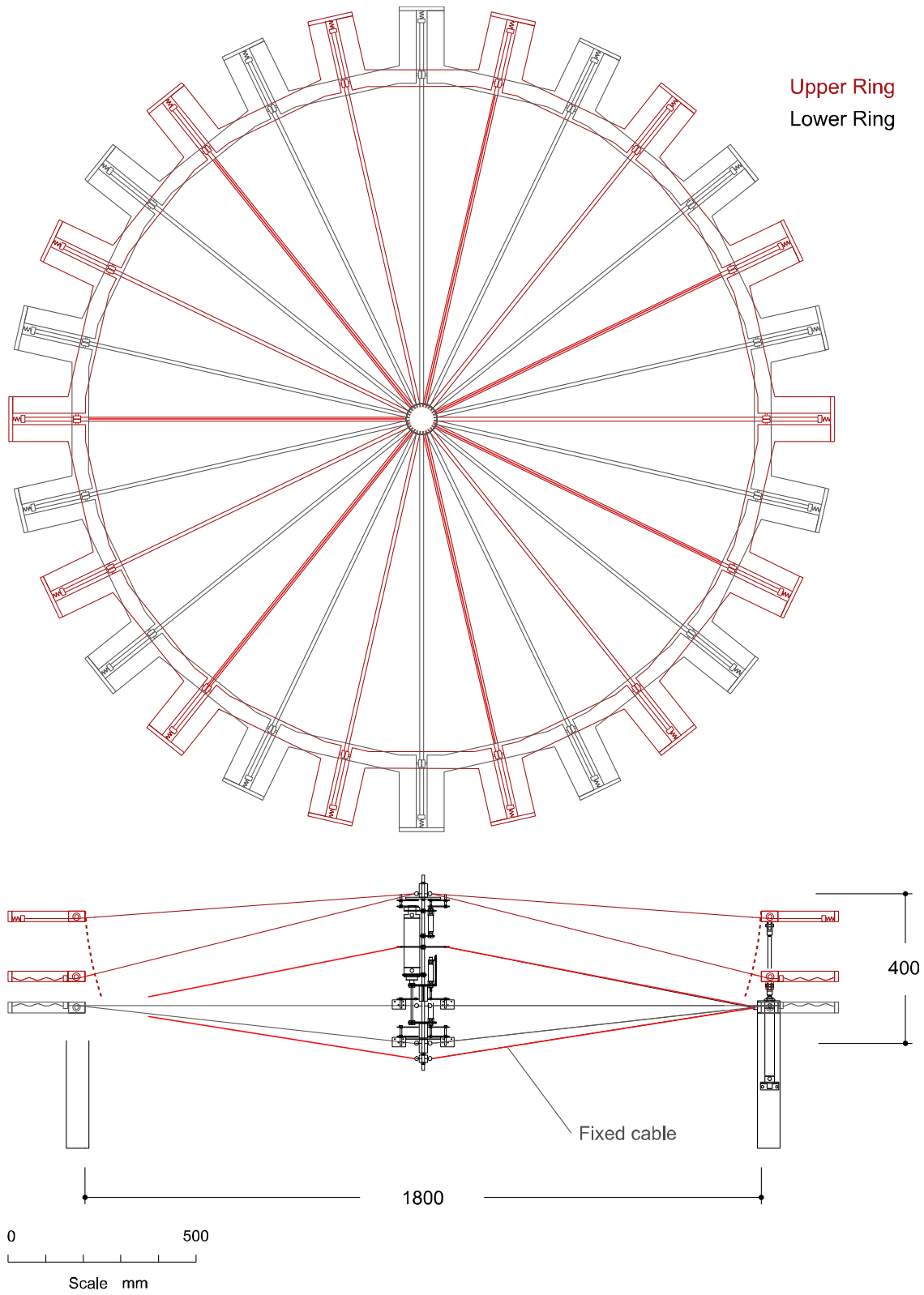


Figure 8.18 Design drawing of the model in plan (upper) and in section (lower)

8.5.3. Actuator design

An air cylinder is chosen as actuator due to its simplicity of linear motion and its ease of handling. The required force of the air cylinder is estimated by the results from SOFiSTiK. One air cylinder with 40mm diameter is chosen for the actuator at the central flying mast, which can generate theoretically 750 N by 6 bar of air pressure. Two more small air cylinders are also installed on the flying mast for the locking device of the sliding carriage.

7 air cylinders of 20mm diameter are installed under the lower compression ring, which can generate theoretically 188 N by 6 bar of air pressure. These three different kinds of air cylinders are connected to two dampers and one compressor. The diagram in Figure 8.19 shows the schematic design of the air cylinders. The locking device and the tension unit are controlled by the different dampers.

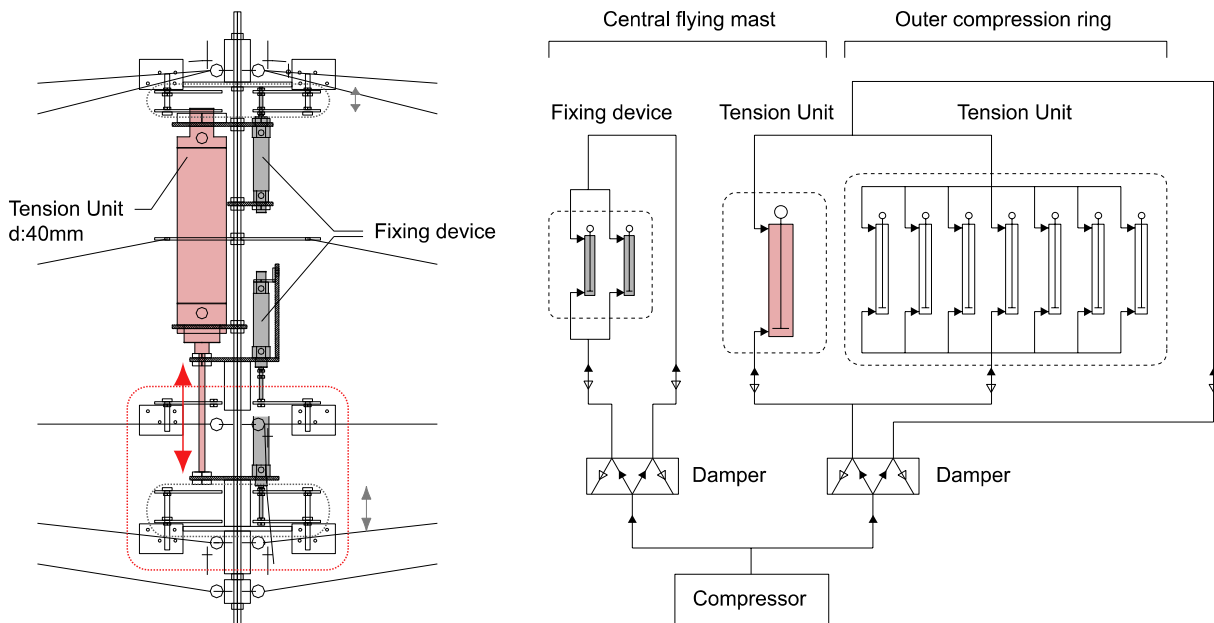


Figure 8.19 Two different kinds of the air cylinders on the flying mast (left) and schematic of the air cylinders

8.5.4. Construction process

The construction process is as follows. After constructing the compression rings, 14 fixing radial cables are installed simultaneously by hand. Since a small error of cable length in construction provokes a disproportionally larger deviation of the roof geometry, the installation of the radial cables is performed with the great care. Figure 8.20 shows one construction scene. While the flying mast is held in the appropriate central position by one person, all fixed radial cables are attached simultaneously to the lower compression ring. Then the central hub was floated appropriately in the center of the roof.



Figure 8.20 *Installation radial cables (left) and flying mast suspended by the radial cables (right)*

The cutting pattern is computed by SOFiSTiK. All 28 membrane strips are cut out from a roll of the membrane fabric and sawed one by one in 3 dimensions by hand. The longitudinal length of it becomes around 11m. This lengthwise membrane fabric is installed between upper and lower compression rings and radial cables. Then the front- and rear edge is sewn together on site to make one continuous form. Finally this donut-like form's membrane fabric is hung by the sliding carriages running on the radial cables.

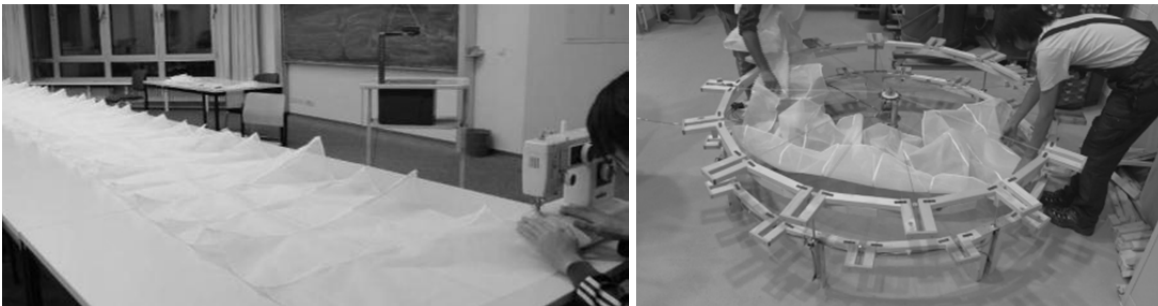


Figure 8.21 *Sew lengthwise textile membrane (left) and installation of membrane (right)*

8.5.5. Result

In the first picture of Figure 8.22, textile membrane is folded at the outer edge of the roof. Next, the membrane is unfolded but not yet stressed. The last picture shows that the upper compression ring is raised up by the air cylinder and the central lower node moves downward in order to prestress the textile membrane.

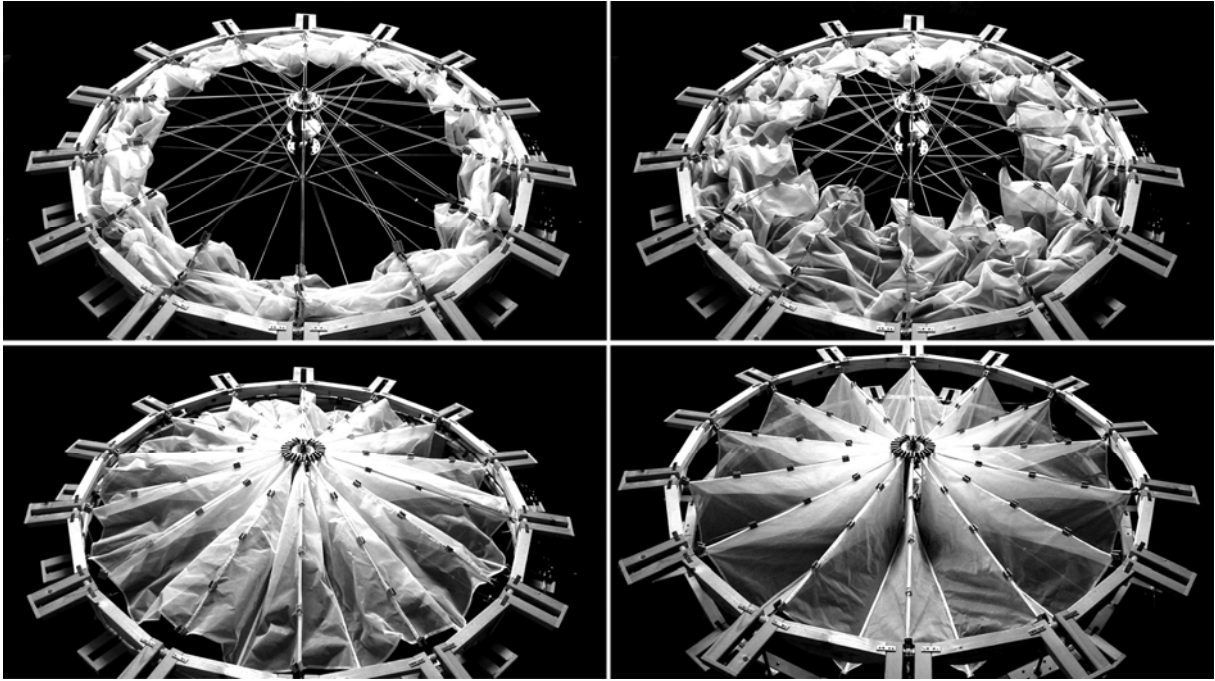


Figure 8.22 The finished model (upper left: folded, upper right and lower left: unfolded, lower right: prestressed status)

Pictures in Figure 8.23 are views from the lower angle. In the last (fourth) picture, the curved radial edge lines of the textile membrane shows that the textile membrane is prestressed successfully.

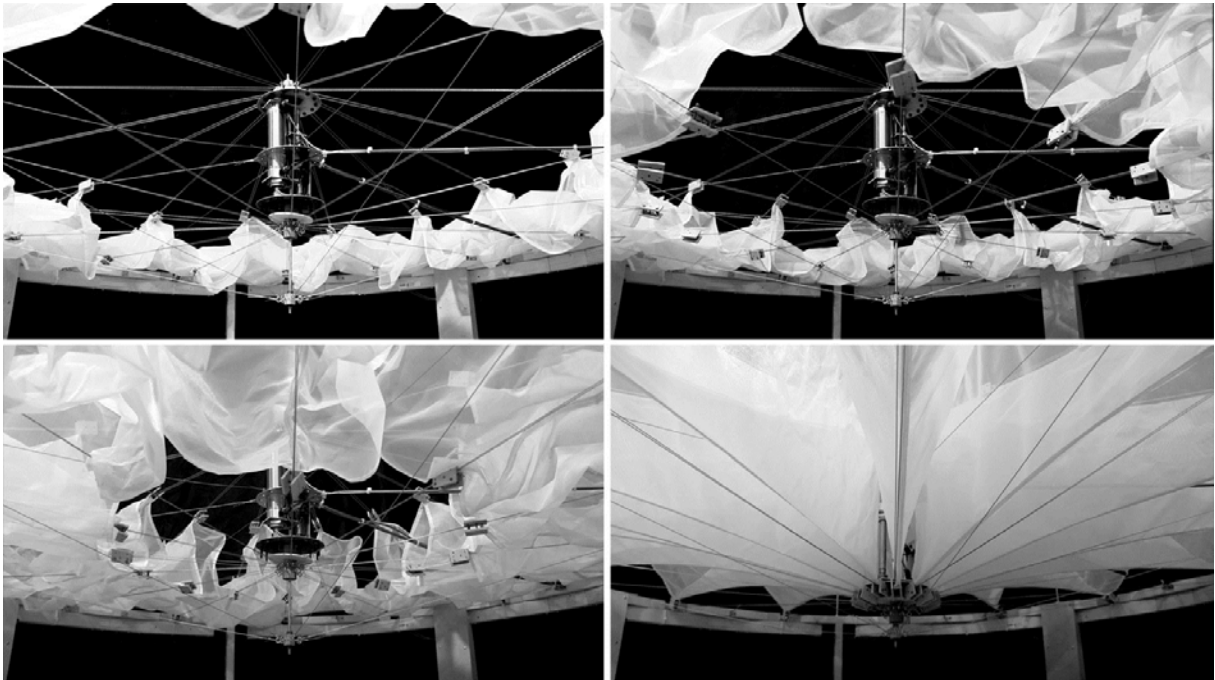


Figure 8.23 The finished model from the lower angle (upper left: folded, upper right and lower left: unfolded, lower right: prestressed status)

8.6. Discussion

In this case study, the raised compression ring method was presented. Since the number of radial cables leads to significant differences in the whole roof's geometry, and since the required width of the membrane strip at the centre of the roof is relatively large in this method, the geometrical considerations as well as drain path were studied at first.

Some detail studies are performed before structural analysis was carried out. The extensional cable system is critical for this method, because the length of the radial cable must be changed in order to introduce prestressing force into the membrane. Two more details are studied: water tightness and minimizing the size of the central hub. The last two are more general themes for a retractable membrane roof folded to the perimeter.

Structural analysis was done for an integrated model in unfolded configuration. The membrane stiffness is changed according to the aim of the analysis: for the stress analysis it is increased and for the ponding analysis it is decreased. This practical analysis provided the basis for the construction of the structure.

Structural analysis was carried out also for the process of introducing prestress by using an iteration calculation method. As the prestress was introduced, the reaction forces of the textile membrane and radial cables of the primary structure were observed and verified.

Even though rational calculation results were obtained from the analysis, it became apparent that the simulation of the exact interaction and behavior of all structural elements in the system was too difficult. Therefore the author designed and constructed one complete physical model. The details and the feasibility of the conceptual design of the raised compression ring method were studied. Due to its simplicity and its ease of the handling, air cylinders are used as devices for intruding prestressing force into the membrane. Construction of the rather large scale model (diameter 1.8m) offered sufficient knowledge and deeper consideration for the details of this method.

Comprehensively, the raised compression ring method seems to provide a reasonable solution for the membrane retractable roof, in which the membrane is folded to the perimeter. However, more careful and detailed analysis, such as checking the global stability and the dynamic behavior of the structure may be required in order to construct the structure in full scale. Also more accurate calculation theory should be developed to simulate the behavior of textile membrane during the introduction of prestress.

9. Case Study B – ‘Minor Shift - Major Lift’ Mechanism

9.1. Introduction

This chapter devotes to study another possible solution for the membrane foldable roof with a unique system for introducing prestressing force into membrane, which was named “minor shift – major lift” mechanism in the last chapter. The chapter consists of two parts. First a study of the statics and the kinematic behaviour of cable girder is performed. Then the analytical results are transferred to the intended retractable membrane roof. One crucial aspect concerning membrane roofs in general and movable ones in particular is the introduction of the prestress. Here the combination of a movable membrane roof with a kinematic cable girder offers a new solution for this major structural challenge.

9.2. Parameter study of static- and kinematic cable girder

The aim of the study in this section is to reveal the behaviour of kinematic cable girders. To fully understand the potential of kinematic cable girders, their behaviour will be studied through a parametrical analysis. The main characteristics like deflection and raising factor will be described and analyzed from an extensive static and kinematic analysis.

9.2.1. Advantage of kinematic cable girders

Flexibility is not a synonym for instability, nor is inflexibility synonymous with stability. On the contrary, flexibility allows new solutions for adaptable light weight structures. Kinematic cable girders for movable and flexible structures have a great advantage in terms of efficiency compared to traditional movable structures. This concerns not only the small amount of necessary material but also the reduction of required energy for the movement. Their lightness as well as their flexibility provide kinematic advantages as well as challenges. For instance, a small error of cable-length in construction can produce significant membrane sag. However this kinetic feature combined with a driving mechanism can be applied to movable structures with surprisingly efficient results. It is, for example, perfectly used for the lift of the “Katzbuckel” bridge in Duisburg, Germany, as shown in the previous chapter. This simple and effective approach can be an answer for one of the most interesting challenges of modern movable structures: how to reach maximum output with minimum input.

A cable girder is composed of a convex downwards forming “supporting” cable and a convex upward forming “prestressing” cable whose curvature are reversed. Both cables are connected by several vertical hangers.

A cable girder can be regarded as one solution to provide more rigidity to the single supporting structure without greatly increasing its weight. Since, like all the cable structures, it functions only in tension and never in compression, stability problems do not occur. This

makes the dimension of all of the structural components relatively small. Its lightness and transparency are great advantages as wide span structures such as roofs or footbridges.

These structural advantages can be directly translated to the kinematic feature of cable girders. One example is that its lightness leads to low required energy for moving the structure. As shown in Chapter 3, the energy for the movable roof depends primarily on its self-weight. The fact that cable girders consist of only axial components can make the required driving mechanism as simple as possible. For instance in the “Katzbuckel” bridge only shortening of the back stay cables cause the lifting up of whole deck of the bridge. Such simplicity is a great advantage to design and to construct a movable structure.

9.2.2. Calculation model and parameters

Here a basic model of a cable girder used for the static as well as for the kinematic study is illustrated. The geometrical features appeared on the following schema. It is composed of 20 vertical hangers connecting the upper with the lower cable, and all cable stiffnesses are the same: $EA_U = EA_L = EA_H$. Both main cables are modeled with a parabolic form, and the distance a between each hangers is constant. Cables with a diameter of 40 mm are used. By default the hangers are prestressed with a force P of 25 kN and loaded with singles loads Q_i of 20 kN applied at the all nodes between the hangers and the lower cable. The note e is the smallest distance between the upper and lower cables.

In static analysis maximal deflection (U) and maximum cable forces (N) will be observed. The loading process is composed of three phases described on the schemas as: Initial state (0), Prestressed state (1), and Loaded state (2). The response of the cable girders in displacement are represented with the variations of deflection ΔU between the prestressed and the loaded state: $\Delta U = U_2 - U_1$. ΔU_{\max} represents the maximum of variation of deflections between the prestressed and the loaded state (2)-(1).

In the kinematic study of the cable girders the source of the move Δ is the main input parameter, which takes a constant value from 0.01m to 0.3m in each calculation. It represents a horizontal outward movement of both upper anchorages. This causes the cable girder to shift upward. The cable girder's elevation E_i at the middle of the upper cable is the output result. Only the elevation of the upper cable is observed because ones of both upper and lower cable are mostly same. By establishing the relation between input and output parameters $E_i = n \cdot \Delta$, another output parameter n as the so called “raising-factor” is introduced. The magnitude of n expresses the cable girder's “efficacy” i.e. the multiplication factor of the input parameter.

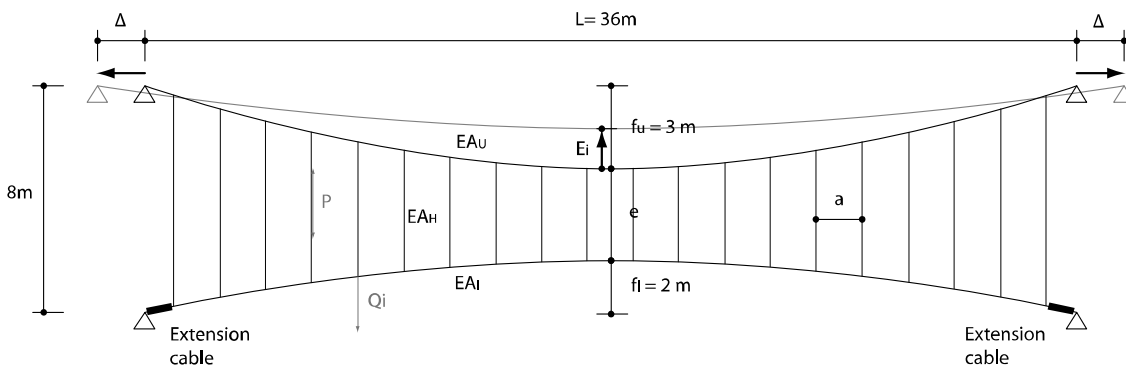
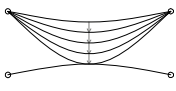
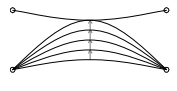
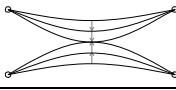
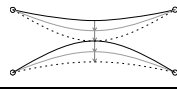
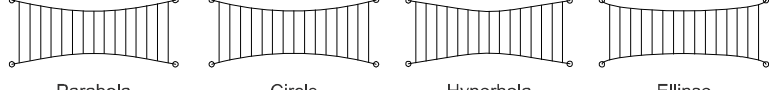
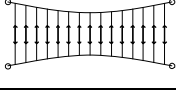
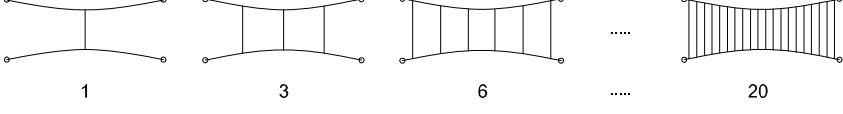
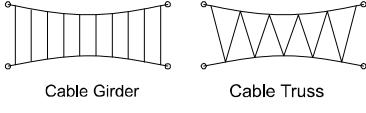
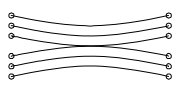


Figure 9.1 Detailed diagram of a concave cable girder

The increase in elevation of the whole cable girder during the kinematic process leads to an elongation of the lower cable. The cable sag increases, and this causes an elongation of the extension cable. In the case of the above mentioned Katzbucket bridge, this problem was managed by additional walkway elements drawn out from the ends during the raising up. It is necessary to develop an accurate model to consider this lower cable's extension. The ideal result is to enable the extension of the lower cable without creating additional internal forces. The author looked for a model which can fulfill both of these contradictory goals and selected one in which the axial stiffness is decreased to $EA/100$. With this, the additional internal forces in the lower cable exist but are limited, while the elevation is affected by the presence of the lower cable.

An input parameter is set for each component of cable girders: cables and hangers. For the cables, variation of upper- and lower cable sag as well as form will be considered. For the hangers, applied prestressing force, quantity, disposition and length will be treated as parameters.

Table 9.1 Defined parameters for this study

Cables	
Cable sag	<div> Variation in upper-cable sag  $f_{u,min} = 0m \ (f_u/l=0)$ $f_{u,max} = 6m \ (f_u/l=0.17)$ </div> <div> Variation in lower-cable sag  $f_{l,max} = 6m \ (f_l/l=0.17)$ $f_{l,min} = 0m \ (f_l/l=0)$ </div>
	<div> Both cable sags (e varying)  $f_{u,min} = 0m \ (f_u/l=0)$ $f_{u,max} = f_{l,max} = 4m \ (f_l/l=0.1)$ $f_{l,min} = 0m \ (f_l/l=0)$ </div> <div> Variation in both cable sags (e constant)  $f_{u,min} = 0m \ (f_u/l=0)$ $f_{u,max} = 6m \ (f_u/l=0.17)$ </div>
Cable form	 <div>Parabola Circle Hyperbola Ellipse</div>
Hangers	
Prestressing force	 $P = 0, 10, 20, 30, 40 \text{ kN}$
Number of hangers	 <div>1 3 6 20</div>
Disposition of hangers	 <div>Cable Girder Cable Truss</div>
Length of hangers	 $e_{max} = 6m$ $e_{min} = 0m$

9.2.3. Summary of the results of the parameter study

The observations were completed for stationary (deflections and tensions) and for kinematic (elevation and raising factor) cable girders. Instead of showing all calculation results, the relationships between the input and the output parameters will be described with a focus on its kinematic features.

a) $f_u \leftrightarrow E_{\max}$

Maximum allowable elevation E_{\max} is equal to the sag of the upper cable f_u when the upper cable is in its initial position.

b) $\Delta U_{\max} \leftrightarrow n_{\max}$

Most of the results of the parameter studies show one tendency: the values of the maximum deflection between the prestressed and the loaded state in the upper cable ΔU_{\max} have a correlation with n_{\max} . Large/small values of ΔU_{\max} corresponds to large/small values of n_{\max} , respectively.. This seems logical because more rigid structures are less sensitive against loading. Lifting the cable girder is nothing more than imposing a deformation. ΔU_{\max} could be defined as an intermediate parameter connecting the static input parameter such as cable form or number of hangers to the kinematic output parameter (n_{\max}) in regard to the “rigidity” of the cable girder.

c) $f_u / l \leftrightarrow n_{\max}$

Since the sag-span ratio of the upper cable f_u/l is also one of the input parameters, it can be related to the raising factor n_{\max} through ΔU_{\max} , as a parameter as described above in (b). However, f_u/l could also be connected to n_{\max} directly. This tendency can be observed by the curves in the left diagram of Figure 9.2, in which, globally, the maximum raising factors in three different studies decrease at the same time that the ratio f/l increases. The influence of the lower cable’s geometry is much less important than that of the upper cables.

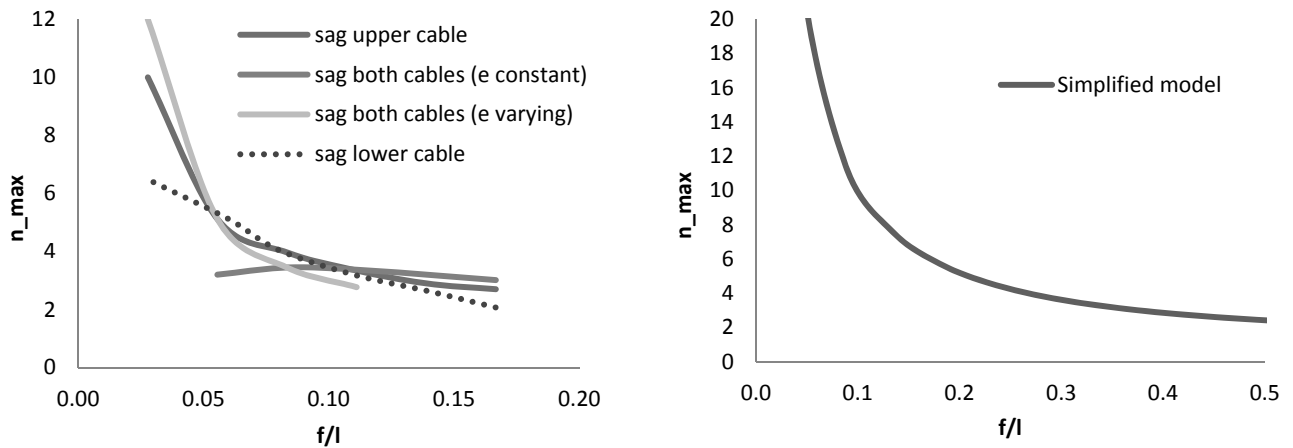


Figure 9.2 The maximum raising factor n_{\max} according to f/l

These results show that the efficiency of the kinematic cable girder depends mostly on the geometry of the upper cable.

The great advantage of kinematic cable girders is, as previously described, that minor shifting causes major lifting. The geometrical trick of this can be explained by Figure 9.3, in which the upper hanging-formed cable is simplified to a linear line with length s . However, the value of the maximum elevation, E_i , remains equal to the sag, f . By a horizontal outward shift of the

end, the middle point of the line is lifted up until the line becomes horizontal. The sag-span ratio can be expressed with the angle α that indicates the inclination of the line at the initial position:

$$\frac{f}{l} = \frac{\tan \alpha}{2} \quad (9.1)$$

From the geometrical configuration the input and the output value, Δ and E_i , can be expressed using the angle α respectively:

$$\begin{cases} E_i = \frac{s}{2} \cdot \sin \alpha \\ \Delta = \frac{s}{2} (1 - \cos \alpha) \end{cases} \quad (9.2)$$

$$\Delta = \frac{s}{2} (1 - \cos \alpha) \quad (9.3)$$

Thus the raising factor can be calculated.

$$n = \frac{E_i}{\Delta} = \frac{\sin \alpha}{1 - \cos \alpha} \quad (9.4)$$

The curve of this equation can be drawn using f/l as a variable with the equation (9.1). It is shown in the right diagram in Figure 9.2. Even though the magnitudes of the variables are different, it can be understood that both graphs in Figure 9.2 show very similar tendencies. Thus we can assume that the geometrical configuration of the sag-span ratio of the upper cable directly relates to the efficiency of kinematic cable girders.

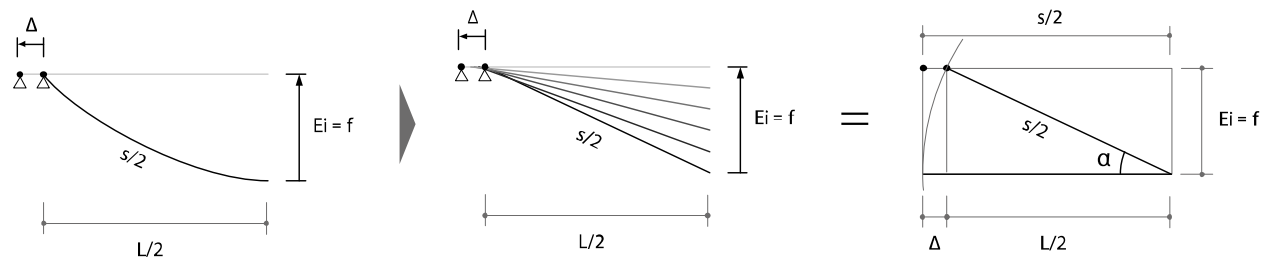


Figure 9.3 Simplified geometrical feature of kinematic cable girder

d) Hanger's length

The parameter study of the hangers revealed that the geometrical configuration of the hangers has no relevance to its kinematic feature.

The derived relationships between the parameters mentioned above could be helpful to understand the kinematic behavior of the cable girder and can be summarized in one figure.

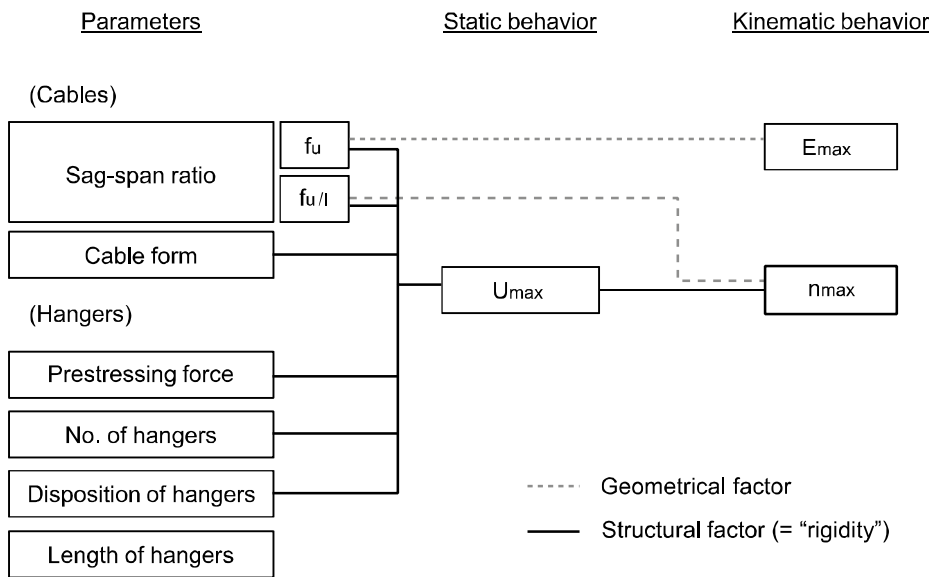


Figure 9.4 A relationship between each parameter of the kinematic cable girder

Input parameters $\leftrightarrow n_{max}$

The relationships between the input parameters and the maximum raising factor are shown in Figure 9.5. The study of prestressing force shows that larger initial prestressing forces lead to a smaller elevation of the cable girder. This is logical because the prestressing force tends to rigidify the cable girder and therefore to limit its displacements, as confirmed in the static study.

The study of the cable form reveals that cable girders whose main cables are parabolic or circular have similar responses, as their geometries are very close. However, the hyperbola behaves slightly differently from the two previous cases. The elliptical curve is globally more flexible which makes it easier to elevate, from a kinematic point of view. This is because the curvature of elliptical curve is zero at mid-span.

The static analysis demonstrates that a large number of hanger cables tends to limit the cables' deformations. However the difference in performance between 6 hanger cables and 20 hanger cables is small.

The static analysis of the hangers shows that a cable truss is less affected by loading than a cable girder, and it therefore has lesser value of the maximum raising factor. In other words it's more rigid. This is due to the fact that in the case of the truss, the hangers are inclined and form triangles, whereas in the case of the cable girder, they are connected with trapezoids (more movable than triangles).

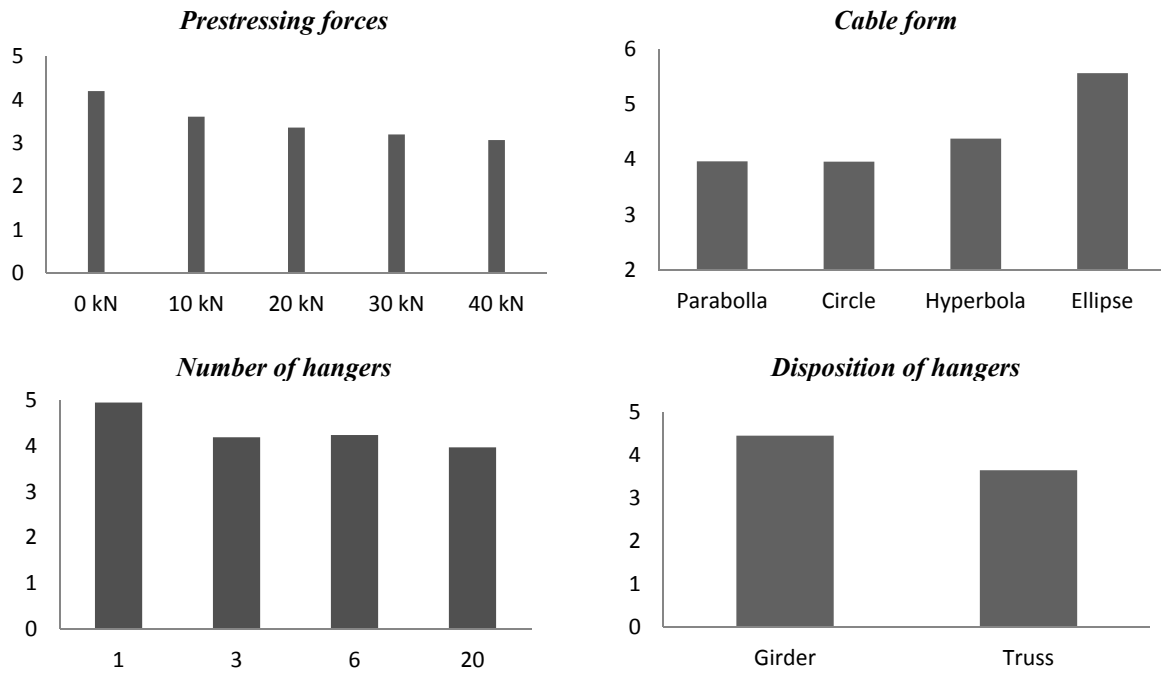


Figure 9.5 The maximum raising factors in each parameter (horizontal axis: input parameters, vertical axis: maximum raising factor n_{max})

Conclusion of the parameter study

The results and of this study are useful in guiding the selection of appropriate parameters to vary according to a target function. It is not easy, but it is also not impossible, to define the ‘best’ performing cable girder in regard to both static and kinematic behavior. For instance, good structural stability (minimization of deflection) must be considered in addition to good kinematic efficiency (maximal raising factor). Thus the target function is very important to design the kinematic cable girder.

9.3. Principle model

Finally the analytical results are transferred to the intended retractable membrane roof. The physical study model demonstrates the proposed mechanisms. The cable girders connected to the masts standing on the outer edge of the roof are arranged radially. The lower cables are not connected, but they run through the mast foot and meet the elastic support that allows the extension of the lower cables. Retracting all backstay cables at the same time causes pivoting outwards of all masts, which leads to the uplifting of the cable girders.

One simple device is applied to the model in order to demonstrate the kinematic cable girder’s behavior; all backstay cables run through the saddles on the outer edge of the roof and connect in a small ring under the roof at the central position. A simultaneous shift of the all mastheads can be invoked by the pushing this ring downward.

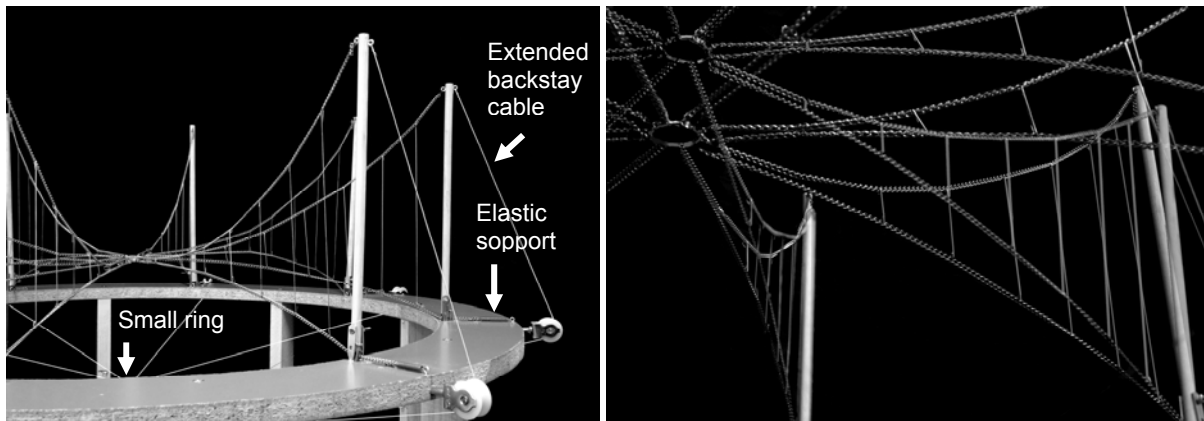


Figure 9.6 *A physical model of cable girders in radial arrangement*

The textile membrane is connected to the cable girder. In unfolded status the membrane would be pulled upwards so that an appropriate prestressing force could be introduced. But a stationary central flying mast supported by additional radial cables becomes necessary, because the lower point of the textile membrane must be fixed in order to introduce prestressing force.

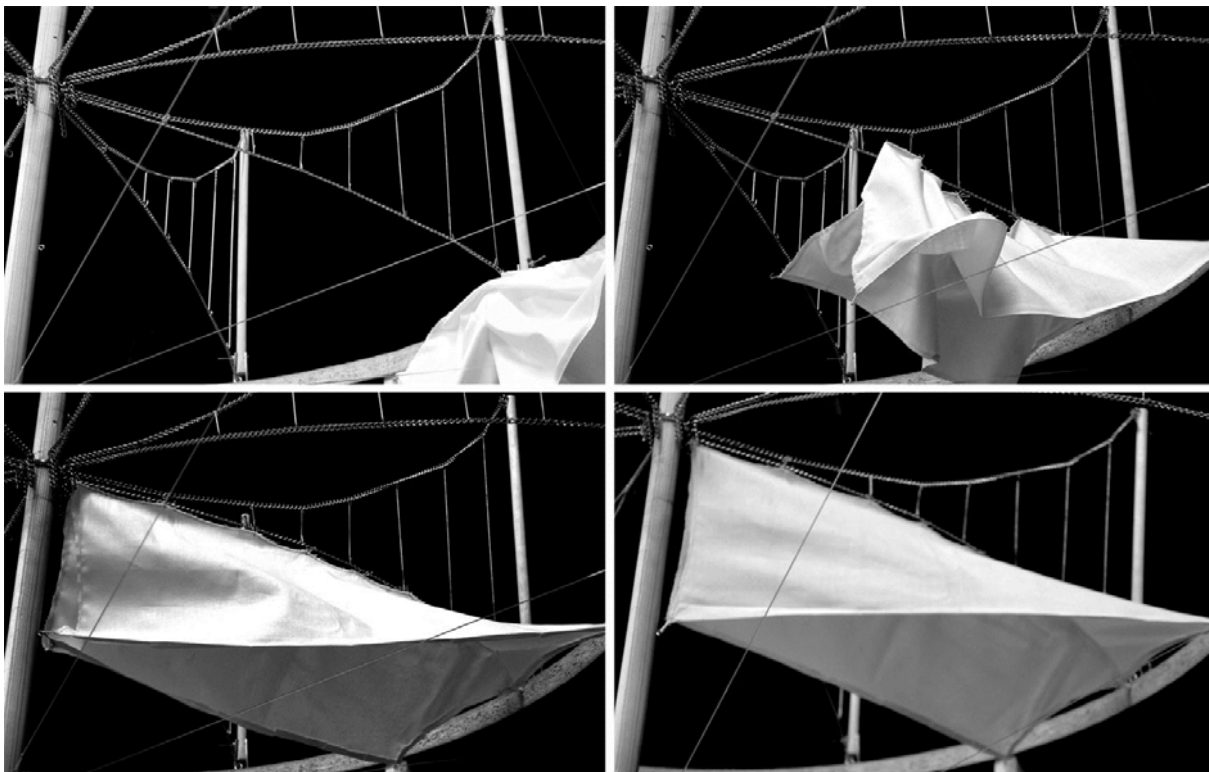


Figure 9.7 *Demonstration of introducing prestressing force into textile membrane*

9.4. Analysis and design of a retractable roof structure

Structural analysis of the textile membrane and the radial cables is carried out using a finite element method.

9.4.1. Geometrical consideration

Some additional geometrical conditions must be considered to realize the cable girders whose edge forms elliptic curve. They will be described step by step.

Cutting the elliptic curve

A cable girder forms a polygon, because all of its components are linear without consideration of the self-weight. If one would like to change the polygon shape of the cable girder to a desired curvature, one simple solution is to increase the number of the hanger cables. The larger the curvature of the curve, the more hanger cables that are necessary. In the case of the ellipse, its slope of the tangent line near the edges is very large and even infinity at the edge point. Therefore, in order to approximate the edge line of cable girders with an elliptic curve, a large number of hanger cables would be required at the edge and placed in a very dense configuration.

This problem can be solved by using only a part of an elliptical curve and by avoiding using the steep part near the edge. Consequently an ellipse would be used whose length of the major axis is larger than the diameter of the target roof (for instance an ellipse 2 m longer than the radius of the roof as shown in Figure 9.8), and only the part within the bounds of the roof is exploited for the lower cable of the cable girder. Thus the equation of the lower cable's form becomes:

$$z_{e2}(y) = \sqrt{h^2 - \frac{h^2}{(r+2)^2} \cdot y^2} \quad (9.5)$$

Two outer compression rings become necessary in this approach.

Additional sag for prestressing

In this approach, the lines of the lower long side edge of the membrane strip must be formed convex upward to achieve the pre-tensioned form as described in the previous chapter (see Figure 7.39). Numerically this convex curve can be obtained by the iterative calculation using the form finding analysis. However, the curve is approximated here as parabola.

$$z_p(y) = -\frac{4 \cdot f}{r^2} \cdot \left(y - \frac{r}{2}\right)^2 + f \quad (9.6)$$

Since the width of the membrane strip must be constant, the geometrical line of the upper long side edge must be also lifted up as much as the lower edge line. Consequently the equation of the upper long side edge of the membrane strip is expressed as the summation of the ellipse and the parabola.

$$z(y) = z_{e2}(y) + z_p(y) \quad (9.7)$$

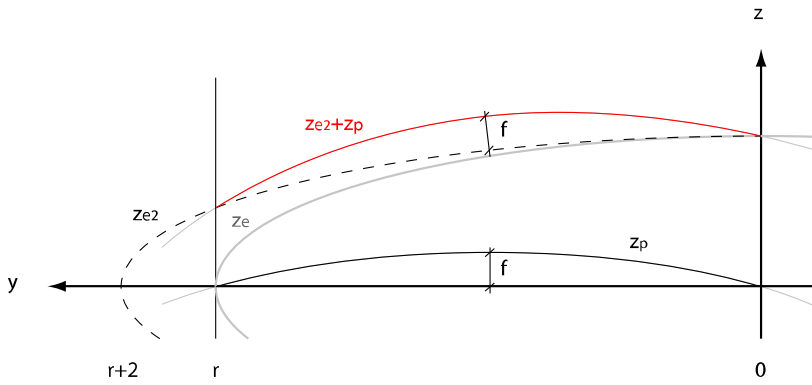


Figure 9.8 Curve lines for the radial edge line of the membrane strip

Inclination

This additional curve causes another geometrical challenge. The convex curve inevitably has a downward inclination at the centre of the roof. The cable girder in one side must be connected continuously to the one in the other side in radial direction to make one cable girder. Therefore, both the upper and the lower long side edge of the membrane strip are inclined upward around the rotation point at the outer edge of the roof until their inclination at the centre of the roof becomes zero. The required rotation angle can be calculated from the inclination angle of the sag line at the lower position. By this geometrical operation, the drain problem is automatically eliminated: rain water always goes down toward the outer edge of the roof.

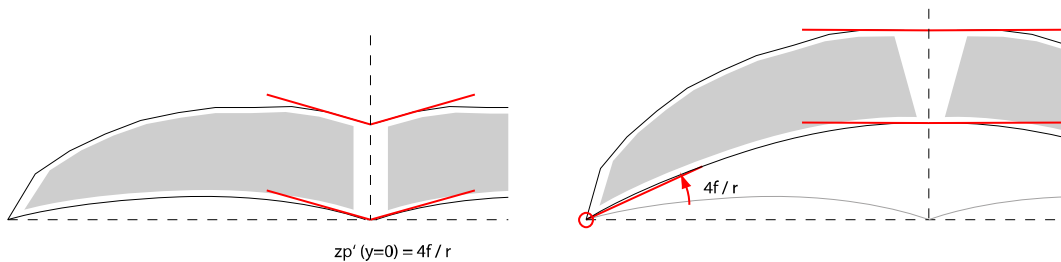


Figure 9.9 Inclination of the geometrical lines of the upper and lower long side edge of the membrane strip

Starting from this position the kinematic cable girder will be lifted up for the introduction of prestressing force into the membrane as shown in Figure 9.10. When the cable girder is in the initial lower position, the membrane strip is not prestressed, and the long side of the membrane strip is straight with its length (L_1). When the cable girder is lifted to the final position, the membrane strip is stressed and the long side of the membrane strip is curved (L_2). The cutting pattern of the membrane strip of this position is calculated, and the length of its long side is (L_3). To meet geometrical conditions, this length L_3 must be longer than L_1 . Otherwise the driving carriage cannot reach the central point of the roof when it moves from the perimeter to the centre of the roof. The amount of lifting of the cable girder must be decided to satisfy this condition.

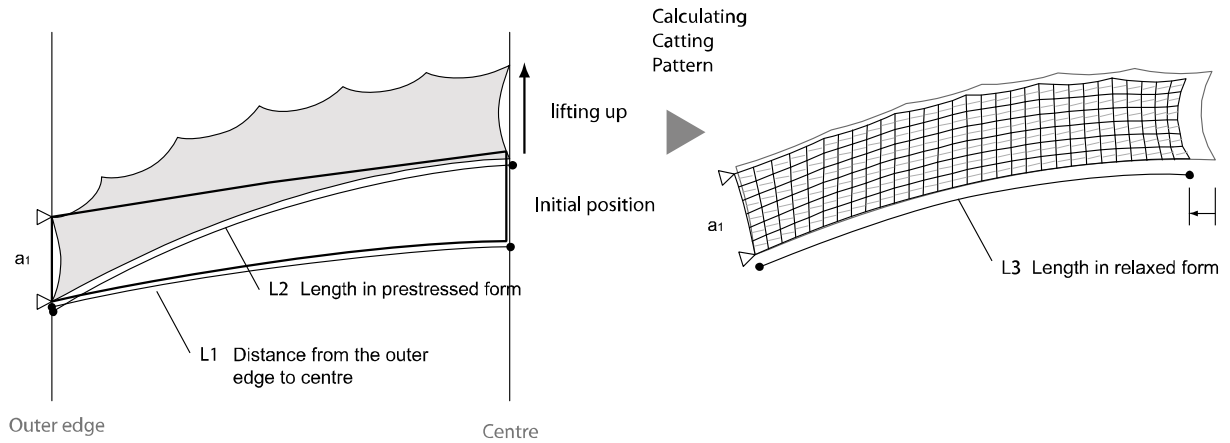


Figure 9.10 The length of the lower long side of the membrane strip in the different positions

9.4.2. Analysis of kinematic cable girder

First the two-dimensional kinematic cable girder is modeled to simulate the lifting and to calculate the raising factor by the same manner as the parameter study. Optimizing for the efficiency of the kinematic cable girder, the smallest possible value for the sag-span ratio of the upper cable was chosen ($f_u/l = 4\text{m}/36\text{m} = 0.11$). Consequently, the maximum raising factor reached nearly 4.0. The graph in figure shows that the allowable maximum elevation of this model (4m) can be obtained by 2m of outward movement of the upper cable. For the retractable roof, approximately 700mm is set for the maximum amount of the input value Δ that causes the upper node to move upward 2.40m.

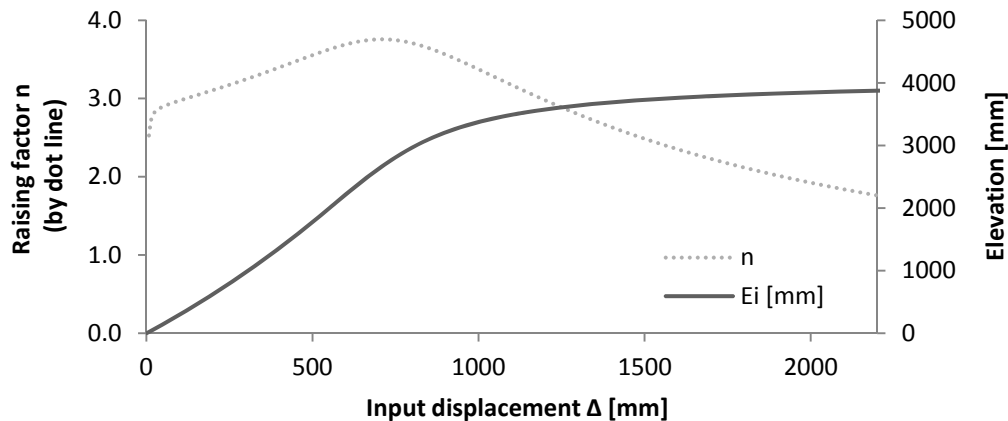


Figure 9.11 The calculation result of the raising factor and the elevation

9.4.3. Global model analysis

A global model is constructed for the structural analysis. The geometrical non-linear calculation is done using the finite element program SOFiSTiK, as was done in case study A.

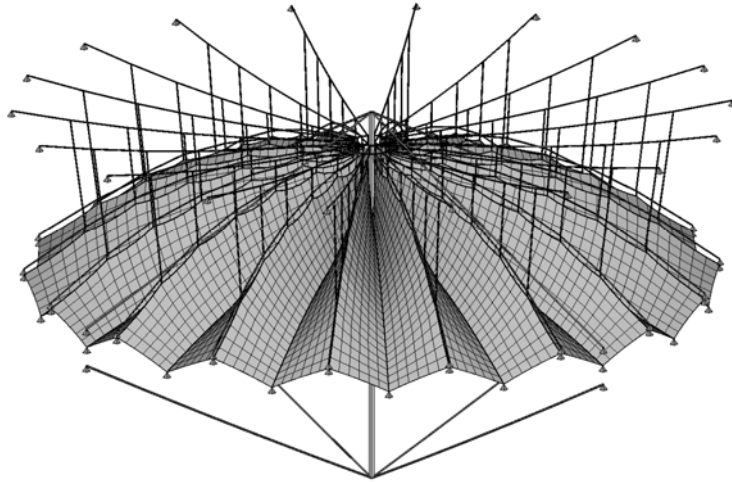


Figure 9.12 Global model for Case study B

The number of radial cables is set at 36. Since the elliptic curve must be trimmed as described above, the width of a single membrane strip can be calculated as:

$$a = \frac{\pi \cdot (d - 4)}{n} = 2.79 \text{ m} \quad (9.8)$$

The retractable roof mainly consists of the following three components:

- Retractable textile membrane with driving and sliding carriage
- Cable girder with extension materials
- Flying mast supported by the eight fixed radial cables

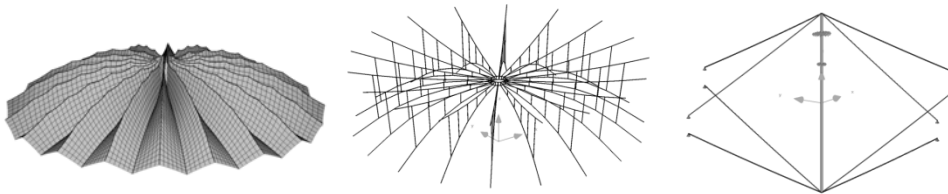


Figure 9.13 Main components of the retractable roof

The lower point of the membrane strip must be attached to the flying mast during the operation of lifting of the cable girder. Therefore, the cable that guides the driving carriage of the lower point of the membrane strip is required at the underside of the textile membrane. However since this guiding cable is not a structural component, it was not included in the model.

9.4.4. Results of static analysis

A stress analysis for the textile membrane is performed. The calculation results shown in Table 9.1 verify that the stress in the membrane under all load cases does not exceed the allowable stress. The membrane stiffness was increased to 130% for this analysis.

Table 9.2 Validation of stress analysis

membrane material										
Type of load-case	load case	number of load-case-combination	warp				fill (weft)			
			Max. membrane force in warp-direction	Max. allowable membrane force in warp-direction	utilization	verification	Max. membrane force in fill-direction	Max. allowable membrane force in fill-direction	utilization	verification
			N_{xx}	$f_{t,d,mem,warp}$	$N_{xx} / f_{t,d,mem,warp}$		N_{yy}	$f_{t,d,mem,fill}$	$N_{yy} / f_{t,d,mem,fill}$	
			[kN/m]	[kN/m]			[kN/m]	[kN/m]		
1)	(P+G)	1	1.96	18.0	0.11	<1.0 ok	1.68	17.2	0.10	<1.0 ok
2)	(P+G)+S	2	7.51	22.5	0.33	<1.0 ok	8.08	21.6	0.37	<1.0 ok
		3	5.15		0.23	<1.0 ok	3.28		0.15	<1.0 ok
3)	(P+G)+W	4	8.04	35.9	0.22	<1.0 ok	5.95	34.4	0.17	<1.0 ok
		5	11.52		0.32	<1.0 ok	14.04		0.41	<1.0 ok

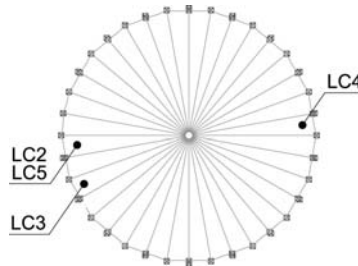
membrane seam										
			N_{xx}	$f_{t,d,seam,warp}$	$N_{xx} / f_{t,d,seam,warp}$		N_{yy}	$f_{t,d,seam,fill}$	$N_{yy} / f_{t,d,seam,fill}$	
			[kN/m]	[kN/m]			[kN/m]	[kN/m]		
1)	(P+G)	1	1.96	12.1	0.16	<1.0 ok	1.68	11.6	0.15	<1.0 ok
2)	(P+G)+S	2	7.51	23.5	0.32	<1.0 ok	8.08	22.4	0.36	<1.0 ok
		3	5.15		0.22	<1.0 ok	3.28		0.15	<1.0 ok
3)	(P+G)+W	4	8.04	32.9	0.24	<1.0 ok	5.95	31.4	0.19	<1.0 ok
		5	11.52		0.35	<1.0 ok	14.04		0.45	<1.0 ok

Others			Strap and Belt			Edge cables in membrane			
			N	$f_{t,d}$	$N / f_{t,d}$		N	$f_{t,d}$	$N / f_{t,d}$
			[kN/m]	[kN/m]			[kN/m]	[kN/m]	
1)	(P+G)	1	88.5	163.3	0.54	<1.0 ok	27.2	86.0	0.32
2)	(P+G)+S	2	110.8		0.68	<1.0 ok	38.9		0.45
		3	108.9		0.67	<1.0 ok	31.5		0.37
3)	(P+G)+W	4	88.1		0.54	<1.0 ok	33.7		0.39
		5	92.1		0.56	<1.0 ok	46.1		0.54

A ponding analysis is also performed. The minimum values of the deformation in z-direction in each load case are described in Table 9.2. The membrane stiffness is decreased with a factor of 0.8 to create favorable conditions for ponding.

Table 9.3 The minimum values of the deformation in z-direction in each load case

LF	min Uz [mm]
LC 2	-174
LC 3	-73
LC 4	-110
LC 5	-221



The iso-area is checked to determine whether water will accumulate on the membrane. The geodesic contour plots shown in Figure 9.14 is taken from load case 5, which has the largest deformation in z-direction. It becomes clear from this figure that the water flows down to the outer edge of the roof, and no ponding occurs on the membrane surface.

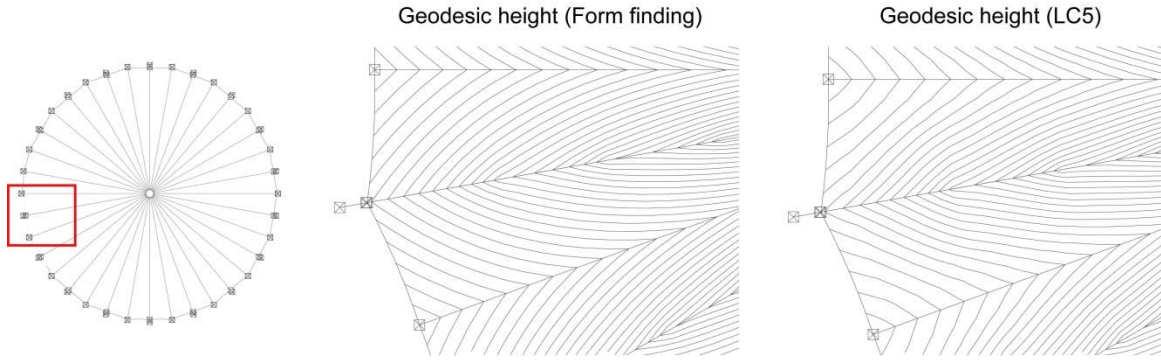


Figure 9.14 Geodesic height (Form finding and Load Case 5)

9.4.5. Results of transition analysis

Next, the transient analysis is performed to observe and check the behavior of the membrane during the introduction of prestressing force into the membrane. It is performed by the iteration of the non-linear static analysis in reverse order. Starting from the prestressed status, the initial prestressing force is released step by step by lowering the cable girder. The reaction forces of the two edge nodes of the membrane at the centre of the roof are observed.

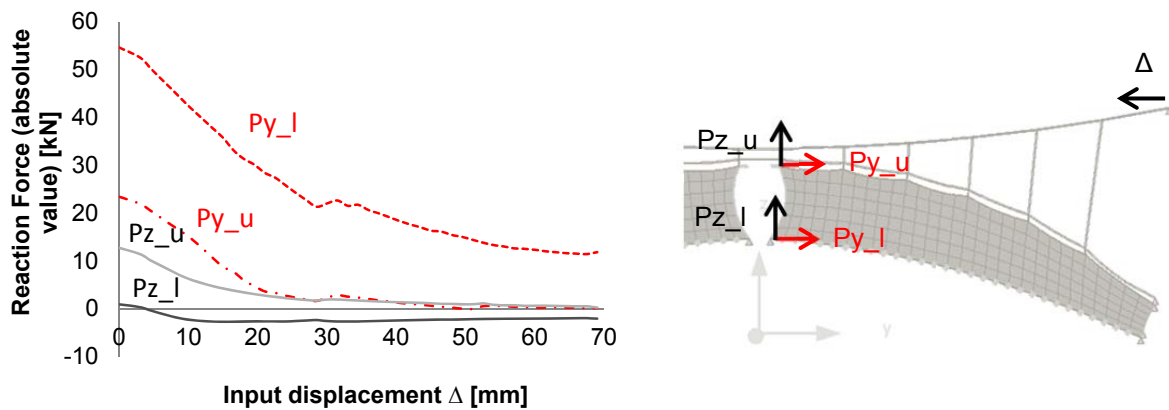


Figure 9.15 Transition of the reaction force on the edge of the membrane strip

The stress conditions of the textile membrane in combination with the kinematic cable girder are displayed in sequence.

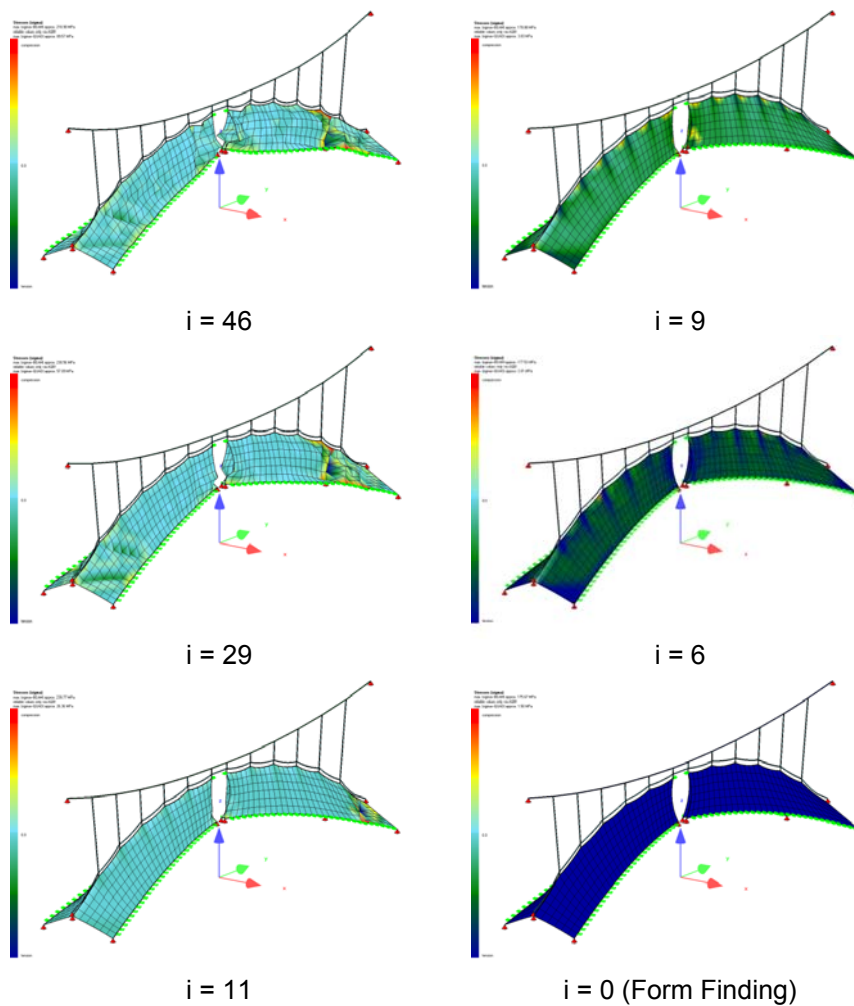


Figure 9.16 Transition of the reaction force in membrane

9.5. Discussion

In combination with a driving mechanism, cable girders can be applied as an efficient kinematic structure. The author firstly revealed the behavior of the kinematic cables through exhaustive parameter studies in both static and kinematic analysis. Most of the calculation results are shown in the appendix, and here only essential information was described. The results and conclusions drawn from this study were applied, in order to choose the right parameters to vary according to the desired target function.

The analytical results of the parameter study were then transferred to the desired retractable membrane roof. The principle of the movable mechanism was demonstrated by the physical study model. Shortening all backstay cables at the same time causes an uplift of the cable girders. The principle of kinematic cable girders is a novel method to introduce prestressing force into an outward folding membrane roof with spoked wheel structure.

Finally, structural analysis of the textile membrane and the radial cables is carried out using geometrical non-linear finite element method. Feasibility of this ‘minor shift and major lifting’ approach was checked through both stationary- and transition analysis. However, the study also revealed that more intensive study is required, especially for the development of details.

For instance, the method for controlling the prestressing force in the lower cable of the kinematic cable girder must be considered.

10. Conclusion and Discussion

The motivation for this dissertation was the development of a foldable membrane roof combined with a primary spoked-wheel structure, and the specific goal was to find a solution how the membrane can be folded to the perimeter in order to create a free opening when the roof opens. The complex geometrical problems arising as a result were the main challenges. The only realized prototype for this type of a retractable roof, the bullfight-ring in Jaén, Spain constructed in 1998 designed by Felix Escrig and Jose Sanchez, was introduced in Chapter 2 as well as the related research.

“Economical” and “sustainable” are the keywords of our time and retractable roofs fit into these ideas perfectly. They can convert a space for multi-use and multi-purpose. To date a wide variety of retractable roofs have been constructed and their characteristics are described in chapter 3. It was possible to classify different roofs and thereby the method of conversion, could be defined as a unique classifier. Through overlapping, folding, rolling, or deforming by air, the roof changes its dimensions and thereby reduces its size. This reduction is important, because the storage space for the retractable roof is limited in many cases. Hence, a membrane is a suitable material for retractable roofs, because it can be folded into a compact form. A study on the required energy for motion revealed the advantage of a membrane retractable roof. They require significantly less energy than rigid convertible roofs, especially in the case of a membrane roof with spoked wheel structure, the necessary energy is very small.

Chapter 4 serves not only as a general description about the membrane material, but also presents details regarding the flexibility and foldability of textile membrane. Among the common combinations of coatings and fabric for membranes, PVC-Polyester and PTFE-PTFE fabric are suitable for retractable roofs due to their flexibility. Especially, PTFE fabric is increasingly being applied to membrane retractable roofs.

The history of development of a retractable membrane roof bunching in a single point has been studied and described in Chapter 5. Key persons like Frei Otto, Roger Taillibert and Jörg Schlaich are described in the context of their contributions to invention and innovation of this principle. All of these individuals are from Stuttgart, Germany, or at least related to this place, and their interaction is also essential for the history. For example, Taillibert stayed in the institute of Otto and sought the aid of Otto for designing his first two realized retractable membrane roofs in Cannes and Carnot in France. Schlaich worked together with Otto for the Olympic Stadium in Munich and consulted for the design of the retractable roof in Montreal Stadium that Taillibert conceived. An important technical innovation concerning the aim of this dissertation had been done by Schlaich for the roof in Zaragoza. The combination of retractable membrane with spoked wheel principle provides enough rationality for the structure. The roof in Zaragoza becomes the milestone for the success of large retractable roofs mostly designed by the office schlaich bergemann und partner since then.

The brief history, the morphology and structural principles of a spoked wheel structure is described in Chapter 6. As it consists of mainly cables, the weight of spoked wheel is small and it results in a very transparent appearance.

Based on the knowledge obtained from the first part of the dissertation, possible folding methods towards the perimeter of the roof were developed in the second part.

Chapter 7 described the principle problems which arise when a continuous circular membrane cover opens towards its perimeter, and the possible solutions were developed and described. First, the geometrical inconsistency between the required shape of the membrane and the radial cables was addressed as follows:

- A flat continuous membrane cannot be folded towards the outer edge of the roof, because the length of the membrane in the direction of circumference changes along the radius.
- If a radial membrane strip, a part of the continuous membrane between each radial cable, is twisted perpendicular against the horizontal edge of the outer ring in order to fit them to the form of a spoked wheel, the minimum distance between two adjacent straight radial cables is not constant along the radial direction.
- It becomes smaller at the centre of the cables; in other words, the form of the membrane strip is “waisted”, which causes problems for movability, because the membrane strip should have the shortest width at the outer edge of the roof.
- Thus, if the membrane strip has a “waisted” shape, it can be fitted to the boundary cables. But a movement outwards is not possible.
- Whereas, a membrane strip with rectangular shape can be moved but it cannot be fitted to the boundary cables arranged in space as radial cables of spoked wheel structure.

Among several approaches to overcome these geometrical questions, two simple as well as practical geometrical solutions were developed, at first without and then with the consideration of the corresponding form of textile membrane in a tensioned state.

In the first approach, the radial cables remains straight in space, whereas the outer edge of the membrane strip must be inclined, and therefore the line of the outer edge of the roof becomes a zigzag shape. From this study, it became clear that varying the twisting angle θ of the membrane strip results in a different required width at the center of the roof, and $\theta=45$ is the most economical solution for this. A great advantage of this approach was the geometrical simplicity of the primary structure. Even hanger cables are not necessary, thus an undisturbed bottom view could be realized.

However, in order to fold this membrane towards the perimeter, the fixed support points of the outer edge of the membrane strip must be moved vertically toward the level of the roof's surface. This geometrical alteration of the boundary condition could be conducted through a vertical movement of the whole compression ring. In Chapter 8, this ‘raised compression ring’ method was developed as 'case study A'.

The whole geometry of the roof and some details including the extension cable, water tightness and minimizing the size of the central hub were studied at first. Using finite element analysis, the statically behavior in prestressed status and the transition process of introducing a prestressing force into the membrane were checked with an integrated model. Also the feasibility of this method and the details were checked through the physical model that author built at the TU-Berlin.

In the second approach, the radial cables are curved in shape by adding the hanger cables that serve as cable girders. To introduce the prestress force uniformly into the textile membrane, the principle of “Katzbukel” Bridge in Germany was adopted: the cable girders are lifted up

together with the textile membrane. So far the flexibility of cable girders is regarded as an unfavorable factor for a stationary structure. Thinking from a different angle allows turning this to be the opposite. In combination with a driving mechanism cable girders can be applied as an efficient kinematic structure. One advantage of this mechanism is that a minor shift of the anchor point of the upper cable causes a major lift of the whole structure. Therefore, in the section of case study B in Chapter 9, the behaviour of kinematic cables was revealed through exhaustive parameter studies in both static and kinematic analysis.

The results and interpretation given in this study was useful to choose the right parameters according to the target function. It is neither easy nor possible to define the ‘best’ solution for a cable girder with regards to both static and kinematic behavior. For instance, good structural stability (minimization of deflection) conflicts with good kinematic efficiency (maximal raising factor). Thus the target function is very important to design kinematic cable girders.

This principle was a novel method for introducing a prestressing force for the membrane, which was demonstrated by a physical study model. Finally, a structural analysis of the textile membrane and the radial cables was carried out.

Further Discussion

Since the membrane retractable roof with spoked wheel principle includes various topics, some of these issues have been remained unclear. However following problems are very important, therefore further study is especially necessary.

Firstly, calculating the required amount of membrane material is always a challenge for a retractable membrane roof folding to the perimeter. The calculations revealed that this retractable system demands at least double the amount of membrane to cover a circular area. Furthermore, for the raised compression ring method, more than 3 times material would be necessary. Thus further study to explore the possibility reducing the amount of membrane is recommended.

A second challenge is its limited geometry. The proposed methods would be possible only in circular form in plan. This would not satisfy a common demand in the real projects such as for a football stadium; oval or rectangular shaped retractable roofs are often called for in these cases. Consideration to overcome this geometrical limitation is required.

Third issue is the reliability of the primary structure. In both proposals, the raised compression ring method and the minor shift – major lift method, the primary structures are kinematically moved to introduce pretensioning force into the membrane. Especially for large scale structures, the number of kinematical parts in the structure should be as small as possible. Thus, new ways of introducing prestressing should be studied further.

LIST OF TABLES

Table 3.1 Typology of retractable roofs	17
Table 4.1 Mechanical properties of common “foldable” fabrics [Kni 11]	26
Table 4.2 Gaussian curvature ($K=k_1 \cdot K_2 = 1/r_1 \cdot 1/r_2$) and the possibility of its surface deformation	27
Table 6.1 Stadium roofs using spoked wheel principle (Courtesy of schlaich bergemann und partner)	57
Table 6.2 Variations of the combination of the two spoked wheels	59
Table 7.1 Geometrical change according to the number of radial cables	71
Table 7.2 Two types (waisted and rectangular) of membrane strips and their problem	79
Table 7.3 Two approaches for geometrical solutions	95
Table 7.4 Global safety factor for material	103
Table 7.5 Global safety factor for welded seams	104
Table 7.6 Snow loads	106
Table 7.7 Wind pressure on the roof per load zone (+: pressure. -: suction)	108
Table 7.8 Load combinations with load factors	108
Table 7.9 Design resistance R_d divided by safety factor	109
Table 8.1 Geometrical change according to the number of radial cables by the half strip method	112
Table 8.2 Validation of stress analysis	118
Table 8.3 The minimum values of the deformation in z-direction in each load case with the corresponding node positions	119
Table 9.1 Defined parameters for this study	133
Table 9.2 Validation of stress analysis	143
Table 9.3 The minimum values of the deformation in z-direction in each load case	143

LIST OF FIGURES

Figure 1.1 Folding in the center (left: open configuration, right: closed configuration)	2
Figure 1.2 Movable roof with the membrane moving along a spoked wheel structure, Frankfurt, Germany [Göp 07a]	2
Figure 1.3 Folding on the perimeter (left: open configuration, right: closed configuration)	3
Figure 1.4 Structure of this dissertation	3
Figure 2.1 Sketch, membrane roof opening toward the perimeter [Ott 72]	7
Figure 2.2 Exterior and interior of the bullring in Jaén, Spain (courtesy of Felix Escrig)	7
Figure 2.3 Radial cable structural system of the bullring in Jaen (left), Plan of bullring in Jaen with the information of the place of the motors (M-1(red): driving motor, m-2(blue): auxiliary motors) (right) (courtesy of Felix Escrig)	8
Figure 2.4 Sequential view of retractable membrane roof from closed state to opened state (courtesy of Felix Escrig)	8
Figure 2.5 Pulleys on the top of the centre flying mast in plan (left) and in 3D (middle) and pulley in vertical on the outer edge of the roof (right) (courtesy of Felix Escrig)	9
Figure 2.6 Folding pattern of cylinder membrane (left), Air-inflated type (upper right) and air-supported type (lower right) [Oza 00]	9
Figure 2.7 Physical test model (courtesy of K. Kawaguchi)	10
Figure 2.8 n-square form in plan (left) and the geometrical lines of the part of the membrane roof (right) [Küh 01]	10
Figure 2.9 A case study model of which membrane roof is folded to the perimeter [Küh 01]	11
Figure 2.10 Iris dome on Expo Hannover, Germany [Hob 12]	11
Figure 2.11 Qi Zhong Centre Court Stadium designed by Environmental Design Institute + Naomi Sato (Architect) and SDG (Engineer) [Bau 12]	11
Figure 3.1 Classification of the retractable roofs [Ott 72]	15
Figure 3.2 6 degree of freedom of a rigid body (left) and 4 degree of freedom of a rigid plate (right)	16

Figure 3.3 Energy required for moving of different types of retractable roofs	18
Figure 3.4 Required devices for the point supporting foldable membrane roof	19
Figure 3.5 Unit of pulleys for the point supporting foldable membrane roof	19
Figure 3.6 Two driving systems for the point supporting foldable membrane roof	20
Figure 3.7 A tractor of the Allwetterbad in Düsseldorf constructed in 1977 (left) (photo taken by author in 06/2012) and sliding carriages of the Frankfurt Stadium constructed in 2005 (right) (courtesy of schlaich bergemann und partner)	20
Figure 4.1 Classification of polymers according to the chemical structures (image figures of the molecules from [Kni 11]) (*A glass fiber is not polymer, but GFRP is a resin which is reinforced by glass fiber.)	22
Figure 4.2 Classification of fibers showing typical ones	23
Figure 4.3 Common combinations of the coating and fabric of membrane with historical transition	24
Figure 4.4 Comparison of three typical membrane materials (best value in each case taken as 100%) (left), Four different membranes with similar strength (right) [Kni 12]	25
Figure 4.5 Anisotropy shown in different fibre orientations [Blu 90]	26
Figure 4.6 Equilibrium models: increasing resistance to loading through alternations of the angle of the system axes to each other [Sei 09]	28
Figure 4.7 Brief difference between the construction process and the designing (numerical simulation) process	28
Figure 4.8 Cable force during the lifting procedure (left) and its schematic illustration (right) [Ber 00]	30
Figure 4.9 Simple model of tension releasing calculation	30
Figure 4.10 The process of the construction and the planning of folding membrane structure	31
Figure 4.11 The investigation of the inner retractable roof of Commerzbank-Arena Frankfurt, computing simulation (left) [Göp 07b] and mock up model (right) [Göp 07a]	32
Figure 5.1 The appearance of the convertible roof of the Colosseum [Gra 79]	33
Figure 5.2 Three types of centrally folding system [Ott 72]	34
Figure 5.3 History of retractable roofs bunching in a single point single mast system	35

Figure 5.4 Portrait of Taillibert and his own description about the design attitude for the curves (Both from [Tai 12])	36
Figure 5.5 Appearance of the retractable roof in Cannes, France (left) [Ner 05] and its driving system (right) [Ott 72]	37
Figure 5.6 Appearance of the retractable roof in Boulevard Carnot in Paris, France (left) [Fab 70] and its driving system (right) [Ott 72]	37
Figure 5.7 Portrait of Frei Otto [Ott 96] and his major works	38
Figure 5.8 Appearance of the retractable roof in Bad Hersfeld, Germany (left) [Ner 05] and its driving system (right) [Ott 72]	39
Figure 5.9 Allwetterbad Düsseldorf, photos taken by author in 06/2012	40
Figure 5.10 Multimedia stadium the sketch and the physical model [Ner 05]	41
Figure 5.11 Retractable Roof of the Olympic Stadium in Montréal [Hol 97]	41
Figure 5.12 Retractable Roof of the Olympic Stadium in Montréal [Hol 97][Ish 99]	42
Figure 5.13 Portraits of Jörg Schlaich [Bög 03]	43
Figure 5.14 Retractable Roof of Bull-fight ring in Zaragoza (left) and Roof of Roman Arena Nîmes (right) [Bög 03]	44
Figure 5.15 Retractable Roof of Bull-fight ring in Zaragoza [Hol 97]	45
Figure 5.16 Retractable Roof of Bull-fight ring in Zaragoza [Ish 99]	45
Figure 5.17 The Rothenbaum Center Court in Hamburg (photos taken by author in 06/2011)	46
Figure 5.18 The Commerzbank-Arena Frankfurt, unfolding of the retractable roof (left) [Göp 07a] and the central video cube protecting the folded membrane (right) (taken by author in 06/2012)	47
Figure 5.19 The retractable roof at Kufstein, Austria (left) [Rei 12], a part of the webbing belt of the retractable roof (PES 50x3mm ultimate strength 80kN) (centre and right, photos taken by author at the office Kugel+Rein in 01/2009)	48
Figure 5.20 National Stadium Warsaw [Göp11]	48
Figure 5.21 National Stadium Warsaw, retractable roof (left) [sbp 12] the driving carriage of the retractable membrane roof in Warsaw [Jae 12]	49
Figure 5.22 BC Place in Vancouver, section and appearance [Göp 11]	49

Figure 5.23 Inflated retractable roof in BC Place (left) (courtesy of schlaich bergemann und partner), Air ducts in the central Hub (right) [Ten 12]	50
Figure 5.24 Historical transition of the size of the retractable roof bunching in a single point	50
Figure 5.25 Uniaxial forces of foldable membrane with spoked wheel primary structure (Left: type of Zaragoza roof, Right: type of Warsaw roof)	51
Figure 5.26 Uniaxial forces of foldable membrane with spoked wheel primary structure (Left: type of cable girder such as Frankfurt Stadium, Right: type of pneumatic system such as BC-Place, Vancouver)	51
Figure 5.27 Different vertical coordinates in circumference direction (left: circle, right: Oval in plan)	52
Figure 6.1 A typical spoked wheel	53
Figure 6.2 The order of structures [Schl 06]	54
Figure 6.3 R. Buckminster Fuller and the model of tensegrity structures [Ful 61]	54
Figure 6.4 Variation of the Cable dome: Geiger Dome (left) and Fuller Dome (right) [Schl 97]	55
Figure 6.5 Weight comparison: Cantilever (dot line)– Spoked wheel Structure (line) (Internal study, Courtesy of schlaich bergemann und partner)	56
Figure 6.6 An aerial view of Gottlieb-Daimler-Stadium in 1993 (Left) and the roof from the lower angle with extended part constructed in 2011 (Right) [sbp 12]	57
Figure 6.7 Sections of Bukit Jalil Stadium (Left) and Gottlieb-Daimler-Stadium (Right) [Ber 00]	58
Figure 6.8 Variation of the forms of the spoked wheel roofs (the figures from [Ber 00])	58
Figure 6.9 Cable truss – Normal forces (left), Development of radial prestress [Ber 00]	59
Figure 6.10 A simple study model; one fourth of an oval-form spoked wheel, axial force (kN) in the tension rings and in radial cables	60
Figure 6.11 Variation of inner roof opening of Pusan Dome, South Korea (The figures from [Ber 00], the pictures from [sbp 12])	61
Figure 6.12 AOL Arena in Hamburg: plan view (left) and the corner as built from the lower angle (right) (The figure from [Ber 00], the picture from [sbp 12])	61

Figure 6.13 AOL-Arena, Hamburg / Jaber Al Ahmad Stadium, Kuwait / Olympic stadium in Sevilla /. Greenpoint Stadium, Cape Town (in clockwise direction from upper left hand) [sbp 12]	62
Figure 7.1 The differences of number of configuration between rigid movable roof and foldable membrane roof	66
Figure 7.2 Diagram of design flow and the corresponding number of the section	66
Figure 7.3 A strip, a part of continuous membrane roof and the width a	67
Figure 7.4: Possible membrane strips with the width a	68
Figure 7.5: A minimal required membrane cylinder composed of rectangular strips	68
Figure 7.6: A membrane strip folded to fit to a radial form	69
Figure 7.7: The rotation of one strip of a continuous membrane	70
Figure 7.8 Possibilities of the combination of spoked wheel structure and membrane and the drain lines (c: compression ring, t: tension ring)	72
Figure 7.9 Two possibilities for drain path, if valley line of the roof surface is sloping down toward the centre of the roof (Left: adding pipes for draining off rainwater, Right: changing the geometry with additional radial cables)	72
Figure 7.10 Physical model: opened into the upward	72
Figure 7.11 Physical model: opened into the downward	73
Figure 7.12 A rectangular strip with the width a twisted in clockwise direction	73
Figure 7.13 A physical model of membrane retractable roof using 'twisting' method (left: closed configuration, right: open configuration)	74
Figure 7.14 The position of the bundle of textile membrane (Left), Membrane textile covered the gap between inner and outer roof (Right) (courtesy of Felix Escrig)	74
Figure 7.15 Figure projected to the perimeter of the roof (Left), Three-dimensional figure of a twisted membrane strip (top view, side view and view from the perimeter) (Right)	75
Figure 7.16 A mathematical model called a hyperboloid	75
Figure 7.17 3-D Diagram of hyperboloid with the twisted angle θ	76
Figure 7.18 Distance between two straight radial cables	77

Figure 7.19 Figure projected to the perimeter of the roof (Left), One projected to the top and side (Right)	77
Figure 7.20 Three-dimensional figure (top view, side view and view from the perimeter)	78
Figure 7.21 An idea to use half of a membrane strip (left) and an appearance of the whole roof (right)	80
Figure 7.22 Diagrams in view from the perimeter (left), the edge line of the long side of the membrane strip on the vertical plane (V) raised up from a straight line of the radial cables (right)	81
Figure 7.23 Required width of the membrane strip against the different twisting angle of the membrane strip	82
Figure 7.24 The 3-D diagram and the imaginary plane between two adjacent radial cables	83
Figure 7.25 Diagrams in view from the perimeter	83
Figure 7.26 Changing a rectangular membrane strip	84
Figure 7.27 A rectangular membrane strip with ellipse curve	85
Figure 7.28 Mathematical ellipse form	85
Figure 7.29 Changing axis of twisting from the center to the edge in two dimensional diagram from the perimeter	86
Figure 7.30 Design flow till the geometrical boundary conditions	87
Figure 7.31 pretensioned fabric between two parallel cables cannot folded to the side but only folded in the middle [Ott 72]	87
Figure 7.32 Problem of the half strip approach	88
Figure 7.33 Some ideas for prestressing membrane strip	88
Figure 7.34 Two geometrical configuration of a membrane strip	89
Figure 7.35 Variation of the edge rope radius and edge rope force [Sei 09]	89
Figure 7.36 FEM model of the whole roof after the form finding process (left) and the cutting pattern of a membrane strip (right)	89
Figure 7.37 A physical model of the one eights of the roof in two different configuration	90
Figure 7.38 A physical model of the one eights of the roof in in unfolding procedure	91

Figure 7.39 Problem of the cable girder approach and its solution (side view of a membrane strip)	92
Figure 7.40 The physical model of one eight of the roof using an arch as upper guide line	93
Figure 7.41 One membrane strip, View from the top, perimeter and the side and the cutting pattern	94
Figure 7.42 Development of the foldable membrane roof opening center to the outside: geometrical study to the method for pretensioning	96
Figure 7.43 One membrane twisted strip and its warp (Nxx) and weft (Nyy) directions	97
Figure 7.44 Introduction for prestressing force into membrane in both surface directions	98
Figure 7.45 Model of the whole roof (sectional view)	98
Figure 7.46 Movable Bridge in Duisburg (eng. schlaich bergemann und partner) [sbp 12]	98
Figure 7.47 Introduction for prestressing force into membrane in both directions	99
Figure 7.48 Development of the foldable membrane roof opening center to the outside	100
Figure 7.49 Zone Definition for the exposure coefficient (conical shape with open side) [For 04]	107
Figure 8.1 Two possibilities for drain path by the half strip method (Left: adding pipes for draining off rainwater. Right: changing the geometry with additional radial cables)	112
Figure 8.2 A physical study model for the extension cable	113
Figure 8.3 Details of a physical study model for the extension cable and internal force flow	113
Figure 8.4 Examples of spring bearings for glass façade (Sony Center in Berlin (left)(photo taken by author)and the entrance area of the University of Bremen (ZBUB) (right) [Sob 04]	114
Figure 8.5 A physical study model for water tightness of the raised compression ring method. a part of the central hub (left and centre), a simple image of the appearance (right)	115
Figure 8.6 Central hub of the Commerz Bank Arena in Frankfurt (left) [Ale 05] and of the National Stadium in Warsaw (right) (Courtesy of schlaich bergemann und partner)	115

Figure 8.7 Equations of the upper and lower radial edge of one membrane strip	116
Figure 8.8 Carriage of retractable roof in Commerz Bank Arena (left) (Courtesy of schlaich bergemann und partner) and the simulated model in the analysis (right)	117
Figure 8.9 Geodesic height (Form finding and Load Case 5)	119
Figure 8.10 Input displacement of the edge node of membrane and radial cables	120
Figure 8.11 Transition of the Reaction force in Membrane	121
Figure 8.12 Reaction force in four edge node of the membrane strip in both y- and z-direction	121
Figure 8.13 Cutting pattern of a membrane strip	122
Figure 8.14 Position of actuators and force balance at the outer edge and the centre of the roof	123
Figure 8.15 Sectional view of primary structure	124
Figure 8.16 Extensional cable system at the outer compression ring	125
Figure 8.17 Two compression ring (red: upper ring and black: lower ring)	125
Figure 8.18 Design drawing of the model in plan (upper) and in section (lower)	126
Figure 8.19 Two different kinds of the air cylinders on the flying mast (left) and schematic of the air cylinders	127
Figure 8.20 Installation radial cables (left) and flying mast suspended by the radial cables (right)	128
Figure 8.21 sewed lengthwise textile membrane (left) and installation membrane (right)	128
Figure 8.22 The finished model (upper: folded. middle: unfolded. lower: prestressed status)	129
Figure 8.23 The finished model from the lower angle (upper 1 and 2: folded. middle 3: unfolded. lower 4: prestressed status)	129
Figure 9.1 Detailed diagram of a concave cable girder	132
Figure 9.2 The maximum raising factor n_{\max} according to f/l	134
Figure 9.3 Simplified geometrical feature of kinematic cable girder	135
Figure 9.4 A relationship between each parameter of the kinematic cable girder	136

Figure 9.5 The maximum raising factors in each parameter	137
Figure 9.6 A physical model of cable girders in radial arrangement	138
Figure 9.7 Demonstration of introducing prestressing force into textile membrane	138
Figure 9.8 Curve lines for the radial edge line of the membrane strip	140
Figure 9.9 Inclination of the geometrical lines of the upper and lower long side edge of the membrane strip	140
Figure 9.10 The length of the lower long side of the membrane strip in the different positions	141
Figure 9.11 The calculation result of the raising factor and the elevation	141
Figure 9.12 Global model for Case study B	142
Figure 9.13 Main components of the retractable roof	142
Figure 9.14 Geodesic height (Form finding and Load Case 5)	144
Figure 9.15 Transition of the reaction force on the edge of the membrane strip	144
Figure 9.16 Transition of the Reaction force in membrane	145

Reference

- [AIJ 93] Architectural Institute of Japan (ed.), Recommendations for Design of Retractable Roof Structures with Realized Examples, Architectural Institute of Japan, Tokyo, 1993. (in Japanese)
- [Ale 05] Alexander, M., Orth, F., Faszination des Ovals : vom Waldstadion zur Commerzbank-Arena, Societäts-Verlag, Frankfurt am Main, 2005. (in German)
- [Ank 77] Anka (Akzo-Gruppe), Information - Technische Game, Industrial Fibres, Fils Technique, Nr.4/1977(20) Jahrgang V, 1977. (in German)
- [ASC 10] ASCE, Tensile Membrane Structures (ASCE/SEI 55-10) (Asce Standard), American Society of Civil Engineers, Reston, 2010.
- [Bau 12] Baunetzwissen, Qi Zhong Centre Court Arena in Shanghai, Accessed May 12, 2012. www.baunetzwissen.de (in German)
- [Beu 05] Beukers, A. and van Hinte, E., Lightness: The Inevitable Renaissance of Minimum Energy Structures, 010 publishers, Rotterdam, 2005.
- [Ber 92a] Bergermann, R. and Schlaich, J., "Movable membrane roofs for the arenas in Nîmes and Zaragoza," IABSE congress report, Volume 14, Fourteenth congress New Delhi, pp. 151-162, 1992.
- [Ber 92b] Bergermann, R. and Schlaich, J., "Cable-Membrane Roof for the Arena in Zaragoza, Spain," Structural Engineering International, Volume 2, Number 4, pp. 238-241, November 1992.
- [Ber 95] Bergermann, R., Göppert, K. and Schlaich, J., "Die Membranüberdachungen für das Gottlieb-Daimler-Stadion, Stuttgart und den Gerry Weber Centre Court, Halle," Bauingenieur 70, Heft 6, 1995. (in German)
- [Ber 00] Bergermann, R. and Göppert, K., "Das speichenrad – Ein Konstruktionsprinzip für weitgespannte Dachkonstruktionen," Stahlbau 69, Heft 8, pp. 595-604, 2000. (in German)
- [Ber 04] Bergermann, R., Gugeler, J., Keck, T., "Wandelbares Membrandach im Innenhof des Wiener Rathauses," Stahlbau Vol. 73, Issue 6, pp.373–380, June 2004. (in German)
- [Bög 03] Bögle, A., Schmal, P. and Flagge, I. (ed.), leicht weit – Light Structures, Jörg Schlaich, Rudolf Bergermann, Prestel Verlag, München, 2003.
- [Bög 09] Bögle, A., Schlaich, M. and Hartz, C., "Pneumatic structures in motion", Proceedings of IASS Symposium 2009, Valencia.

- [Bla 99] Blaser, W. and Sobek, W., art of engineering, Werner Blaser, illustriert, Birkhäuser, Basel, 1999.
- [Blu 90] Blum, R., "Zeltbaumaterialien," in Leicht und Weit, Deutsche Forschungsgemeinschaft (ed.), pp. 200-224, Weinheim, 1990. (in German)
- [Det 99] Pedestrian Bridge in the Inner Harbour of Duisburg, DETAIL (Brücken), Serie 1999, Volume 8, pp. 1455-1458, December 1999.
- [Det 11] DETAIL engineering 1: schlaich bergemann und partner, München, 2011
- [DIN 96a] DIN V ENV 1991-2-3 (1996-01), Eurocode 1 - Basis of Design and Actions on Structures - Part 2-3: Actions On Structures - Snow Loads, 1996.
- [DIN 96b] DIN V ENV 1991-2-4 (1996-12), Eurocode 1 - Basis of Design and Actions on Structures - Part 2-4: Actions On Structures - Wind Actions, 1996.
- [Dre 08] Drew, P., New Tent Architecture, Thames & Hudson, London, 2008.
- [Edm 87] Edmondson, A.C., A Fuller Explanation: The Synergetic Geometry of R. Buckminster Fuller, Birkhäuser, Boston, 1987.
- [Fab 70] Fabian, D., Aquatic Buildings 2 Reference Book on Aquatic Buildings Establishments and Facilities Construction Plant Equipment Operation Economy, Georg D. W. Callwet, München, 1970.
- [For 04] Forster, B. and Mollaert, M.(ed.), European Design Guide for Tensile Surface Structures, TensiNet, 2004
- [Fre 11] Freidman, N. and Farkas, G., "Roof structures in motion – On retractable and deployable roof Structures enabling quick construction or adaption to external excitations," Concrete Structures (Journal of the Hungarian Group of fib), vol. 12, pp. 41-50, 2011.
- [Ful 61] Fuller, R. Buckminster, "Tensegrity," Portfolio and Art News Annual, No. 4 1961, pp. 112-127, 144, 148.
- [Gen 01] Gengnagel, C. and Barthel, R. "Bewegliche Dächer," Detail 5/2001, pp.841 - 846 (in German)
- [Gen 05] Gengnagel, C., Mobile Membrankonstruktionen, TU München, Dissertation, 2005.
- [Göp 02] Göppert, K. and Schlaich, J., "The essence of Lightweight Structures," Brussels University Press, 2002.
- [Göp 04] Göppert, K., "Membrankonstruktionen – Form und Detail," Stahlbau73(2004), Heft12, pp. 990-1000, 2004. (in German)

- [Göp 05a] Göppert, K., "Gottlieb-Daimler-Stadion, Stuttgart," Stahlbau Spezial 2005, pp.192-197, 2005. (in German)
- [Göp 05b] Göppert, K., "Adaptive Tragwerke - Wandelbare Dachkonstruktionen für Sportbauten," Bautechnik, Vol.82, No.3, pp.157-161, 2005. (in German)
- [Göp 07a] Göppert, K., "A Spoked Wheel Structure for the World's largest Convertible Roof – The New Commerzbank Arena in Frankfurt, Germany," Structural Engineering International 4, pp282-287, 2007.
- [Göp 07b] Göppert, K, Structures for Stadium Projects, IABSE E-Learning Project IABSE Lecture Series 22, Zürich 2007, Accessed May 12, 2012.
- [Göp 11] Göppert, K., Haspel L. and Paech C., "New retractable roof solutions for sports stadia," IABSE-IASS London Symposium 2011 Proceeding.
- [Gra 79] Graefe, R., VELA ERUNT - Die Zeltdächer der römischen Theater und ähnlicher Anlagen, Philipp von Zabern, Mainz, 1979 (in German)
- [Hob 12] Hoberman Associates, Accessed May 12, 2012.
<http://www.hoberman.com>
- [Hol 97] Holgate, A., The Art of Structural Engineering. The Work of Jörg Schlaich and his Team., Edition Axel Menges, Stuttgart/London, 1997.
- [Hou 00] Houtman, R. and M. Orpana, "Materials for Membrane Structures," Bauen mit Textilien Heft 4, 2000.
- [Ino 02] Inoue, S. and Tsuboi, N., "Safety and Comfort Technology for Bicycles," Koutsuu-anzen-gakkai-shi, vo.27, No.2, 2002. (in Japanese)
- [Ish 93] Ishii, K., Membrane Structures in Japan, SPS Publication, Tokyo, 1993.
- [Ish 99] Ishii, K., Membrane Designs and Structures in the World, Shinkenchiku-sha Co. Ltd, Tokyo, 1999.
- [Ish 00] Ishii, K., Structural Design of Retractable Roof Structures, WIT Press, Southampton, 2000.
- [Ish 01] Ishii, K., "Retractable Roof Structures": in IASS Journal - Recent Spatial Structures In Japan, vol. 42, n. 1-2, pp. 27-32, Oct 2001.
- [Ish 04] Ishii, K., "Large Retractable Roof Structures in Japan", Journal of the International Association for Shell Structures, n. 1-2 vol. 42, April 2004.
- [Jae 12] Jaeger, F. (ed.), Next 3 Stadia: Warsaw Bucharest Kiev, Jovis, Berlin, 2012.
- [Kal 04] Kaltenbach, F. (ed.), Detail Praxis, Translucent Materials Glass, Plastic, Metals, Birkhäuser Architektur, Regensburg, 2004.

- [Kni 11] Knippers, J., Cremers, J., Gabler, M. and Lienhard, J., Construction Manual for Polymers + Membranes, Institut für internationale Architektur-Dokumentation, München, 2011
- [Koc 04] Koch, K.M. (ed.), Membrane Structures, Prestel, Munich, 2004.
- [Kra 99] Krausse, J. and Lichtenstein, C., Your Private Sky, R. Buckminster Fuller, Lars Müller Publishers, Baden, 1999.
- [Küh 01] Kühner, C., Wandelbares Membrandachsystem - Entwicklung eines peripher raffenden und fugenlosen Membrandachsystems, Diplomarbeit, ILKE, Universität Stuttgart, 2001. (in German)
- [Lai 88] Lainey, L., Schlaich, J., Morin, N. and Bergermann, R., "Retractable Roof Olympic Stadium Montreal," IABSE congress report Vol. 13, 1988.
- [Lew 03] Lewis, W. J., Tension Structures. Form and Behaviour., A monograph, Thomas Telford, 2003.
- [Mas 10] Masubuchi, M., Bögle, A. and Schlaich, M., "Study of retractable membrane roofs folding to the perimeter", Proceedings of IASS Symposium 2010, Shanghai, China, pp.505-506.
- [Mas 12] Masubuchi, M., Dessien, G., Bögle, A. and Schlaich, M., "Kinematic Cable Girders – Parametrical Analysis and Its Application", Proceedings of IASS Symposium 2012, Seoul, pp.323.
- [Min 81] Minte, J., Das mechanische Verhalten von Verbindungen beschichteter Chemiefasergewebe, RWTH Aachen, Dissertation, 1981. (in German)
- [Mor 04] Morgan, C. L. and Sobek, W., Show Me the Future: Engineering and Design by Werner Sobek, Av Editions, 2004.
- [Mun 11] Mungan, I. and Abel, J. F. (ed.), Fifty years of progress for shell and spatial structures : in celebration of the 50th anniversary Jubilee of the IASS (1959-2009), CEDEX - Laboratorio Central de Estructuras y Materiales, Madrid, 2011.
- [Ner 05] Nerdinger, W., Frei Otto: Complete Works : lightweight construction, natural design, Birkhäuser, Basel/Boston, 2005.
- [Ott 72] Otto, F., IL5 Wandelbare Dächer/Convertible Roofs, Wittenborn and Company, New York, 1972.
- [Ott 96] Otto, F., Rasch B., Finding Form: Towards an Architecture of the Minimal, Edition Axel Menges, 1996
- [Oza 00] Ozawa, Y. and Kawaguchi, K., "Research on Retractable Roof System with Twisted Membrane", JOI JST.JSTAGE/seisankenkyu/Vol. 52 (2000) , No. 4 pp.189-192, Tokyo 2000. (in Japanese)

- [Pae 08] Paech, C. and Hanssum, R., "Untersuchungen zu einem am äußeren Rand geparkten Innendach," Internal paper of schlaich bergemann und partner, 2008.
- [Rei 12] Alfred Rein Ingenieure, Accessed May 12, 2012.
www.ar-ingenieure.com
- [sbp 12] schlaich bergemann und partner: Accessed March 12, 2012.
www.sbp.de
- [Schl 94] Schlaich, J. and Bergemann, R., "Conceptual Design of Long-Span Roofs," Proceedings of the IABSE-Symposium Birmingham, pp13-24.1994.
- [Schl 97] Schlaich, J., "Seiltragwerk", in Baukonstruktion (Auflage 4.), Dierks, K., Schneider, K. and Wormuth, R. (ed.), Werner Verlag, Düsseldorf, 1997 (in German)
- [Schl 98] Schlaich, J., Bergemann, R. and Göppert, K., "Textile Überdachungen für die Sportstätten der Commonwealth Games 1998 in Kuala Lumpur/Malaysia," Bauen mit Textilien 2, pp.13–19, 1999. (in German)
- [Schl 00] Schlaich, M., "Kuppel und Kissen - Stierkampf-Arena in Madrid," db Deutsche Bauzeitung, 134. Jahrgang, Nr. 9/2000, Deutsche Verlags-Anstalt, pp. 59-69, 2000. (in German)
- [Schl 04] Schlaich, M., "Future Engineering Structures for the Urban Habitat and Infrastructure," Proceedings IABSE Symposium in Shanghai, pp.102, China, 2004.
- [Schl 06] Schlaich, M., "Challenges in Education – Conceptual and Structural Design," Proceedings of the IABSE Symposium Budapest, IABSE Report Vol. 92, 2006
- [Schu 10] Schumacher, M., Schaeffer, O. and Vogt, M., move - Architektur in Bewegung - dynamische Komponenten und Bauteile, Birkhäuser, Basel, 2010 (in German)
- [Sei 09] Seidel, M., Tensile Surface Structures. A Practical Guide to Cable and Membrane Construction, Ernst & Sohn Verlag, Darmstadt, 2009.
- [Sob 93] Sobek, W. and Speth, M., "Von der Faser zum Gewebe," DB nr 9, pp.74-81, Sept 1993. (in German)
- [Sob 02] Sobek, W. and Teuffel, P. "Adaptive Lightweight Structures," Proceedings of the International IASS Symposium, 24–28 June 2002, Warsaw, Poland. Micro Publisher, pp. 203–210.
- [Sob 04] Sobek, W. and Rehle, N., "Beispiele für verglaste Vertikalseilfassaden," Stahlbau 73, pp-224–229, 2004. (in German)

- [Sob 12] WERNER SOBEK Engineering & Design, Accessed May 12, 2012.
www.wernersobek.com
- [Sto 68] Stromeyer, Textiles Bauen, Konstanz, 1968 (in German)
- [Tai 12] Taillibert International, Accessed May 12, 2012.
www.agencetaillibert.com
- [Ten 12] TENARA® Fabric “TENARA“ Accessed March 12, 2012.
www.tenarafabric.com
- [Top 07] Topping, B.H.V. and Ivanyi, P., Computer Aided Design of Cable-Membrane Structures, Saxe-Coburg Publications, Stirling, 2007.
- [Tsu 12] Tsuboi, Y. et al., Mechanics Material and Structural Design (Rikigaku Sozai Kouzou Design), Kenchiku-Gijyutsu, Tokyo, 2012 (in Japanese)
- [Wag 02] Wagner, R. and Bögle, A., ”Double-Curved Space Structures – Function and Construction.” International Journal of Space Structures 17, no. 2-3, pp.117-127, 2002.

Appendix A – Required Energy for Motion - Reference data for the diagram in Fig. 3.3

The diagram in Fig. 3.3 was drawn based on the numbers shown in the tables in this appendix. For the “membrane” retractable roof, the weight of textile membrane and pulleys were taken into account. For the “rigid” retractable roofs, the data of the weight was directly drawn from the reference shown in Appendix D. Since the swing center of a “rigid rotate” retractable roof lies on a stationary point on a building, it is approximated that half of the weight of the roof is transferred to this point, and therefore only the other half is relevant to the required energy for motion.

Table A-1 Required energy for motion of membrane retractable roofs (1 kN \approx 100 kg)

		Area of a retractable roof	weight of membrane	weight of pulleys		Effective weight	Factor of Required Energy (Weight /Area)
		A	W_m	W_p		$W = W_m + W_p$	W/A
approximation			1kg/m ²	200kg/ one with a motor 100kg/ one without motor			
		[m ²]	[kN]		[kN]	[kN]	[kN/m ²]
Membrane + single mast	Cannes	800	8	100kg*16=	16	24	0.03
	Bad Hersfeld	1315	13	200kg*14+100kg*7=	35	48	0.04
	Paris	1800	18	200kg*14+100kg*14=	42	60	0.03
	Montreal	20000	200	100kg*43=	43	243	0.01
Membrane + spoked wheel	Zaragoza	1017	10	100kg*80=	80	90	0.09
	Kufstein	2000	20	100kg*120=	120	140	0.07
	Rothenbaum	3000	30	100kg*126=	126	156	0.05
	Frankfurt	8000	80	100kg*256=	256	336	0.04

Table A-2 Required energy for motion of rigid retractable roofs (1 kN \approx 100 kg)

		Area of a retractable roof	Weight of a retractable roof	Effective weight	Factor of Required Energy (Weight /Area) [kN/m ²]
		A	W	W _e	W _e /A
		[m ²]	[kN]	[kN]	[kN/m ²]
Rigid - Parallel	Bullring in Logrono	1300	1200	1200	0.92
	Stadium in Cardiff	8960	8000	8000	0.89
	Stadium in Kobe	9794	13200	13200	1.35
	Stadium in Copenhagen	11000	14000	14000	1.27
	Stadium in Phoenix	22400	40000	40000	1.79
	Ocean Dome	22660	27240	27240	1.20
	Minute Maid Park	25276	90000	90000	3.56
	Skydome	32374	110000	110000	3.40
	SafeCo Field	36000	110000	110000	3.06
Rigid - Rotate	Mukogawa Gakuin	2231	7810	3905	1.75
	Mellon Arena	12500	30000	15000	1.20
	Miller Park	22000	120000	60000	2.73
	Fukuoka Dome	33000	80000	40000	1.21

Appendix B – An Alternative Solution (Pneumatic system)

Another geometrical solution for the rectangular strip is an application of a pneumatic structural principle. A double layered rectangular textile membrane for which all edges are sealed can be inflated by air pressure. If only the four corners are fixed, the maximum deformation would occur in the middle of the strip, and the distance between the edge lines of long side becomes smallest there. As the form of this air cushion would be “waisted” in plan, this may be fit to the shape of the straight lines of the radial cables discussed in Section 7.2.

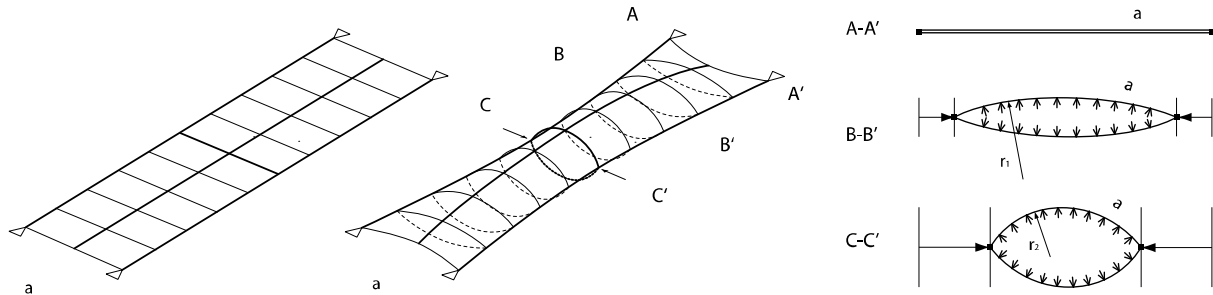


Figure B-1 Rectangular air cushion with four corners fixed: no air pressure (Left), with air pressure (centre) and cross section of a rectangular membrane strip inflated by constant air pressure (right)

The curves shown in the transverse cross section would be calculated as follows. The ‘waisted’ membrane strip is twisted onto a horizontal plane to simply define the geometrical curve in two-dimensions. Physical phenomena such as elongation of membrane material are ignored here.

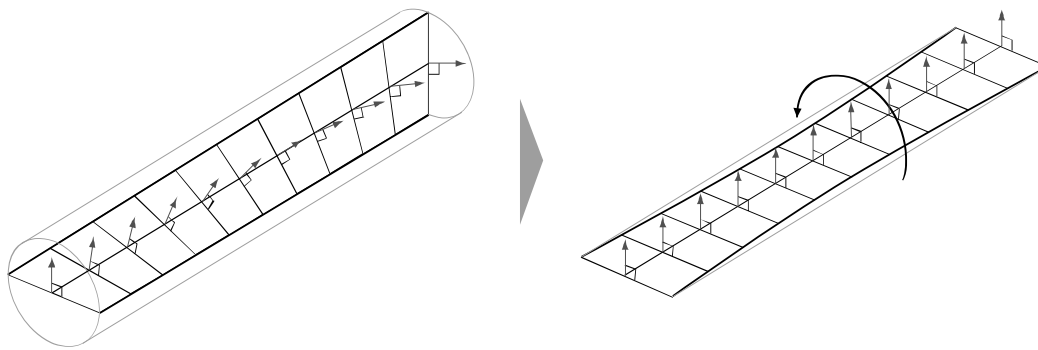


Figure B-2 The twisted “waisted” membrane strip

The origin point is set on the center of the roof. The y-axis is overlapped on the rotational axis so that the surface of the membrane strip lies on the x-y plane. The z-axis orients in the vertical direction. The inflation curve is shown on the y-z plane and expressed with a z-coordinate. The number m corresponds to the one used in Figure 7.3 in Chapter 7.

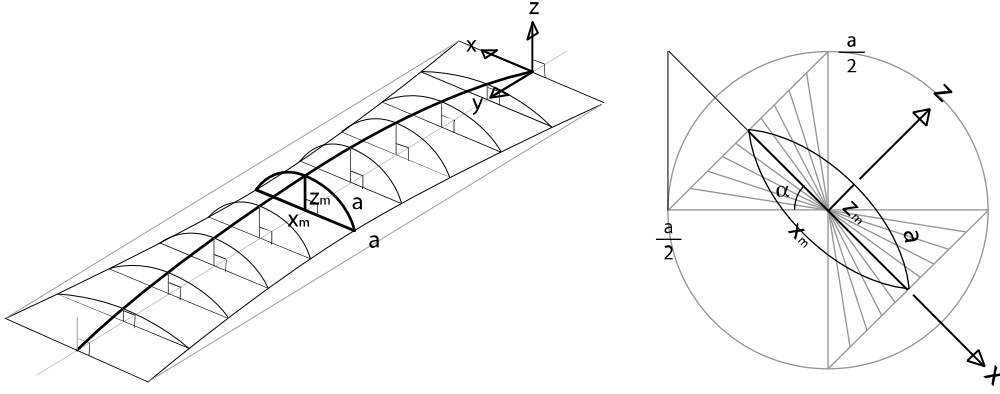


Figure B-3 3-D figure of membrane strip and figure on xz-plane

At first, the distance between two boundary cables x_m is calculated. This is simply calculated in the view from the perimeter using the angle α that indicates the rotation angle from the x-y plane. x_m is expressed by a similar function as:

$$Xm(\alpha) = \frac{a}{2} \cdot \frac{1}{(1 + \tan \alpha) \cdot \cos \alpha} \quad (B-1)$$

Since the curve of the cross-section in the transverse direction of the air cushion is approximated as circle, the distance between two boundary cables x_m and the deviation z_m correspond to the chord and arc of this circle, respectively. z_m is expressed with Huygens' approximation and the Pythagorean theorem:

$$Zm^2 = \left(\frac{3 \cdot a + Xm}{8} \right)^2 - \left(\frac{Xm}{2} \right)^2 \quad (B-2)$$

From the equation above, the curve can be expressed as follows. This curve indicates the minimum required height of membrane strip to apply this principle to a twisted membrane strip.

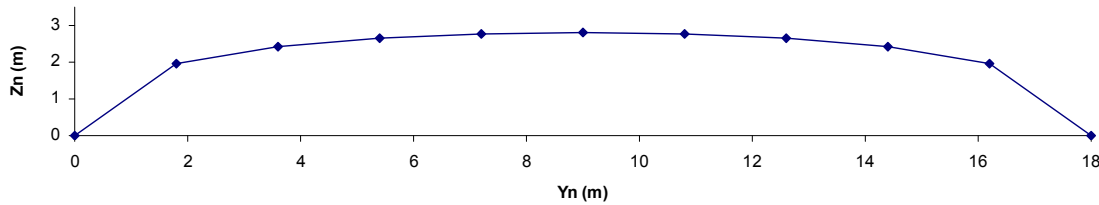
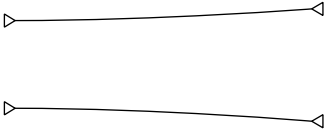
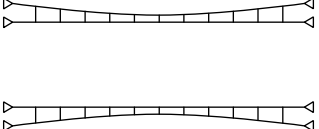
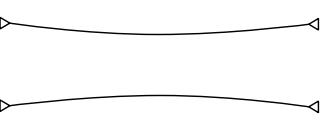

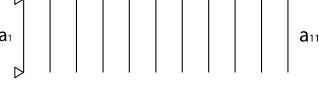

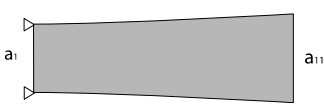
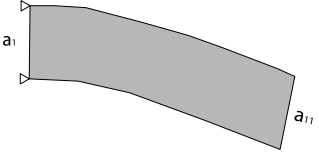
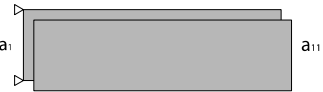


Figure B-4 A desired curve appeared on yz-plane with radius of the roof $r=18m$

This is just an approximation, because the membrane strip is actually twisted. Twisting a membrane strip causes large deformation in the surface especially at the middle of the membrane strip. However, in general, the large deformation does not cause serious damage on the surface of the membrane. Therefore, this approach seems reasonable.

One disadvantage of this approach is the required amount of material, which demands $4 \cdot A_c$, double the area of the cable girder approach, as shown in table below.

Table B-1 Comparison between the three approaches

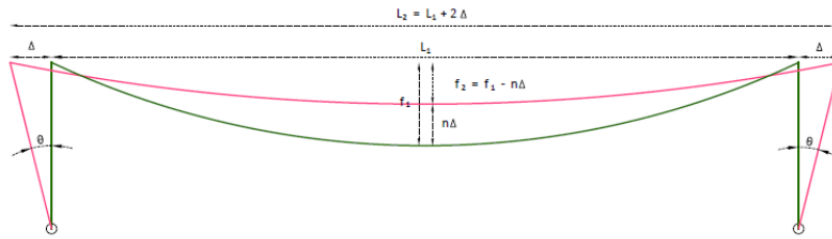
	Half strip approach	Cable girder approach	Air cushion approach
Radial cable			
Distance between adjacent radial cables			
Shape of a membrane strip			
Required Amount of membrane	$3.2 \cdot A_c$	$2 \cdot A_c$	$4 \cdot A_c$
Possible way for introduction of prestressing force	Kinematic	kinematic	pneumatic

Appendix C –Parameter Study of Kinematic Cable Girders

The analysis of the ‘Katzbuckel’ bridge and the results of the parameter study that were discussed in chapter 9 will be shown here.

C-1 Analysis of the ‘Katzbuckel’ Bridge

The kinematic behavior of the ‘Katzbuckel’ bridge shown in Chapter 9 will be analyzed first. Even though it is not a cable girder but instead a suspension bridge, it is the only realized example which uses the raising-principle of kinematic cable girders. Kinematic features of the Katzbuckel bridge is studied by simulating the main cable as a single hanging cable. The outwards move Δ of the anchorages of a single hanging cable are caused by a rotation of both supporting masts. The elevation of the single hanging cable E_i is the target of this analysis. The “raising-factor” n defines the ratio between E_i and Δ . A diagram of principles is drawn with related captions.



Index 1:	cable in lower position
Index 2:	cable in upper position
L_i	Span ($l_1 = 73\text{m}$)
S_i	cable length
F_i	cable sag ($l_1 = 18.9\text{ m}$)
Δ	horizontal outwards displacements of cable-anchorage as a result of mast rotations
$E_i = n\Delta$	cable elevation expressed as a multiple of the original horizontal displacement Δ
N	“raising-factor”

Figure C-1 Diagram of principles of the kinematic cable girders

Some simplifications are applied: only horizontal move is considered, the cable has no self-weight, no elongation ($EA = \infty$) and is flexible ($EI = 0$).

From geometry:

$$l_2 = l_1 + 2\Delta \quad (\text{C-1})$$

$$f_2 = f_1 - n\Delta \quad (\text{C-2})$$

From cable theory, cable lengths in each position are expressed as:

$$s_1 = l_1 + \frac{8 \cdot f_1^2}{3 \cdot l_1} \quad (\text{C-3})$$

$$s_2 = l_2 + \frac{8 \cdot f_2^2}{3 \cdot l_2} \quad (\text{C-4})$$

From geometrical compatibility,

$$s_1 = s_2 \quad (C-5)$$

Therefore the equation (C-5) becomes by substitution from (C-1) to (C-4):

$$l_1 + \frac{8 \cdot f_1^2}{3 \cdot l_1} = l_1 + 2\Delta + \frac{8 \cdot (f_1 - n \cdot \Delta)^2}{3 \cdot (l_1 + 2\Delta)} \quad (C-6)$$

This equation whose only unknown is n can be simplified as:

$$\Delta + \frac{4}{3} \cdot \left[\frac{(f_1 - n \cdot \Delta)^2}{(l_1 + 2\Delta)} - \frac{f_1^2}{l_1} \right] = 0 \quad (B-7)$$

From the equation it is clear that the input values and output values are nonlinearly related. This second degree equation is solved and expressed in a graph below. The horizontal force at the edge of the cable is also calculated with $q=17\text{kN}$ using cable theory:

$$H_2 = \frac{ql^2}{8f_2} \quad (B-8)$$

The calculation results are presented with the evolution of the cable-elevation ($E_i = n\Delta$) as a function of Δ .

The elevation increases according to an increase of input displacement. The raising factor changes negligibly and stays at approximately the value 2. The horizontal force at the edge becomes large according to the increasing of the value of the input displacement, and it goes to infinity at $\Delta=6.0\text{m}$. This is because the hanging cable reaches the limit height and becomes flat in shape.

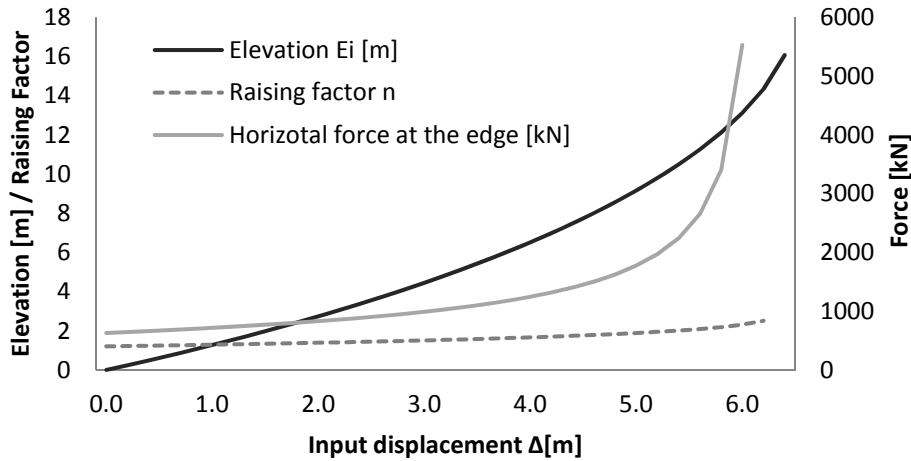


Figure C-2 Hand calculation results of Elevation, Raising factor and normal force in upper cable of the 'Katzbuckel' bridge

C-2 Calculation results of the parameter study of the kinematic cable girder

The results of the parameter study performed in chapter 9 are shown here.

All results of the kinematic study showed that the internal force in the upper cable increases dramatically during the movement, as shown in the last graph. However, the difference between two iterations remains almost constant. This means that the driving force required to perform the anchorage movements don't increase, and a large force is not necessary.

Parameters of the hanger cables

1) Prestressing forces in the hanger cables

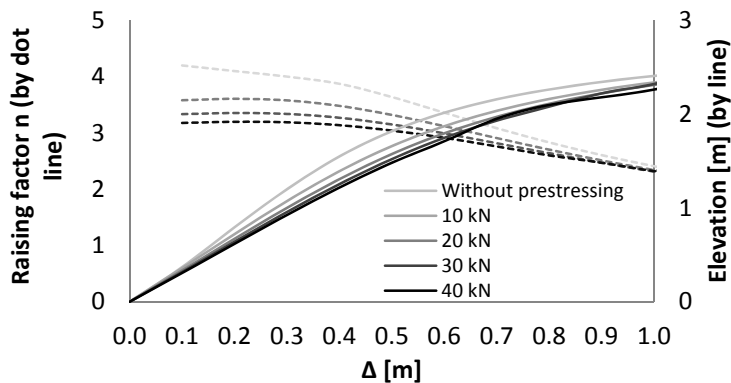


Figure C-3 Kinematic curves for a variation of the prestressing forces introduced in hangers

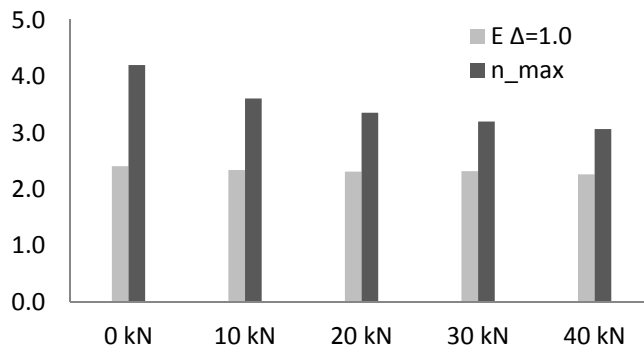


Figure C-4 Diagrams of the main results for a variation of the prestressing forces introduced in hangers

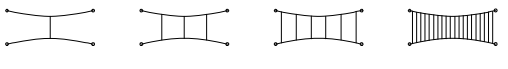
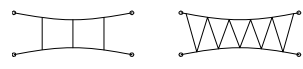
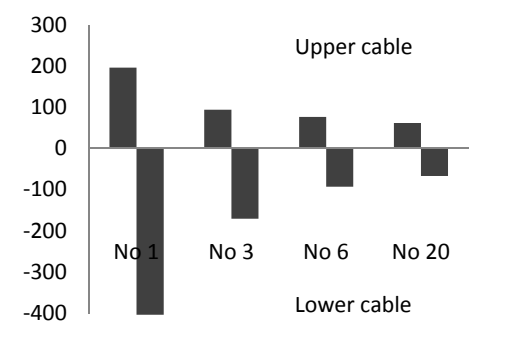
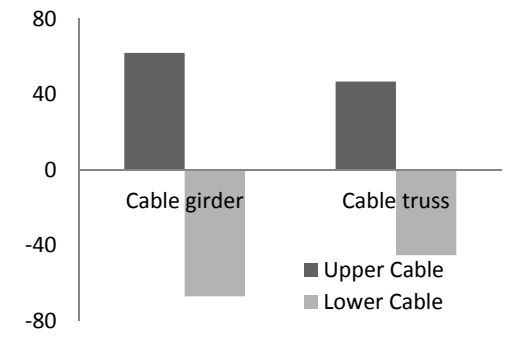
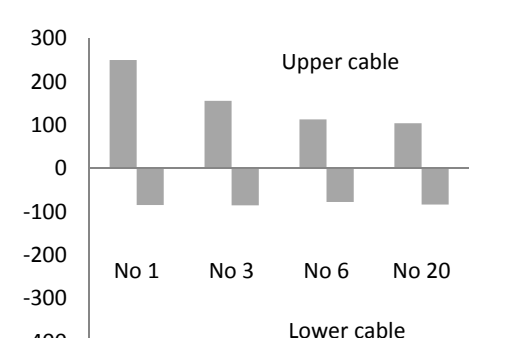
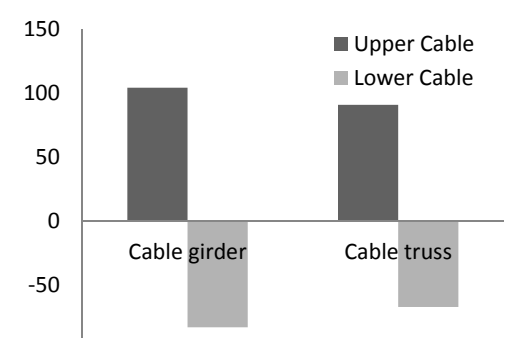
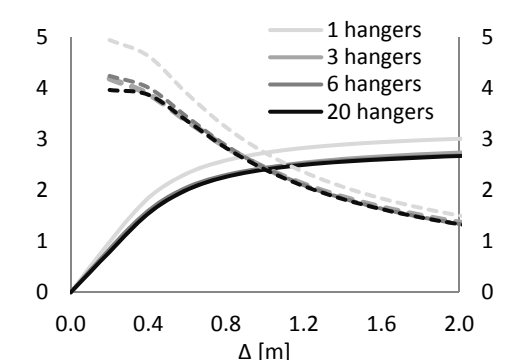
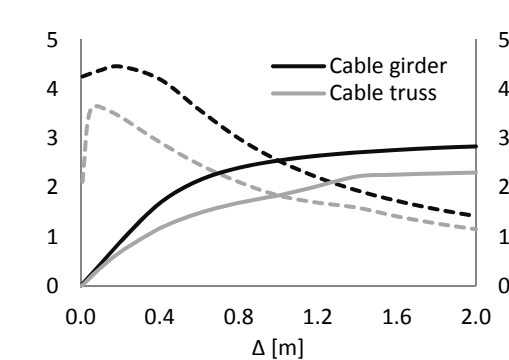
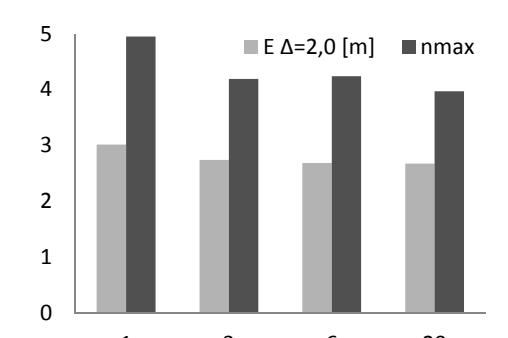
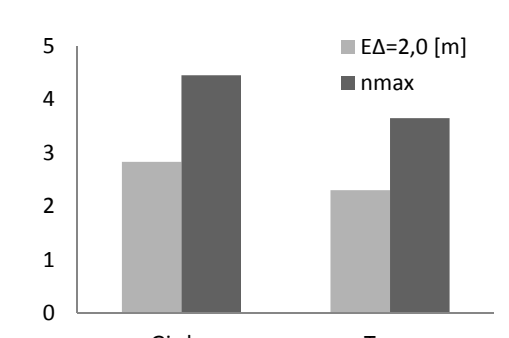
2) Length of hanger

The hanger's length is varied here, so the distance between the main cables e (1, 3 and 5m) can be adjusted. The sag of the main cables remain the same, and the anchorage positions are simply translated in the vertical direction to accommodate the variation in hanger length. From the studies it reveals that the hanger's length has no influence on both static and kinematic behavior of the cable girders. All output results including deflection, cable force, elevation and raising factor, are the same.

3) Number and 4) Disposition of hangers

The numbers of hangers are varied from 1 to 20. However, only the results of the number of hangers 1, 3, 6 and 20 are shown here.

Table C-1 The results of Static and kinematic study of Number of hangers

		Number of hangers	Disposition
		 1 3 6 20	 Cable Girder Cable Truss
Statically Analysis	Deflection: ΔU max [mm]		
	Cable force: ΔN max [kN]		
Kinematically Analysis	Left axis: Raising Factor N (by dot line) Right axis : Elevation [m] (by line)		
	Elevation E (when $\Delta=2.0$) Max. Rising Factor n_{max}		

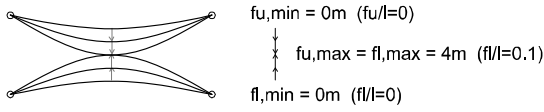
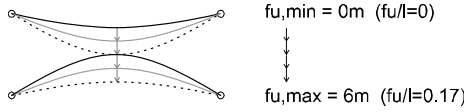
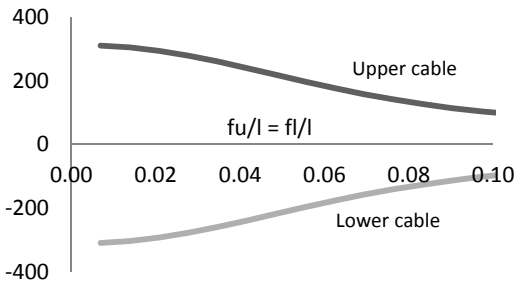
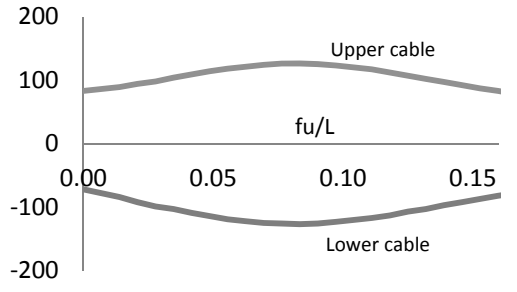
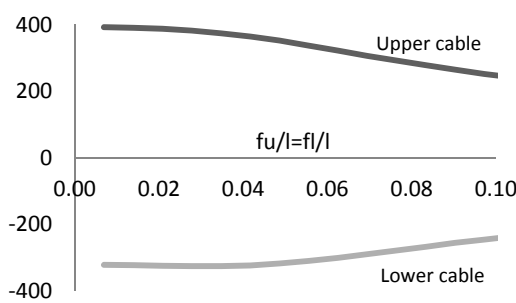
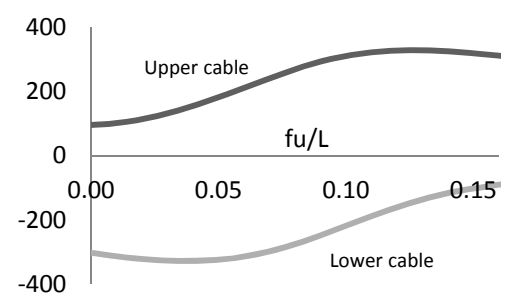
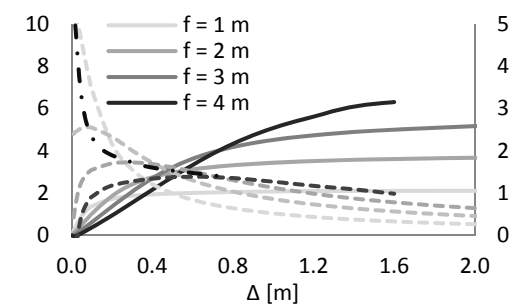
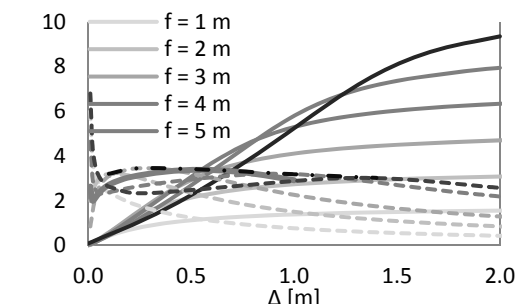
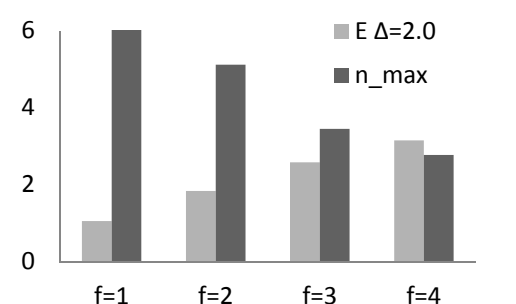
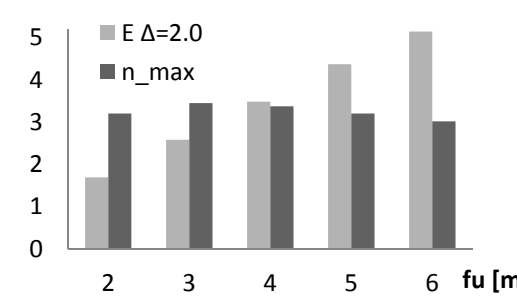
Parameter of the cables

1) Parameter study of the cable sag

Table C-2 The results of Static and kinematic study of variation in upper and lower cable sag

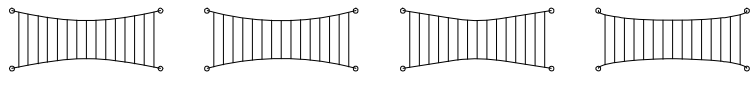
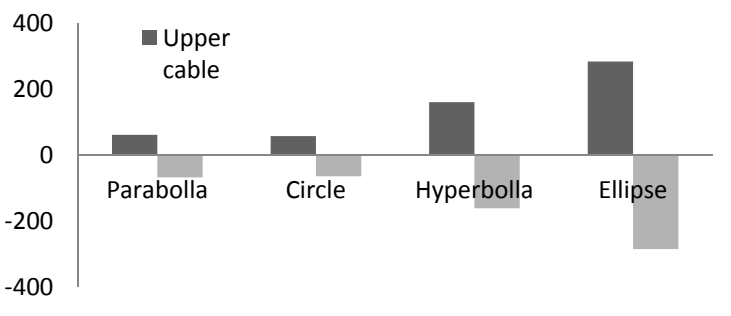
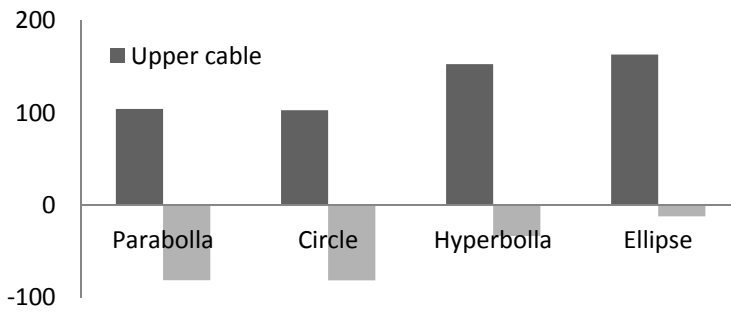
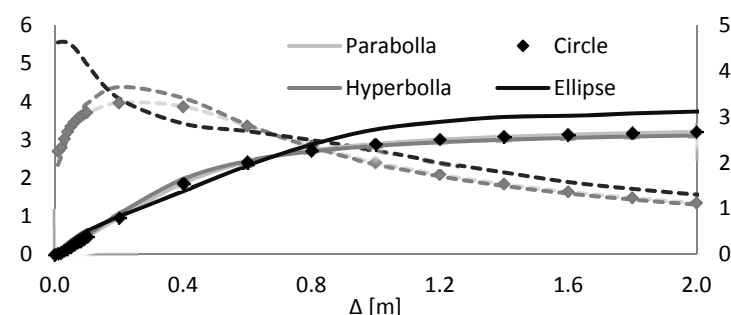
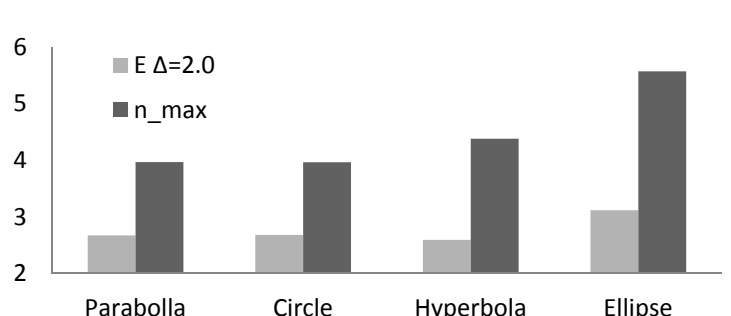
		Variation in upper-cable sag	Variation in lower-cable sag
Statically Analysis	Deflection: ΔU max [mm]		
	Cable force: ΔN max [kN]		
Kinematically Analysis	Left axis: Raising Factor N (by dot line)		
	Elevation E (when $\Delta=2.0$) Max. Rising Factor n. max		

Table C-3 The results of Static and kinematic study of variation in both upper and lower cable sag

		Both cable sags (e varying)	Variation in both cable sags (e constant)
			
Statically Analysis	Deflection: ΔU max [mm]		
	Cable force: ΔN max [kN]		
Kinematically Analysis	Left axis: Raising Factor N (by dot line) Right axis: Elevation [m] (by line)		
	Elevation E (when $\Delta=2.0$) Max. Rising Factor n_{max}		

2) Parameter study of the cable form


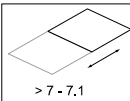
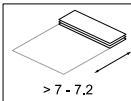
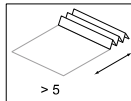
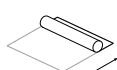
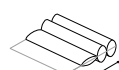
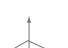
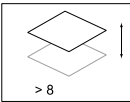
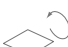
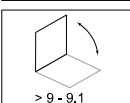
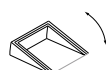
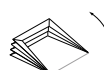
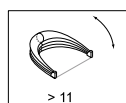

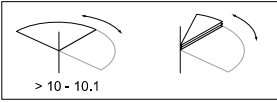
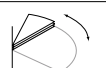
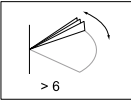

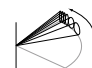
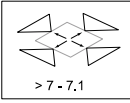
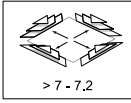
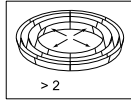
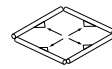
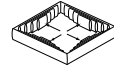
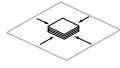
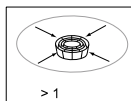
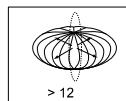
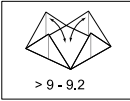
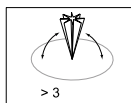
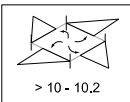

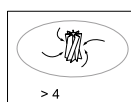
Table C-4 The results of Static and kinematic study of variation in cable form

		 Parabola Circle Hyperbola Ellipse
Statically Analysis	Deflection: ΔU max [mm]	
	Cable force: ΔN max [kN]	
Kinematically Analysis	Left axis: Raising Factor N (by dot line) Right axis: Elevation [m] (by line)	
	Elevation E (when $\Delta=2.0$) Max. Rising Factor n_max	

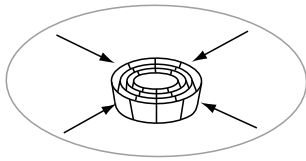
Appendix D – List of Retractable Roofs

A list of existing retractable roofs all over the world is shown here according to the typology that the author defined in Chapter 3. Small scale and very common types of retractable roofs are not listed here because there exist countless examples.


Table D-1 Typology of the retractable roofs and the section number



Coordinate System		none	Size reduction for storage				
			overlap	fold / bunch	role	deform by air	
Single - axis motion							
Translation	Horizontal						
	Vertical						
Rotation	Horizontal						
	Vertical						
Multiple - axis motion							
Translation	Horizontal	peripheral					
	Horizontal	Central					
Rotation	Horizontal	peripheral					
		Central					
	Vertical	peripheral					
		Central					


1 Folding/bunching - Horizontal translation to the center




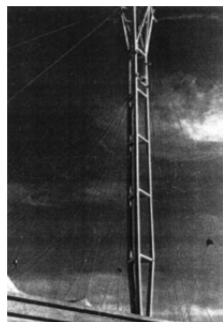
1.1 A single mast


Name	Open air theatre Masque de Fer Casino Palm Beach	 <p>[Ner 05]</p>
Location	Cannes, France	
Start of design	1965	
Year of completion	1965	
Function	Roof over terrace of casino palm beach	
Designer	R. Taillibert (arch.) F. Otto (EL: Entwicklungsstätte für Leichtbau Berlin) St. du Chateau (eng.) Stromeyer (membrane)	
Material	Membrane: polyester fabric coated with PVC	
Area of retractable roof [m ²]	ca. 800 (D = ca.33m)	
Operation time	ca. 12 min.	
Remarks	-First convertible roof of this type -Membrane is not tensioned	
Reference	[Ner 05][Ott 72]	

Name	Swimming pool Boulevard Carnot	
Location	Paris, France	
Start of design	1966	
Year of completion	1966	
Function	Swimming pool	
Designer	R. Taillibert (arch.) F. Otto (EL) Stromeyer (membrane)	
Area of retractable roof [m ²]	ca.1,800 (length 62m, width 32m)	
Operation time	ca. 12 min.	 <p>[[Ner 05]</p>
Remarks	Combination of stationary winch and cable tractor system	
Reference	[Ner 05][Ott 72][Fab 70]	

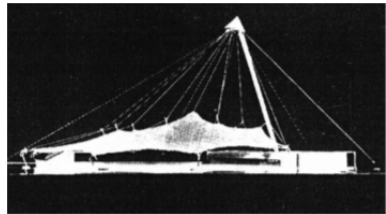
Name	Open-air Theatre of the abbey ruins of Bad Hersfeld	 <p>[Ner 05]</p>
Location	Bad Hersfeld, Germany	
Start of design	1966 (designed in competition 1959)	
Year of completion	1968	
Function	Open-air theatre	
Designer	F. Otto (EL) Leonhardt, Andrä und Partner (eng.) Stromeyer (membrane)	
Material	Membrane polyester fabric coated with PVC	
Area of retractable roof [m ²]	1,315 (length 45m, width 37m)	
Operation time	ca. 4 min.	
Remarks	-Prestressed only by the tractors -Renovation in 1993 and still used	
Reference	[Ott 72] [Ner 05][Sto 68]	


Name	Swimming pool Rue David D'Angers	 <p>[maps.google.com]</p>
Location	Paris, France	
Start of design	1968	
Year of completion	1969	
Function	Swimming pool	
Designer	R. Taillibert (arch.)	
Area of retractable roof [m ²]	ca.1,800 (length 63m, width 37m)	
Operation time	ca. 12 min.	
Reference	[Ott 72]	


Name	Swimming pool St. Fons	 <p>[Ott 72]</p>
Location	Lyon, France	
Start of design	1969	
Year of completion	1970	
Function	Swimming pool	
Designer	R. Taillibert (arch.) Stromeyer (membrane)	
Area of retractable roof [m ²]	ca. 2,000 (length 67m, width 39m)	
Operation time	ca. 10 min.	
Reference	[Ott 72]	


Name	Hoechst exhibition pavilion	 <p>[Sto 68]</p>
Location	Hannover fair 1970, Germany	
Start of design	1969	
Year of completion	1970	
Function	Temporary roof for the fair	
Designer	Stromeyer (design and construction)	
Area of retractable roof [m ²]	250 (length 17m, width 12m)	
Operation time	2.5 min.	
Remarks	Four wheels tractor operated by a self-locking worm drive	
Reference	[Ott 72][Sto 68]	

Appendix

Name	Swimming pool Reim	
Location	Reim, France	
Start of design	1969	
Year of completion	1971	
Function	Swimming pool	
Designer	R. Taillibert (arch.)	
Area of retractable roof [m ²]	1,400 (length 44.2m, width 40.7m)	
Operation time	5 min.	
Reference	[Ott 72]	


Name	Swimming pool Kleinostheim	
Location	Kleinostheim, Germany	
Year of completion	1971	
Function	Swimming pool	
Designer	R. Taillibert (arch.)	
Area of retractable roof [m ²]	ca. 1,800 (length 65m, width 33m)	
Operation time	ca. 15 min.	
Reference	[Ott 72]	
		[www.aschaffenburg.dlrg.de]


Name	Westbad Regensburg	
Location	Regensburg, Germany	
Start of design	1970	
Year of completion	1972	
Function	Swimming pool	
Designer	Schmaz, Schmid, Mehr and Eckel (arch.) Frei Otto (AW: Atelier Warmbronn) (consultant) Stromeyer (membrane)	
Material	Membrane polyester fabric coated with PVC	
Area of retractable roof [m ²]	ca. 2,300 (length 70m, width 40m)	
Operation time	15 min.	
Remarks	-25 tractors and 9 trolleys are used -Pneumatic cushion is installed in the gap between the wall and the roof	
Reference	[Ott 72][Ner 05]	
		[Ner 05]


Name	Allwetterbad Düsseldorf	
Location	Düsseldorf, Germany	
Year of completion	1977	
Function	Swimming pool	
Designer	IPL Ingenieurplanung Leichtbau (design) Verseidag, Stromeyer (membrane)	
Material	PVC-Diolen fabric	
Operation time	ca. 10 min.	
Reference	[Ner 05][Ank 77]	
		(taken by the author)


Name	Montréal Olympic Stadium	 <p>[profit.bg/news/Naj-skupite-stadioni-v-sveta/nid-86128.html]</p>
Location	Montréal, Canada	
Start of design	1972	
Year of completion	1987	
Function	Multifunctional sports facility	
Designer	Roger Taillibert (arch.) Lavalin (eng.) schlaich bergemann und partner (consultant)	
Material	PVC coated Kevlar-membrane	
Area of retractable roof [m ²]	20,000 Spans: 200 x 140 m (elliptical shape)	
Reference	[Lai 88] [Hol 97]	

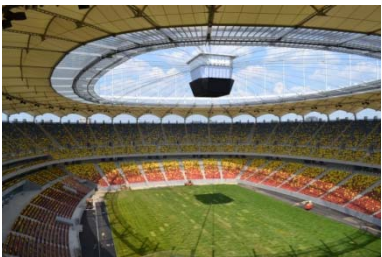

1.2 Spoked wheel structure

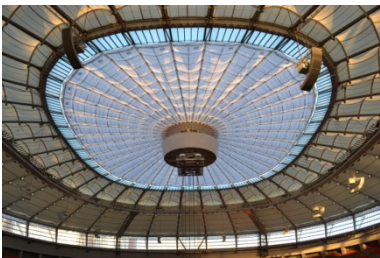

Name	Bull-fight Ring	 <p>[Hol 97]</p>
Location	Zaragoza, Spain	
Year of completion	1989	
Function	Bull-fight + Multi-events	
Designer	schlaich bergemann und partner (arch.+ eng.)	
Material	Membrane: Polyester fabric coated with PVC	
Area of retractable roof [m ²]	1,000 (D = 36m)	
Operation time	2-3 min.	
Remarks	-The outer fixed roof: ca. 4000m ² , 64 upper and 32 lower radial cables -The inner roof : 16 cables +16 motors	
Reference	[Hol 97] [Ber 92a] [Ber 92b] [Bög 03]	

Name	Centre court Rothenbaum	 <p>[Sob 12]</p>
Location	Hamburg, Germany	
Year of completion	1999	
Function	Tennis stadium	
Designer	ASP Schweger (arch.) Sobek + Rieger (eng.)	
Material	Membrane: Polyester fabric coated with PVC	
Area of retractable roof [m ²]	3,000 (D = 63 m)	
Operation time	ca. 5 min.	
Remarks	-The outer fixed roof (ca. 5300m ²) -18 motors (5.5kW/motor, traction force 1.5t) -Driving system: ECCON Engineering Computer Consulting	
Reference	[Koc 04] [Bla 99] [Sob 12]	

Name	Commerzbank-Arena	 <p>[sbp 12]</p>
Location	Frankfurt, Germany	
Year of completion	2005	
Function	Football + Multi-events	
Designer	von Gerkan, Marg und Patner (arch.) schlaich bergemann und partner (eng.)	
Material	Membrane: polyester fabric coated with PVC + additional PVDF (Polyvinylidene Flouride) coating on upper side	
Area of retractable roof [m ²]	8,000	
Operation time	ca.15 min.	
Remarks	-The outer fixed roof: ca. 29,000m ² -44 radial cables (outer) and 32 (inner upper) -Driving system: ECCON Engineering Computer Consulting	
Reference	[Göp 07a] [sbp 12]	



Name	Fortress Kufstein, Josefsburg Arena	 <p>[Rei 12]</p>
Location	Kufstein, Austria	
Year of completion	2006	
Function	Open-air theatre	
Designer	Nikolai Kugel (arch.) Alfred Rein Ingenieure (eng.)	
Material	Membrane: Fluoropolymer-coated Fabric woven from ePTFE fabric (product: TENARA® Fabric 4T40)	
Area of retractable roof [m ²]	2,000 (D = 52 m)	
Operation time	within 4 min.	
Remarks	-16 trolleys -Driving system: ECCON Engineering Computer Consulting	
Reference	[Rei 12][Kni11][Ten 12]	

Name	National stadium Bucharest	  <p>Courtesy of schlaich bergemann und partner</p>
Location	Bucharest, Romania	
Year of completion	2011	
Function	Football stadium	
Designer	von Gerkan, Marg und Patner (arch.) schlaich bergemann und partner (eng.)	
Material	Membrane: Polyester fabric coated with PVC	
Reference	[sbp 12] [Det 11]	

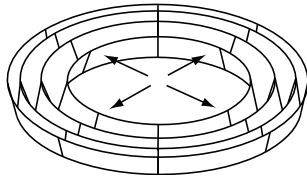
Name	BC Place	  <p>Courtesy of schlaich bergemann und partner</p>
Location	Vancouver, Canada	
Year of completion	2011	
Function	Multi-events	
Designer	schlaich bergemann und partner (eng.) Geiger Engineers (eng.)	
Material	Cushion: Fluor-polymer (PTFE) coated woven PTFE fabric (product: Tenara) (Translucency 40%)	
Area of retractable roof [m ²]	8,500	
Operation time	ca. 20 min.	
Remarks	-The outer fixed roof: ca. 32,500m ² (PTFE glass fabric) -The inner retractable: 36 radial cables and 36 inflated inflated cells -One unit of air cushion: ca.105 m ³	
Reference	[Det 11] [Göp 11]	


Name	National stadium Warsaw	 <p>[sbp 12]</p>
Location	Warsaw, Poland	
Year of completion	2012	
Function	Football stadium	
Designer	von Gerkan, Marg und Patner (arch.) JSK Architekten (arch.) schlaich bergemann und partner (eng.)	
Material	Membrane: Polyester fabric coated with PVC	
Area of retractable roof [m ²]	11,000	
Remarks	-Capacity: 55,000 -The outer fixed roof: ca. 54,000m ² -Total covered area: 70,000m ² (280x245m) -60 upper radial cables (inner retractable)	
Reference	[sbp 12][Det 11][Göp 11]	

1.3 Others

Location	Kazakhstan	  <p>[www.planex-gmbh.de]</p>
Year of completion	2009	
Function	Hotel / sunshade	
Designer	Planex	
Area of retractable roof [m ²]	470	
Reference	[www.planex-gmbh.de]	

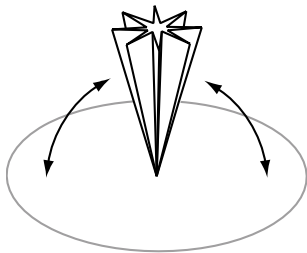
2 Folding/bunching - Horizontal translation to the periphery



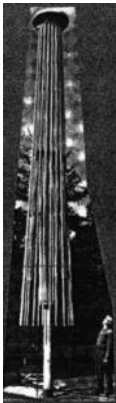
Name	Bull-fight Ring	
Location	Jaén, Spain	
Year of completion	1998 (-1999 demolished)	
Function	Bull-fight + Multi-events	
Designer	F. Escrig and J. Sanchez	
Area of retractable roof [m ²]	3,000	
Operation time	less than 20 min.	
Remarks	The outer fixed roof: ca. 2,000m ²	

Courtesy of Felix Escrig

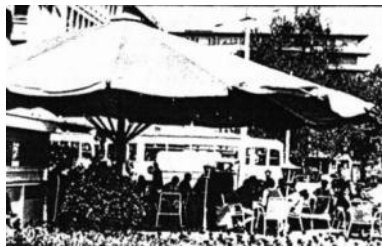
3 Folding/bunching - Horizontal axial rotation to the centre




3.1 Foldable membrane with umbrella-like structures


Name	Hotel Baur au Lac	
Location	Zürich, Switzerland	
Year of completion	1943	
Function	Sun umbrella	
Area of retractable roof [m ²]	(D = 12 m)	
Reference	[Ott 72]	


[Ott 72]


Name	Café am wasserturm	
Location	Mannheim, Germany	
Year of completion	1968	
Function	café terrace	
Area of retractable roof [m ²]	130 (D = 12m)	
Remarks	Electrical motor located in the canopy base	
Reference	[Ott 72]	


[Ott 72]


Name	Department Store Hertie	
Location	Bad Godesberg, Germany	
Year of completion	1969	
Function	Café terrace	
Area of retractable roof [m ²]	14 x 10m (mushroom), 14 x 8m (funnel)	
Remarks	-Combination of mushroom-like canopies and funnel-shaped canopies -Electrical motor located in the canopy base	
Reference	[Ott 72]	

Name	Café Kranzler	
Location	Frankfurt, Germany	
Year of completion	1970	
Function	Café terrace	
Area of retractable roof [m ²]	8 x 3m	
Reference	[Ott 72]	


Name	BUGA Canopies, National Garden Show (Bundesgartenschau)	
Location	Köln (Cologne), Germany	
Year of completion	1971	
Function	Sunshade	
Designer	F. Otto with B. Rasch and H. Isler Stromeyer (membrane)	
Material	PVC-coated polyester fabric	
Area of retractable roof [m ²]	ca. 200 (D = 19m)	
Operation time	2.5 min.	
Reference	[Ner 05], [Ott 72]	

Name	Stage umbrellas for a concert tour of the group Pink Floyd	
Location	USA	
Year of completion	1978	
Function	Weather protection	
Designer	F. Otto with B. Rasch Buro Happold	
Reference	[Ner 05] [www.freiotto.com]	


Name	Schirm Prototyp	
Location	The Red Sea Coast in Arabia	
Year of completion	1987 (temporary)	
Function	Sunshade	
Designer	B. Rasch and F. Otto	
Area of retractable roof [m ²]	5 x 5m	
Remarks	-Height: 5.4m (opened) - 6.5m (closed) -Used 6 months	
Reference	[Ott 96] [www.sl-rasch.de]	

Name	Prophet's Holy Mosque	
Location	Medina, Saudi Arabia	
Year of completion	1992	
Function	Weather protection	
Designer	B. Rasch with J. Bradatsch	
Material	PTFE (Teflon) fabric	
Area of retractable roof [m ²]	17 x 18m, height 9m	
Reference	[Ott 96] [www.freiotto.com]	

[Ott 96]

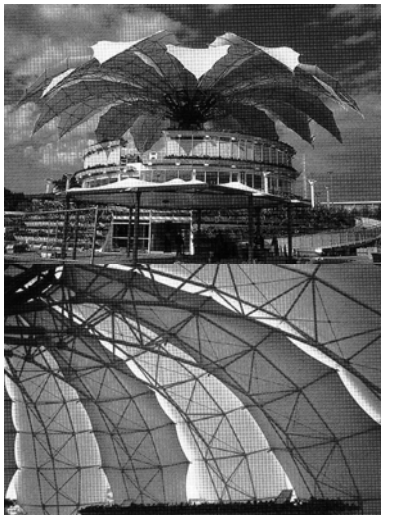
Name	Canopies for Buckingham Palace	
Location	Buckingham Palace, London	
Year of completion	1994	
Function	Shelters for visitors to the courtyards	
Designer	Richard Horden Associates	
Reference	[www.hcla.co.uk]	

[www.hcla.co.uk]


Name	Alden Biesen	
Location	Alden Biesen, Belgium	
Year of completion	2003	
Function	Deployable shelter for the castle's courtyard	
Designer	Ney & Partners	
Area of retractable roof [m ²]	676 (13 x 13m when open)	
Reference	[www.ney.be]	

[www.ney.be]

3.2 Other types

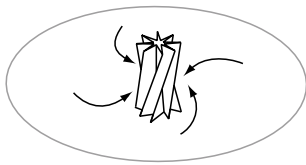
Name	Venezuela Pavilion	
Location	Hannover, Germany	
Year of completion	2000 (temporary)	
Function	Pavilion for EXPO 2000 in Hannover	
Designer	F. Otto, Rasch & Bradatsch, F. Vivas, Arqintegral with J. Llorens (arch.) Buro Happold (eng.)	
Area of retractable roof [m ²]	1,480	
Reference	[Ner 05] [tensinet.com]	


[Ner 05]

Name	Tsurumi-blossom (Flower Center)	
Location	Osaka, Japan	
Year of completion	1995	
Function	Shopping mall	
Designer	Nikken Sekkei	
Area of retractable roof [m ²]	1,330	
Reference	[www.nikken.co.jp]	


[www.nikken.co.jp]

4 Folding/bunching - Vertical axial rotation to the centre



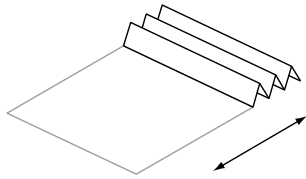
Name	Rotationspneu	
Location	Munich, Germany (Portable)	
Year of completion	1997	
Function	Shelter / Art work	
Designer	D. Baumüller (artist)	
Material	TYVEK polythene fleece (65 g/m ²)	
Remarks	-Open by rotating -Inflated by rotating using an electric motor (up to 4.5 m/sec.)	
Reference	[Dre 08]	

[Dre 08]

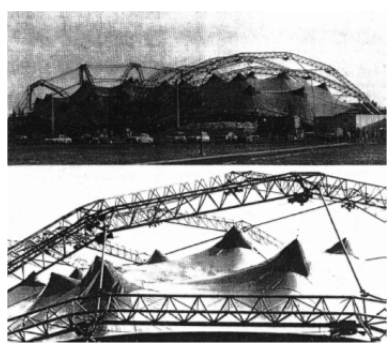
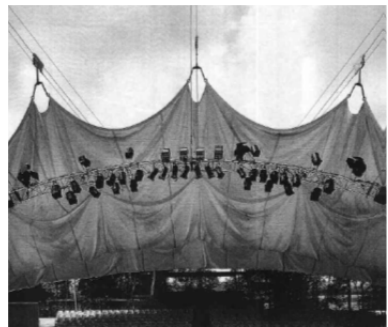
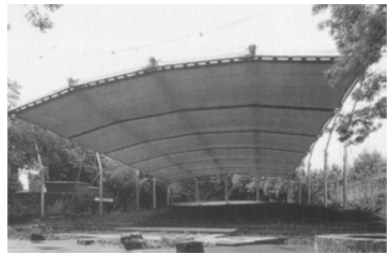
Name	Spokeless fabric umbrella	
Location	Stuttgart, Germany	
Year of completion	2003	
Function	Experimental model	
Designer	Werner Sobek + Transsolar	
Remarks	-Open by rotating -An electric motor mounted in the mast head	
Reference	[Sob 12]	

[Sob 12]

5 Folding/bunching – Horizontal translation




5.1 Radial movement

Name	Eisbahn Conflans St. Honorine	
Location	Conflans St. Honorine, France	
Year of completion	1971	
Function	Ice rink	
Designer	Blasco and Girard (arch.) F. Otto (AW) (consultant) Stromeier (membrane)	
Material	Polyester fabric with PVC coating	
Area of retractable roof [m ²]	3,300 (Length: ca.90m, width: ca.50m)	
Remarks	Membrane travels on the three-chord lattice girder	
Reference	[Ott 72] [Ner 05]	
		[Ott 72]
Name	Open-air Theatre in historical castle	
Location	Wiltz, Luxemburg	
Year of completion	1988	
Function	Open-air theatre	
Designer	B. Rasch and J. Bradatsch (arch.)	
Material	Membrane PES/PVC	
Area of retractable roof [m ²]	1,200	
Reference	[Ott 96] [www.sl-rasch.de] [Baus U., Leicht im Sattel, db 9/93.] [www.tensinet.com]	
		[Baus U., Leicht im Sattel, db 9/93.]
Name	Freilichttheater Tecklenburg	
Location	Tecklenburg, Germany	
Start of design	1993	
Year of completion	Open-air theatre	
Function	IPL (eng.) Carl Nolte (design)	
Area of retractable roof [m ²]	1,200 (30x40m)	
Remarks	Pneumatic system	
Reference	[Baus U., Leicht im Sattel, db 9/93.] [www.tensinet.com]	
		[Baus U., Leicht im Sattel, db 9/93.]


5.2 Parallel movement

Name	Quba Mosque
Location	Medina, Saudi Arabia
Year of completion	1987
Function	Shade for the courtyard
Designer	B. Rasch
Reference	[Ott 96] [www.sl-rasch.de]




[www.sl-rasch.de]

Name	Jaen Shortage
Location	Jaen, Spain
Year of completion	1998
Function	Cover for the audience
Designer	F. Escrig and J. Sanchez
Material	polyester fiber covered with PVC
Operation time	less than 20 min.
Reference	[www.performance-starbooks.com]




[www.performance-starbooks.com]

Name	Rathaus
Location	Vienna, Austria
Year of completion	2000
Function	Protect the courtyard from the weather for public events
Designer	Silja Tillner (arch.), schlaich bergmann und partner (eng.)
Material	PVC Polyester Typ I
Area of retractable roof [m ²]	1,100 (34 x 32m)
Reference	[Ber 04] [Dre 08]





[sbp 12]


Name	Toyota Stadium
Location	Toyota City, Japan
Year of completion	2001
Function	Football and rugby stadium
Designer	Kisho Kurokawa Architect & Associates (arch.) Ove Arup & Partners Japan Limited (eng.)
Material	Fabric: PVC-coated polyester fiber (top-coated with polyvinylidene fluoride compound)
Area of retractable roof [m ²]	Membrane covered area: 17,420+5,730m ² 45x90m (opened) / 224x90m (closed)
Operation time	50 min.
Remarks	-Capacity: 45,000 -Drive system: Rack-and-pinion system -Weight of the retractable roof: 2,400t
Reference	[Kayashima M. et al., AIJ Gakujutsukouen kougaisuu (Kantou), 09/2001 (in Japanese)]



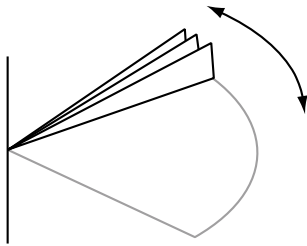
Photos taken by the author

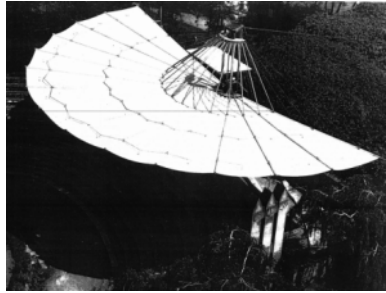
Name	Summer Theatre Burgas	 <p>[Dakov, D., V. Tanev, IABSE, Chicago, 2008.]</p>
Location	Burgas, Bulgaria	
Year of completion	2008	
Function	Summer theatre	
Designer	Archcom Ltd. (arch.) Proremus Ltd., Tanev and Partners Ltd. (eng.) IF (membrane)	
Material	Polyester with PVC coating	
Area of retractable roof [m ²]	1,600	
Operation time	ca. 20 min.	
Reference	[Dakov, D., V. Tanev, IABSE, Chicago, 2008.]	

Name	Wimbledon Centre Court	 <p>[www.tatasteelconstruction.com]</p>
Location	Wimbledon, UK	
Year of completion	2009	
Function	Tennis court	
Designer	Populous (arch.) Capita Symonds (eng.)	
Material	Fluoropolymer-coated ePTFE fabric (Product name: TENARA® Fabric 4T40 / 4T20)	
Area of retractable roof [m ²]	5,220	
Remarks	1,100t	
Reference	[www.tatasteelconstruction.com] [Ten 12]	

Name	Shopping Mall Athens Heart	 <p>[form-tl.de]</p>
Location	Athens Heart	
Function	Shopping mall	
Designer	Conran & Partners, Diarchon (arch.) form-tl (eng.)	
Area of retractable roof [m ²]	3,400	
Remarks	The main structure has 13 crescent-shaped arched girders, which span freely up to 50 m	
Reference	[form-tl.de]	

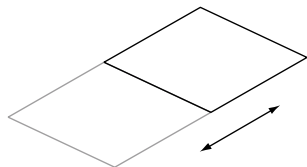
6 Folding/bunching – Vertical axial rotation



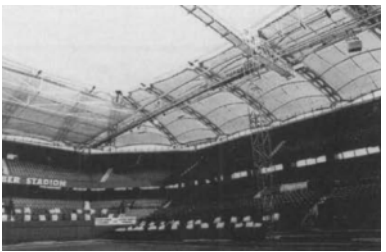
Name	Open-air Theater Neuenstadt	
Location	Neuenstadt / Kocher, Germany	
Year of completion	1971	
Function	Open-air theater	
Designer	E. Kress	
Material	PVC-coated Polyester	
Area of retractable roof [m ²]	260 (R=12m)	
Operation time	10 min.	
Reference	[Ott 72]	



7 Horizontal translation

7.1 No size reduction




Small scale roofs

Name	Gerry Weber Stadium	
Location	Halle/Westfalia, Germany	
Year of completion	1994	
Function	Tennis stadium	
Designer	schlaich bergemann und partner (arch.+eng.)	
Material	Foil, Hostafloan ET (Pneumatic)	
Area of retractable roof [m ²]	1,400	
Operation time	90 sec.	
Remarks	Capacity: 12,400	
Reference	[Ish 00]	


Name	Fahrbares Bühnendach in Landschaftspark Duisburg-Nord	 
Location	Duisburg, Germany	
Year of completion	2003	
Function	Open-air theatre	
Designer	Planinghaus Architekten (arch.), schlaich bergemann und partner (eng.)	
Material	ETFE Membrane	
Area of retractable roof [m ²]	600 (24x3m, 9 cushions)	
Reference	[Dre 08] [sbp 12] [Detail: Heft 7+8/2004]	

[Dre 08]


Name	Sport- and Wellness Bath Kelsterbach	
Location	Kelsterbach, Germany	
Year of completion	2010	
Function	Swimming pool	
Designer	kplan AG (arch.) schlaich bergemann und partner (eng.)	
Material	ETFE-cushions	
Area of retractable roof [m ²]	ca. 504 (cushion 4-ply, 6 x 3 m)	
Reference	[sbp 12]	

[sbp 12]


Large scale roofs


Name	National Tennis Center (Rod Laver Arena)	
Location	part of the Melbourne Park complex, in Melbourne, Victoria, Australia	
Year of completion	1988	
Function	Tennis court	
Designer	Cox Architects + Peddle Thorp Learmonth	
Area of retractable roof [m ²]	ca. 5,800	
Reference	[Ish 00]	


[www.nap.com.au]

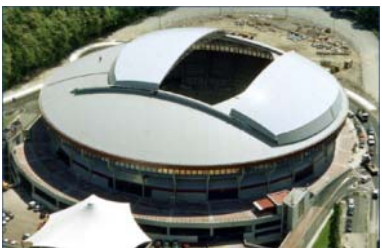
Name	Ariake Coliseum	
Location	Tokyo, Japan	
Year of completion	1991	
Function	Multi-purpose	
Designer	Kenchiku Mode Kenkyujo (arch.+eng.)	
Area of retractable roof [m ²]	17,366	
Reference	[Ish 04]	


[Ish 04]

Name	Amsterdam Arena	 [www.conbit.nl]
Location	Amsterdam, The Netherlands	
Year of completion	1996	
Function	Football and multipurpose Stadium	
Designer	Grabowsky & Poort B.V. (arch. + eng.) Ballast Nedam Engineering B.V. (roof-structure)	
Material	Steel frame + Translucent plastic sheets	
Area of retractable roof [m ²]	7,668	
Reference	[Ish 00] [www.conbit.nl]	


Name	Komatsu Dome	 [Ish 04]
Location	Komatsu, Japan	
Year of completion	1997	
Function	Baseball stadium	
Designer	Yamashita Sekkei + Taisei Co.	
Area of retractable roof [m ²]	3,750	
Reference	[Ish 04]	


Name	Gelredome	 [www.coachvanhetjaar.nl/parool/stadiuminfo.do?stadiumid=16]
Location	Arnhem, Netherlands	
Year of completion	1998	
Function	football and multi-use	
Designer	Alynia Architecten (arch.)	
Material	steel	
Area of retractable roof [m ²]	ca. 7,000	
Remarks	Capacity: 26,600	
Reference	[www.gelredome.nl] [nl.wikipedia.org/wiki/GelreDome]	

Name	Plaza de toros Illunbe	 [www.lanik.com]
Location	San Sebastián, Vascongadas, Spain	
Year of completion	1998	
Function	Bull-fight Ring	
Designer	Lanik (eng.)	
Remarks	-60t /plate -Capacity: 16,000	
Reference	[www.lanik.com]	

Name	SafeCo Field	 [www.ballparksofbaseball.com/al/SafecoField.htm]
Location	Seattle, USA	
Year of completion	1999	
Function	Baseball stadium	
Designer	NBBJ (arch.)	
Area of retractable roof [m ²]	36,000	
Operation time	ca. 10 min.	
Remarks	-11,000t (13,000t with the roof-moving equipment) -Capacity: 46,621	
Reference	[www.scotforge.com/sf_articles_fieldofdreams.htm]	

Name	Docklands Stadium (Colonial Stadium, Telstra Dome, Etihad Stadium)	 <p>[stadiumvibe.com/tag/etihad-stadium/]</p>
Location	Melbourne, Victoria, Australia	
Year of completion	2000	
Function	multi-purpose sports and entertainment stadium	
Designer	Daryl Jackson Architects Hok Sport Architecture	
Material	Steel	
Area of retractable roof [m ²]	ca. 18,000	
Operation time	8 min.	
Reference	[stadiumvibe.com/tag/etihad-stadium/]	


Name	Hisense Arena	 <p>[www.skyscrapercity.com/showthread.php?t=809808&page=7]</p>
Location	The Melbourne Park complex, in Melbourne, Victoria, Australia	
Year of completion	2000	
Function	Tennis court	
Designer	Peddle Thorp Architects	
Area of retractable roof [m ²]	ca. 4,500	
Reference	[en.wikipedia.org/wiki/Hisense_Arena]	


Name	Oita Big Eye Stadium	 <p>[Ish 04]</p>
Location	Oita, Japan	
Year of completion	2001	
Function	Football stadium	
Designer	Kisho Kurokawa (arch.) Takenaka Co. (eng.)	
Material	Steel truss + Membrane	
Area of retractable roof [m ²]	20,000	
Remarks	-Driving system: wire traction -Capacity: 43,000	
Reference	[Ish 04]	

Name	Plaza de toros La Rivera de Logroño	 <p>[www.lanik.com]</p>
Location	Logroño, Spain	
Year of completion	2001	
Function	Bull-fight Ring	
Designer	Diego Garteiz y Javier Labad (arch.), Lanik (eng.)	
Material	Membrane + steel truss	
Area of retractable roof [m ²]	1,300	
Remarks	-60t /plate -Capacity: 11,046	
Reference	[www.lanik.com]	


Name	Plaza de toros de Morzarzal	 <p>[www.lanik.com]</p>
Location	Morzarzal, Madrid, Spain	
Year of completion	2003	
Function	Bull-fight Ring	
Designer	Lanik (eng.)	
Area of retractable roof [m ²]	30 x 30m (D = 49m)	
Reference	[www.lanik.com]	

Name	ESPRIT arena (LTU Arena)	
Location	Düsseldorf, Germany	
Year of completion	2005	
Function	Football Stadium	
Designer	JSK Architekten (arch.)	
Material	Steel	
Area of retractable roof [m ²]	ca. 8,100	
Reference	[de.wikipedia.org/wiki/ESPRIT_arena]	
		[www.fck-news.de/?p=9160]

Name	University of Phoenix Stadium	
Location	Glendale, Arizona, USA	
Year of completion	2006	
Function	Multipurpose football stadium	
Designer	Eisenman Architects (arch.) Walter P Moore (eng.)	
Material	Steel truss	
Area of retractable roof [m ²]	8,030 (55x73m, 2 Panels)	
Reference	[Waggoner, M. IABSE-IASS 2011, London], [www.walterpmoore.com]	
		[Waggoner, M. IABSE-IASS 2011, London]


Name	Plaza de toros Vitoria	
Year of completion	2006	
Function	Bull-fight Ring	
Designer	Lanik (eng.) et al.	
Area of retractable roof [m ²]	2,500	
Remarks	Capacity: 7,800	
Reference	[www.lanik.com]	
		[www.lanik.com]

Name	Plaza de Toros de Elvas	
Location	Elvas, Portugal	
Year of completion	2006	
Function	Bull-fight Ring	
Designer	Lanik (eng.)	
Remarks	Capacity: 6,500	
Reference	[www.lanik.com]	
		[www.lanik.com]


Name	Wembley National Stadium	
Location	London, England, UK	
Year of completion	2007	
Function	Multi-purpose sports stadium	
Designer	Foster and Partners, Populous, Nathaniel Lichfield and Partners (arch.), Mott MacDonald (eng.)	
Area of retractable roof [m ²]	13,722	
Remarks	Capacity: 90,000	
Reference	[www.wembleystadium.com/buildingwembley/statsandfacts/]	
		[www.designbuild-network.com/projects/wembley/]

Name	Plaza de toros Illescas	
Location	Illescas, Toledo, Spain	
Year of completion	2007	
Function	Bull-fight Ring	
Designer	Diego Garteiz (arch) Lanik (eng.)	
Area of retractable roof [m ²]	2,600	
Reference	[www.lanik.com]	

[www.lanik.com]

Name	Lucas Oil Stadium	
Location	Indianapolis, Indiana, USA	
Year of completion	2008	
Function	American Football and a multi-purpose sports stadium	
Designer	HKS, Inc. (arch.) Walter P Moore (eng.)	
Material	Steel truss	
Area of retractable roof [m ²]	16,000	
Operation time	9 min.	
Reference	[Waggoner, M. IABSE-IASS 2011, London] [www.walterpmoore.com]	


[Waggoner, M. IABSE-IASS 2011, London]

Name	Cowboys Stadium	
Location	Arlington, Texas, USA	
Year of completion	2009	
Function	American Football	
Designer	HKS, Inc. (arch.) Walter P Moore (eng.)	
Material	Steel frame + Membrane	
Area of retractable roof [m ²]	9,750	
Operation time	12 min.	
Remarks	-14,100t -Capacity: 80,000 -The largest domed stadium in the world	
Reference	[Waggoner, M. IABSE-IASS 2011, London] [www.walterpmoore.com]	

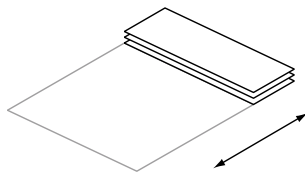
[Waggoner, M. IABSE-IASS 2011, London]

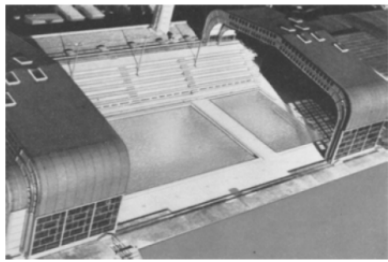
Name	Astana arena	
Location	Astana, Kazakhstan	
Year of completion	2009	
Function	Football Stadium	
Designer	Tabanlıoglu (arch.) HOK Sport Buro Happold (eng.)	
Material	Steel + Polycarbonate	
Area of retractable roof [m ²]	ca. 7,000	
Remarks	Capacity: 30,000	
Reference	[www.sezerler.net/blog/m-t-k-dugun-foto/astana-arena-gurur-fotografлари?nggpage=5]	

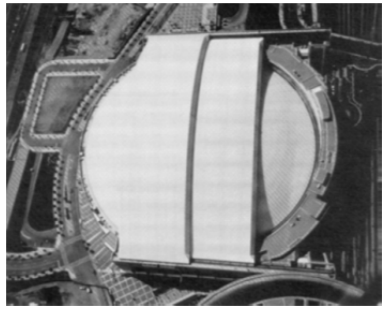
[www.worldarchitecturenews.com/index.php?fuseaction=wanappln.projectview&upload_id=1285]


Name	Nantong Stadium	 [en.structurae.de/structures/data/index.cfm?ID=s0022996]
Location	Nantong, Jiangsu, China	
Year of completion	2010	
Function	Sports Conference and Exhibition Center	
Designer	Enerpac (Hydraulics)	
Material	Steel	
Remarks	1,100t /plate	
Reference	[en.structurae.de/structures/data/index.cfm?ID=s0022996]	


7.2 Overlapping




Name	Schwimmbad Nyon	 [Ott 72]
Location	Noyon, France	
Year of completion	1967	
Function	Swimming pool	
Area of retractable roof [m ²]	ca. 2,200 (60.5 x 37.5 m)	
Reference	[Ott 72]	

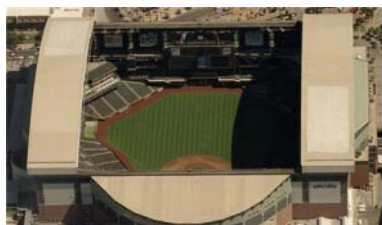
Name	Toronto Sky Dome (Rogers Centre)	 [Ish 00]
Location	Toronto, Canada	
Year of completion	1989	
Function	Baseball stadium (Toronto Blue Jays)	
Designer	Rod Robbie (arch.)	
Material	Steel frames	
Area of retractable roof [m ²]	32,374	
Operation time	20 min.	
Remarks	-Capacity: 54,000 -11,000 t -3 plates (horizontal translation + vertical axial rotation) -open and close 100 times/year -91% of the stadium seats opened -First retractable roof for a stadium	
Reference	[Ish 00]	

Name	Parken Stadium	 <p>[www.pinkfloydz.com/roger2013/aug11copenhagen/aug11copenhagen.htm]</p>
Location	Copenhagen, Denmark	
Year of completion	1992	
Function	Football stadium	
Designer	Gert Andersson (arch.)	
Material	Steel	
Area of retractable roof [m ²]	ca. 11,000	
Remarks	Capacity: 38,000	
Reference	[en.wikipedia.org/wiki/Parken_Stadium]	


Name	Ocean Dome	 <p>[Ish 04]</p>
Location	Miyazaki, Japan	
Year of completion	1993	
Function	Swimming pool	
Designer	Mitsubishi Heavy Industries (arch.+ eng.)	
Material	Steel truss + membrane	
Area of retractable roof [m ²]	22,600	
Reference	[Ish 04]	


Name	Shin-Amagi Dome	 <p>[www.kajima.co.jp]</p>
Location	Tagata-gun, Shizuoka, Japan	
Year of completion	1997	
Function	Multifunctional	
Designer	Yamashita Sekkei	
Area of retractable roof [m ²]	1,044 (29 x 36m)	
Reference	[Ish 00]	


Name	Bank One Ballpark	 <p>[www.acdellovade.com/work/sports.php#img/Sports/heinzfield.jpg]</p>
Location	Phoenix, Arizona, USA	
Year of completion	1998	
Function	Baseball stadium	
Area of retractable roof [m ²]	21,000	
Reference	[Ish 00]	


Name	Chase Field (formerly Bank One Ballpark)	 <p>[www.virtualbirdseye.com/2008/04/12/arizona-diamondbacks-chase-field-aerial-view/]</p>
Location	Phoenix, Arizona, USA	
Year of completion	1998	
Function	Baseball stadium (Arizona Diamondbacks)	
Designer	Ellerbe Becket (arch.)	
Area of retractable roof [m ²]	ca. 22,400	
Operation time	4 min.	
Remarks	-4,000 t -Capacity: 49,033	
Reference	[arizona.diamondbacks.mlb.com]	


Name	Minute Maid Park (aka The Ballpark at Union Station /Enron Field/Astros Field)	 <p>[Waggoner, M. IABSE-IASS 2011, London]</p>
Location	Houston, USA	
Year of completion	1999	
Function	Baseball stadium	
Designer	HOK Sports Facilities Group (arch.) Walter P Moore (eng.)	
Material	Steel truss panel	
Area of retractable roof [m ²]	25,276	
Remarks	-9,000t roof system featuring truss panels -A movable glass wall rides along with the roof to open in 12 min. -Open/close 160 times a year -Capacity: 42,000	
Reference	[Waggoner, M. IABSE-IASS 2011, London] [www.walterpmoore.com]	

Name	Millennium Stadium	 <p>[www.millenniumstadium.com/information/facts_and_figures.php]</p>
Location	Cardiff, Wales, UK	
Year of completion	1999	
Function	Rugby, football and multi-use	
Designer	Populous, WS Atkins	
Operation time	20 min.	
Area of retractable roof [m ²]	8,960	
Remarks	-400t /plate -Capacity: 74,500	
Reference	[www.millenniumstadium.com/information/facts_and_figures.php]	

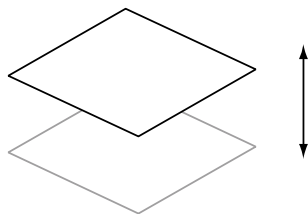
Name	Veltins Arena	 <p>[en.wikipedia.org/wiki/Veltins-Arena]</p>
Location	Gelsenkirchen, Germany	
Year of completion	2001	
Function	Football stadium (Schalke)	
Reference	[en.wikipedia.org/wiki/Veltins-Arena]	

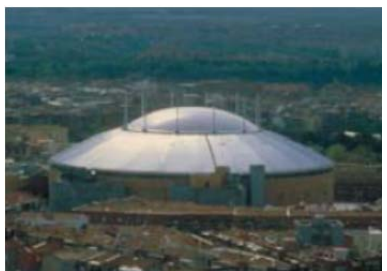

Name	Reliant Stadium	 <p>[Waggoner, M. IABSE-IASS 2011, London]</p>
Location	Houston, USA	
Year of completion	2002	
Function	American Football Stadium	
Designer	Walter P Moore (eng.)	
Material	Steel truss + fabric cover	
Area of retractable roof [m ²]	ca. 290 x 110 m	
Reference	[Waggoner, M. IABSE-IASS 2011, London] [www.walterpmoore.com]	

Name	Misaki Park Stadium / Kobe Wing Stadium	
Location	Kobe, Japan	
Year of completion	2003	
Function	Football stadium	
Designer	Ohbayashi corp.+Shinko Wire Co	
Area of retractable roof [m ²]	9,794	
Operation time	20 min.	
Remarks	One plate: 82x30m, 330t	
Reference	[Ish 04]	[Ish 04]

Name	Marlins' Ballpark (Miami Ballpark)	
Location	Miami, Florida	
Year of completion	2012	
Function	Baseball stadium	
Designer	Populous (arch.) Walter P Moore (eng.)	
Material	Steel truss	
Reference	[Waggoner, M. IABSE-IASS 2011, London]	
		[Waggoner, M. IABSE-IASS 2011, London]

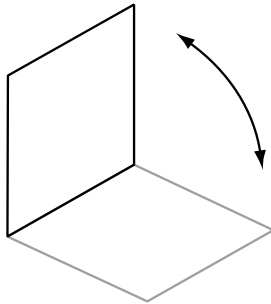
8 Vertical translation





Name	Centro Integrado de Vista Alegre	 
Location	Madrid, Spain	
Year of completion	2000	
Function	Bull-fight ring	
Designer	Jaime Pérez, Ayuntamiento de Madrid (arch.) schliach bergermann und patner (eng.)	
Material	Upper: PVC-coated polyester Lower: ETFE	
Area of retractable roof [m ²]	1,960 (D = 50 m)	
Opening time	ca. 5 min.	
Remarks	-Total weight of cushion: 60t -Lifted upwards vertically by 10m	
Reference	[Schl 00]	[Schl 00]


9 Horizontal axial rotation

9.1 Single axis

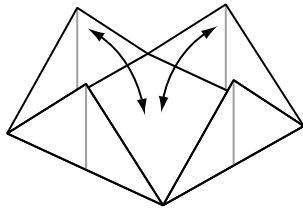


Name	Resonare Obuchizawa Garden Chapel ZONA	 [www.archi-map.jp]
Location	Japan	
Year of completion	2004	
Function	Wedding chapel	
Designer	Klein Dytham architecture (arch.)	
Area of retractable roof [m ²]	122 (building area)	
Reference	[www.archi-map.jp]	

Name	Horizon Serono	 [Sob 12]
Location	Geneva, Switzerland	
Year of completion	2004	
Function	Commercial building (pharmaceutical company Merck/Serono)	
Designer	Helmut Jahn (arch.) Werner Sobek Engineering & Design (eng.)	
Material	Glass roof	
Area of retractable roof [m ²]	1,000	
Remarks	The world's largest openable glass roof	
Reference	[Sob 12]	

Name	Olympic Tennis Centre Complex	 [Detail: Heft 6/2010]
Location	Madrid, Spain	
Year of completion	2009	
Function	Tennis court + Multi hall	
Designer	Dominique Perrault (arch.) TYP SA (eng.)	
Material	Steel truss + sheet-aluminium covering	
Remarks	-Move horizontally+ tilt by hydraulic jacks -Capacity:12000, 5000 and 3000	
Reference	[Detail: Heft 6/2010]	

9.2 Multiple axes

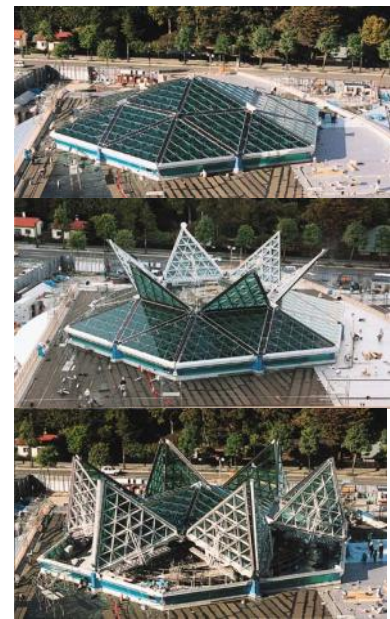


Name	Aircraft Hanger
Location	Stuttgart, Germany
Start of design	1993 (temporary)
Reference	[Koc 04]



[Koc 04]

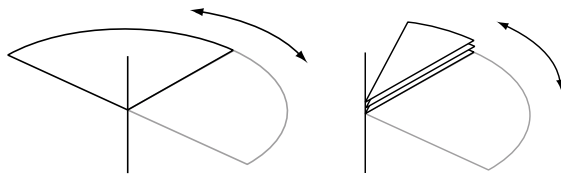
Name	Sapporo Media Park
Location	Sapporo, Japan
Year of completion	2000
Function	Multi-use hall
Designer	Isaka Design (arch.) SDG (eng.)
Material	Steel, glass
Area of retractable roof [m ²]	841
Remarks	18 out of 24 Triangle plates move
Reference	[www.kajima.co.jp]





[www.kajima.co.jp]


10 Vertical axial rotation


10.1 Single axis



Name	Mellon Arena (the Civic Auditorium, Civic Arena, “The Igloo”)	 <p>[en.wikipedia.org/wiki/Mellon_Arena]</p>
Location	Pittsburgh, Pennsylvania, USA	
Year of completion	1961 (2010 closed)	
Function	Ice hockey stadium (NHL) and Multi-use	
Designer	Mitchell and Ritchey (arch.)	
Material	Stainless steel	
Area of retractable roof [m ²]	12,500	
Remarks	2,950t	
Reference	[Ish 00]	


Name	Piscine	 <p>[www.jds.fr/guide-des-sorties/piscines/piscine-ferrette-694_L]</p>
Location	Ferrette, France	
Reference	[www.jds.fr/guide-des-sorties/piscines/piscine-ferrette-694_L]	

Name	Mukogawa Gakuin School Pool	 <p>[Ish 93]</p>
Location	Hyogo, Japan	
Year of completion	1991	
Function	Swimming Pool	
Designer	Takenaka Co.	
Material	Steel truss + Membrane	
Area of retractable roof [m ²]	2,237	
Reference	[Ish 93] [Ish 00]	

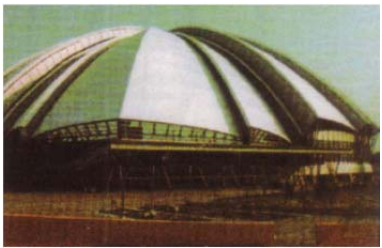
Name	Ball Dome	 <p>[Ish 00]</p>
Location	Toyama, Japan	
Year of completion	1991	
Function	Training Center	
Designer	Sato Kogyo (arch.+eng.)	
Material	Steel truss + Membrane	
Area of retractable roof [m ²]	1,134	
Remarks	Horizontal translation + Vertical axial rotation	
Reference	[Ish 93] [Ish 00]	

Name	Fukuoka Stadium	
Location	Fukuoka, Japan	
Start of design	1993	
Year of completion	General Sports/ Entertainment Complex	
Function	Baseball stadium	
Designer	Takenaka Corp. + Maeda Corp. (arch.+eng.)	
Area of retractable roof [m ²]	33,000 (D = 218m, H = 84m)	
Operation time	20 min.	
Remarks	4,000t /plate	
Reference	[Ish 00][Ish 01]	


[Ish 01]

Name	Tajima Dome	
Location	Hyogo, Japan	
Year of completion	1998	
Function	Baseball stadium	
Designer	M. Senda + Daiken Sekkei, Mitsubishi Heavy Industries	
Area of retractable roof [m ²]	4,700	
Material	PTFE glass fiber fabric	
Reference	[Ish 01]	

[www.oku.co.jp]

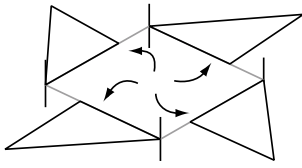
Name	Sendai Dome (Shellcom Sendai)	
Location	Sendai, Japan	
Year of completion	2000	
Function	Football stadium	
Designer	Sogo Keikaku + Mitsubishi Heavy industries	
Material	PTFE glass fiber fabric	
Area of retractable roof [m ²]	6,900	
Reference	[Ish 01]	


[Ish 01]

Name	Miller Park	
Location	Milwaukee, Wisconsin, USA	
Year of completion	2001	
Function	Baseball stadium	
Designer	HKS, Inc., NBBJ, Eppstein Uhen Architects	
Material	Steel	
Area of retractable roof [m ²]	ca. 22,000	
Operation time	10 min.	
Remarks	-12,000t -Capacity: 41,900	
Reference	[www.baseballpilgrimimages.com/national/milwaukee.html]	

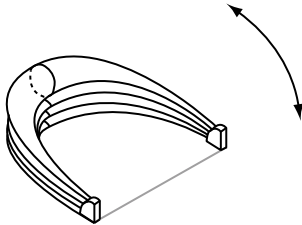
[fingerfood.typepad.com/finger-food/slumping-offense/]


10.2 Multiple axes



Name	Qi Zhong Centre Court Stadium	
Location	Shanghai, China	
Year of completion	2005	
Function	Tennis court	
Designer	SDG (eng.) Environmental Design Institute + Naomi Sato (arch.)	
Material	Steel	
Area of retractable roof [m ²]	15,050	
Operation time	8 min.	
Reference	[Bau 12]	

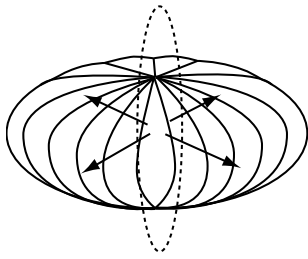
11 Pneumatic deformation – Horizontal axial rotation




Name	Osservatorio Astronomico	
Location	Tenerife, Canary Islands, Spain	
Year of completion	2008	
Function	Astronomical Observatory	
Designer	Airlight Ltd	
Material	polyester / PVC	
Area of retractable roof [m ²]	(D=11.8 m, H=6.3 m)	
Operation time	Inflated in 7 min.	
Remarks	-14 "banana" shaped "Tenserity" -Inflated with an overpressure of 100mbar -Deflated under the weight of steel supports	
Reference	[www.airlight.biz]	

[www.canobbio.com]

12 Pneumatic deformation – Horizontal translation to the centre



Name	Mush-balloon	
Location	Expo 1970, Osaka, Japan	
Year of completion	1970 (temporary)	
Designer	Shigeru Aoki	
Material and Area of retractable roof	D = 30m > PVC coated PVA fabric D = 20m > PVC coated PVA fabric D = 15m > PVC coated Polyester fabric	
Reference	[Ott 72]	[Ott 72]